Universitat Autònoma de Barcelona

Kazrin C Controls Endocytic Trafficking and is a Double Regulator of Actin Polymerisation and Microtubule Transport

Inés Hernández Pérez

Doctoral Thesis

Kazrin C Controls Endocytic Trafficking and is a Double Regulator of Actin Polymerisation and Microtubule Transport

Doctoral candidate: Inés Hernández Pérez

Supervisor: María Isabel Geli

Tutor: Joaquín Ariño

Universidad Autónoma de Barcelona

Doctoral program in Biochemistry, Molecular Biology and Biomedicine

Instituto de Biología Molecular de Barcelona - CSIC

Barcelona, 2020

Acknowledgements

Quiero agradecer a Maribel su dedicación, su entusiasmo por la ciencia y su empeño en este proyecto. Sobre todo, le agradezco su confianza en mí y el haberme enseñado tanto. Agradezco a J. Ariño, J. A. Biosca, E. Boix y F. Tebar su ayuda en las comisiones de seguimiento. A E. Rebollo le agradezco su ayuda con la adquisición de imágenes y el desarrollo de la macro para la cuantificación de la actina endosomal. A esta tesis también han contribuido mis compañeros de laboratorio. Agradezco a Javi sus consejos y el jamón, a Adrian el haberme allanado el camino, a Isa su amabilidad y su trabajo con la kazrina y a Laura el venir todos los días desde Granollers para amenizarme el día.

Gracias a mi madre por ayudarme siempre y por enseñarme a verlo todo, incluida la ciencia, desde un punto de vista estético. A mi padre, por no dudar de mis decisiones y por haberme impulsado a ser, sobre todo, profesional. A Julia, por poner esta tesis en perspectiva. A mi abuela Maruja, experta en CRISPR. A Olga, por compartir mi forma de entender la vida y el trabajo. A Andrea, que es la mejor compañera de piso posible, por su ayuda con la maquetación. Por último, gracias a Craig por motivarme y haberme sacado tantas veces de la espiral infinita del trabajo de laboratorio.

Abstract

Eukaryotic cells internalise and redistribute the molecules from their surface through the endocytic pathway. This process is key to nutrient uptake and catabolism, and controls the surface exposure of signalling receptors and cell adhesion complexes, among others. Previous work in the laboratory identified kazrin C as a protein that blocked Clathrin-Mediated Endocytosis (CME) when overexpressed.

The work presented in this thesis further supported the role of kazrin in CME, as kazrin KO cells generated with the CRISPR-cas9 system were defective in the uptake of the endocytic marker Transferrin (Tfn). Kazrin C co-localised with markers of adherence junctions, such as N-cadherin, at the plasma membrane and on intracellular structures. Indeed, subcellular fractionation analysis showed the localisation of kazrin in Early Endosomes (EEs). Consistent with a role of kazrin in EEs, kazrin depletion caused an accumulation of N-cadherin-loaded EEs, which showed a more peripheral distribution as compared to WT cells. Kazrin KO cells loaded with Tfn were unable to transport the cargo towards the Endocytic Recycling Compartment (ERC) and had a concomitant defect in Tfn recycling. All phenotypes on KO cells were recovered by the re-expression of GFP-kazrin C but not GFP. These evidences indicated a role of kazrin C in endosomal recycling and the transport of EEs towards the ERC. In agreement with this hypothesis, kazrin depletion caused defects in cellular processes that strongly depend on recycling through the ERC, such as cell migration and cytokinesis.

This study also analysed the molecular mechanisms of kazrin C function in endocytic traffic. Kazrin C was found to interact with the microtubule motors kinesin-1 and dynein, and directly bind to the dynein Light Intermediate Chain LIC1. In fact, kazrin C contains a coiled-coil domain similar to those found in dynein adaptors. Also similar to those, GFP-kazrin C localised to the pericentriolar region, where it seemed to trap EEs. Therefore, we proposed that kazrin C promoted microtubule-dependent transport of EEs, possibly as an EE dynein adaptor. Accordingly, this and previous studies in the laboratory showed direct interactions and partial co-localisations of kazrin C with EE components, such as the AP-1 clathrin adaptor complex and EHD1/3 GTPases. In addition, kazrin C interacted with PI3P and the class III PI3K, and its depletion caused an increase in the endosomal levels of the PI3P probe GFP-FYVE. Finally, we linked kazrin C with another player in endocytic traffic: the Arp2/3-associated machinery for actin polymerisation. Direct interactions were observed with cortactin and N-WASP, as well as co-localisation of GFP-kazrin C with cortactin at the plasma membrane and intracellular structures. Moreover, kazrin depletion caused a reduction in cortical and an increase in endosomal branched actin.

Altogether, we proved that kazrin C functions in endosomal recycling and propose that this function is mediated by the regulation of microtubule-dependent transport, actin polymerisation and PI3P metabolism.

Resumen

Las células eucariotas internalizan y redistribuyen las moléculas de su superficie a través de la ruta endocítica. Este es un proceso clave para la adquisición de nutrientes y el catabolismo que también controla la exposición de receptores y complejos de adhesión celular, entre otros. Trabajos anteriores de nuestro laboratorio identificaron la kazrina C como una proteína que bloqueaba la endocitosis dependiente de clatrina (CME) cuando se sobreexpresaba.

El trabajo expuesto en esta tesis confirma el papel de la kazrina en la CME, al demostrar que células KO de kazrina generadas por el sistema de CRISPR-cas9 no internalizaban correctamente la transferrina (Tfn), un marcador endocítico. La kazrina C co-localizó con marcadores de uniones adherentes como la N-cadherina en la membrana plasmática y en estructuras intracelulares. De hecho, un fraccionamiento subcelular demostró la presencia de la kazrina en endosomas tempranos (EEs). Además, la depleción de la kazrina provocó una acumulación de EEs con N-cadherina, y estos tenían una distribución más periférica que en las células control, lo cual es coherente con un papel de la kazrina en EEs. Las células KO de kazrina incubadas con Tfn no transportaban el cargo hacia el compartimento de reciclaje endocítico (ERC) y tenían el consiguiente defecto en el reciclaje de Tfn. Todos los fenotipos en las células KO de kazrina se recuperaron con la re-expresión de GFP-kazrina C pero no con la de GFP. Estas evidencias apuntan hacia un papel de la kazrina C en el reciclaje endosomal y el transporte de EEs hacia el ERC. De acuerdo con esta hipótesis, la depleción de la kazrina causó defectos en procesos celulares que dependen del reciclaje a través del ERC, tales como la migración celular y la citoquinesis.

Este estudio también analiza los mecanismos moleculares de la función de la kazrina C en el tráfico endocítico. Se demostró que la kazrina C interacciona con los motores asociados a microtúbulos kinesina-1 y dineína, y que se une directamente a la cadena intermedia ligera de la dineína, LIC1. De hecho, la kazrina C tiene un dominio coiled-coil similar a los de los adaptadores de la dineína. La kazrina C tiene también en común con estos adaptadores su localización en la región pericentriolar, donde parecía atrapar EEs. Por lo tanto, proponemos que la kazrina C promueve el transporte de EEs a través de microtúbulos, probablemente como un adaptador de EEs y la dineína. En consonancia, este y anteriores estudios del laboratorio mostraron una interacción directa y co-localizaciones parciales de la kazrina C con componentes de EEs, tales como el adaptador de clatrina AP-1 y las GTPasas EHD1/3. Además, la kazrina C interaccionó con PI3P y con la PI3K de clase III, y su depleción causó un aumento en los niveles endosomales de la sonda de PI3P GFP-FYVE. Por último, hemos establecido una relación entre la kazrina C y otro elemento clave del tráfico endocítico: la maquinaria de polimerización de actina asociada a Arp2/3. Se observaron interacciones directas con la cortactina y el N-WASP, así como la co-localización de la GFP-kazrina C y la cortactina en la membrana plasmática y estructuras intracelulares. La depleción de la kazrina causó una reducción en la actina ramificada cortical y un aumento en la endosomal.

En conjunto, probamos una función de la kazrina C en el reciclaje endosomal y proponemos que esta función está mediada por la regulación del transporte a través de microtúbulos, la polimerización de actina y el metabolismo de PI3P.

Resum

Les cèl·lules eucariotes internalitzen i redistribueixen les molècules de la superfície a través de la ruta endocítica. Aquest és un procés clau per a l'adquisició de nutrients i el catabolisme que també controla l'exposició de receptors i complexos d'adhesió cel·lular, entre d'altres. Treballs anteriors del nostre laboratori van identificar la kazrina C com una proteïna que bloquejava l'endocitosi depenent de clatrina (CME) quan es sobreexpressava.

El treball exposat a aquesta tesi confirma el paper de la kazrina en CME, ja que les cèl·lules KO de kazrina generades pel sistema de CRISPR-cas9 no van internalitzar correctament la transferrina (Tfn), un marcador endocític. La kazrina C va co-localitzar amb marcadors d'unions adherents com la N-cadherina a la membrana plasmàtica i en estructures intracel·lulars. De fet, un fraccionament subcel·lular va demostrar la presència de la kazrina als *early endosomes* (EEs). En concordança amb un paper de la kazrina a EEs, la seva depleció va provocar una acumulació de EEs que contenien N-cadherina, que a més tenien una distribució més perifèrica que a les cèl·lules control. Les cèl·lules KO de kazrina no transportaven Tfn cap al compartiment de reciclatge endocític (ERC) i tenien el conseqüent defecte al reciclatge de Tfn. Tots els fenotips en les cèl·lules KO de kazrina es van recuperar amb la re-expressió de GFP-kazrina C però no amb la de GFP. Aquestes evidències apunten cap a un paper de la kazrina C al reciclatge endosomal i al transport de EEs cap al ERC. En consonància amb aquesta hipòtesi, la depleció de kazrina va causar defectes en processos cel·lulars que depenen del reciclatge a través del ERC, com ara la migració cel·lular i la citoquinesi.

Aquest estudi també va analitzar els mecanismes moleculars de la funció de la kazrina C en el tràfic endocític. Es va demostrar que la kazrina C interacciona amb els motors associats a microtúbuls kinesina-1 i dineïna, i que s'uneix directament a la cadena intermitja lleugera de la dineïna, LIC1. De fet, la kazrina C té un domini coiled-coil similar als dels adaptadors de la dineïna. La kazrina C també té en comú amb aquests adaptadors la localització a la regió pericentriolar, on semblava atrapar EEs. Per tant, proposem que la kazrina C promou el transport de EEs a través de microtúbuls, probablement com un adaptador de EEs i la dineïna. En la mateixa línia, aquest i anteriors estudis del laboratori van mostrar una interacció directa i co-localitzacions parcials de la kazrina C amb components de EEs, com l'adaptador de clatrina AP-1 i les GTPases EHD1/3. A més, la kazrina C va interaccionar amb PI3P i amb la PI3K de classe III, i la seva depleció va causar un augment als nivells endosomals de la sonda de PI3P GFP-FYVE. Finalment, establim una relació entre la kazrina C i un altre element clau del trànsit endocític: la maquinària de polimerització d'actina associada a Arp2/3. Es van observar interaccions directes amb la cortactina i el N-WASP, així com la co-localització de la GFP-kazrina C i la cortactina a la membrana plasmàtica i estructures intracel·lulars. A més, la depleció de la kazrina va provocar una reducció en l'actina ramificada cortical i un augment en l'endosomal.

En conjunt, hem provat una funció de la kazrina C al reciclatge endosomal i proposem que aquesta funció ocorre a través de la regulació del transport a través de microtúbuls, la polimerització d'actina i el metabolisme de PI3P.

List of contents

List of figures

List of tables

Abbreviations

CCV	Clathrin-Coated Vesicle
CHC	Clathrin Heavy Chain
CIE	Clathrin-Independent Endocytosis
CLC	Clathrin Light Chain
CME	Clathrin-Mediated Endocytosis
ECM	ExtraCellular Matrix
EE	Early Endosome
EGF	Epidermal Growth Factor
EGFR	Epidermal Growth Factor Receptor
EMT	ExtraCellular Matrix
ER	Endoplasmic Reticulum
ERC	Endocytic Recycling Compartment
FACS	Fluorescence-Activated Cell Sorting
GAP	GTPase-Activating Protein
GDI	Guanosine nucleotide Dissociation Inhibitor
GEF	Guanosine nucleotide Exchange Factor
GPCR	G Protein Coupled Receptor
gRNA	guide RNA
GST	Glutathione S-Transferase
IB	ImmunoBlot
IC	Intermediate Compartment
IDR	Intrinsically-Disordered Region
ILV	IntraLuminal Vesicle
KO	Knock-Out
LE	Late Endosome
LIC	Light Intermediate Chain
MEF	Mouse Embryonic Fibroblast
MTOC	MicroTubule Organising Centre
MVB	MultiVesicular Body

NPF	Nucleation Promoting Factor
PCM	PeriCentriolar Material
PCR	Polymerase Chain Reaction
PIP	PhosphatidylInositol Phosphates
PM	Plasma Membrane
RE	Recycling Endosome
RTK	Receptor Tyrosine Kinase
Tfn	Transferrin
TfnR	Transferrin Receptor
TGN	*Trans*-Golgi Network
WT	Wild-Type

1 Introduction

This thesis focuses on the study of kazrin C, a protein that was first found to impede Clathrin-Mediated Endocytosis (CME) when overexpressed. Further analysis suggested that kazrin C controls endocytic transport through its interaction with the actin cytoskeleton and clathrin coat components. This thesis expands on the molecular mechanisms by which kazrin C regulates endocytic traffic, which involves not only the interaction with the actin cytoskeleton but also with the tubulin cytoskeleton and with membrane phosphoinositides. It also explores the involvement of kazrin C in physiological functions that require proper endocytic recycling, such as cell migration and division. Therefore, the introduction reviews the endosomal system and its role in cell physiology as well as the molecular players involved in endocytic membrane traffic, including the actin and tubulin cytoskeletons. Finally, it gives an overview of the structure and previously known functions of kazrin C, according to the available literature.

1.1 The secretory and endocytic pathways

Eukaryotic cells are compartmentalised into membrane-limited and membrane-less organelles with different compositions and functions. These cellular compartments function in a coordinated manner to efficiently fulfil the physiological processes, which sustain life, including nutrient uptake and processing for energy production, anabolism, waste disposal, cell migration, cell division, and adaptation to environmental cues or stress. Proteins and lipids are effectively transported from one compartment to another. They are often transported as cargoes within membrane-limited organelles or transport intermediates, in a process collectively known as membrane trafficking. Membrane trafficking has been classically divided into the secretory and the endocytic pathways. The secretory pathway allows the distribution of newly synthesised proteins and lipids from the Endoplasmic Reticulum (ER). These travel through the Golgi apparatus to the Plasma Membrane (PM), in the case of transmembrane cargoes, or to the extracellular space, in the case of soluble cargoes. The ER is an extended tubular network throughout the cytoplasm, whereas the Golgi is formed by *cis*, medial and *trans* cisternae in close proximity, usually in the perinuclear region. An Intermediate Compartment (IC) connects the ER and the Golgi, and a *Trans*-Golgi Network (TGN) sorts cargo into the endosomal system or to the PM (**Figure 1.1**).

On the other hand, the endocytic pathway allows the internalisation of proteins and lipids that come from the PM or the extracellular media, and their distribution in the cytoplasm (**Figure 1.1**). They are internalised in endocytic vesicles of different nature, termed clathrin-coated vesicles (CCVs) in the case of CME. Endocytic vesicles are delivered to Early Endosomes (EEs), also called sorting endosomes (Lamaze and Prior, 2018; Wang *et al.*, 2018). EEs are a network of vacuolar and tubular structures from where cargoes will be sorted to different destinations, either to the degradative compartments, to the Golgi or back to the PM (Sönnichsen *et al.*, 2000). Membrane proteins destined for degradation are packed into IntraLuminal Vesicles (ILVs) in the EE. ILVs fill the Late Endosomes (LE), that will deliver

cargo into the lysosome. Cargoes that reach the lysosome are degraded into their structural units, which will in turn be used for the biogenesis of new proteins (Huotari and Helenius, 2011; Hu *et al.*, 2015). If, however, cargoes are to be recycled back to the PM, they can follow the direct route from the EE (van der Sluijs et al., 1992) or can go first to the Recycling Endosome (RE) and then to the PM. The RE is a reticular and tubular compartment that is usually next to the nucleus, in close to the TGN (Maxfield and McGraw, 2004; Grant and Donaldson, 2009; **Figure 1.1**). The secretory and endocytic pathway crosstalk at different points, mainly the PM and the TGN. Of note, many lipids and proteins follow retrograde transport in order to be recycled back to their original organelle and maintain homeostasis. Retrograde transport occurs from the Golgi to the ER or from the endosomes to the Golgi or the PM (**Figure 1.1**).

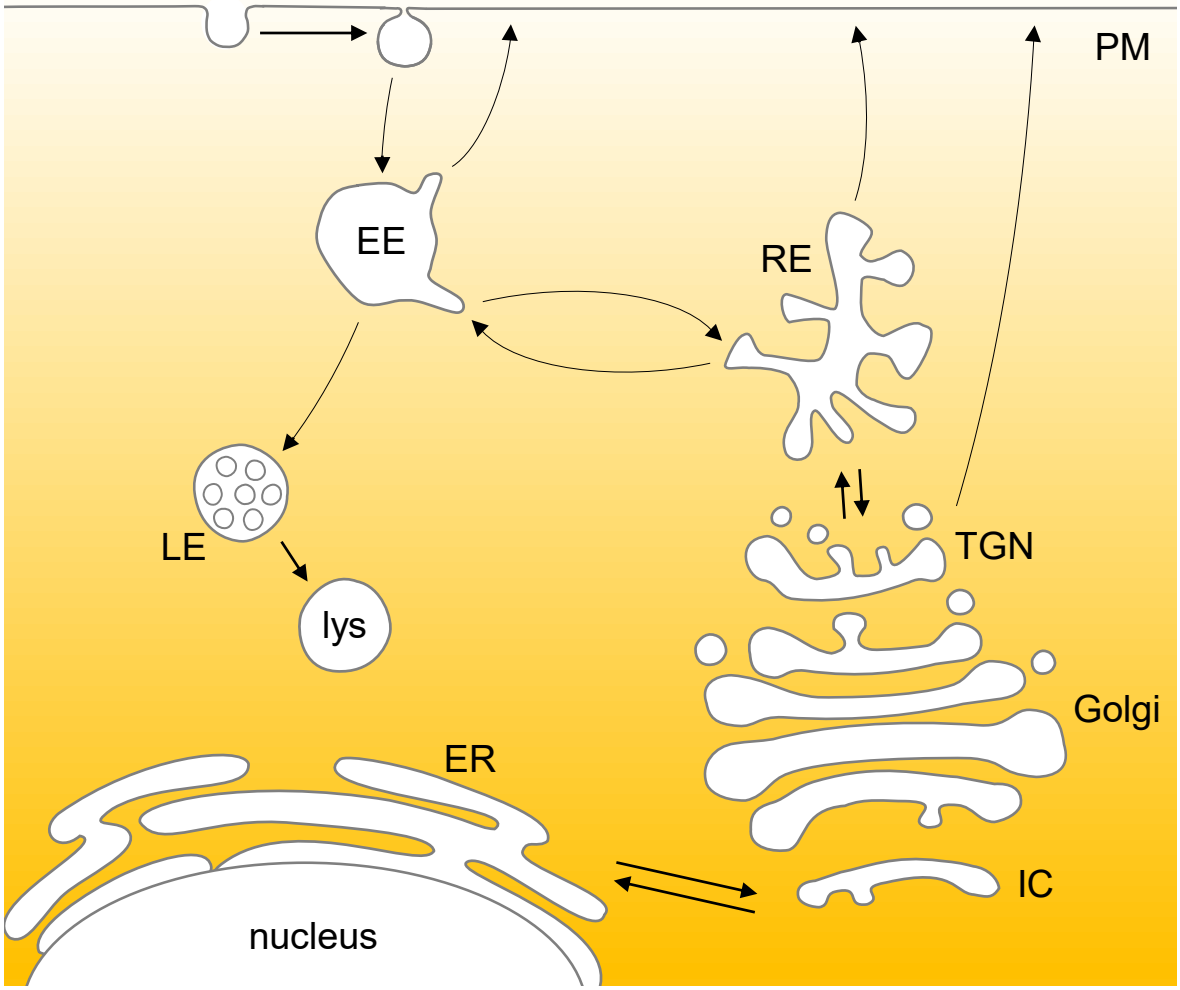

Figure 1.1. The secretory and endocytic pathways. The pathways followed by endocytic cargoes are depicted, starting from the invagination of the PM (plasma membrane) during endocytosis and transport to the EE (early endosome). Cargoes then follow the degradation route to the LE (late endosome) and lys (lysosome) or they are recycled to the PM (plasma membrane). Recycling can be direct from the EE or indirect, through the RE (recycling endosome). The nucleus, ER (endoplasmic reticulum), IC (intermediate compartment), Golgi apparatus and TGN (*trans*-Golgi network) are depicted to show the connexion between the endosomal pathways and the secretory pathway.

Along the secretory and endocytic pathways, proteins and lipids are transported to a particular cellular destination as cargo. Cargo can follow the bulk flow, but membrane proteins normally bear specific sequences on their cytosolic-exposed regions that target them to specific routes. Luminal cargo can bind to membrane receptors that will in turn define their transport pathway. Trafficking signals can either be constitutively exposed or be available only upon a conformational change that is induced by chemical or mechanical cues. Further, cargo can be selectively labelled by covalent modifications, such as phosphorylation or ubiquitination, that will change their initial fate.

The secretory pathway has an obvious role in anabolism, whereas endocytosis essentially contributes to nutrient uptake and catabolism, as well as to waste disposal (Palm and Thompson, 2017; Gilleron, Gerdes and Zeigerer, 2019; Sun and Brodsky, 2019). In addition, coordinated endocytosis and secretion play key roles in cell reprograming. They control the surface exposure of a particular set of signalling and cell adhesion receptors, transporters, channels or enzymes, essentially contributing to define the cell identity. Inputs from environmental stress, developmental cues or nutritional demands cause transcriptional or post-transcriptional modifications that label particular PM proteins for their internalisation and degradation or that affect the set of secreted cargoes (Di Fiore and Zastrow, 2014; Watanabe and Boucrot, 2017; Sicari, Igbaria and Chevet, 2019).

Endosomal traffic is also used to quickly redistribute membrane components and reshape the cell. In fact, membrane organelles serve as a platforms to spatially redistribute signalling (Schmid, 2017). Thereby, endosomal trafficking and polarised secretion play essential roles in sustaining cell polarity (Lecuit and Pilot, 2003; Scita and Di Fiore, 2010). They are also essential in any other process that requires membrane reshaping or a rapid redistribution of cell adhesion molecules or signalling complexes at the PM. The most relevant roles of endosomal trafficking for this thesis are those in cell migration (Lecuit and Pilot, 2003; Sigismund and Scita, 2018), and cytokinesis (Albertson, Riggs and Sullivan, 2005; Nähse *et al.*, 2017), which will be discussed in more detail in section 1.5. In this respect, the tubulin cytoskeleton plays a key role by providing long-range directional movement of organelles and defining how the Golgi and the endosomal system are placed within the cell.

Finally, specialized forms of secretion and endocytosis have important roles in particular cell types in multicellular organisms. Some examples are the secretion of synaptic vesicles and subsequent regeneration in neurons, the regulation of the pigmentation in melanocytes and the antigen presentation in the immune system. Since these are not the focus of this thesis, the reader can refer to Dengjel *et al.* (2005) and Lou (2018) for further information.

The understanding of membrane trafficking mechanisms is a fundamental question in biology but it is also of great biomedical interest. For instance, neurodegenerative diseases such as Parkinson's or Alzheimer's are characterised by the accumulation of dysfunctional

proteins in the cells of patients (Kovacs, 2018), and therefore are strongly linked to the dysfunction of the degradative capacity of the endosomal system (Hu *et al.*, 2015). These protein aggregates in turn affect the structural integrity of the Golgi and affect the secretory pathway (Fan *et al.*, 2008). Also, deregulation of the levels of cell surface proteins can lead to neuronal synapsis malfunction and affect neuronal viability (McMillan, Korswagen and Cullen, 2017). In addition to neurodegenerative diseases, aberrant endosomal trafficking is linked to bad cancer prognosis. The stabilisation or degradation of oncogenic or tumour supressing proteins, respectively, can influence malignant cell transformation (Tanaka, Kyuuma and Sugamura, 2008). Also, the secretory and recycling machineries regulate the amount of cell-surface proteins involved in cell invasion, such as metalloproteases, integrins or the epidermal growth factor (EGF) receptor (EGFR; Caswell and Norman, 2008; Zahoor and Farhan, 2018). In fact, some breast cancer therapies are based in blocking the trafficking of ErbB2, a protein that is overexpressed in the cell surface of patients with poor prognosis (Austin *et al.*, 2004). Finally, the endosomal and secretion systems are often exploited by pathogens as part of their infection process, and their intervention can prevent pathogen infection and propagation (Gruenberg and Van Der Goot, 2006; Allgood and Neunuebel, 2018).

1.2 Mechanisms of membrane traffic

The mechanisms of membrane trafficking can be divided in three types: non-vesicular transport, transport using transport intermediates and maturation of organelles. Non-vesicular transport is mainly associated with the transport of lipids by shuffling in membrane contact sites. It works together with vesicular transport to maintain organelle homeostasis. Non-vesicular transport is not the aim of this thesis and therefore, it will not be further described. The reader can refer to its review in Funato, Riezman and Muñiz (2020).

In addition to non-vesicular traffic, proteins and lipids can be transported between organelles via the formation of membrane-limited vesicular or tubular intermediates that bud from the donor membrane, travel into the cytosol and fuse with the acceptor organelle (**Figure 1.2**). This transport mechanism is well established between the PM and the EE, between the endosomes and the PM or the Golgi, and between the ER and the Golgi for anterograde and retrograde transport (Bonifacino and Glick, 2004). The formation of these intermediates generally requires a coat, composed of proteins that transiently assemble on the cytoplasmic leaflet of the donor membrane. Coats often bind certain phosphoinositides and small GTPases that are landmarks of each organelle. They recruit the cargo and contribute to curve the lipid bilayer to generate the transport intermediate (Wang *et al.*, 2018). Besides coats, other mechanisms can contribute to the remodelling of the lipid bilayer for membrane budding. These include the insertion of amphipathic helices, molecular crowding, the binding of intrinsically curved domains like the F-BAR domains, changes in the lipid composition and the exertion of mechanical forces by actin polymerisation and actin or tubulin molecular

motors (Simunovic, Bassereau and Voth, 2018). The scission of transport intermediates usually requires a specialized machinery to overcome the energy barrier of membrane fusion. For example, the GTPase dynamin and related proteins such as the EHD family. Also N-BAR domain-containing proteins contribute to fission by stabilising highly curved membranes, bringing the actin polymerisation machinery or creating lipid boundaries to promote fission (Renard, Johannes and Morsomme, 2018).

The resulting vesicles or tubules are transported along actin fibres or at the tip of actin comets (for short-range movements close to the cortex), or along microtubules (for long-range centripetal or centrifugal movements within the cell) until they interact with the target membrane. Recognition between the transport intermediate and the acceptor organelle is ensured by tethers that expand from the organelle into the cytosol to fish the incoming vesicles and tubules, together with the rab GTPases present on both approaching membranes (Witkos and Lowe, 2017; Podinovskaia and Spang, 2018). Once tethered, the unfavourable fusion of the membranes takes place, which is achieved by the formation of a *trans*-SNARE complex (Witkos and Lowe, 2017; **Figure 1.2**).

Besides the formation of transport intermediates, material can be transported within the organelle body as it is converted into another compartment in a process called maturation (Podinovskaia and Spang, 2018). This mechanism is well established for the transition from EE to LE, but it may also apply to the formation of RE from EE or transport through the Golgi cisternae. The acquisition of a new organelle identity is led by the exchange of rab GTPases and the conversion of phosphoinositides. It often involves changes in the organelle shape and positioning and the recruitment of specialised enzymatic machinery, membrane transporters, channels or receptors needed for the new organelle function. Maturation also implies the acquisition of new tethers and fusion-mediating complexes that will redefine the transport intermediates that will fuse with it (Del Conte-Zerial *et al.*, 2008; Mindell, 2012; Marat and Haucke, 2016; Bonifacino and Neefjes, 2017).

The key molecular players defining organelle identity and effecting membrane trafficking are discussed in more detail in the following sections. These include small GTPases, phosphoinositides, coat and fission machineries, tethering and SNARE complexes, as well as actin filaments, microtubules and their respective molecular motors.

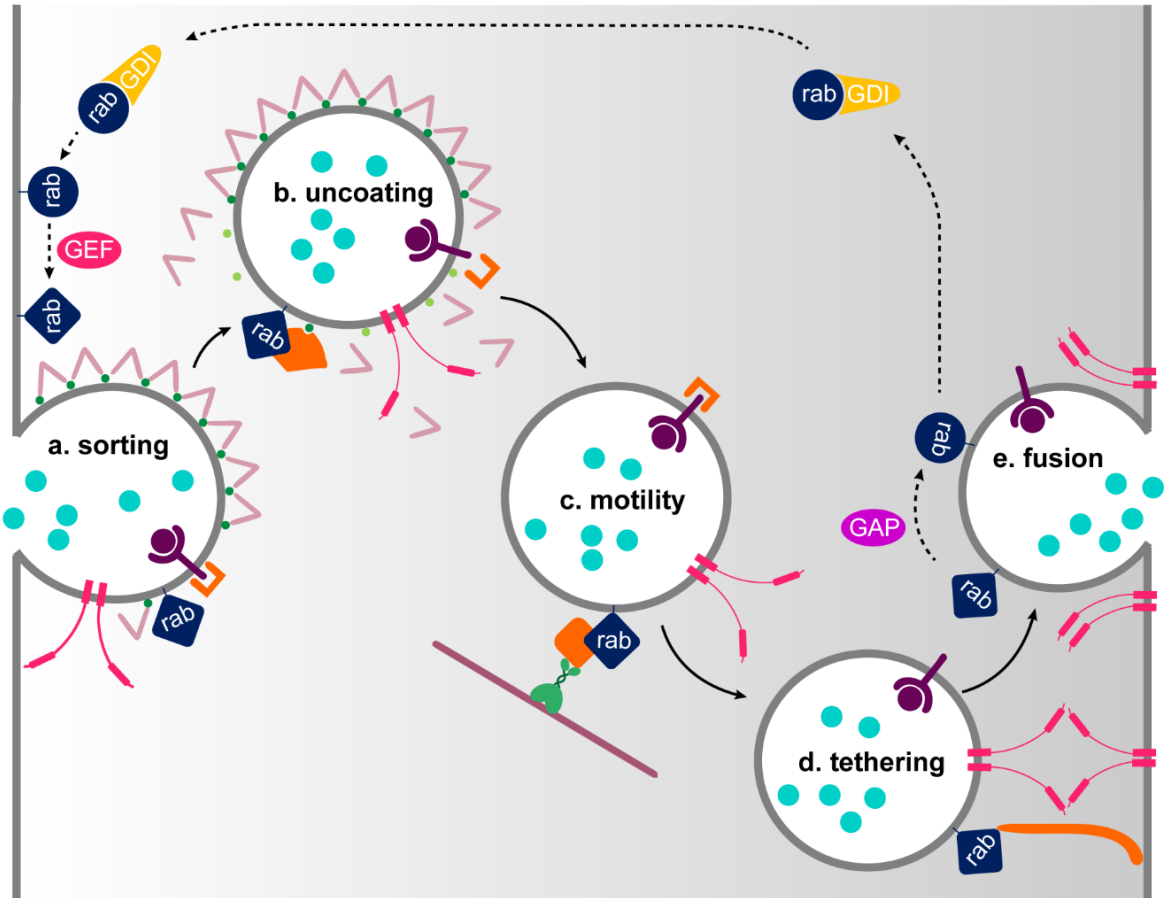

Figure 1.2. Vesicular transport of cargo. Cargoes are sorted into a specialised domain of the donor membrane as a result of a rab and PIP double coat, triggered by the activation of the rab by its GEF (a). The budding of the vesicle starts as the coat proteins are recruited. The coat is detached after fission of the vesicle, often due to a change in the phosphoinositide (PI) composition of the membrane as PIP kinases and phosphatases are recruited (b). The vesicle is transported along a cytoskeletal track through its interaction to motor proteins (c) until a tether connects it to the acceptor membrane (d). Fusion occurs through a SNARE complex (e). After fusion, the rab protein is inactivated by its GAP and joins the cytoplasmic pool in its GDI-binding form. Note that the rab GTPase cycle guides the different steps of vesicle transport by recruiting various effectors, which are marked in orange. From Stenmark (2009).

1.3 Molecular players in membrane traffic

The main molecules implicated in membrane trafficking are described in this section. They are classified in small GTPases, phosphoinositides, phosphoinositide kinases and phosphatases, coats, membrane fission machinery, tethers, membrane fusion machinery, the actin cytoskeleton and microtubules. Special sections are dedicated to molecules of particular importance in this thesis.

1.3.1 Small GTPases

The identity of organelles within the secretory and endocytic pathways is thought to be mostly defined by phosphoinositides and small GTPases. Phosphoinositides can be rapidly interconverted by phosphoinositide kinases and phosphatases, whereas small GTPases quickly transit between activated GTP-loaded states and inactive forms (Barr, 2013). The fact that organelle identity depends on short-lived molecules and molecular states reveals how plastic and dynamic membrane transport is.

Rab (*Ras*-like in rat Brains) proteins are small GTPases of around 70 kDa that recruit specialised machinery to the cytoplasmic surface of endocytic compartments, forming a transient membrane subdomain (Novick, Field and Schekman, 1980; Salminen and Novick, 1987; Chavrier *et al.*, 1991; Wandinger-Ness and Zerial, 2014). Their GTP/GDP cycle induces conformational changes that determine membrane and effector binding (**Figure 1.2**; Wittinghofer *et al.*, 1993). GDP-bound rabs are inactive in the cytosol bound to GDIs (Guanosine nucleotide Dissociation Inhibitors). GEF (Guanine nucleotide Exchange Factor) proteins favour GDP to GTP exchange, impede GDI binding, and therefore activate rabs. Activated rabs associate with membranes through prenylation of their C-terminus and interact with multiple effectors (Andres *et al.*, 1993). The cycle is closed by the hydrolysis of GTP to GDP, which is promoted by GAPs (GTPase-Activating Proteins) and which entails the inactivation of the rab (**Figure 1.3**). Importantly, many rab GEFs are effectors of rabs other than the one they activate, which leads to rab activation cascades (Zhang *et al.*, 2006). Reciprocally, rabs can also activate GAPs (Rivera-Molina and Novick, 2009), allowing the exclusion of other rabs and imposing negative feedback mechanisms to stop the previous rab in the cascade (Pfeffer, 2013). Thus, both rab GEFs and GAPs are essential to spatially and temporally regulate rab function (Lamber, Siedenburg and Barr, 2019).

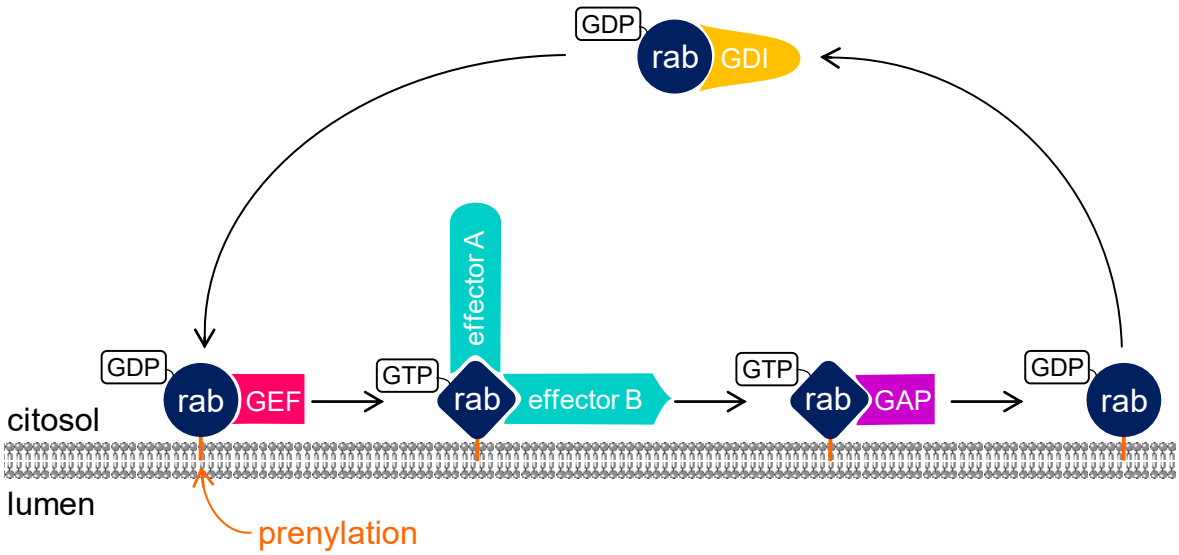

Figure 1.3. Rab GTPase cycle. Rab GTPases follow an activation/inactivation cycle that is linked to their GTP/GDP state. The inactive, GDP-bound rab is maintained in a cytosolic pool in association with a GDI protein. Upon recognition by its GEF in the target membrane, the rab exchanges GDP for GTP and becomes active. The active rab binds to membranes through a prenyl moiety and acquires a new conformation that allows binding to its different effectors. Eventually, the rab GAP enhances the GTPase activity of the rab. The resulting GDP-bound rab detaches from the membrane and binds the GDI, ready to start a new cycle.

Rabs are necessary for cargo selection, vesicle formation, interaction with the cytoskeleton, vesicle tethering and fusion, and signalling. The best characterised rabs involved in endocytic trafficking are rab4, rab5, rab7 and rab11, but many other have been described. Along the secretory pathway, rab1, rab2, rab8 and rab29 are the most prominent ones (Zhen and Stenmark, 2015; **Figure 1.4**).

Another family of small GTPases, arfs (ADP Ribosylation Factors), plays a role in organelle identity. Like rabs, arfs are also localised in specific compartments and recruit multiple effectors (Behnia and Munro, 2005; Cherfils, 2014). Their GTP-GDP cycle is similar to that of other small GTPases. However, their membrane association is mediated through a myristyl group and an amphipathic helix. A mechanism involving the latter ensures that the GDP to GTP exchange is sufficient for membrane binding, which explains the absence of a GDI equivalent for arf proteins (Pasqualetto, Brancale and Young, 2018). Although the localisation and function of most arfs is not well characterised, many are known to be important for membrane trafficking and sorting, such as arf1, arf3, arf4 and arf6 (Donaldson and Jackson, 2011; **Figure 1.4**).

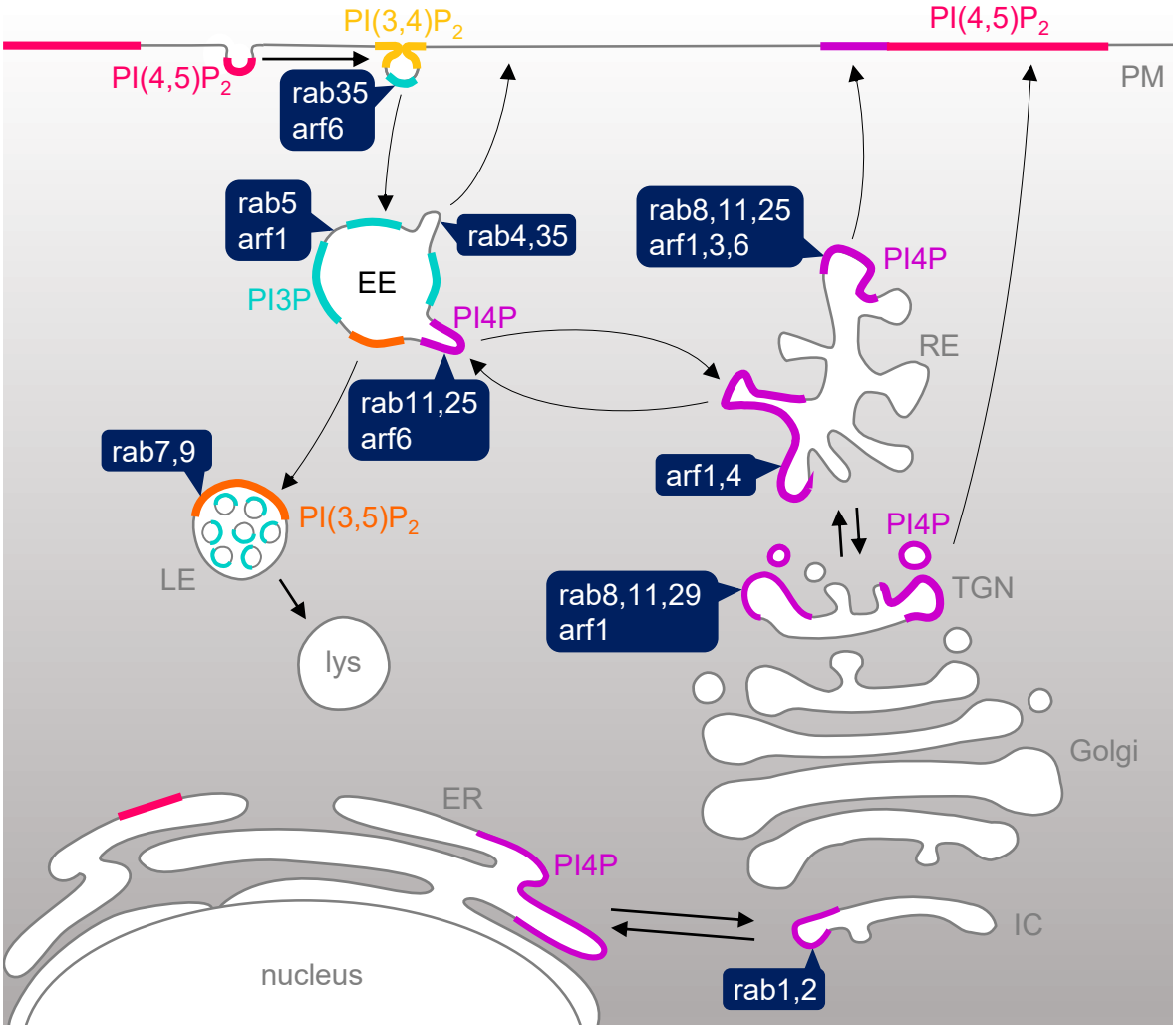

Figure 1.4. Small GTPases and phosphoinositides involved in membrane trafficking. The best characterised PIPs and rab and arf GTPases in secretory and endosomal pathways are shown. At the PM $PI(4,5)P_2$ recruits and activates the endocytic machinery, and is essential for nucleation, maturation and fission of the endocytic vesicle (Posor, Eichhorn-Grünig and Haucke, 2015). As invagination proceeds, $PI(4,5)P_2$ is converted to $PI(3,4)P_2$ for vesicle fission. Upon fission, phosphates are recruited to generate PI (Posor *et al.*, 2013). Rab5 is recruited to endocytic vesicles, where it plays a role in cargo recruitment. Endocytic vesicles then reach EEs, where rab5 and arf1 GTPases accumulate. PI3P is the predominant PIP in endosomal membranes and is implicated in homotypic fusion of EEs, endosomal sorting and ILV formation in EEs (Marat and Haucke, 2016). Specific endosomal subdomains acquire different PIPs and rabs depending on the destiny of the cargoes in them (Sönnichsen *et al.*, 2000). For instance, the enrichment in $PI(3,5)P_2$ and rab7 promotes conversion to LE and lysosomes (lys; Jin, Lang and Weisman, 2016). Rab4 and rab35 can direct direct trafficking to the PM (Kouranti *et al.*, 2006). Trafficking towards the RE is driven by the hydrolysis of PI3P, coupled to the generation of PI4P, and to rab11, rab25 and arf6 recruitment. Rab8, rab11, rab25, arf1, arf3 and arf6 are required for recycling to the PM. Trafficking between the RE and the TGN depends on arf1, arf4, rab8, rab11 and rab29 (D'Angelo *et al.*, 2008; Nakai *et al.*, 2013). Rab1 and rab2 are involved in membrane exchange between the ER and the IC (Tisdale *et al.*, 1992).

An essential mechanism by which small GTPases ensure compartment and subcompartment identity is the formation of lipid platforms for the recruitment of specialised machinery (Behnia and Munro, 2005). Indeed, phosphoinositides are an important hallmark for specific membrane compartment.

1.3.1.1 Rab5, rab4 and rab11

Rab4, rab5 and rab11 are the best described in the early endocytic pathway, and therefore most relevant for this thesis. Rab5 is located in the PM and in the EE and it is involved in the formation of CCV, in the tethering and fusion of CCV with the EE and in the fusion between EEs (Chavrier *et al.*, 1990). The GEF rabex5 binds to endocytic cargoes and activates rab5 on endocytic vesicles. Interestingly, the rab5 effector rabaptin5 interacts with rabex5 to induce a positive feedback loop and a rab5 endosomal subdomain (Horiuchi *et al.*, 1997). Rab5 also activates VPS34, which catalyses PI3P formation and defines EE identity (this is described in more detail in section 1.3.2.1; Shin *et al.*, 2005). Other effectors of rab5 include EEA1 and CORVET, tethers that allow vesicle-endosome fusion and homotypic endosomal fusion, respectively (see section 1.3.5; Christoforidis *et al.*, 1999; Perini *et al.*, 2014).

Rab4 is found on CCVs, EEs and REs. It is important for cargo sorting at EEs and the recycling of cargoes such as integrins, receptor tyrosine kinases (RTKs) and G-protein coupled receptors (GPCRs; van der Sluijs *et al.*, 1992a; Arjonen *et al.*, 2012). Specifically, rab4 seems to recruit tubule and vesicle-formation machinery in EEs, thus creating sorting subdomains (D'Souza *et al.*, 2014). Two isoforms of rab4, rab4a and rab4b, have different roles in recycling, with rab4a being involved in the short recycling pathway (Yudowski *et al.*, 2009) and rab4b in the long recycling pathway (Perrin et al., 2013). Among rab4 effectors is rabaptin 5, which points towards a mechanism linking cargo arrival to EE to its recycling (Kälin *et al.*, 2015).

Finally, rab11 functions at the TGN for the delivery of secretory vesicles, as well as in endocytic recycling (Urbé *et al.*, 1993; Ullrich *et al.*, 1996). The recycling pathway regulated by rab11 is slower than that dependent on rab4a, and delivers cargoes such as the transferrin (Tfn) receptor (TfnR), integrins and cadherins (White, Caswell and Norman, 2007; Desclozeaux *et al.*, 2008). Some rab11 effectors are rab11-FIP3, the exocyst complex and cytoskeletal motors, which allow transport and fusion of recycling transport intermediates (Zhang *et al.*, 2004; Horgan *et al.*, 2010; Delevoye *et al.*, 2014). The importance of rab11-dependent trafficking is highlighted by its implication in numerous cellular processes like ciliogenesis, cytokinesis and neuritogenesis (Welz, Wellbourne-Wood and Kerkhoff, 2014).

1.3.2 Phosphoinositides, kinases and phosphatases

Cellular membranes are formed by a wide variety of lipids (Harayama and Riezman, 2018). Different lipid composition can be found in different organelles, but also in different domains within (**Figure 1.4**). For instance, apical and basal membranes in polarised cells, PM or endosomal nanodomains, or the inner and outer leaflet within one lipid bilayer, are enriched in particular lipids. This has functional implications in the membrane physiochemical properties and in protein function. The size and saturation of the hydrophobic tails determines the direction and degree of the membrane curvature, and also the fluidity and the formation of nanodomains by phase separation (Sezgin *et al.*, 2017). Lipid composition influences the localisation and conformation of transmembrane proteins, but also determines the recruitment of lipid-binding proteins and curvature-sensing proteins from the cytoplasm (Harayama and Riezman, 2018).

Cellular membranes are composed of three types of lipids, namely glycerophospholipids, sphingolipids and esterols (Harayama and Riezman, 2018). Phosphatidylinositides are a type of glycerophospholipids consisting of a glycerol esterified by two fatty acid chains and linked to an inositol ring through a phosphate group (**Figure 1.5A**), and account for most phosphoinositides in the cell (Posor, Eichhorn-Grünig and Haucke, 2015). The fatty acid hydrophobic tail is embedded in the lipid bilayer, whereas the hydrophilic head is exposed in the cytoplasm. Importantly, the inositol ring can be phosphorylated and de-phosphorylated in positions 3, 4 and 5, giving rise to a variety of PhosphatidylInositol Phosphates (PIPs): phosphatidylinositol (PI), phosphatidylinositol 3-phosphate (PI3P), PI4P, PI5P, PI(3,4)P_2, PI(3,5)P_2, PI(4,5)P_2 and PI(3,4,5)P_3 (**Figure 1.5B**). Many endocytic proteins bear lipid binding domains, such as the FYVE, PH, PX, BAR, ENTH, ANTH, PROPPIN and GRAM domains, that specifically recognize certain PIPs (Lemmon, 2008). PIPs are dynamically interconverted by specific kinases and phosphatases (**Figure 1.5B**), whose localisation and activation often depends on GTPases. In turn, GTPase GAPs and GEFs can be recruited by PIPs, thereby establishing positive and negative feedback loops (Wang, Lo and Haucke, 2019). On the other hand, rab and arf effectors often bear PIP binding domains, which synergizes with their GTPase binding sites, imposing a double code that ensures organelle and subdomain identity.

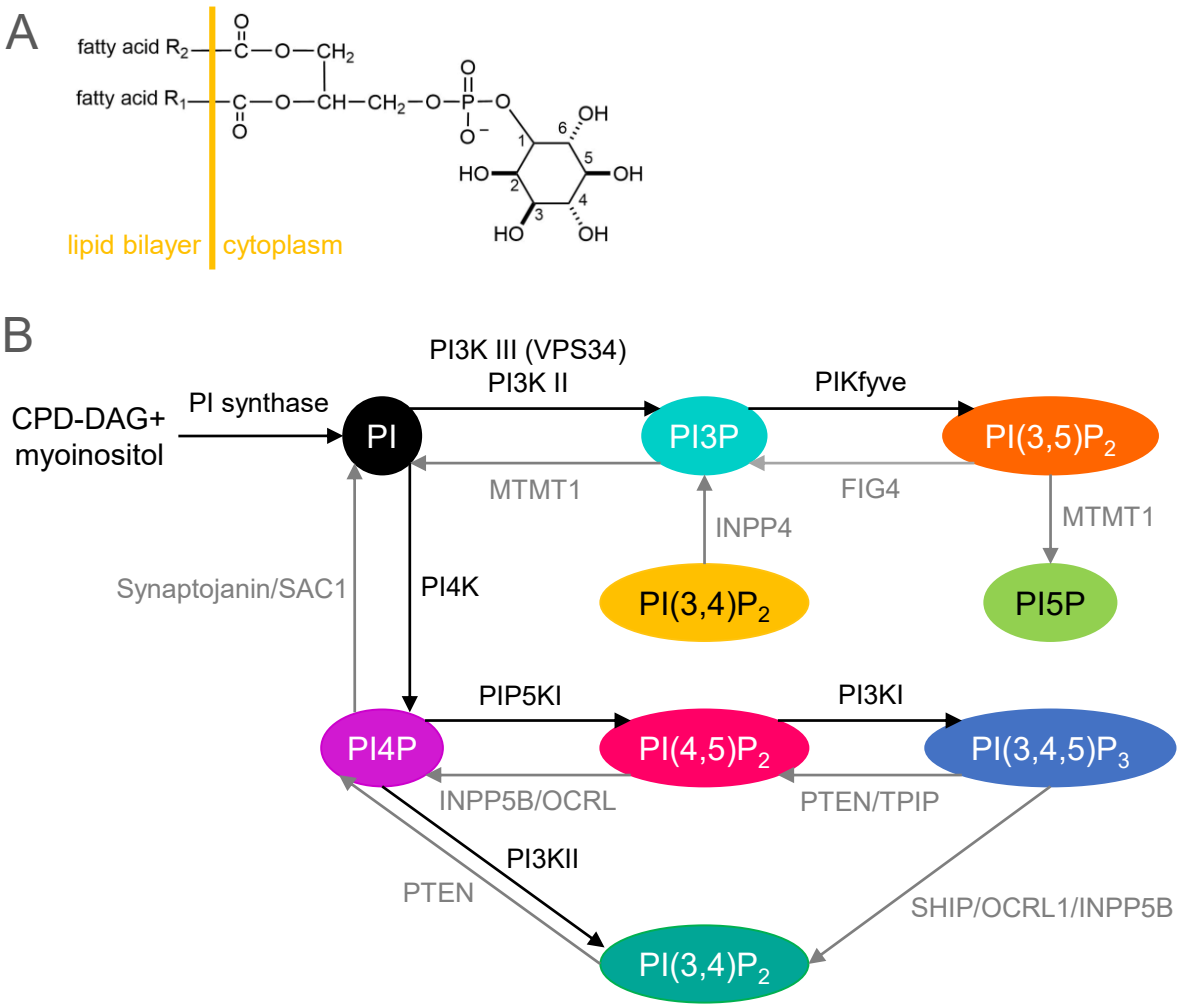

Figure 1.5. Phosphoinositides structure and metabolism. A. Structure of phosphatidylinositol, the base of PIPs. It is formed by a glycerol that is esterified by two fatty acid chains embedded in the lipid bilayer. An inositol ring is joined to the glycerol by a phosphate group that has negative charge in the cytoplasmic pH. Note positions 3, 4 and 5 in the inositol ring, which are susceptible to phosphorylation. **B.** Metabolic routes for the synthesis of PIPs by phosphorylation or dephosphorylation of the inositol ring. The enzymes catalysing each step in humans are specified. Kinases are shown in black and phosphatases in grey. Adapted from De Craene *et al.* (2017).

1.3.2.1 VPS34 and MTM1

Most PI3P is formed by the class III PI3K, although a small proportion is formed by class II PI3K (Backer, 2016). The catalytic subunit of class III PI3K is VPS34, which is active as a heterodimer with VPS15. In addition, the complex includes a heterodimer of beclin and UVRAG that regulates the activity and membrane binding capacity of the complex (Rostislavleva *et al.*, 2015). This complex is important in EE fusion and maturation, as well as in autophagy (Schu *et al.*, 1993; Devereaux *et al.*, 2013). An alternative complex containing ATG14L instead of UVRAG is mainly involved in autophagy (Kihara *et al.*, 2001). Binding of VPS34 to EEs is mediated by rab5 and to LEs by rab7 (Murray *et al.*, 2002; Stein *et al.*, 2003). The VPS34 inhibitor IN1 is often used to study its function (Bago *et al.*, 2014).

The function of VPS34 on EEs is counteracted by PI 3-phosphatases of the myotubularin family, of which the best known is MTM1 (Cao *et al.*, 2008; Singla *et al.*, 2019). MTM1 forms homodimers through its coiled-coil domain or heterodimers with catalytically-inactive myotubularins. Interestingly, MTM1 can assemble into heptameric rings. It also contains a PH-GRAM domain that allows its binding to PI3P, a PDZ domain and the catalytic domain (Lorenzo, Urbé and Clague, 2006). VPS34 and MTM1 regulate the availability of PI3P on endosomal membranes and therefore determine the recruitment of specialised machinery, often in synergy with rab GTPases. For instance, the tether EEA1 binds to both rab5 and PI3P to mediate fusion of EEs (Simonsen *et al.*, 1998). Also in EEs, PI3P contributes to rab11 recruitment, which in turns brings the PI3P phosphatase MTM1 to enable trafficking to the RE (Ketel *et al.*, 2016; Campa *et al.*, 2018).

1.3.3 Coats

Coats are protein complexes that bind cargo and specialised machinery in particular membrane domains in order to sort cargo and produce a transport intermediate. A list of coats and their components can be found in **Table 1.1**, and the localisation of coats in the different membrane trafficking pathways is in **Figure 1.6**. Coats work, together with their adaptors, as sorting platforms that accumulate a specific type of cargo to follow a particular pathway. The coats clathrin, caveolin, COPI and COPII also give rise to coated vesicles or tubules independent from the donor membrane. The most relevant coats in endosomal trafficking are described in more detail in the following sections.

Coat	Subcomplexes and subunits
Clathrin	CHC, CLC.
Caveolin	Caveolin, cavin.
COPI	Outer coat: α-COP, β'-COP, ε-COP. Inner coat: β-COP, δ-COP, γ-COP, ζ-COP.
COPII	Outer coat: sec13, sec31. Inner coat: sec23, sec24.
ESCRT	ESCRT-0: HRS, STAM1/2. ESCRT-I: TSG101, VPS28, VPS37A/B/C/D, MVB12A/B, UBAP1. ESCRT-II: EAP30, EAP20, EAP45. ESCRT-III: CHMP2A/B, CHMP6, CHMP3, CHMP4A/B/C, CHMP5, CHMP1A/B, V7, IST1. VPS4A/B, VTA. ALIX.
Retromer	VPS26, VPS29, VPS35.
Commander	Retriever: VPS26C, VPS29, VPS35L. CCC complex: CCDC93, CCDC22, COMMD.

Table 1.1. Composition of coats. Membrane traffic coats are listed together with the complexes and subunits that form them.

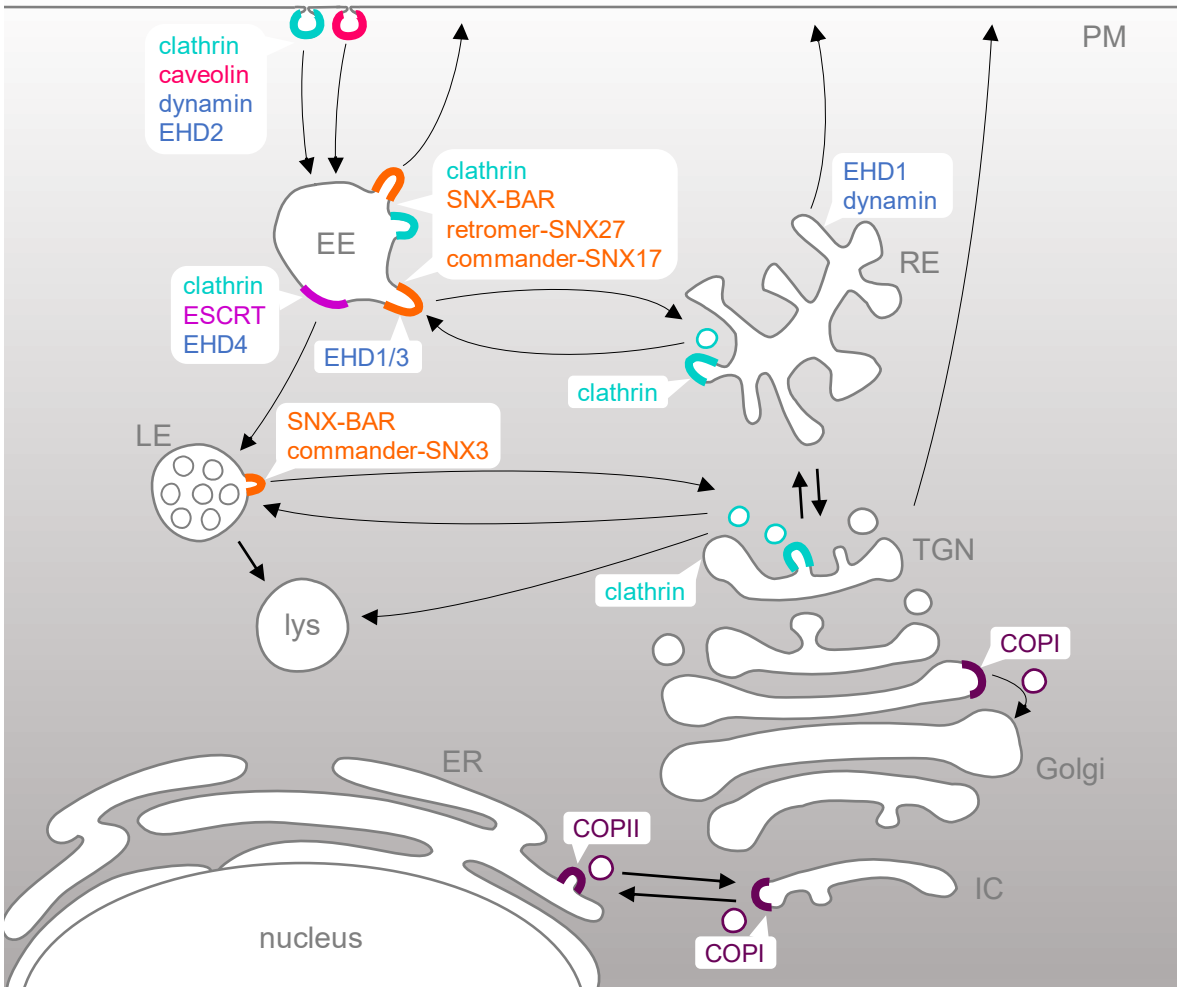

Figure 1.6. Coats and fission machinery in membrane trafficking. A model for the involvement of coats and the fission proteins dynamin and EHDs in membrane trafficking routes. Clathrin and caveolin are the two coats known to mediate endocytosis from the PM. The constricting proteins dynamin and EHD2 can mediate scission in CME. Different coats participate in sorting at the EE. Clathrin and ESCRT allow the formation of ILVs and maturation towards LE, a process aided by EHD4. Clathrin, BAR-containing SNX dimers, SNX27-associated retromer and SNX17-associated commander direct trafficking routes towards the PM, although it is not clear if these are direct routes or through the RE. Clathrin is the only coat reported in transport from the RE or the TGN to SEs or LEs. EHD1 and 3 form tubules in EEs for the recycling of cargo. EHD1 and dynamin are required for recycling from the RE. Retrograde transport along the Golgi or from the Golgi to the ER occurs in COPI-coated vesicles, whereas COPII-coated vesicles transport cargo from the ER.

1.3.3.1 The clathrin coat and its adaptors

Clathrin is an evolutionary-conserved complex formed by three heavy chains (CHC) and three light chains (CLC) assembled into a triskelion (Brodsky, 2012). The structure of the triskelion is achieved by the convergence of the three CHCs in a central vertex. Each CHC adopts a conformation in which a proximal leg, knee, distal leg, linker and terminal domain can be distinguished (**Figure 1.7B**; Fotin *et al.*, 2004). The triskelions that assemble into

lattices can drive the formation of CCVs from the PM, the TGN and the endosomes. Clathrin adaptors and regulators are found between the coat and the vesicle within (**Figure 1.7A**). In addition to curved lattices on vesicles, clathrin can form larger flat structures assembled at the PM or endosomes. The terminal domain of the CHC consists of a β-propeller and mediates most of the interactions with adaptors or regulatory proteins, many of which contain a peptide sequence termed the 'clathrin box' (Kirchhausen, Owen and Harrison, 2014).

The transport of cargo in CCVs requires the function of clathrin adaptors that link clathrin to cargo and often to lipids. Therefore, they are important for cargo selection at specific membrane domains. They are also thought to promote clathrin coat assembly and aid in the induction of curvature on the clathrin lattice (Lacy *et al.*, 2018). The best described clathrin adaptors are the AP family of heterotetramers (**Figure 1.8**). AP-1 functions in the delivery of cargo from endosomes and the TGN, as well as from EEs to REs and to the PM in recycling routes. AP-2 functions at the PM to deliver cargoes to EEs. AP-3, from EEs to lysosomes. Finally, AP-4 and AP-5 have been identified but they do not seem to work with clathrin (Sanger *et al.*, 2019). AP-1 and AP-2 are the best-known and the most relevant for this thesis. They are formed by two large subunits, α and β_1 in AP-1 and α and β_2 in AP-2, a medium μ subunit, and a small δ subunit. The C-terminus of the large subunits extends outside the core of the complex and form two appendages (ears) that are connected to the core by unstructured linkers (**Figure 1.7A**). These linkers contain various clathrin boxes that interact with the clathrin terminal domain. Several accessory and regulatory proteins bind to both the clathrin terminal domain and the AP ears.

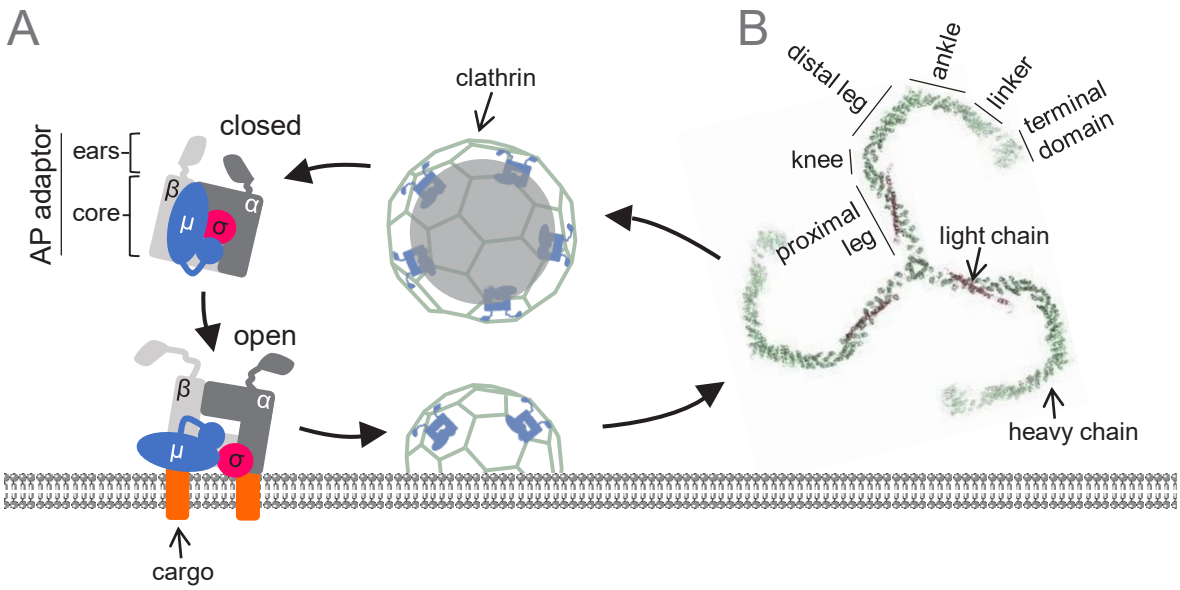

Figure 1.7. Structure of the clathrin coat and AP adaptors. A. AP-1 and AP-2 adaptors have α, β, μ and σ subunits assembled to form a core and two ears. Binding to transmembrane cargo induces an open conformation of the AP, which is now able to bind clathrin. Clathrin assembles into a lattice that surrounds the budding vesicle and the adaptors. **B.** Three clathrin heavy chains and three clathrin light chains assemble into a triskelion. The segments in each heavy chain are named.

Recruitment to membranes is in part due to the binding of the μ subunits to YXXØ endocytic motifs and of β subunits to LL endocytic motifs in the cytoplasmic tails of transmembrane cargoes (Ohno *et al.*, 1995; Doray *et al.*, 2007). However, organelle specificity is thought to be defined by PIP binding. AP-2 binds to $PI(4,5)P_2$ in the PM, whereas AP-1 binds to PI4P, which is enriched in Golgi and endosomal membranes (Gaidarov and Keen, 1999; Wang *et al.*, 2003). APs cycle between different conformations that correspond to different activity states. It has been shown that in the AP-2 closed conformation, clathrin-binding sites are hidden within the core, while in the open conformation they are exposed. AP-2 is activated by $PI(4,5)P_2$, and a similar mechanism is inferred for AP-1 activation upon PI4P binding. AP-1 is also known to be activated by the small GTPases arf1 and rab4b (Stamnes and Rothman, 1993; Perrin *et al.*, 2013; Beacham, Partlow and Hollopeter, 2019).

Another type of clathrin adaptors working at Golgi membranes and endosomes are monomeric GGA adaptors (Golgi-localised, γ-ear-containing, Arf-binding proteins; **Figure 1.8**). The structure of GGAs differs from that of the large AP subunits but they also have an appendage and a linker that contains clathrin-binding boxes. GGAs are well-established to mediate transport of membrane proteins from the TGN to endosomes (Puertollano *et al.*, 2001). However, they are also involved in sorting from endosomes. GGA3, in particular, is required to sort a number of cargoes from EEs to the PM and prevent their degradation (Puertollano and Bonifacino, 2004; Parachoniak *et al.*, 2011; Ratcliffe *et al.*, 2016). It is not clear whether these clathrin adaptors work together in the same pathways, but evidence in yeast shows that GGAs and AP-1 assemble sequentially on Golgi membranes as they mature (Daboussi, Costaguta and Payne, 2012; Uemura and Waguri, 2020).

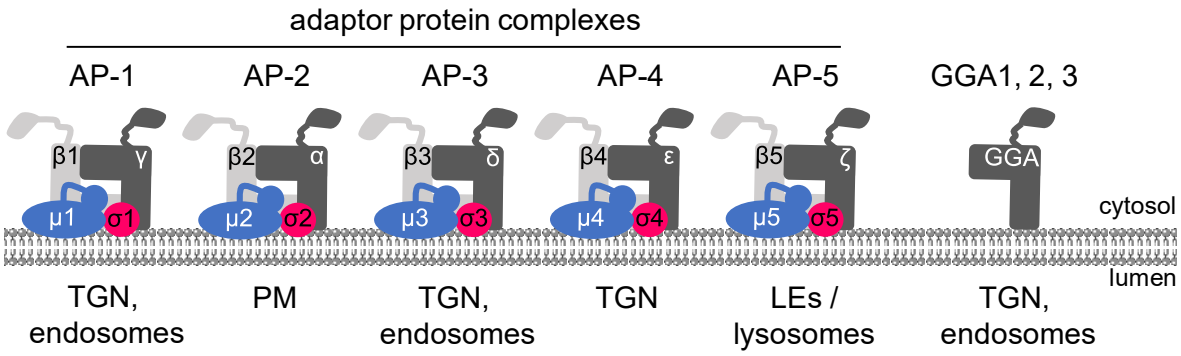

Figure 1.8. Clathrin adaptors. The subunits of the adaptor protein complexes and GGAs are shown. The organelles in which they function are listed underneath.

A number of co-adaptors have been identified for AP-2 at the PM (Robinson, 2004). They bind to the AP-2 ears, to clathrin, and to cargoes. Those include β-arrestins, which are involved in the endocytosis of GPCRs and dab2 (disabled-2), numb and ARH (Autosomal Recessive Hypercholesterolemia), which are involved in the endocytosis of LDL (Low

Density Lipoprotein) receptor and integrins. The only identified AP-1 co-adaptors are Eps15 (Epidermal growth factor receptor Substrate 15) and epsinR, which work in TGN to endosome transport of hydrolytic enzymes and SNARE components (Hirst *et al.*, 2004; Merrifield and Kaksonen, 2014; Wei *et al.*, 2014; Eichel and von Zastrow, 2018).

In addition to CCVs, clathrin can form large flat lattices on membranes (Sochacki and Taraska, 2019). These work as scaffolds for sorting cargo and recruitment of machinery or cytoskeletal components. The best known examples are clathrin plaques at the basal membrane of adherent cells. They form large, stable subdomains that can recruit cargo, such as TfnR or integrins. In fact, clathrin plaques are required for normal integrin uptake. As with the internalisation of CCVs, the internalisation of plaques depends on AP-2, numb, dab2 and on the polymerisation of actin through N-WASP (see section 1.3.7.3). The mechanistic details are, however, not known. Other functions of clathrin flat lattices involve their association to the cytoskeleton. They associate to adherens junctions and are required for their maturation, including the recruitment of cytoskeletal proteins (see section 1.5.1; Bonazzi *et al.*, 2012). Clathrin can also work as an endosomal recruitment platform. This is well described during the formation of ILVs by the ESCRT machinery (see section 1.3.3.2; Sachse *et al.*, 2002). This might also be the case in retromer-dependent retrograde traffic, in which clathrin is known to participate (see section 1.3.3.3; Popoff *et al.*, 2009; McGough and Cullen, 2013).

1.3.3.2 ESCRT machinery

ESCRT (Endosomal Sorting Complex Required for Transport) mediates the formation of ILVs, which accumulate as EEs mature into MultiVesicular Bodies (MVBs) or LEs. Therefore, ESCRT is essential for the sorting of membrane associated-cargoes destined for degradation. These cargoes are most often ubiquitinated and recognised by ESCRT-0, specifically by its hrs subunit. ESCRT-0 also recruits clathrin, which forms lattices in specific endosomal subdomains. The activation of ESCRT-0 leads to the recruitment of one of two possible core ESCRT machinery: ESCRT-I, -II, -III and VPS4, on one branch; or ALIX, ESCRT-III and VPS4 on the alternative branch (**Figure 1.9**). These complexes function in a sequential manner (Wenzel *et al.*, 2018). ESCRT-III subunits assemble into filaments that form variable structures like flat spirals, helices or cones (Schöneberg *et al.*, 2017). The disassembly of the ESCRT is prompted by the ATPase VPS4, which together with ESCRT-III generates the force for scission (Schöneberg *et al.*, 2018). The ESCRT-III complex can also mediate fission or fusion of membranes in many other cellular processes, such as nuclear envelope sealing after mitosis, virus budding, PM repair, or sealing of the PM after cytokinesis. These ESCRT-dependent processes share the characteristic inverted topology, in which the vesicle is liberated towards the concave side of the donor membrane (Gatta and Carlton, 2019).

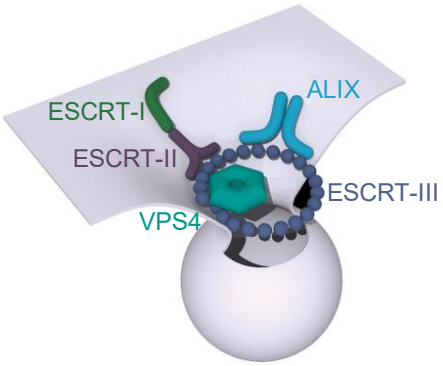

Figure 1.9. ESCRT machinery. A model of the arrangement of the ESCRT machinery is represented in a budding membrane. ESCRT-I and ESCRT-II, or ALIX, recognise ubiquitinated cargo and induce membrane budding. They also recruit ESCRT-III, which forms a spiral for constriction of the budding neck. The final scission is prompted by VPS4. Adapted from Hurley (2015).

1.3.3.3 Retromer, commander and sorting-nexins

The retromer complex promotes the formation of endosomal-derived tubular transport intermediates, which deliver protein cargoes to the TGN or the PM, thereby avoid their degradation (Burd and Cullen, 2016; Lucas and Hierro, 2017). It is composed of a core trimer of VPS26, VPS29 and VPS35, which is always bound to a SNX (Sorting NeXin) dimer (**Figure 1.10**). Six of the total 33 SNXs in mammalian cells are known to interact with the retromer: SNX1, SNX2, SNX3, SNX5, SNX6 and SNX27. All SNXs have a PX domain that binds PI3P or PI(3,5)P_2. In addition, SNX1, 2, 5 and 6 contain a BAR (Bin/Amphiphysin/RVS) domain that senses membrane curvature and SNX27 has a FERM domain, which binds additional PIPs and proteins, and a PDZ domain for protein-protein interactions. The recruitment of retromer to endosomal membranes is partly mediated by GTP-rab7 (Balderhaar *et al.*, 2010). SNXs can modify membrane curvature and their activity is amplified by their association to retromer (Purushothaman and Ungermann, 2018). SNXs can also work as cargo adaptors for the retromer (Simonetti *et al.*, 2017). Thus, different SNXs associate with the retromer, depending on the pathway (Lucas *et al.*, 2016). Once the cargo is recognised at the membrane, the retromer complex oligomerises to form a coat-like structure (Kovtun *et al.*, 2018; Kendall *et al.*, 2020). Finally, there is a strong interaction between the retromer and the activator of endosomal actin polymerisation WASH (Lee, Chang and Blackstone, 2016). Overall, the retromer complex directs the assembly of curvature-inducing proteins and provides a scaffold for regulatory proteins in order to regulate endosomal tubule formation.

A complex that is structurally-related to retromer has recently been discovered to function at endosomes in the recycling of specific cargoes to the PM. It is called retriever and it works in conjunction with the CCC complex, forming a supercomplex named commander (Mallam and Marcotte, 2017; McNally *et al.*, 2017). Retriever shares the VPS29 subunit with

retromer. It contains another two subunits that are structurally similar to VPS26 and VPS35 and thus have been renamed VPS26C and VPS35L. The retriever complex associates with SNX17, a FERM domain-containing SNX (**Figure 1.10**; McNally *et al.*, 2017).

The CCC complex is formed by CCDC93, CCDC22 and COMMD proteins. In humans, there are ten isoforms of COMMD proteins and several of them are thought to exist in complex with retriever. However, exactly which of them or the stoichiometry of the complex are not known (Chen, Healy and Collins, 2019). The role of the CCC complex within commander is not exactly understood. It is known that it maintains endosomal PI3P levels and that this role is required for the correct recycling of $\alpha_5\beta_1$ (Singla *et al.*, 2019). Importantly, the function of commander, as well as that of the retromer, depends on its association with the WASH complex, which occurs through the fam21 subunit of WASH. Of note, the CCC complex is also implicated in the recycling of retriever-independent, retromer-dependent cargoes, as it has been shown for GLUT1 (Singla *et al.*, 2019). An integrative vision of ESCRT, retromer, commander and the WASH complexes is shown in **Figure 1.20**.

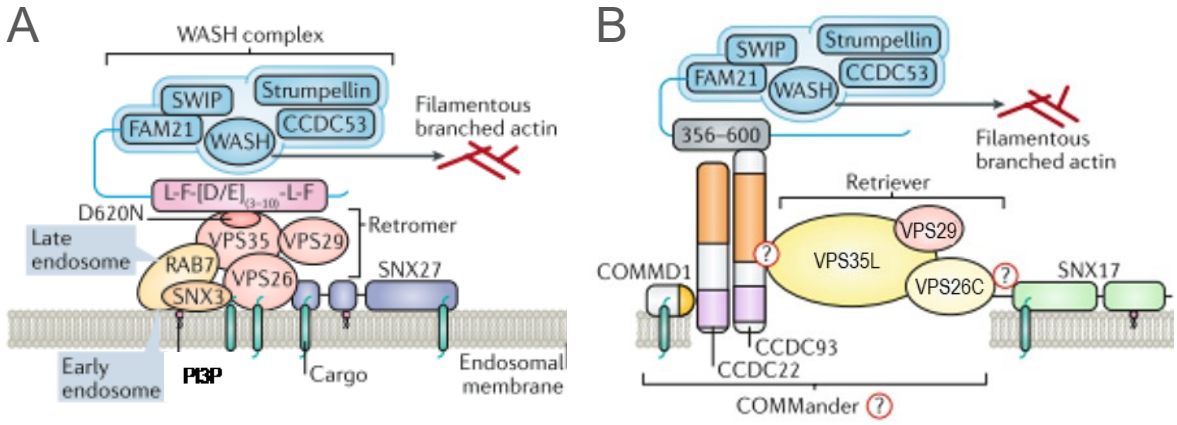

Figure 1.10. Composition of the retromer and retriever complexes and their interactions with endosomal membranes and the WASH complex. A. The retromer complex, formed by VPS35, VPS29 and VPS26, is depicted in association to SNX27. It is bound to an endosomal membrane through its interaction with the cargo, with PI3P through SNX3 and with rab7. A specific motif in VPS35 recognises the fam21 tail and links the retromer with the WASH complex, which in turn promotes actin polymerisation. **B.** The retriever complex, composed by VPS35L, VPS29 and VPS26C, forms commander in association with the CCC complex, composed by COMMD1, CCDC22 and CCDC93. SNX17 interacts with retriever and with cargo and PI3P at the endosomal membrane. CCDC93 interacts with the WASH complex, which in turn induces actin polymerisation. Adapted from Cullen and Steinberg (2018).

1.3.4 Membrane fission machinery

In order to produce an autonomous vesicle or tubule there must be a scission from the donor membrane. According to the most accepted model, there is a hemifission intermediate in which the proximal membrane has coalesced, but not the distal one. Proteins that mediate fission are diverse but they all have lipid-binding domains and tend to form oligomers (Renard, Johannes and Morsomme, 2018). A common mechanism for inducing curvature is the reorganisation of lipids by the insertion of an amphipathic helix of proteins like endophilins, amphyphisins, epsins or the small GTPases sar1 and arf1. The insertion enhances the membrane curvature and prompts fission (Yorimitsu, Sato and Takeuchi, 2014; Zhukovsky *et al.*, 2019). A passive mechanism of fission is the formation of lipid domains and thus of unfavourable lipid domain boundaries that induce tension. A similar effect has been proposed for protein crowding (Renard, Johannes and Morsomme, 2018).

Other fission processes involve membrane-constricting proteins, such as the dynamin superfamily of GTPases or the ESCRT machinery, in the case of inverted topology. The localisation of these proteins in the endosomal and secretory systems is shown in **Figure 1.6**. Other proteins, such as endophilins, use their curvature-sensing BAR domains to induce friction in the membrane. Microtubule-dependent motors can generate tension on the membrane invagination. A mechanism has been shown by which endophilin-A2 creates a scaffold in the neck as the microtubule motor dynein pulls the membrane until it 'breaks' (Simunovic *et al.*, 2017). Finally, the actin cytoskeleton is also important in many fission contexts, as actin polymerisation itself can exert forces that produce tension or compression to aid scission. At the tubule or vesicle neck, the activators of actin polymerisation are often recruited by F-BAR domain-containing proteins that recognize highly curved membranes (Gautreau, Oguievetskaia and Ungermann, 2014). The actin-associated motor myosin-1b can also form tubules from endosomes (Yamada *et al.*, 2014). The best-known fission machinery is that of dynamin. It oligomerises into helices around the neck of the budding vesicle, constricts it and eventually hydrolyses GTP to exert fission. Different models have been proposed for the last step but none of them have been demonstrated to prevail so far. It is known, however, that the GTPase activity is enhanced by the binding of PI4P or PI(4,5)P_2 to the PH domain. Moreover, the PH domain contains a loop that inserts in the membrane and is required for scission. A certain degree of membrane tension is also required (Antonny *et al.*, 2016; Ford and Chappie, 2019).

1.3.4.1 EHD proteins

EHDs (Eps15-Homology Domain-containing proteins) are tubulating and fission-promoting proteins that are sometimes included in the dynamin family. They have an N-terminal domain that is structurally similar to the GTPase domain of dynamin. However, it hydrolyses ATP, and its activity is lower than that of dynamin. The catalytic domain of EHDs also mediates oligomerization, allowing the formation of ring-like structures on membranes. Next to the

catalytic domain there is a helical domain and a EH domain. The EH domain interacts with PIPs and with NPF motifs in proteins. Interestingly, it binds to the catalytic domain in an autoinhibited conformation. Upon binding to membranes, the helical domain is inserted in the lipid bilayer and the autoinhibition is released. Activated EHDs exhibit a tighter membrane binding and oligomerisation (Daumke *et al.*, 2007; Shah *et al.*, 2014).

EHDs bend membranes and induce curvature to either tubulate endosomes or cause scission of transport intermediates. There are four isoforms in mammals. EHD1 promotes tubule or vesicle fission at EEs and REs during slow recycling. EHD3, on the other hand, is thought to rather stabilise tubules at EEs. Also at EE functions EHD4, probably to allow trafficking towards the degradation pathway. Finally, EHD2 is involved in internalisation of caveolae at the PM (**Figure 1.6**; Naslavsky and Caplan, 2011).

1.3.5 Tethers

Tethers are proteins or protein complexes that interact with rab GTPases, act as a bridge between membranes, and prime these for SNARE-mediated fusion. The localisation of tethers and SNAREs in the endosomal and secretory pathways is shown in **Figure 1.11**. There are two types of tethers: long coiled-coil proteins (Gillingham and Munro, 2003) and multisubunit tethers (van der Beek *et al.*, 2019). Coiled-coil tethering proteins are rab effectors that extend from the target organelle and fish another fusion-compatible organelle or transport intermediate. An example of this kind of tethers is EEA1, which is explained in detail in the next section. More recently, the coiled-coil TANGO1 has been described to recruit ERGIC membranes to specific patches of the ER (Santos *et al.*, 2015). However, the best known long-coiled coil tethering proteins are the golgins. Golgins localise at Golgi membranes to tether vesicles or cisterna through their N-terminal domains (Muschalik and Munro, 2018).

Most multimeric tethering complexes contain at least a rab binding site and a SNARE binding site. These complexes can be subdivided according to their structure in class C VPS complexes and CATCHR (Lürick, Kümmel and Ungermann, 2018). Class C VPS complexes are conserved and predicted to contain an N-terminal β-propeller and a C-terminal α-helical solenoid. They include CORVET, HOPS and CHEVI (van der Beek *et al.*, 2019). A more recently described class C tether of EEs is FERARI (Solinger *et al.*, 2020). Another family of multimeric tethers is the CATCHR group. These fold into a rod-shaped structure formed by a stack of helical bundles (Ungermann and Kümmel, 2019). It includes GARP, EARP, dsl1, COG, TRAPPII, TRAPIII and the exocyst (Spang, 2012; Rosa-Ferreira *et al.*, 2015; Schindler *et al.*, 2015; Kim, Lipatova and Segev, 2016; Blackburn, D'Souza and Lupashin, 2019). In the mammalian exocyst, eight subunits are divided into two subcomplexes that bind the vesicle independently. Once at the acceptor membrane, the whole complex 'clicks' together through the four conserved α-helices found in each subunit (Picco *et al.*, 2017; Ahmed *et al.*, 2018).

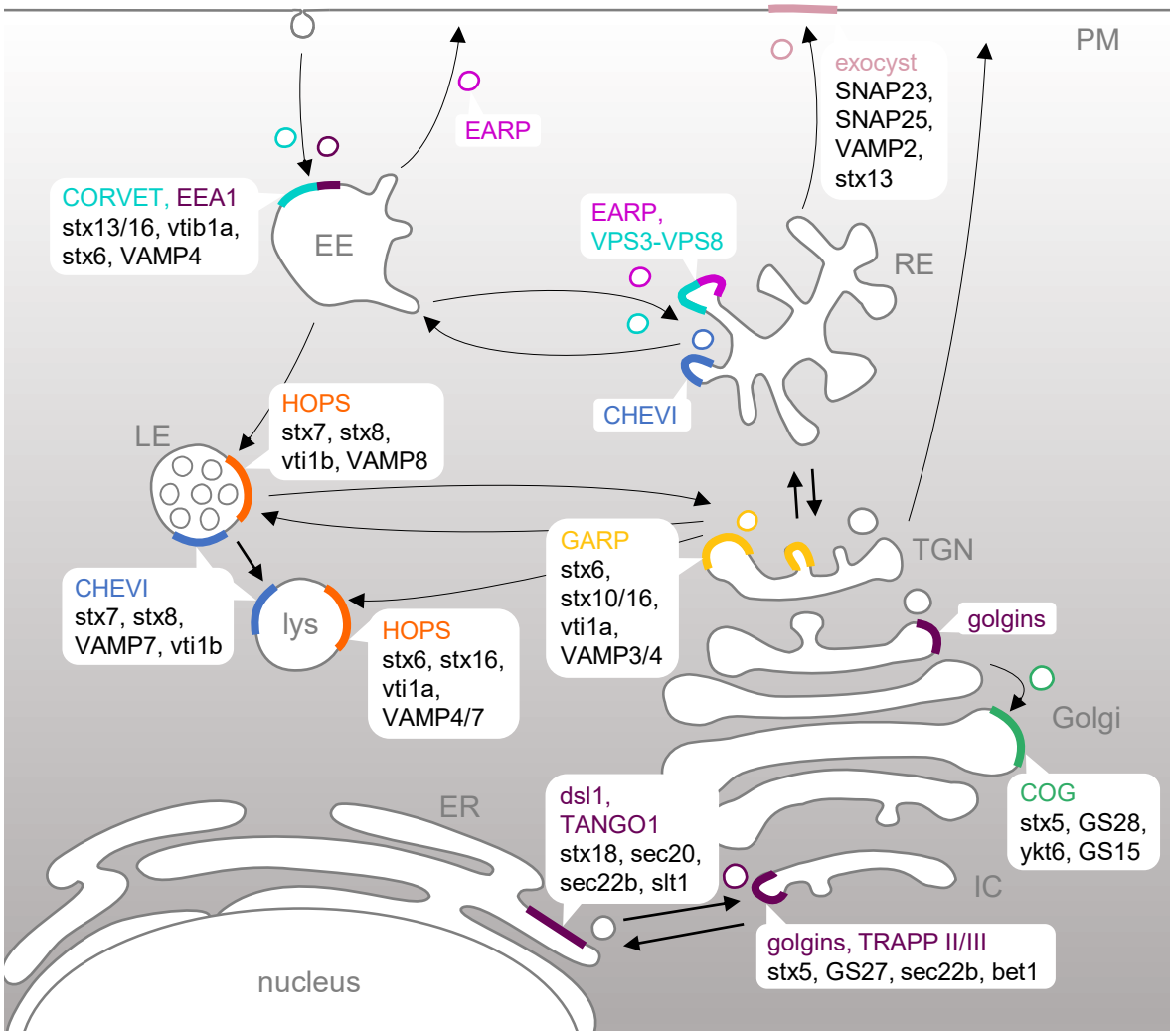

Figure 1.11. Tethers and SNAREs in membrane trafficking. A model for the localisation of tethers and SNAREs in fusion events throughout the endosomal and secretory systems. EE membranes contain CORVET and EEA1 for homotypic fusion and fusion of incoming vesicles. CORVET is substituted by HOPS as endosomes mature to LEs and lysosomes, which use CHEVI to fuse with each other. Recycling through the RE can depend on EARP, as well as on the CORVET subunits VPS3 and VPS8, and on CHEVI. Fusion of vesicles with the TGN requires GARP, and transport between Golgi stacks, COG. Golgins fulfil tethering functions along the whole Golgi apparatus. Dsl1 and TANGO1 tether incoming vesicles at the ER, and TRAPPII and III at the IC. The SNAREs responsible for the fusion of membranes in the different organelles are shown in black.

1.3.5.1 EEA1

EEA1 is a dimer that brings endocytic vesicles and EEs together for fusion (Mills, Jones and Clague, 1998; Rubino *et al.*, 2000). In particular, EEA1 allows the fusion of rab5-containing vesicles with PI3P-containing membranes (Simonsen *et al.*, 1998). It has a C-terminal FYVE domain that interacts with PI3P with high affinity and a Zn^{2+}-finger in its N-terminus that interacts with GTP-rab5 with lower affinity. Both domains are linked by a long coiled-coil

region that mediates homodimerisation. The length of this coiled-coil impedes binding of rab5 and PI3P on the same membrane. Its interesting molecular mechanism of action has been elucidated. In the absence of GTP-rab5, EEA1 has a stiff conformation and extends approximately 200 nm from PI3P-containing vesicles. Upon binding to GTP-rab5, the coiled-coil becomes flexible and changes into a more stable compact conformation. This entropic collapse generates a force that is used to pull both membranes together (Murray *et al.*, 2016).

1.3.6 Membrane fusion machinery: SNARE complexes

Once the membranes from the fusing organelles have been targeted towards each other, the SNAREs bring them into direct contact (**Figure 1.11**). First, SNARE proteins recognise their complementary SNAREs in the opposing membrane, then they interact to form a *trans*-SNARE complex that brings the membranes into such close proximity that the fusion is promoted. The *trans*-SNARE complex is formed by four SNAREs, of which at least one belongs to each of the fusing membranes. They oligomerise through the coiled-coils SNARE motifs. The hydrophobic residues interact, leaving a 'zero layer' zone with the negatively-charged residues. These are three glutamines from the three so-called Q-SNAREs and one arginine from the R-SNARE. SM family proteins work as chaperones for the assembly of the complex (Ungermann and Kümmel, 2019). Additional proteins are recruited to the fusion site, like Sec17/SNAP and Sec18/NSF. Sec17/SNAP binds the *trans*-SNARE complex and inserts its hydrophobic N-terminal loops into the bilayer to induce reorganisation of the lipids that leads to fusion. Then, SEC17/SNAP and Sec18/NSF hydrolyse ATP to disassemble the resulting *cis*-SNARE complex (Wickner and Rizo, 2017). Tethers and SNAREs work synergistically to produce fusion (Ungermann and Kümmel, 2019).

1.3.7 Actin in membrane traffic

Actin is one of the most abundant proteins in eukaryotic cells. In vertebrates there are three main isoforms. α-Actin is present in muscle cells and is essential for their contraction, β-actin works at the leading edge of most cell types, and γ-actin is mainly associated to stress fibres, also in most cell types (Dugina *et al.*, 2009). Actin forms fibres and networks that govern numerous functions in the cell. It participates in whole-cell motility, cell-cell adhesions, cell shape, muscle contraction and, most importantly for this thesis, intracellular transport (Bachir *et al.*, 2017; Svitkina, 2018; Titus, 2018). Actin filaments can work as tracks for the transport of vesicles and other cargoes throughout the cytoplasm, generally for short distance movements close to the cortex or the membranes of intracellular organelles. Key mediators of this type of movement are the myosins, actin-dependent molecular motors that convert the hydrolysis of ATP into mechanical force. Actin polymerisation can also be used as a propeller force for vesicles and tubules, via the formation of the so-called actin tails, and as a bending force to assist membrane budding and fission.

Actin filaments organise into two kinds of higher-order structures: bundles and networks. Actin bundles are formed by parallel actin filaments and give rise to projections from the PM, such as microvilli and filopodia, and also to contractile structures like the mitotic ring and stress fibres. They serve as tracks for the processive myosin movement. Stress fibres are large actin bundles connected to contact sites with the extracellular matrix (Bartles, 2000). Actin bundles are normally induced by formins or spire-like actin nucleators (see section 1.3.7.2). Actin filaments can also organise into 3D branched arrays with a semi-gel consistency. These actin networks are known to form cortical actin in the inner surface of the PM, to form lamellipodia in the leading edge and to work at membrane reshaping during vesicle formation and fission (Alekhina, Burstein and Billadeau, 2017). This kind of actin structures can also form membrane subdomains that may act as cargo sorting platforms. Actin networks require the function of the Arp2/3 complex actin nucleator. The principles controlling actin polymerisation and myosin function in the context of membrane traffic are described below.

1.3.7.1 Actin structure and dynamics

The actin monomer is a 43 kDa globular protein with an ATP-binding site that determines its affinity for other actin molecules (Kabsch *et al.*, 1990). Each filament is a right-handed helix composed by two strands. Since monomers are asymmetric, filaments have an intrinsic polarity, with a barbed or plus end, and a pointed or minus end (Huxley, 1963). The polymerisation process can be divided in three phases: nucleation, elongation and steady-state (Nosworthy *et al.*, 2003). Actin nucleation is the process by which three ATP-bound monomers associate to conform a ‘seed’ that will further polymerise. Since nucleation is energetically unfavourable, specialised proteins called actin nucleators are required to overcome the energy barrier to initiate polymerisation (Sugino and Hatano, 1982; Pollard and Borisy, 2003). Once the ‘seed’ is formed, ATP-bound monomers are continuously added to both ends to elongate the filament. After ATP hydrolysis, the resulting ADP-actin has less affinity for the adjacent subunit and is therefore more likely to detach (Pollard, 1986). The monomer in the cytoplasm has its ADP exchanged for ATP and is ready to join a new filament. In dynamic equilibrium state, called treadmilling, there is a turnover of monomers but the length of the filament is maintained (Wegner, 1976; Fujiwara, Vavylonis and Pollard, 2007).

Actin polymerisation and depolymerisation are tightly regulated to give rise to numerous structures that can be rapidly remodelled. This regulation is carried out by a subset of actin-binding proteins with actin monomer sequestering, actin nucleating, actin capping and/or actin severing activities (**Table 1.2**). Once synthesized, the actin filaments can be arranged into different structures by actin crosslinking proteins and a number of adaptors that link actin to cellular structures, mostly cellular membranes (**Figure 1.12**; Pollard, 2016). From all these proteins, those initiating actin polymerisation at particular locations, the

actin nucleators, are the ones that mostly define the nature of the emerging structure and therefore they will be discussed in more detail.

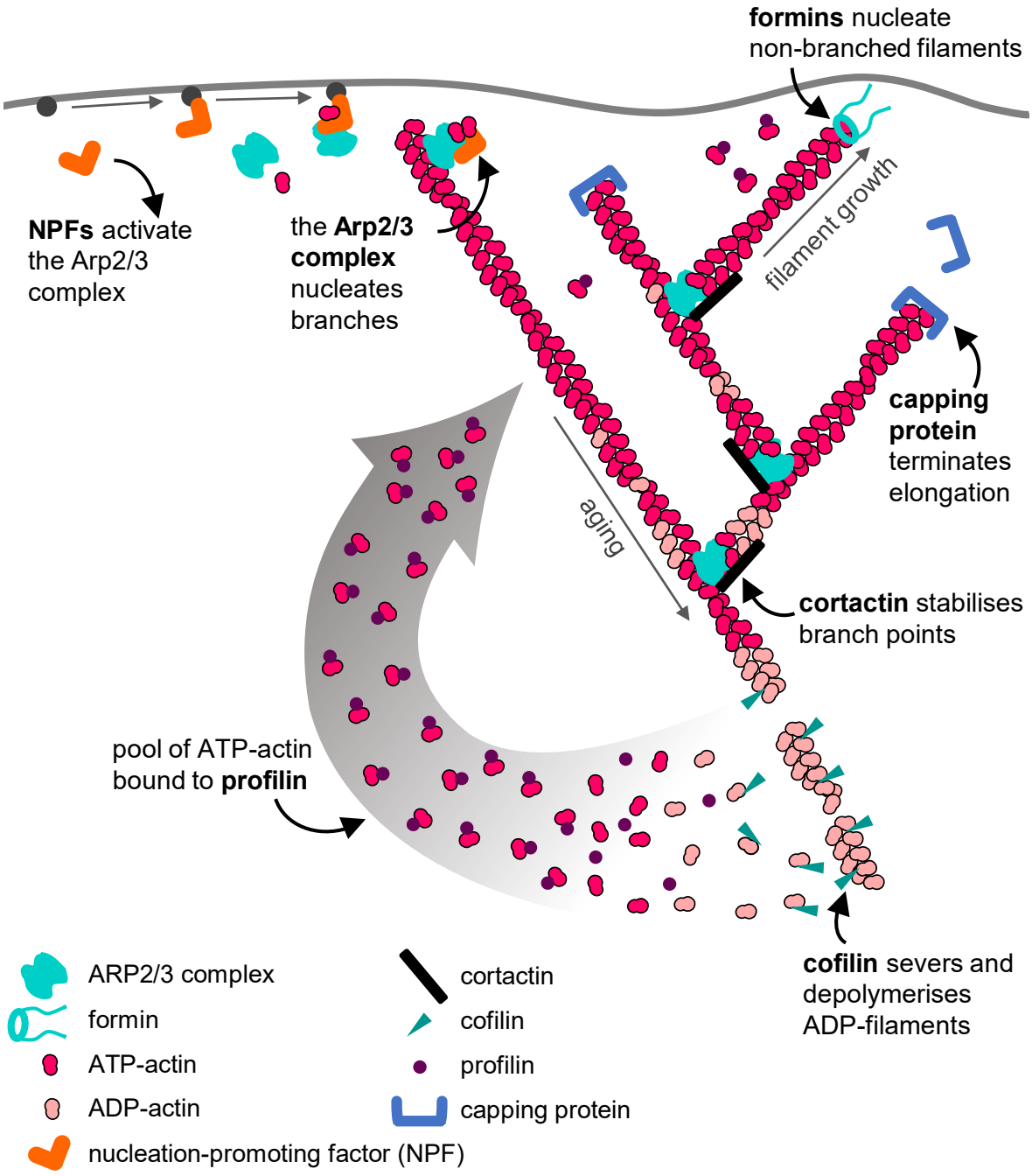

Figure 1.12. Actin polymerisation regulation by actin-binding proteins. The function of some actin binding proteins are depicted to illustrate actin polymerisation regulation. Actin polymerisation is nucleated by formins and spire proteins for linear filaments and by the Arp2/3 complex for branched networks. The latter is activated by nucleation-promoting factors (type I NPFs) that are recruited to the membrane. The resulting branching points are stabilised by type II NPFs such as cortactin. New actin monomers are added in the ATP-bound form, but as the filament grows, the ATP is hydrolysed, leaving an ADP-enriched filament. Capping protein restrics filament growth. Severing by cofilin fragments ADP-actin filaments and causes depolymerisation. Free actin monomers bind profilin, which promotes nucleotide exchange and inhibits their nucleation. Adapted from Svitkina (2018) and Pollard and Cooper (2009).

ABP	Function
Profilin	Monomer sequestering, nucleotide exchange catalysis, recruitment of elongation factors.
Thymosin-β4	Monomer sequestering.
Cofilin	Severing, nucleotide exchange inhibition.
Gelsolin	Severing, capping.
Arp2/3 complex	Branched filament nucleation.
Formins	Unbranched filament nucleation, filament elongation.
Spire	Unbranched filament nucleation.
Ena/VASP	Filament elongation, uncapping.
Capping protein	Capping.
Tropomodulin	Capping.
Fimbrin	Filament cross-linking to form bundles.
Fascin	Filament cross-linking to form bundles.
Filamin	Filament cross-linking to form networks.
Tropomyosin	Filament stabilisation, myosin adaptor.

Table 1.2. Actin binding proteins. The main actin binding proteins (ABPs) and their main functions are listed.

1.3.7.2 Actin nucleators

Three types of actin nucleators can be found in metazoans: the Arp2/3 complex, formins and spire-like proteins (**Table 1.2**). Formins stabilise actin dimers by wrapping themselves closely around it. The polymerisation-promoting activity of formins allows for rapid growth of the nucleated filament (**Figure 1.12**). Spire and related proteins like cordon blue connect three monomers in a longitudinal manner and stay at the minus end, preventing depolymerisation. Both formins and spire nucleate linear, unbranched actin networks (Pollard, 2016).

The Arp2/3 complex is composed of seven subunits: the actin-related proteins Arp2 and Arp3 and the actin-related complex proteins Arpc1/p41, Arpc2/p34, Arpc3/p21, Arpc4/p20 and Arpc5/p16 (Robinson *et al.*, 2001). Arp2 and Arp3 have a sequence and a structure similar to actin (Lees-Miller, Henry and Helfman, 1992; Schwob and Martin, 1992). This similarity allows them to mimic an actin dimer that would work as the initiating seed of a new filament. The prevailing model suggests that Arpc2 and Arpc4 bind a previously existing filament, and Arp2 and Arp3 conform the minus end of the daughter filament (Beltzner and Pollard, 2004; Rouiller *et al.*, 2008). The Arp2/3 complex remains at the branching point and caps the minus end of the daughter filament, which continues to grow from the more dynamic plus end. The result is a branched actin network (**Figure 1.13A**; Mullins *et al.*, 1998; Svitkina and Borisy, 1999).

The Arp2/3 complex is an inefficient nucleator and needs activation by the so-called nucleation-promoting factors (NPFs; **Figure 1.12**; Zimmet *et al.*, 2020). A number of NPFs work on specific cell structures and fine-tune Arp2/3-dependent actin polymerisation (Campellone and Welch, 2010). There are two types of NPFs. Type I NPFs contain a WCA domain that binds the Arp2/3 complex and monomeric actin to promote nucleation. In mammals, these is the WASP (Wiscott-Aldrich Syndrome Protein) superfamily (**Figure 1.13B**). Type II NPFs bind the Arp2/3 complex and F-actin and stabilise the branching point. The main type II NPF in mammals is cortactin (Campellone and Welch, 2010).

WASP superfamily proteins vary in their N-terminal regions but they all share a highly conserved WCA domain in their C-terminus (**Figure 1.13B**). This domain is composed of one or more WH2 (WASP-Homology 2) motif that binds actin monomers, a Connector (C) peptide that binds actin and Arp2, and an Acidic (A) peptide that also binds the Arp2/3 complex. Within the acidic peptide is a conserved tryptophan. The CA sequence binds to the Arp2/3 and brings Arp2 and Arp3 to the right conformation to allow nucleation (Goley *et al.*, 2004; Kreishman-Deitrick *et al.*, 2005). The WH2 motif recruits actin monomers that become available to bind the barbed ends of Arp2 and Arp3 and initiate the new filament (Hertzog *et al.*, 2004). The best characterised NPFs are WASP or the more ubiquitous N-WASP (Neural-WASP). Other type I NPFs are WAVE (WASP and VErprolin homolog), WASH (WASP and Scar Homolog), WHAMM (WASP Homolog associated with Actin, Membranes and Microtubules) and JMY (Junction-Mediating and regulatorY protein; Kollmar, Lbik and Enge, 2012). Of those, N-WASP, WASH and WHAMM have prominent and direct functions in membrane traffic and have been implicated in membrane budding and/or fission of transport intermediates from the PM, the endosomes and the ER, respectively. N-WASP, WASH and cortactin are the most relevant NPFs for this thesis and will be discussed in more detail.

1.3.7.3 N-WASP

N-WASP contains, from N- to C-terminus, the following domains: WH1 (WASP homology 1), B (Basic), GBD (GTPase-Binding Domain), PRD (Proline-Rich Domain), and a WCA domain with two WH2 (**Figure 1.13B**). The activity of N-WASP is autoinhibited, as the GBD interacts with the C and A components of the WCA in the closed, inactive conformation (Campellone and Welch, 2010). Several mechanisms act in combination to drive N-WASP activation. The WH1 of the inactive N-WASP is bound to WIP (WASP Interacting Protein). WIP detaches from this domain for the activation of N-WASP, but remains bound to the WCA domain, presumably assisting in the function (Fried *et al.*, 2014). In addition, PIPs and GTPases bind to the N-terminal part in order to decrease its affinity for the WCA and activate the protein. $PI(4,5)P_2$ binds to the B domain and cdc42 to the GBD (Higgs and Pollard, 2000; Rohatgi, Ho and Kirschner, 2000). The PRD attracts SH3 domain-containing proteins that also promote an open conformation of N-WASP and work as recruiting platforms for other actin-binding proteins (Stradal *et al.*, 2004). Membrane curvature has also been shown to

impact N-WASP dependent polymerisation (Daste *et al.*, 2017). Finally, tyrosine kinases are known to phosphorylate the GBD that in turn would recruit SH2 domain-contaning proteins that work as recruiting platforms, such as Grb2 and Nck (Carlier *et al.*, 2000; Rivera *et al.*, 2004).

There are many cellular functions that require N-WASP (**Figure 1.13C**). N-WASP promotes protrusion of the PM in different situations, such as the formation of filopodia and ruffling (Miki *et al.*, 1998; Gryaznova *et al.*, 2018) or podosomes (Linder *et al.*, 1999). This capacity to induce PM protrusions is also used in phagocytosis (Dart *et al.*, 2012). On the other hand, N-WASP-induced actin polymerisation is important for PM invagination and fission in CME (see section 1.4.1; Girao, Geli and Idrissi, 2008). In addition, it has been implicated in exocytosis (Tran *et al.*, 2015). In the cytoplasm, N-WASP is found on EEs and might be of importance in sorting and fission (Taunton *et al.*, 2000; Bu *et al.*, 2010; Tanabe *et al.*, 2011). It also has a clear role in the formation of actin tails for the motility of endosomes (Taunton *et al.*, 2000; Benesch *et al.*, 2002). Finally, WASP has a nuclear role in gene transcription that is independent of its WCA domain (Sadhukhan *et al.*, 2014).

1.3.7.4 WASH

As opposed to N-WASP, the NPF WASH is not autoinhibited. Similar to N-WASP, WASH has a polyproline-rich region and a WCA domain in the C-terminus. The N-terminus is composed of a WASH-Homology Domain (WHD1) and a tubulin-binding region (TBR; **Figure 1.13B**). WASH works as a complex that requires all seven subunits to maintain its stability. These subunits are: WASH, KIAA1033, fam21 (also called VPEF or KIAA0592), ccdc53, strumpellin and the capping protein subunits capZ α and β (Derivery *et al.*, 2009). The regulatory mechanisms that change the spatial conformation of the WASH complex to control its activation are largely unknown. However, some studies have proposed activation mechanisms of the WASH complex by rho (Liu *et al.*, 2009), the lipid kinase phosphatidylinositol-4-kinase type IIα (PI4KIIα; Ryder *et al.*, 2013) or ubiquitination (Hao *et al.*, 2013).

The WASH complex is known to localise at endosomes (**Figure 1.13C**), where it influences their shape and sorting function (Derivery *et al.*, 2009; T. S. Gomez and Billadeau, 2009; Monteiro *et al.*, 2013) Interestingly, these functions might be mediated by the interaction of WASH with tubulin, as it has been demonstrated for the exocytosis of a metalloprotease in cancer invasion (Marchesin *et al.*, 2015). Also linking WASH to the tubulin cytoskeleton is the fact that WASH is implicated in the nucleation of centrosomal actin (Farina *et al.*, 2016). Finally, there is a balance between cortical actin and endosomal actin that seems to be maintained by WASH during epithelial tube formation (Tsarouhas *et al.*, 2019).

1.3.7.5 Cortactin

As mentioned above, cortactin is a class II NPF that can activate Arp2/3-dependent actin branching (Uruno *et al.*, 2001; Weaver *et al.*, 2001). The binding to the Arp2/3 complex occurs in this case through an N-terminal acidic region. This region is followed by a series of repeats for actin filament-binding, a PRD and an SH3 domain (**Figure 1.13B**; Uruno *et al.*, 2001). Cortactin is regulated by tyrosine kinases that bind to the SH3 domain and also by several post-translational modifications (Schnoor, Stradal and Rottner, 2017). The acidic and the actin filament-binding domains are required for cortactin localisation. Accordingly, cortactin is found at branched actin structures such as those associated with lamellipodia, endosomes, cell-cell and cell-matrix contacts and invadopodia (Kaksonen, Peng and Rauvala, 2000), although it also has Arp2/3-independent functions (Schnoor, Stradal and Rottner, 2017). Interestingly, $PI(3,5)P_2$ competes with actin for cortactin binding and thus promotes detachment of cortactin from late endosomal membranes (Hong, Qi and Weaver, 2015). Importantly, the efficiency by which cortactin activates the Arp2/3 complex is less than that of class I NPFs. In fact, it is not essential for the formation of branched actin structures and rather seems to increase their stability. There is a synergy between cortactin and class I NPFs, although the interplay between them varies (Helgeson and Nolen, 2013). For example, cortactin seems to work downstream of N-WASP and displace it, but to rather work upstream of WAVE (Siton *et al.*, 2011; Han *et al.*, 2014).

Cortactin is key to the formation of lamellipodia and invadopodia and therefore for cell directional migration and invasion (Bryce *et al.*, 2005; Kowalski *et al.*, 2005; Mader *et al.*, 2011). It is also involved in membrane trafficking events, such as CME (Merrifield, Perrais and Zenisek, 2005), exocytosis (González-Jamett *et al.*, 2017), LE maturation (Kirkbride *et al.*, 2012), and transport from the Golgi (Cao *et al.*, 2005). Furthermore, cortactin is required for sorting at EEs, in particular for the establishment of endosomal subdomains that allow sequence-dependent recycling (Puthenveedu *et al.*, 2010; Ohashi *et al.*, 2011; Tanabe *et al.*, 2011).

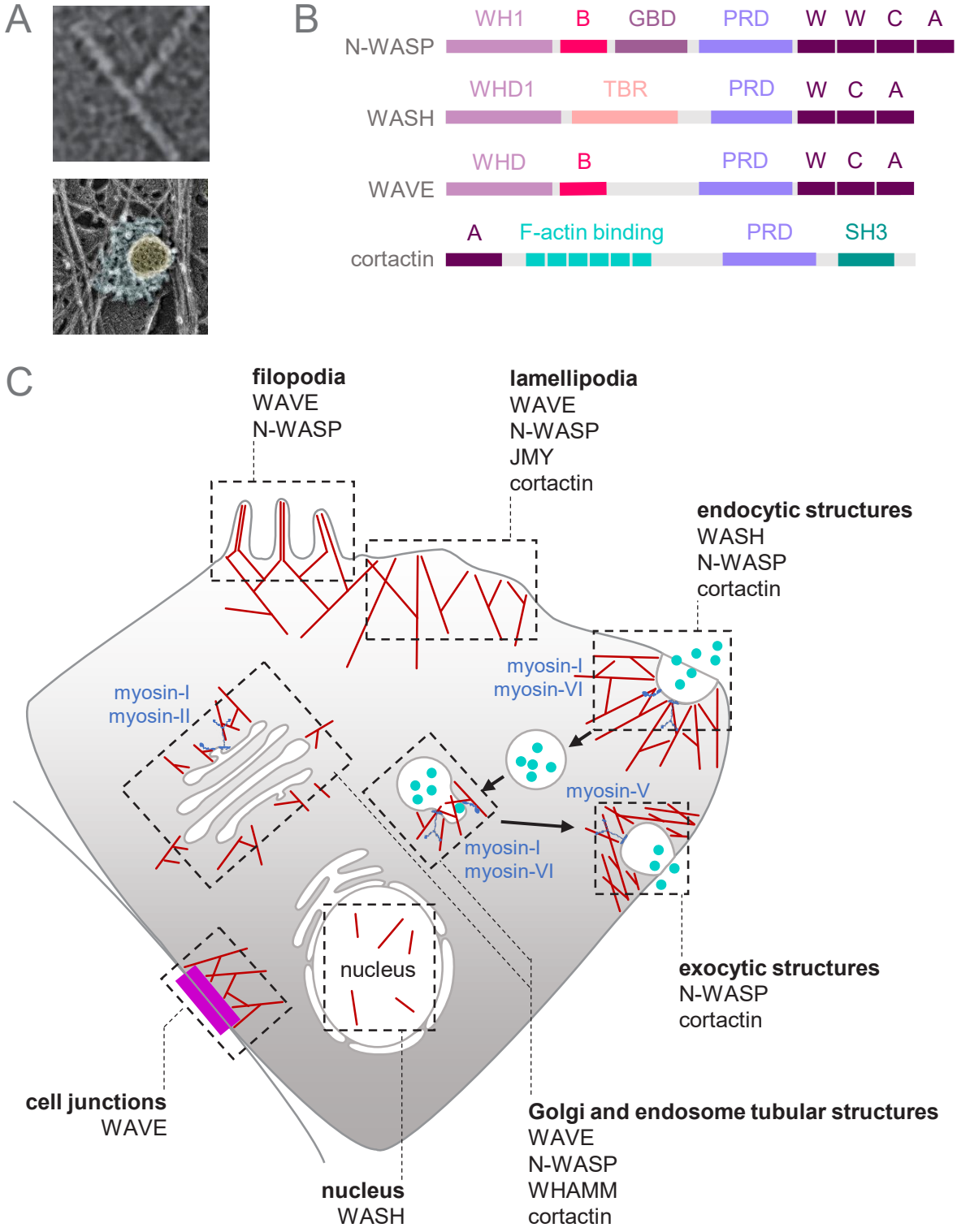
A
B
WH1
B
GBD
PRD
W
W
C
A
N-WASP
WHD1
TBR
PRD
W
C
A
WASH
WHD
B
PRD
W
C
A
WAVE
A
F-actin binding
PRD
SH3
cortactin
C
filopodia
WAVE
N-WASP
lamellipodia
WAVE
N-WASP
JMY
cortactin
endocytic structures
WASH
N-WASP
cortactin
myosin-I
myosin-II
myosin-I
myosin-VI
myosin-V
myosin-I
myosin-VI
nucleus
exocytic structures
N-WASP
cortactin
cell junctions
WAVE
nucleus
WASH
Golgi and endosome tubular structures
WAVE
N-WASP
WHAMM
cortactin

Figure 1.13. Cellular functions of branched actin. A. Electron microscopy images of a ramified actin filament (above; Campellone and Welch, 2010) and a clathrin-coated in yellow surrounded by branched actin patch in blue (below; Collins et al., 2011). **B.** Domain structure of the class I NPFs N-WASP, WAVE and WASH, and of the class II NPF cortactin. Note the WCA domain in at the C-terminus of N-WASP, WAVE and WASH, and the A motif at the N-terminus of cortactin. **C.** Branched actin structures in the cell. Filopodia, lamellipodia, endocytic and exocytic structures, cell junctions and tubules in endosomes and Golgi are all structures that depend on Arp2/3-induced polymerisation. Note that specific NPFs activate Apr2/3 in the different structures. Those myosins implicated in membrane trafficking are indicated. Modified from Campellone and Welch (2010) and Rotty, Wu and Bear (2013).

1.3.7.6 Arp2/3 inhibitors

In order to tune the formation of branched actin, the presence of Arp2/3 inhibitors in addition to the activators is required. Direct Arp2/3 inhibitors such as GMF, PICK1, gadkin and arpin, contain an acidic domain that is analogous to that of NPFs. The acidic domain allows Arp2/3 binding and is needed for Arp2/3 inhibition, although the molecular mechanisms for this inhibition vary among inhibitors. Gadkin, for instance, sequesters the Arp2/3 complex at specific cell sites, whereas PICK1 and arpin compete with the NPFs for its binding. GMF induces an open conformation in Arp2/3 to impede nucleation and also catalyses debranching of existing networks (Chánez-Paredes, Montoya-García and Schnoor, 2019). Physiological roles requiring Arp2/3 inhibition by PICK1, gadkin and arpin have been described, including membrane trafficking-related functions. For example, PICK1 inhibits internalisation of the AMPA receptor. Gadkin localises to endosomes and the TGN and controls the balance between endosomal and PM Arp2/3. Specifically, gadkin sequesters Arp2/3 at endosomes and its downregulation leads to an increase in cortical Arp2/3 (Rocca *et al.*, 2008; Maritzen, Zech, Michael R. Schmidt, *et al.*, 2012; Gorelik and Gautreau, 2015; Li *et al.*, 2018).

1.3.7.7 Myosins in membrane traffic

Myosins are actin-associated motors that hydrolyse ATP to produce force. They transport cargo towards the plus end of the actin filament except for myosin VI, which does so in the opposite direction (Fili and Toseland, 2020). They bind cargo in order to transport it or link it to an actin track. Each myosin contains a motor head, a neck and a tail (**Figure 1.14**). The tail contains dimerisation domains, as well as cargo-binding domains. The binding to PIP or small GTPases of the tail often induces conformational changes that activate the myosin. Other forms of regulation are the binding of Ca^{2+} to calmodulin light chains that interact with the myosin neck, as well as post-translational modifications or applied tension (Fili and Toseland, 2020). Of the 13 classes of myosins found in humans, myosins I, II, V and VI have functions related to membrane trafficking (**Figure 1.13C**). Myosin I and VI exert forces in CME (Buss *et al.*, 2001; Taylor, Perrais and Merrifield, 2011). Myosin I also works in recycling from EEs, endosome tubulation, lysosome fusion and TGN secretion, in which myosin II and VI are also required (Neuhaus and Soldati, 2000; Warner *et al.*, 2003;

Almeida *et al.*, 2011; Brandstaetter *et al.*, 2014; Yamada *et al.*, 2014; Miserey-Lenkei *et al.*, 2017). Myosin V drives exocytic vesicles through cortical actin and to the PM (Lapierre *et al.*, 2001).

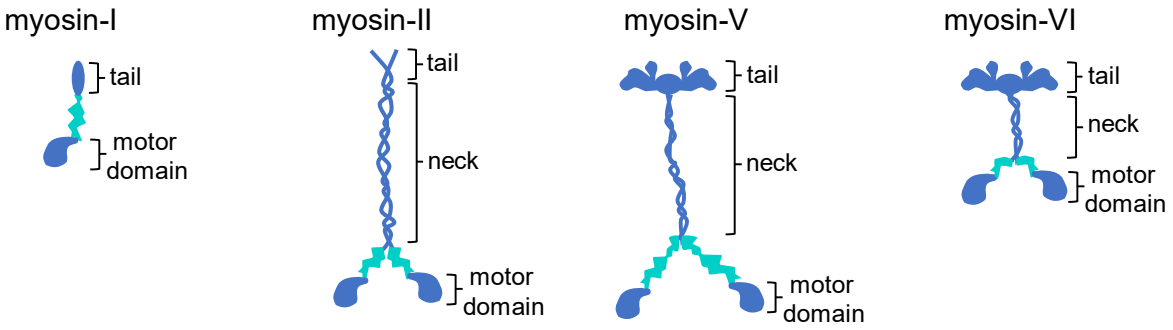

Figure 1.14. Structure of myosins. The structure of myosin is depicted for the main classes involved in membrane trafficking. The tail, neck and motor domains are marked. The light chains associated to the myosins are shown in light blue.

1.3.8 Microtubules in membrane traffic.

The tubulin cytoskeleton is composed of bundles of tubulin filaments termed microtubules. Microtubules conform cellular structures essential in cellular processes such as cell division, motility, and intracellular movement of vesicles and organelles for cell organisation and polarisation (Goodson and Jonasson, 2018). During the interphase of most cells, including fibroblasts, the microtubule network has a radial distribution. Microtubules emanate from the Microtubule-Organising Centre (MTOC), adjacent to the nucleus, and expand towards the PM. In mitosis, the network rearranges to form the mitotic spindle, which separates the chromosomes for the two daughter cells (Richard Mcintosh, 2016). At the end of mitosis, an accumulation of microtubule bundles, called midbody, is formed at the point of abscission of the two cells. The midbody is thought to work as a signalling platform to regulate abscission (Dionne, Wang and Prekeris, 2015). Microtubules are also the core of flagella and cilia that protrude in interphase from the PM to allow motility of the cell and, in the case of the primary cilia, work as signalling platforms and cell antennas (Mirvis, Stearns and Nelson, 2018). Therefore, microtubule distribution and function is tightly linked to cell cycle progression.

In the context of membrane traffic, the major role of the microtubules is to serve as tracks to transport organelles, vesicles and tubules. This type of transport is important in many contexts. For instance, the distribution of LEs and lysosomes changes from more dispersed to more concentrated around the MTOC in a regulated manner, in response stress situations or for specific cell functions (Heuser, 1989; Vyas *et al.*, 2007; Korolchuk *et al.*, 2011). Microtubule-dependent transport also impedes EE clustering at the perinuclear regions and allows correct recycling of receptors (Hoepfner *et al.*, 2005). The molecular motors kinesins and dyneins transport their cargo centripetally or centrifugally, respectively. In doing so, microtubules also have a key role defining the position of the Golgi, the endosomes, the

lysosomes and the ER within cells (Bonifacino and Neefjes, 2017). In addition, kinesins and dyneins have been suggested to assist tubulation and fission on endosomes (Skjeldal *et al.*, 2012; Delevoye *et al.*, 2014). In contrast to actin, tubulin polymerisation has not been directly implicated in membrane traffic.

1.3.8.1 Structure and dynamics of microtubules

α- And β-tubulin heterodimers assemble into hollow polymers of approximately 25 nm in diameter. The result is a bundle of linear protofilaments that bind laterally to each other. Most common microtubules are formed by 13 protofilaments. In these, the attachment between two of the protofilaments is different to the rest, and it can be thought of as a "seam" (**Figure 1.15A**). Like actin, microtubules are polar and contain a more dynamic plus end with exposed β-tubulin and a less dynamic minus end with exposed α-tubulin. However, microtubules are more rigid than actin filaments. Because the C-terminus of both tubulin isoforms are rich in glutamic acid, the external surface of microtubules is negatively-charged, which is key for many interactions. The internal surface of microtubules is less well-known but is also subjected to interactions with proteins and small molecules that bind as the tubule forms or that enter through holes in the microtubule wall. Tubulin has GTPase activity that controls polymerisation dynamics. Microtubules are characterised by a dynamic instability (Mitchison and Kirschner, 1984). This means that they stochastically transition from growth to depolymerisation. This transition is called 'catastrophe', whereas the transition from depolymerisation to growth is called 'rescue' (**Figure 1.15B**). In addition to α- and β-tubulin, there are other isoforms. γ-Tubulin is involved in the nucleation of newly formed microtubules, and others like δ-, ε- and ζ-tubulin form part of specialised structures, such as flagella, cilia and basal bodies (Goodson and Jonasson, 2018).

The polarisation and depolarisation mechanisms of microtubules are not completely understood. The intrinsic dynamic instability of microtubules is modulated by microtubule-associated proteins. They can be divided in stabiliser, destabilisers, capping proteins and crosslinkers (**Table 1.3**; **Figure 1.15D**; Sanchez and Feldman, 2016). Since microtubule polymerisation itself is not directly implicated in membrane trafficking, it will not be further discussed. The reader can refer to Goodson and Jonasson (2018) for a review of the available models and the evidence supporting them. Post-translational modifications of microtubules are common and influence the binding and processivity of motors (Marx *et al.*, 2006). Phosphorylation, sumoylation, detyrosination and polyglutamylation occur on the outer surface, and acetylation occurs on the lumen. These are mainly found in older, more stable microtubules but it is not clear whether the modifications are the cause of such stability. Certain post-translational modifications alter the affinity for microtubule-binding proteins and motors. For example, detyrosination of α-tubulin promotes kinesin-1 recruitment (Garnham and Roll-Mecak, 2012).

Function	Microtubule-associated proteins
Stabilisers	XMAP15/DIS1, CLASP, EB1, NDC80, CLIP-170, tau, MAP2, MAP4, STOP proteins, doublecortin, EMAP.
Sequestering (destabilisers)	Stathmin.
Tip destabilisers	KIF13, stathmin.
Severing proteins (destabilisers)	Katanin, spastin, fidgetin.
Capping	Patronin, CAMSAPs, γ-TuRC.
Cross-linkers	MAP65/ase1/PRC1.

Table 1.3. Microtubule-associated proteins. The main microtubule associated proteins are classified according to their function.

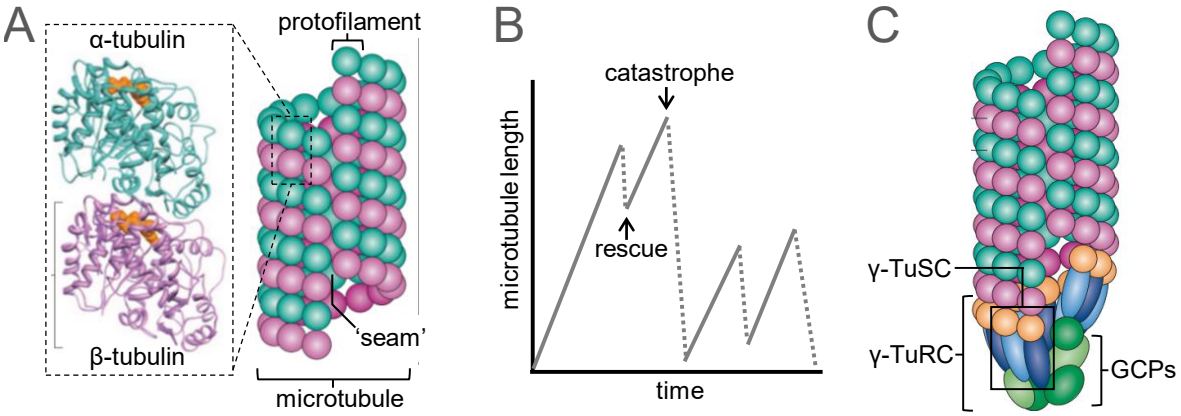

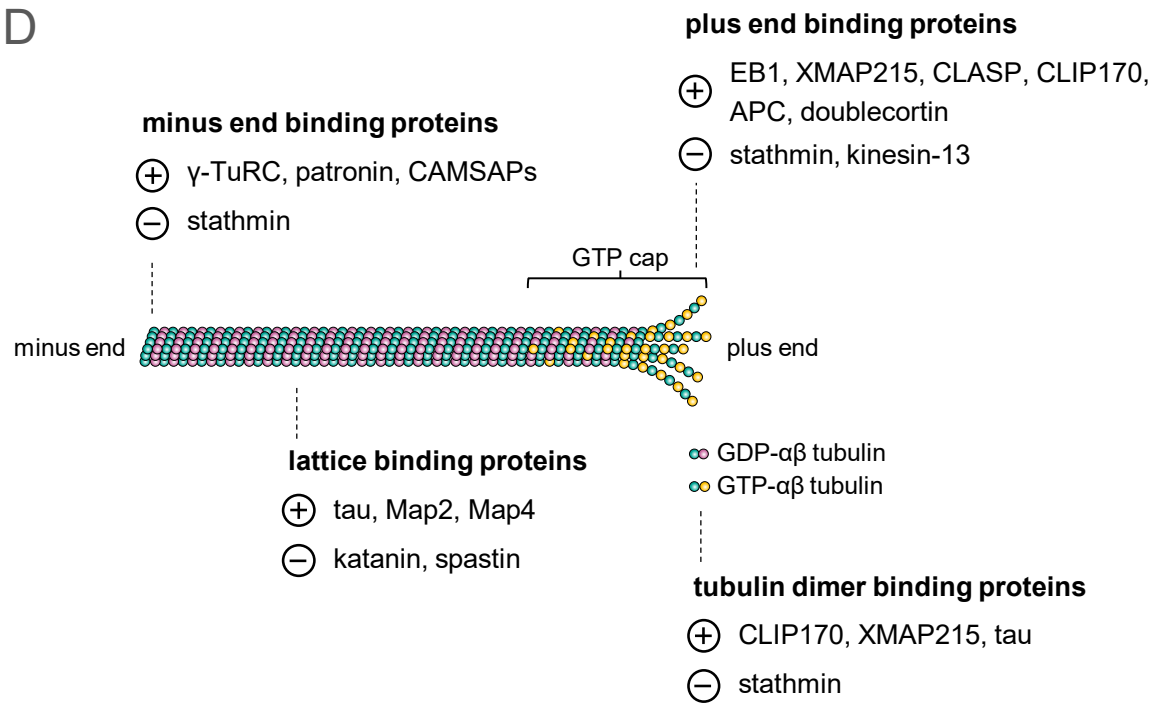

Figure 1.15. Microtubule structure and dynamics. A. A microtubule fragment is shown, composed of 13 protofilaments that are laterally bound to each other. The binding between two of the protofilaments is different to the rest and conforms the 'seam'. Each protofilament is formed by successive dimers of α-tubulin and β-tubulin bound to GTP or GDP (shown in orange). Adapted from Kollman et al. (2011). **B.** Graph of an example of a microtubule's length along time, showing the growing and the shrinking phases, which change stochastically from one to another. These transitions are called rescue and catastrophe. Adapted from Goodson and Jonasson (2018). **C.** The nucleation of a microtubule by the γ-TuRC complex is depicted. The γ-TuRC complex is formed by GPC4, GPC5 and GPC6 (in green), and by the γ-TuSC complex, which in turn is composed by a γ-tubulin dimer (in orange), GPC2 and GPC3 (in blue). The γ-TuRC complex acts as a template in which the γ-tubulin subunits account for the first subunit in each protofilament, promoting the formation of a new microtubule. Adapted from Kollman et al. (2011). **D.** A growing microtubule is illustrated. Note the accumulation of GTP-bound tubulin dimers that form the GTP cap at the plus end. The main microtubule binding proteins affecting microtubule dynamics are shown, classified upon their site of binding to the microtubule. The '+' sign indicates the proteins promote microtubule growth or stabilisation, whereas the '-' sign indicates that the proteins promote depolymerisation or destabilisation.

The nucleation of the first tubulin dimers for the formation of a microtubule is, like in the case of actin, an unfavourable process. This allows special and temporal control of nucleation by microtubule nucleators. Classic microtubule nucleators have a γ-tubulin core with associated proteins (**Figure 1.15C**), although an increasing amount of evidence points towards non-γ-tubulin nucleators (Tovey and Conduit, 2018). The minimal nucleating structure is γTuSC (γ-tubulin small complex), formed by two γ-tubulin subunits, γ-tubulin complex protein 2 (GCP2) and GPC3. γTuSC in animal cells forms part of the larger and more efficient nucleator γTuRC (γ-tubulin ring complex). The γTuRC contains multiple γ-TuSC, GCP4, GCP5, GPC6, MOZART1 and MOZART2, and NEDD1, among others (Guillet *et al.*, 2011). γTuSC works as a template for nucleation. In the complex, γ-tubulin subunits interact with each other laterally, and longitudinally with αβ-tubulins of the forming microtubule (**Figure 1.15C**; Guillet *et al.*, 2011; Kollman *et al.*, 2011).

As mentioned before, microtubules emanate from MTOCs, in which their (-) ends are embedded. Therefore, MTOCs determine microtubule patterning in the cell. They also have functions of nucleation, stabilisation and anchoring. In fibroblasts, with a radial microtubule distribution, the centrosome is the main but not the only MTOC (Sanchez and Feldman, 2016). The mammalian centrosome is composed of two centrioles, mother and daughter, the pericentriolar material (PCM), and satellites (**Figure 1.16**).

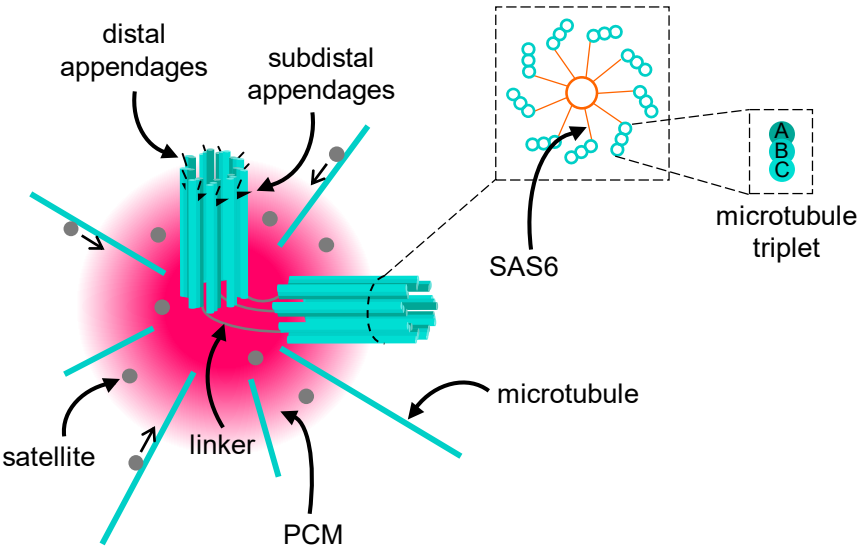

Figure 1.16. Structure of the centrosome. The centrosome is formed by two centrioles, mother and daughter, the PCM and the satellites. Microtubules emerge from the centrosome and satellites often travel along them. Each centriole is formed by nine concentric microtubule triplets connected to a central hub by spokes of SAS6. The mother centriole has distal and subdistal ears.

Each centriole is a barrel-shaped structure formed by a central hub of SAS6 oligomers, surrounded by nine microtubule triplets. Each triplet is linked to the centre by a spoke of SAS6 homodimers (**Figure 1.16**; Kitagawa *et al.*, 2011). The integrity of the centriole is maintained by a helical structure bound to the inner face of the microtubule triplets, formed by centrin 2, among others (Le Guennec *et al.*, 2020). The mother centriole has distal appendages, which dock it to the PM for ciliogenesis (Yang *et al.*, 2018). Attached to the minus end of the centriole are the subdistal ears, which anchor the centriole to the centrosome. The mother centriole is completely matured, whereas the daughter centriole was formed in the last mitosis. Both centrioles are surrounded by γ-TuRCs in the PCM that nucleate microtubules. However, only the mother centriole has microtubules anchored to its subdistal ears. Cells in G_0 phase have a primary cilium that is formed from the mother centriole docking to the PM. In this context, the mother centriole is called basal body (Sanchez and Feldman, 2016).

The PCM is an electron-dense lattice that nucleates microtubules directly or through γ-TuRC (**Figure 1.16**). One of its components is pericentrin, which is often used as a centrosomal marker. The PCM is scaffolded by P1p (Pericentrin-like Protein 1), which is disposed radially, with its C-terminus to the centriole wall (Mennella *et al.*, 2012). The PCM contains satellites, granules that deliver centrosomal components from the cytoplasm (Hori and Toda, 2017). They are important for centrosomal and primary cilium assembly. Satellites are non-membranous compartments of 70 to 100 nm size. Their major component and scaffold is the coiled-coil rich protein PCM-1. BBS4 and OFD1 are also required to maintain these structures.

1.3.8.2 Microtubules-dependent motors in endosomal trafficking

The motors that drive microtubule-dependent transport are mainly the kinesin superfamily (KIF) for transport towards the plus end, and the dynein complex in transport towards the minus end. The attachment to organelles is often mediated by adaptor molecules that bind to small GTPases or PIPs (**Table 1.4**).

Organelle	Motor	Cargo adaptors and regulators
EE	KIF5B	KLC, gadkin, AP-1.
	KIF16B	Rab5, PI3P, VPS34.
	Dynein-dynactin	Rab5, FTS, HOOK, FHIP.
RE	KIF13A	BLOC-1, Rab11.
	KIF13B	-
	Dynein	Rab11, FIP3.
LE/lysosome	KIF1A	BORC, arl8.
	KIF1Bβ	BORC, arl8.
	KIF2A	-
	KIF3A	KAP3.
	KIF5B	KLC, BORC, arl8B, SKIP.
		Rab7, FYCO1.
	Dynein-dynactin	Rab7, RILP, ORP1L, JIP3, HPS6.
Proto-lysosome	KIF5B	$PI(4,5)P_2$, clathrin.
Apical RE	KIF3A	Rab11, FIP5.
	KIF3B	-
Transcytotic / SARA endosomes	KIF16B	Rab11.
Cytokinetic RE	KIF5B	Arf6, JIP4.
	Dynein-dynactin	Arf6, JIP4.
Melanosomes	KIF5B	Rab1A, SKIP.
	Dynein-dynactin	Rab36, RILP.
		Melanoregulin.
Lytic granules	KIF5B	Rab27a, slp3, KLC1.
		Arl8, SKIP.
	Dynein-dynactin	HkRP3.
		Rab7, RILP.

Table 1.4. Motors and adaptors in the microtubule-dependent transport of endolysosomal organelles. Organelles of the endosomal system are listed next to the motors that mediate their transport along microtubules. The adaptors and regulators described for each organelle and motor are also listed (Bonifacino and Neefjes, 2017).

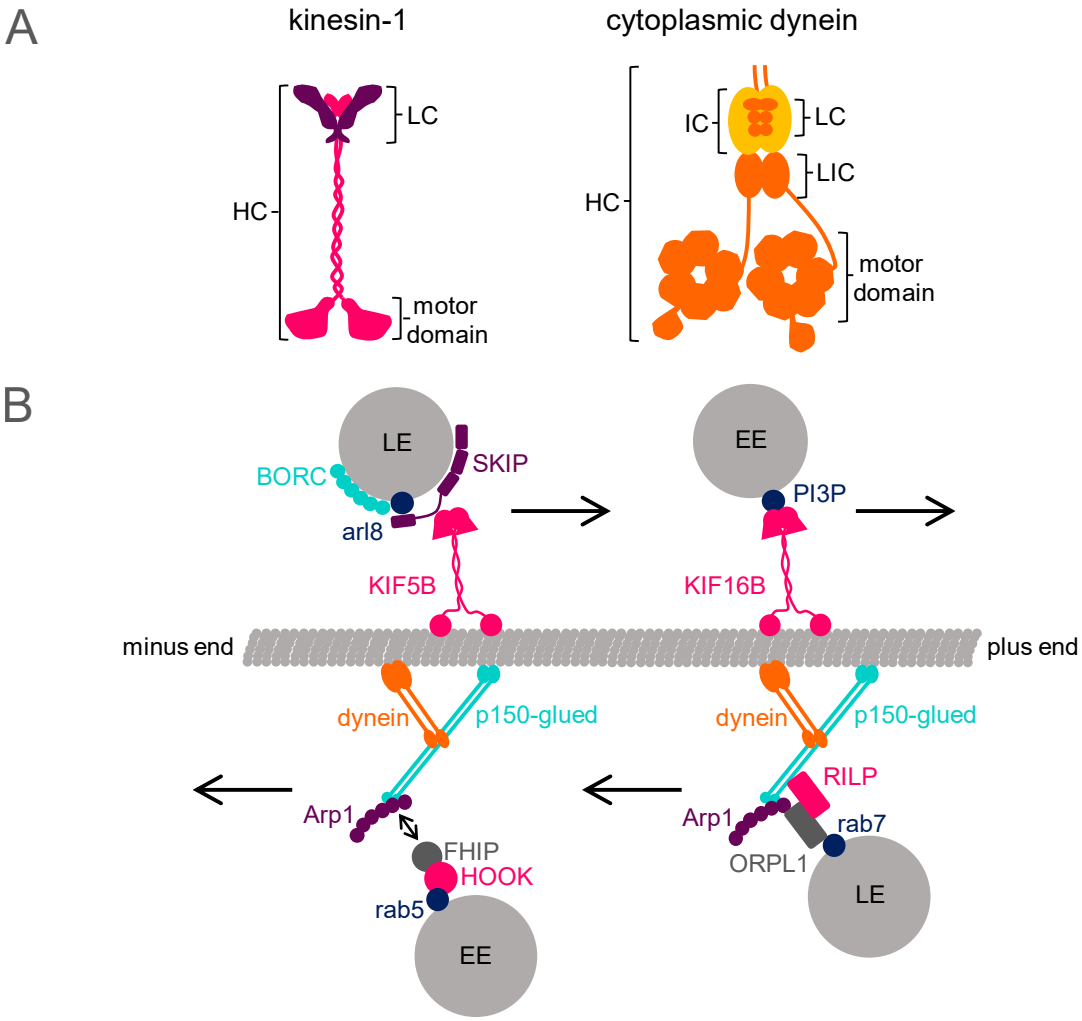

Figure 1.17. Transport along microtubules. A. The composition of kinesin-1 and cytoplasmic dynein, as examples of microtubule motors, is shown. They both have a heavy chain (HC) that contains the motor domain, which binds to the microtubule. The HCs also mediate dimerisation. Kinesin-1 has one light chain (LC) bound to each heavy chain, whereas dynein has a LC, an intermediate chain (IC) and a light intermediate chain (LIC) per HC. **B.** Transport along microtubules is mediated by kinesin in the minus to plus end direction and by dynein in the opposite direction, as exemplified by the depicted mechanisms. KIF16B binds EEs through PI3P. KIF5B transport LEs, to which the motor is bound through the adaptor proteins SKIP and BORC. These adaptors identify the LE by the presence or arl8. Dynein transports cargo along microtubules in conjunction with dynactin, of which two components are shown in the image: p150-glued and the Arp1 repeats. For EE transport, FHIP can simultaneously bind rab5 in EEs and HOOK, which in turn interacts with both dynein and dynactin. For LEs, the interaction with dynein requires rab7, and it is mediated by the interaction of RILP with p150-glued, and by ORPL1, which simultaneously interacts with both the Arp1 filament and rab7-RILP (Pu *et al.*, 2016; Bonifacino and Neefjes, 2017).

Kinesins use the energy from ATP hydrolysis to produce forces. There are at least 14 subfamilies, all of which share the motor domain. Most kinesins work as tetramers formed by two Kinesin Heavy Chains (KHC) that contain the motor domain and that oligomerise

through the coiled-coil regions, and two Kinesin Light Chains (KLC) that mediate the interaction to the cargo or the cargo adaptor (**Figure 1.17A**; Marx, Hoenger and Mandelkow, 2009). Kinesins are processive, and their processivity varies from one kinesin to another and ranges from a few steps to more than a thousand (Mickolajczyk and Hancock, 2017).

Retrograde transport requires cytoplasmic dynein-1. Dynein is a complex of 1.4 MDa conformed by two copies of each of its six components. These include the Dynein Heavy Chain (DHC), which contains the motor and the dimerization domains, and a series of Light and Intermediate Chains (LCs, ICs, LICs; **Figure 1.17A**). Dynactin works with its co-factor dynactin, a 23 subunits complex of 1.1 MDa. Among others, dynactin contains a central actin-like filament of Arp1 and the subunit p150-glued, which is implicated in microtubule binding. In addition, BICD2, BICDR1, HOOK1, HOOK3 and other coiled-coil proteins, collectively called activating adaptors, activate the dynein-dynactin complex for long-range transport and mediate binding to the cargoes (Reck-Peterson *et al.*, 2018). Some examples of kinesin and dynein-mediated transport are listed in **Table 1.4** and depicted in **Figure 1.17B**.

1.4 Endosomal pathways

The previous section described the main machineries in membrane trafficking. Here, the mechanisms involved in each endosomal trafficking step will be discussed in detail.

1.4.1 Endocytosis: from the PM to the EE

There are different ways of internalising cargo into the cell. Phagocytosis and micropinocytosis are large-scale processes, whereas the processes involving smaller invaginations are divided into CME (Roth and Porter 1964; Kaksonen and Roux 2018) and clathrin-independent endocytosis (CIE; Hemalatha and Mayor, 2019). CIE processes are classified according to the machinery involved and the cargo internalised. **Figure 1.18** summarises the different routes for internalisation in metazoans. From here on only CME is discussed, which is the major endocytic route in eukaryotic cells and is the most relevant for the trafficking of the cargoes described in this thesis.

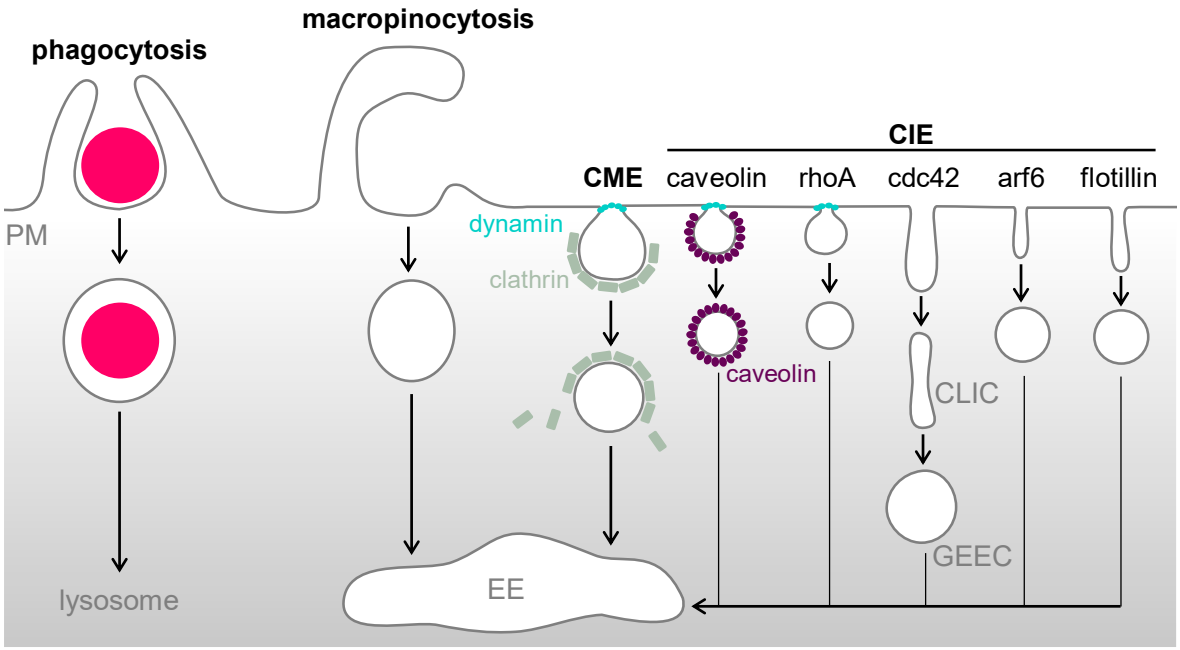

Figure 1.18. Diversity of endocytic pathways. Different routes of cargo internalisation in metazoans are depicted. Phagocytosis and macropynocytosis are processes that capture big particles and fluids, respectively. Distinct CIE routes are referred to by the proteins effecting them. Caveolae are stable structures that form on lipid rafts and allow the internalisation of proteins like albumin and pathogens like SV40. This type of endocytosis requires caveolin and cavin, dynamin and SNX9. The uptake of interleukin-2 requires rhoA, as well as rac1, PI3K, endophilin and dynamin. Cdc42-mediated endocytosis produces carriers termed CLIC that fuse with GEEC endocytic compartments. This pathway allows the internalisation of glycosylphosphatidylinositol (GPI)-anchored proteins and transmembrane proteins. In addition to cdc42, it implicates arf1, Arp2/3 and SNX9. Arf6 has been shown to mediate endocytosis of viruses. Finally, flotillins are required for the internalisation of receptors and GPI-anchored proteins, probably by clustering them at the PM. Generally, carriers derived from the different endocytic routes converge in the EE (Sandvig, Kavaliauskiene and Skotland, 2018).

CME is a sequential process in which proteins are recruited following a very specific order and timing (**Figure 1.19**). This has allowed their classification into functional modules: the clathrin coat module, the actin module, the scission module and the uncoating module (Idrissi *et al.*, 2012; Kaksonen and Roux, 2018). The progress in CME is concomitant to the metabolism of the implicated PIPs. Indeed, the conversion of PI4P to $PI(4,5)P_2$ by PIPK1, an AP-2 binding kinase, allows the recruitment of the machinery that is necessary to initiate endocytosis, including clathrin adaptors. Also dynamin is recruited by $PI(4,5)P_2$. As the invagination progresses, synaptojanins catalyse the formation of PI4P, which is converted to $PI(3,4)P_2$ by PIK3C2A. $PI(3,4)P_2$ recruits machinery involved in membrane bending, such as SNX9. Finally, the PI4 phosphatase and OCRL1 catalyse the formation of PI3P, which provides endosomal identity to the vesicle (Posor, Eichhorn-Grünig and Haucke, 2015; Wang, Lo and Haucke, 2019).

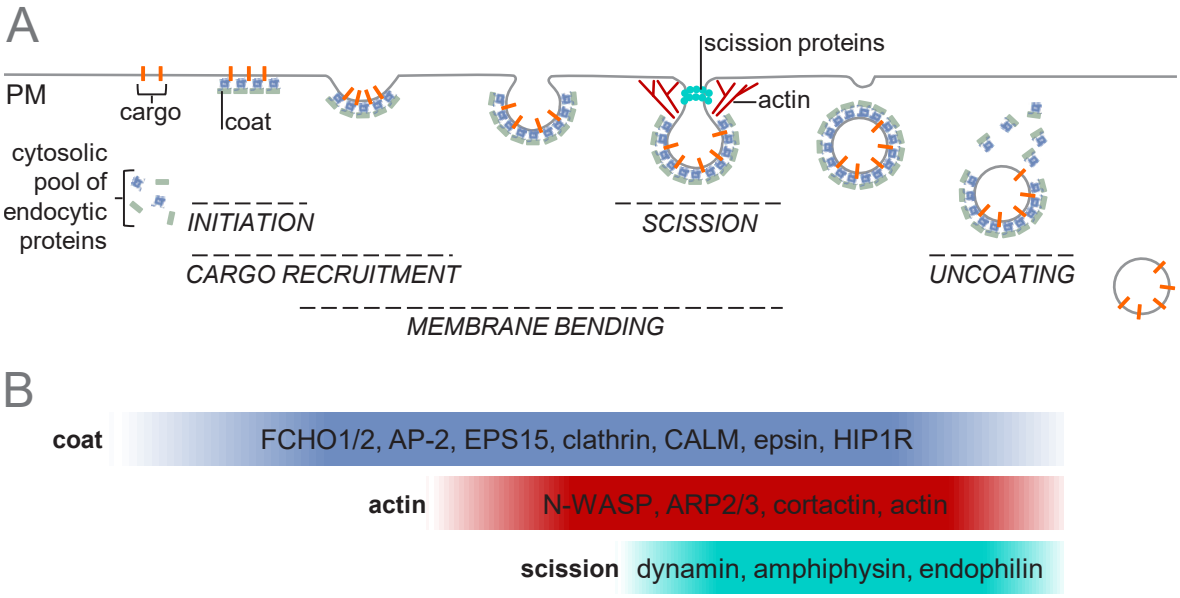

Figure 1.19. Sequential recruitment of proteins during CME. A. The cargo is recognised by the cargo adaptor on the flat plasma membrane (PM), which promotes cargo concentration and the recruitment of endocytic proteins. The membrane is bent to produce an invagination until the actin polymerisation machinery and scission proteins induce scission. The resulting vesicle moves inwards, and the coat is detached. **B.** The main proteins involved in CME are classified as coat, actin or scission proteins. These are depicted depending on the timing of their function along the timeline in A (Kaksonen and Roux, 2018).

Although the initial steps of endocytosis are not completely understood, the best accepted model states that a pioneer set of proteins accumulate in the inner leaflet of the PM to initiate CME. In mammals, it includes the cargo adaptors FCHO1/2 and AP-2 and scaffolds EPS15, EPS15R and intersectins 1 and 2. Clathrin then clusters on the endocytic site (**Figure 1.19**). AP-2 integrates PIP and cargo information, as it binds $PI(4,5)P_2$, but also cargo like TfnR (Kelly *et al.*, 2014). Interestingly, a 'cargo checkpoint' ensures that only cargo-packed domains are susceptible to bending and vesicle formation. It is not clear whether clathrin assembles into flat lattices and induces curvature or whether it stabilises the curvature by binding directly as a curved lattice (Kaksonen and Roux, 2018). The actin module, on the other hand, is known to aid membrane bending at late stages of invagination, forming a network at the rim (**Figure 1.19**). This module is essential in yeast, where a high force is needed to invaginate the plasma membrane due to the high osmotic pressure. In mammals, however, the requirement of the actin module is thought to depend on the context. Actin has been shown to participate in the invagination of clathrin plaques, and proposed to mediate tubulation before dynamin recruitment (Benesch *et al.*, 2005; Ferguson *et al.*, 2009). It is also implicated in CME when the membrane tension is high, which is dependent on the cell type, the differentiation state or external stimulation (Boulant *et al.*, 2011). In mammals, this module consists of actin, the Arp2/3 complex and N-WASP. Also cortactin and myosin-1E, among others, are thought to be recruited at the moment of scission (Taylor, Perrais

and Merrifield, 2011). Coordination of endocytosis and actin polymerisation is achieved by epsins and HIP1R, which interact with PI(4,5)P_2, clathrin and actin filaments (Engqvist-Goldstein *et al.*, 2001; Itoh *et al.*, 2001; Messa *et al.*, 2014). Actin filament polymerisation from the base to the tip of the invagination produces force for bending and abscission, and myosins I and VI are thought to facilitate this role (**Figure 1.19**; Buss *et al.*, 2001; Lewellyn *et al.*, 2015).

The scission module is comprised by N-BAR domain proteins (endophilins and amphiphysins) and by the GTPase dynamin, although dynamin-independent fission can occur in yeast. (**Figure 1.19**). N-BAR-containing proteins serve as linkers to the actin polymerisation machinery that acts in fission, mostly N-WASP. PIP conversion controls the sequential recruitment of BAR proteins (Kaksonen and Roux, 2018). Finally, the uncoating module is formed by chaperones, protein kinases and lipid phosphatases. First, the dephosphorylation of PI(4,5)P_2 causes the release of the coat. Rab5 and its GEFs induce dephosphorylation of PI(4,5)P_2 and also AP-2 that lead to uncoating (Semerdjieva *et al.*, 2008). Second, dynamin, PI3P and PI(3,4)P_2 bind auxilin, which binds to the ATPase HSC70 and clathrin. HSC70 promotes the disassembly of the clathrin coat by steric hindrance or by pressing the vertices as the ATP is hydrolysed (Sousa *et al.*, 2016; Kaksonen and Roux, 2018). Uncoating is also promoted by AAK1 and GAK family kinases and CK2 (Korolchuk and Banting, 2003).

The endocytic vesicle then travels through the cytoplasm, probably propelled by actin comets, and fuses with other vesicles or with EEs (Merrifield *et al.*, 1999). Activated rab5 controls its fusion by binding to the EEA1 tethering factor. EEA1 has a double function of tethering and activation of the SNAREs (McBride *et al.*, 1999; Simonsen *et al.*, 1999). On endosomes, rab5 is activated by rabaptin-5, which in turn binds and activates the PI3K VPS34 (Simonsen *et al.*, 1998). The resulting increase in PI3P, together with GTP-rab5, recruits EEA1, thereby establishing a positive feedback loop.

1.4.2 The degradation pathway: from EEs to lysosomes

The machinery and cargoes that are not recycled to the PM or targeted to the TGN follow the degradation pathway (**Figure 1.1**). This is the case for most lumenal cargoes and ubiquitinated membrane proteins (Frankel and Audhya, 2018). EEs mature into LEs approximately eight minutes after their formation. Once mature, the LE are thought to deliver their luminal content to the lysosomes using mostly a ‘kiss-and-run’ mechanism. The maturation of EE to LE implicates changes in shape and density, progressive lowering of the lumenal pH, microtubule-dependent transport towards the MTOC, acquisition of enzymes involved in the catabolism of biomolecules and a switch of tether complexes. All these changes are coordinated by a rab switch and a PI conversion (Huotari and Helenius, 2011; Podinovskaia and Spang, 2018).

The ESCRT machinery mediates the formation of vesicles that bud into the lumen of the endosome, the ILVs, loaded with membrane proteins sorted for degradation (**Figure 1.9**). The acidification of the lumen is important for lysosomal functions and also works as a signal for membrane trafficking. Indeed, the difference with the cytosolic pH promotes the release of cargo from the receptors. It also allows the progressive activation of acid hydrolyses. The change in the fusion specificity of endosomes is based on the switch in SNARE proteins and from the tethering complex CORVET to HOPS. Most of the specialised machinery of LEs and lysosomes comes from the Golgi and the TGN, only after the formation of ILVs. In addition, LEs accumulate at the perinuclear region along microtubules (Huotari and Helenius, 2011).

Some of the mechanisms that direct the maturation process have been elucidated. Importantly, there is a transition from rab5 to rab7 and from PI3P to $PI(3,5)P_2$ (**Figure 1.4**). According to the 'cut-out switch' model, a negative feedback loop is initiated when the GTP-rab5 levels reaches a threshold (Del Conte-Zerial *et al.*, 2008). It leads to the recruitment of Mon1/Ccz1, a complex that inactivates the rab5 GEF rabex5 and acts as a GEF for rab7 (Nordmann *et al.*, 2010; Poteryaev *et al.*, 2010). Rab7 and also arl8B recruit HOPS. HOPS and Mon1 activate each other, creating a positive feedback loop that stabilises rab7 domains. The enrichment in PI3P depends on the presence of the class III PI3K VPS34. VPS34 forms a complex with Beclin-1, UVRAG and VPS15. It binds GTP-rab5, but also rab7, especially GDP-bound rab7. As rab7 is activated, there will be a reduction in the levels of VPS34, and hence, of PI3P (Schu *et al.*, 1993; Wang, Lo and Haucke, 2019). In addition, GTP-rab7 also actively inhibits PI3K by sequestering the UVRAG subunit. The released UVRAG, in turn, activates HOPS (Sun *et al.*, 2010). Also needed for EE to LE maturation is the PI(3)P-5-kinase PIKfyve, which converts PI3P into $PI(3,5)P_2$. The decrease in the PI3P levels entails a detachment of FYVE-containing proteins. HOPS interacts with RILP, which recruits retrograde transport motors, and allows an enrichment of lysosomes in the pericentriolar region (**Figure 1.17**; van der Beek et al., 2019). As for the acidification of the lumen as the endosome matures, the mechanism is not well understood. The main complex responsible for lowering the pH is the V-ATPase, which is indirectly activated by the rab7 effector RILP (De Luca *et al.*, 2014; Wang, Lo and Haucke, 2019).

The formation of lysosomes might occur through a continuation of the maturation process from EEs, or through the delivery of transport intermediates from LEs to lysosomes. However, evidence best supports the existence of 'kiss-and-run' contacts that allow transfer of machinery while maintaining organelle identity, in addition to complete fusion events of LEs with pre-existing lysosomes (Bright, Gratian and Luzio, 2005).

1.4.3 Recycling pathways: from endosomes to the PM

Those cargoes that are not targeted for degradation in EEs are retrieved. These cargoes are targeted to the PM or to the TGN to join the secretory pathway (**Figure 1.1**; Dai *et al.*,

2004; Cullen and Steinberg, 2018). Most retrieved cargoes contain a sorting sequence that is recognised by cargo adaptors. A study by Sönnichsen *et al.* (2000) revealed that markers of different endosomal routes (rab5, rab4 and rab11) form distinct subdomains within EEs, from which they might promote cargo delivery to one destination or another (**Figure 1.20**; Geuze *et al.*, 1983; Sönnichsen *et al.*, 2000).

Routes to the PM have been classified according to their kinetics into fast recycling routes and slow recycling routes. TfnR, which is 99% recycled to the PM, is partly delivered to the PM within approximately 2 min in CHO cells, and the rest reaches the PM in around 15 min after internalisation (Hao and Maxfield, 2000). The fast route is thought to be direct from EEs to the PM, and to involve rab4a. Cargoes following the slow route are first delivered to the RE and then to the PM, in a process dependent on rab11 (van der Sluijs *et al.*, 1992; Sheff *et al.*, 1999). The role of rab4 in recycling is not clear. Dominant negative rab4 strongly inhibits fast recycling events (Yudowski *et al.*, 2009). However, previous reports indicated that rab4 silencing accelerates a fast TfnR recycling pathway (Deneka *et al.*, 2003). The conflicting results might derive from the fact that rab4a is involved in the short recycling pathway and rab4b in the long recycling pathway (Perrin *et al.*, 2013).

Rabs and PIPs recruit the machinery required in each pathway. The localisation of coats and fission machinery, and of the actin polymerisation machinery along the endosomal system can be visualised in **Figure 1.6** and **Figure 1.13**, respectively. Many tethers and SNAREs are also associated to recycling routes, as described in **Figure 1.11**. The following sections review roles of clathrin, retromer, commander and branched actin, which are thought to sort cargo and establish specific recycling routes form EEs. The role of the fission factors in recycling is also reviewed.

1.4.3.1 Clathrin-dependent recycling

Clathrin-decorated endosomal vesicles have been identified (Stoorvogel, Oorschot and Geuze, 1996). However, the role of clathrin in recycling processes is not well understood. Both rab4a and rab4b seem to be linked to the recruitment of AP-1 and clathrin. Rab4a does it indirectly through the activation of arf1 (Stamnes and Rothman, 1993; D'Souza *et al.*, 2014), whereas rab4b directly interacts with AP-1 (Perrin *et al.*, 2013). Clathrin structures named gyrating-clathrin, associated to GGA1 and GGA3, have been found in rab4 endosomal subdomains and to mediate EE to PM transport, important for β1-integrin recycling (Zhao and Keen, 2008; Parachoniak *et al.*, 2011; Majeed *et al.*, 2014). The formation of a clathrin coat that includes the arf6 GAP ACAP-1 allows correct recycling of TfnR, GLUT-4 and integrins (Van Dam and Stoorvogel, 2002; Dai *et al.*, 2004; Li *et al.*, 2007). There is evidence that at least some cargoes need clathrin for their retrograde transport to the TGN, in a process that involves the clathrin coat-associated protein Hsc70 (Popoff *et al.*, 2009; Shi *et al.*, 2009). Furthermore, AP-1 is required for the tubulation of endosomes together with SNX18 (Håberg, Lundmark and Carlsson, 2008; Kural and Kirchhausen, 2012).

1.4.3.2 Recycling dependent on retromer, commander and the cytoskeleton

As mentioned above, ESCRT-enriched degradatory subdomains are separated from retrieval subdomains, in which retromer, retriever and the CCC complex co-localise (**Figure 1.20**; McNally *et al.*, 2017). Retromer and commander direct trafficking to the PM, and in the case of retromer, also to the TGN. Retromer and commander drive the recycling to the PM of different sets of cargoes. TfnR, β2-adrenergic receptor and GLUT-1 depend on retromer, whereas the copper transporters ATP7A and B, LDL receptor and $\alpha_5\beta_1$ integrin depend on commander (McNally and Cullen, 2018).

The recycling of more than 100 cargoes depends on SNX27-retromer (Steinberg *et al.*, 2013). SNX27 binds PI3P, cargoes, and the VPS26 subunit of retromer. Retromer can also bind cargo directly through its PDZ domain, an interaction enhanced by the binding to SNX27 (Gallon *et al.*, 2014). Furthermore, the binding of SNX3 to the retromer increased its ability to bind cargo (Lucas *et al.*, 2016). SNX5 and SNX6 were shown to bind the dynactin component p150-glued to coordinate sorting and microtubule-based transport, as well as tethering at the TGN (Wassmer *et al.*, 2009). Retromer recruits the WASH complex to retrieval subdomains by binding to fam21 (Gomez and Billadeau, 2009). The tail of fam21 interacts with several retromer complexes, suggesting that actin polymerisation only occurs when the accumulation of cargo reaches a threshold and that WASH-induced actin polymerisation might delimit endosomal subdomains and impede cargo diffusion (**Figure 1.20**; Jia *et al.*, 2012). In addition, WASH recruits retriever and the CCC complex. Retriever works in conjunction with SNX17, which binds PI3P and also cargo (**Figure 1.20**; McNally *et al.*, 2017).

The importance of retromer in endosome to Golgi transport is clear in yeast (Seaman, McCaffery and Emr, 1998). It is also generally accepted for mammals, as the retromer was known to interact with the model cargo CI-MPR. However, two later independent studies showed that the core retromer is dispensable for CI-MPR trafficking and that endosome to TGN transport mostly relies on BAR-containing SNXs dimers (Kvainickas *et al.*, 2017; Simonetti *et al.*, 2017). A more recent study demonstrated that, indeed, there is retromer-dependent and independent transport. SNX3-retromer forms carriers that are tethered by GCC88 at the TGN, whereas SNX-BAR dimers on their own mediate transport that requires golgin-245 (Cui *et al.*, 2019). The interaction of commander with COG suggests a role for commander in Golgi-related trafficking (Chen, Healy and Collins, 2019).

The WASH complex plays a role in endosomal sorting, as WASH-induced actin polymerisation delimits endosomal subdomains and impede cargo diffusion (Jia *et al.*, 2012). This function might be dependent or independent of retromer and commander. Of note, also microtubules are involved in sorting and both kinesins and dynein have also been proposed to segregate endosomal subdomains containing different SNXs (Hunt *et al.*, 2013).

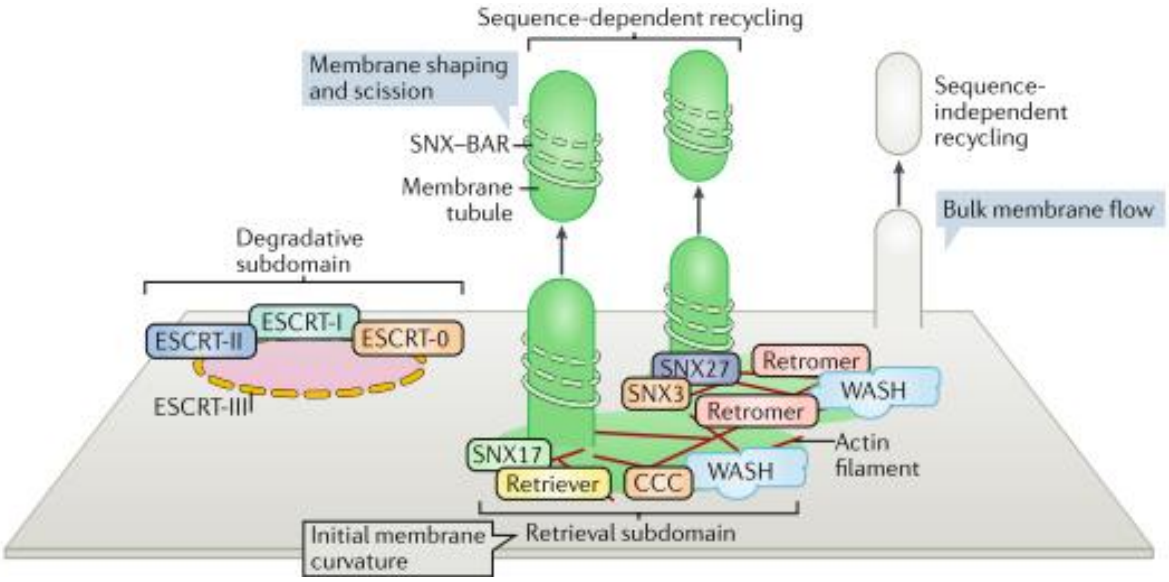

Figure 1.20. Sorting platforms in endosomes. In the endosomal membrane, a degradative subdomain is formed by the ESCRT machinery, and is distinct of the retrieval subdomain. Retromer, SNX27 and WASH, on one side, and retriever, SNX17, CCC and WASH, on the other side, induce the formation of membrane tubules for sequence-dependent cargo recycling. Modified from Cullen and Steinberg (2018).

1.4.3.3 Membrane tubulation in recycling

The formation of vesicles or tubules requires the action of tubulating factors, many of which have been linked to retrieval pathways. The role of dynamin in the pathway is not well established but it has been proposed to work in RE to PM transport (Van Dam and Stoorvogel, 2002; Søreng *et al.*, 2018). EHD1 and EHD3 are both important for recycling (**Figure 1.21**). Both are located in EEs, whereas only EHD1 has been found in RE. EHD1 is thought to induce tubulation, probably downstream of the rab4 and rab5 effector rabenosyn-5, and EHD3 to stabilise tubules (Naslavsky *et al.*, 2004; Bahl *et al.*, 2016). The EHD1 interactor MICAL-L1 seems to work as a hub that links rab8, EHD1 and others in tubular REs (Sharma *et al.*, 2009; Cai *et al.*, 2014). Also, EHD1 interacts with the retromer and the rab5 effector rabankyrin-5 and participates in CI-MPR trafficking (Gokool, Tattersall and Seaman, 2007; Zhang et al., 2012). EHD3 binds rab11-FIP2 and allows TfnR trafficking to the RE (Naslavsky *et al.*, 2006).

The cytoskeleton also plays a role in endosomal tubulation, as mentioned in section 1.3.4 (**Figure 1.21**). N-WASP-induced actin polymerisation might provide pushing forces for the tubulation or scission (Qualmann *et al.*, 1999; Cullen and Steinberg, 2018). Indeed, EHDs bind to the BAR-containing protein PACSIN, which in turn binds N-WASP. Actin polymerisation activated by WASH has also been shown during the scission of CI-MPR carriers (Gomez and Billadeau, 2009). This function might be due to its association with retromer and retriever. In fact, WASH depletion leads to juxtanuclear collapse of endosomes, long tubular structures and defects on the recycling of cargoes that depend on

retromer, retriever or the CCC complex (Cullen and Steinberg, 2018). Also actin motors aid in endosome tubulation (Yamada *et al.*, 2014). The forces exerted by microtubule motors are important in this context too (Simunovic *et al.*, 2017). Dynein and SNX4 are required for sorting of TfnR for recycling (Traer *et al.*, 2007). KIF13A cooperates with rab11 to form recycling tubules and, interestingly, its function requires a link to actin by BLOC-1 (Delevoye *et al.*, 2014, 2016).

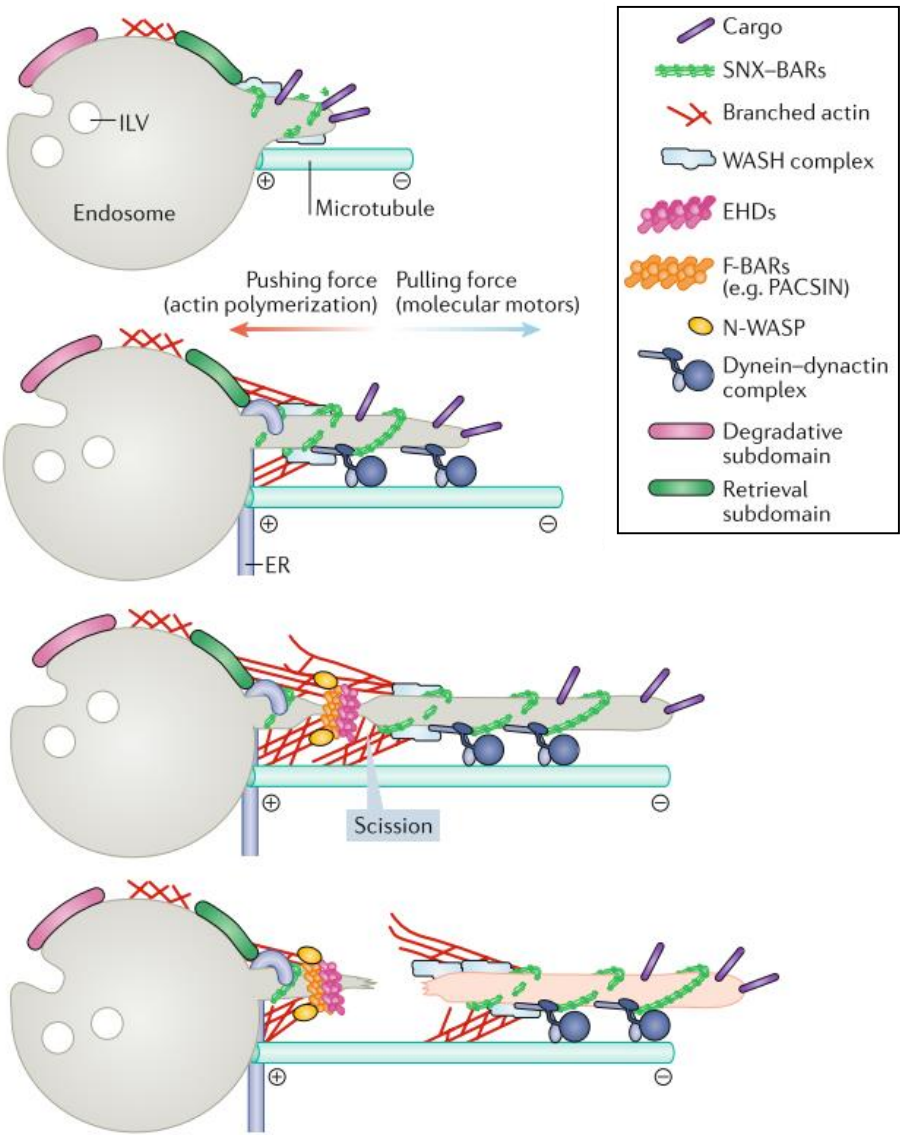

Figure 1.21. A model for endosomal tubule formation. A retrieval subdomain is formed on the endosome by branched actin. BAR-containing sorting nexins (SNX-BARs) induce curvature. Pushing forces are exerted by WASH-induced actin polymerisation, and opposing pulling forces by microtubule motors (a dynein-dynactin complex in this case) promote tubulation and create tension. Fission is promoted by EHD proteins, WASH and N-WASP-induced actin polymerisation, and constriction is promoted by ER tubules. From Cullen and Steinberg (2018).

1.4.3.4 Unanswered questions on recycling pathways

Sorting platforms, coats, fission factors, motors and tethers have been identified in the recycling of specific cargoes. However, the precise nature of the distinct endosomal routes is far from understood. Endosomes are dynamic compartments that constantly fuse with each other and that are subjected to maturation processes. As a consequence, the nature of a specific endosome changes fast and compartments at intermediate maturation stages are found in cells. This complicates the characterisation of recycling routes, because the origin and destination transport intermediates are difficult to identify. It seems clear that there is rapid recycling from EEs soon after endocytosis, but the pathway followed by cargoes during slow recycling is not well defined (Naslavsky and Caplan, 2018).

The definition of the RE is particularly vague. In many cells, including fibroblasts, REs accumulate around the MTOC, grouped in the endocytic recycling compartment (ERC). The ERC is a mesh formed by tubular and vesicular compartments. The origin of these membranes is under debate and can be explained by three general models. First, REs might be independent compartments that receive transport carriers form EEs or the TGN (model 1 in **Figure 1.22**). In this model the identity of the ERC could be maintained by recycling the transport machinery back to the organelle of origin or to a cytosolic pool, and by converting PIPs and inactivating rabs that reach the new organelle. The identity of REs would also be maintained if the delivery of cargo occurred through a ‘kiss-and-run’ mechanism in which there was no membrane exchange.

An independent ERC could also be constituted by EE-derived membranes (model 2 in **Figure 1.22**). That is, tubulovesicular compartments that contain RE markers, such as rab11 and PI4P, might be formed in EEs, transported to the MTOC and fused with pre-existing REs. Models 1 and 2 are supported by the fact that the fission of tubules by EHDs and dynamin is required for the transport of cargo to the perinuclear region during recycling (Sharma, Naslavsky and Caplan, 2008; Chi *et al.*, 2014). Similarly, retromer and SNXs-mediated tubulation allows transport to the MTOC region (Gallon and Cullen, 2015). Evidence that SNARE proteins are also required for transport from EEs to the perinuclear region also points in this direction (Prekeris *et al.*, 1998; Zeng *et al.*, 2003).

A third model to explain the origin of ERC membranes is the maturation of EEs towards REs (model 3 in **Figure 1.22**), similar to the process of LE and lysosome formation in the degradation pathway. In this model the ERC is not completely independent from the pool of EE, but rather a continuation of it. Transport carriers towards the PM would be generated from endosomes at different stages of maturation. The maturation into REs would involve the acquisition of new markers, such as rab11 and rab8, and the conversion of PI3P to PI and then PI4P. EEs would change shape into a more tubular form. They would also be transported to the perinuclear region, presumably along microtubules. In fact, a group of evidence shows that microtubule motors are required for cargo transport towards

the MTOC, but it is not clear whether whole EEs are transported or only carriers derived from these. In favour of the maturation model is the fact that a particular mutation in rab11 causes EEA1-positive membranes to accumulate at the perinuclear region, suggesting the maturation process is affected (Pasqualato *et al.*, 2004). In addition, a study by van Weering, Verkade and Cullen (2012) shows that SNX4 promotes tubule formation from endosomes undergoing a rab4-to-rab11 transition. The models are not mutually exclusive, as EE to RE carriers could be formed as maturation progresses. Also, it could be that only a part of the EE pool matures into RE while the rest preserves its identity.

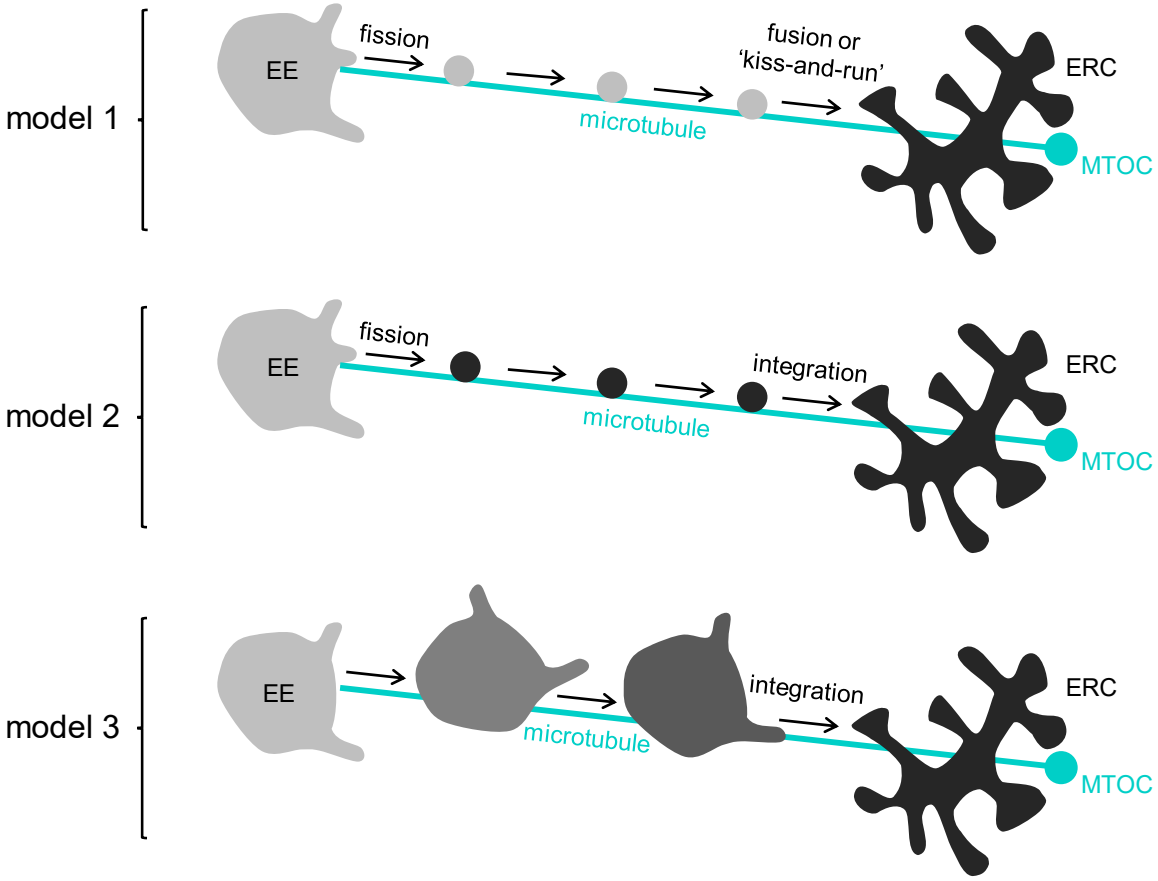

Figure 1.22. Models of transport from the EE to ERC. Three hypothetical models of cargo transport from EEs to REs are illustrated. The models also account for the origin of the membranes that give rise to the ERC. All models include membrane transport towards the MTOC area along microtubules, but differ in the nature of the intermediate carriers or organelles.

Another uncertainty is the relationship between budding machineries and whether they form part of the same or distinct recycling routes. Retromer and retriever are known to form part of different routes, while the CCC complex and SNXs can work together or independently of them (Chen, Healy and Collins, 2019). The relationship of these complexes with the clathrin coat is particularly obscure. On one hand, clathrin or clathrin adaptors and retromer are known to mediate retrograde traffic of common cargoes (Popoff et al., 2009), and RME-8 is known to link clathrin and SNXs in retrograde traffic (Håberg, Lundmark and Carlsson, 2008;

Skånland et al., 2009; Danson et al., 2013). On the other hand, clathrin was found not to be required for SNX-BAR-dependent carrier formation (McGough and Cullen, 2013). These conflicting results might indicate that clathrin and SNX-BARs (maybe in association with the retromer) function in the same retrograde routes but that the function of clathrin is not on membrane bending but rather sorting, or that they function in different routes. A further uncertainty is the interplay of the coats with fission factors and with the actin polymerisation machinery, as well as the role of the different NPFs in endosomal sorting and tubulation. In particular, both WASP and WASH are found in endosomes and are necessary for sorting, but their molecular mechanisms are not well-established and differentiated.

Finally, little is known about the second step in recycling, from the RE to the PM. Although EHD1 and the exocyst are involved, no coats or transport intermediates are specifically found for this route (Caplan et al., 2002; Prigent et al., 2003). The absence of a RE to PM coat would be consistent with the maturation model (model 3), in which it would be difficult to differentiate between carriers derived from EEs and REs. Another open question is the relationship between the ERC and the TGN. At least some cargoes are delivered from the RE to the TGN, either through transport intermediates, 'kiss-and-run' or a partial overlap of both organelles. Cargoes for endosomal recycling would then join the secretory pathway for their transport back to the PM. Many studies refer to recycling pathways through the TGN. In fact, this is the main route for recycling in yeast (Zeng et al., 2003; Arighi et al., 2004; Dyve et al., 2009). In addition, markers like rab11, rab8, arf1 and PI4P are shared between RE and TGN. These evidences point towards a physical and functional overlap between TGN and REs (Chen et al., 1998; De Graaf et al., 2004; Cao et al., 2005). Furthermore, a recent study shows that REs have the ability to attach and detach from Golgi membranes in mammals. This feature was already known of TGN membranes in plants, proving that the difference between RE and TGN should be reconsidered (Fujii et al., 2020).

1.5 Endosomal trafficking in the control of cell adhesion, migration and cytokinesis

The reorganisation of molecules at the cell surface is part of many physiological processes, which therefore depend on the regulation of endosomal transport. Cell differentiation during development or tissue homeostasis implies changes in size, shape, contacts and polarisation of the PM. The control of endocytosis, secretion and recycling has been proven to be of importance for these rearrangements (Lecuit and Pilot, 2003). Endocytic recycling, in particular, allows the establishment of dynamic domains in the PM. For instance, it maintains a specialised leading edge in migrating cells or a growth cone in developing nerves (Jones, Caswell and Norman, 2006; Winckler and Choo Yap, 2011). Finally, the PM is remodelled in the creation of the cleavage furrow during cell division (Frémont and Echard, 2018). The following sections review the role of endosomal trafficking in the regulation of cellular processes of special relevance in this thesis.

1.5.1 Endosomal traffic in the regulation of cell adhesions

Adhesions communicate the cell with the extracellular matrix (ECM) or the neighbouring cell and influence the organisation and function of the cytoskeleton, working as signalling hubs. There are four types of anchoring junctions. Adherens junctions and desmosomes are cell-cell junctions and are mediated by proteins of the cadherin family, whereas focal adhesions and hemidesmosomes are cell-matrix junctions and require integrins (**Figure 1.23A**; Alberts et al., 2019).

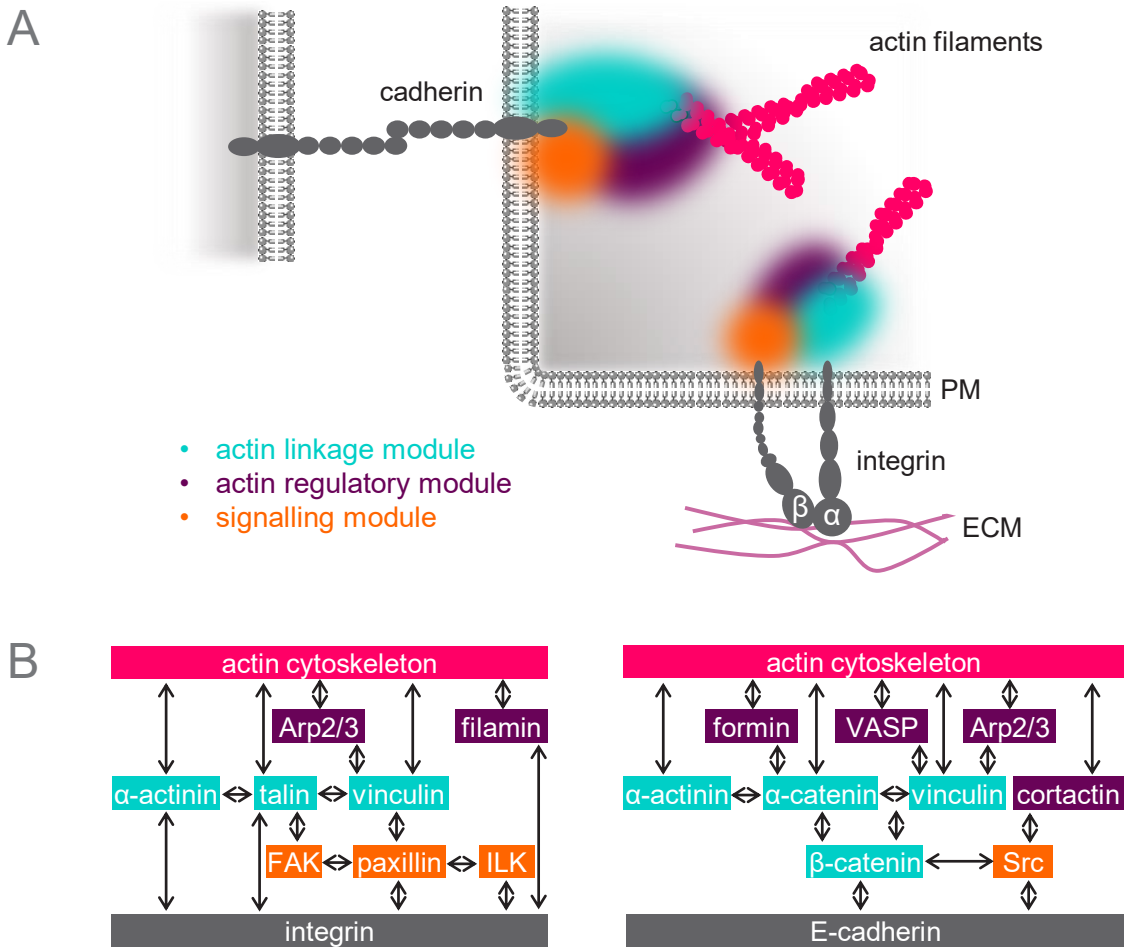

Figure 1.23. Modular structure of cell adhesions. A. Cell-cell contacts are mediated by cadherins and cell-ECM contacts are mediated by integrins, formed by an α and a β chain. The intracellular domains of both cadherins and integrins interact with proteins that link and regulate the actin cytoskeleton. These proteins are classified into the actin linkage (in blue), the actin regulatory (in purple) and the signalling (in orange) modules. **B.** The scheme shows examples of proteins belonging to each of the mentioned modules in the case of integrin-mediated adhesions and E-cadherin-mediated adhesions. The interactions between the different proteins and modules are also shown. Adapted from Bachir *et al.* (2017).

Cadherins from opposing cells interact through their extracellular domains in the presence of Ca^{2+}. Different cadherins are expressed in different tissues, for example, fibroblasts mainly express N-cadherin. The intracellular domains of cadherins are attached to catenins

like α-catenin, β-catenin or p120-catenin, which regulate their function and link them to the cytoskeleton (**Figure 1.23**; Gooding, Yap and Ikura, 2004; Ishiyama and Ikura, 2012). Integrins, on the other hand, have an α and a β chain. Their extracellular domain binds to their ligands in the ECM, like collagen or fibronectin (**Figure 1.23**). This binding induces a conformational change in the integrin that starts an outside-in signal. There is also an inside-out signalling by which cells regulate the activation state of their integrins and therefore their attachment (Margadant *et al.*, 2011). The intracellular domains of cadherins and integrins are linked to the cytoskeleton. The actin cytoskeleton, in particular, takes part in adherens junctions and in focal adhesions. Desmosomes and hemidesmosomes are linked to intermediate filaments (Alberts *et al.*, 2019). The intracellular part of adherens junctions and focal adhesions can be divided into modules: actin linkage, actin regulatory and signalling modules, whose composition varies (**Figure 1.23**). Examples of proteins of each module are shown in **Figure 1.23B** (Bachir *et al.*, 2017).

Many cellular processes rely on the regulation of cell adhesion. Cell migration, for instance, requires a fine turnover of cell-matrix adhesion, as described in section 1.5.2. In the particular case of collective migration, adherens junction turnover ensures cohesion and rapid migration (Peglion, Llense and Etienne-Manneville, 2014). Also during morphogenesis and growth there is a need to redistribute cell contacts in order to change the architecture of the tissue (Katsuno-Kambe and Yap, 2020). Polarisation of cell-cell contacts allows differentiation of epithelial cells, neurons, etc. (Suyama *et al.*, 2002). Therefore, cell adhesion regulation is important in Epithelial-to-Mesenchymal Transition (EMT). This process involves changes in contacts and cadherins and has a direct effect on the migration of cancer cells and their invasiveness (Nieto *et al.*, 2016; Lindsay and McCaffrey, 2017). The regulation of cadherin availability is a way of regulating cell adhesion. In effect, cadherin internalisation breaks cell junctions, whereas cadherin recycling promotes the formation of new ones. However, this cadherins cycle also maintains homeostasis (Cadwell, Su and Kowalczyk, 2016).

CME is best described for the internalisation of E-cadherin, N-cadherin and VE-cadherin. Their endocytosis depends on clathrin, dynamin and AP-2. The adaptors numb and dab2 are also known to be required to maintain apico-basal polarity of cadherins in epithelial cells, probably by regulating their endocytosis (Traub, 2003). As for the implication of the actin cytoskeleton, N-WASP and cortactin are required for the internalisation of *Lysteria monocytogenes* through its binding to E-cadherin (Sousa *et al.*, 2007). In mammals, cadherin internalisation is controlled by p120-catenin. It impedes AP-2 binding and thus blocks cadherin internalisation. p120-Catenin is also thought to impede cadherin ubiquitination by E3-ligases that would lead to internalisation and degradation. Other p120-catenin family members, such as δ-catenin, p0071 and ARVCF, also block cadherin internalisation. β-catenin, on the other hand, exerts a different regulation. It is co-trafficked with cadherins after their biosynthesis, from the ER to the PM, and stabilises them in the junctions (Cadwell, Su and Kowalczyk, 2016).

Less is known about cadherin recycling. The adaptor AP-1B is required for trafficking of E-cadherin in epithelial cells, as well as the retromer (Ling *et al.*, 2007; Lohia, Qin and Macara, 2012). The trafficking of E-cadherin and N-cadherin depends on rab5 and rab11 (Lock and Stow, 2005; Kawauchi *et al.*, 2010). E-cadherin can also be recycled in a rab4a and PI4P-dependent manner (Kachhap *et al.*, 2007). Interestingly, a different route has been demonstrated for the recycling of E-cadherin in epithelial cells. E-cadherin is delivered from the TGN to the RE, and then to the PM in order to maintain polarisation (Suyama *et al.*, 2002). Furthermore, N-cadherin recycling is mediated by rab5, rab4 and rab11. Rab14, which works between rab5 and rab11 in the TfnR recycling pathway, is also required for N-cadherin trafficking (Linford *et al.*, 2012). The rab11 and rab14 effector RCP (Rab Coupling Protein) mediates recycling of N-cadherin, EGFR and $\alpha_5\beta_1$ integrin to promote EMT and invasion (Lindsay and McCaffrey, 2017). E-cadherin and DE-cadherin recycling from REs depends on the exocyst complex (Langevin *et al.*, 2005; Wang, Chen and Margolis, 2007). Desmosomal cahderins, on the other hand, are internalised through CIE, probably mediated by flotillins (Delva *et al.*, 2008; Völllner *et al.*, 2016).

1.5.2 Endosomal trafficking in cell migration

The importance of endosomal trafficking in cell migration generally refers to the recycling of adhesion molecules, integrins or cadherins, and the recycling of RTKs. Recent studies have also shown that the Golgi apparatus positions to the leading edge in cell migrating in 2D substrates (Xing *et al.*, 2016).

Since migration relies to a great extent on propelling and contractile forces produced by the cytoskeleton attached to focal adhesions, integrins play a key role. Integrins in the PM are constantly reorganised during cell migration. They are endocytosed and recycled back to the PM, with only a small percentage following the degradation pathway. Many integrins are endocytosed by CME, although CIE and macropinocytosis are also common (Paul, Jacquemet and Caswell, 2015; Moreno-Layseca *et al.*, 2019). All β_1 integrin tails contain the NPxxY/NxxY motif to bind adaptors for their endocytosis, but a number of additional mechanisms ensure the specificity of the process (Moreno-Layseca *et al.*, 2019). For example, only some α chains with the YxxØ motif are bound by AP-2. Among other adaptors involved are dab2 and numb (Nishimura and Kaibuchi, 2007; Sandri *et al.*, 2012; Paul, Jacquemet and Caswell, 2015). The mechanisms for integrin trafficking are very diverse and context-specific. Accordingly, integrins can be recycled through the rab4, rab11 or TGN pathways, as well as unconventional pathways. Both retromer and SNX-17-retriever have been shown to mediate integrin sorting to elude the degradation pathway (**Figure 1.24**; Shafaq-Zadah *et al.*, 2016; McNally *et al.*, 2017).

The most studied integrin in the context of cell migration is $\alpha_5\beta_1$ integrin (**Figure 1.24**). It promotes the formation of ruffles and fast invasion. In fact, its recycling is enhanced by the mutated oncogene p53. $\alpha_5\beta_1$ integrin is co-trafficked with RTKs, and its recycling implicates

a MAP kinase cascade that leads to rhoA activation at the cell front. This activates formin-mediated actin nucleation that allows the formation of filopodia for 3D invasion (Paul *et al.*, 2015). Also, active $\alpha_5\beta_1$ integrin is trafficked in rab25-containing endosomes and CLIC3-positive lysosomes towards the cell rear, where src signalling induces a forward movement (Dozynkiewicz *et al.*, 2012). Ligand free-β_1 chains are recycled to the leading edge in a retromer, rab6 and syntaxin-16-dependent manner, and they promote directional migration in 2D substrates (Shafaq-Zadah *et al.*, 2016). Interestingly, $\alpha_v\beta_3$ integrin restricts the function of $\alpha_5\beta_1$ integrin. It is recycled through the fast route to the leading edge to promote rac and Arp2/3-dependent lamellipodia formation, conferring persistency in 2D migration. When $\alpha_v\beta_3$ integrin is inhibited, there is an increase in $\alpha_5\beta_1$ integrin recycling and rhoA signalling, which promotes a more random migration based on ruffles rather than a defined lamellipodia (White, Caswell and Norman, 2007). The outcome depends on the context. While $\alpha_v\beta_3$ integrin promotes invasion in low-fibronectin substrates, $\alpha_5\beta_1$ integrin does so in substrates with a high content of its ligand (Wilson, Allen and Caswell, 2018). It was also recently proposed that rab11-positive endosomes remain at the front of the cell and traffic active $\alpha_5\beta_1$ integrin, FAK and src kinases that are able to rapidly form new focal adhesions in a polarised way (**Figure 1.24**; Nader, Ezratty and Gundersen, 2016).

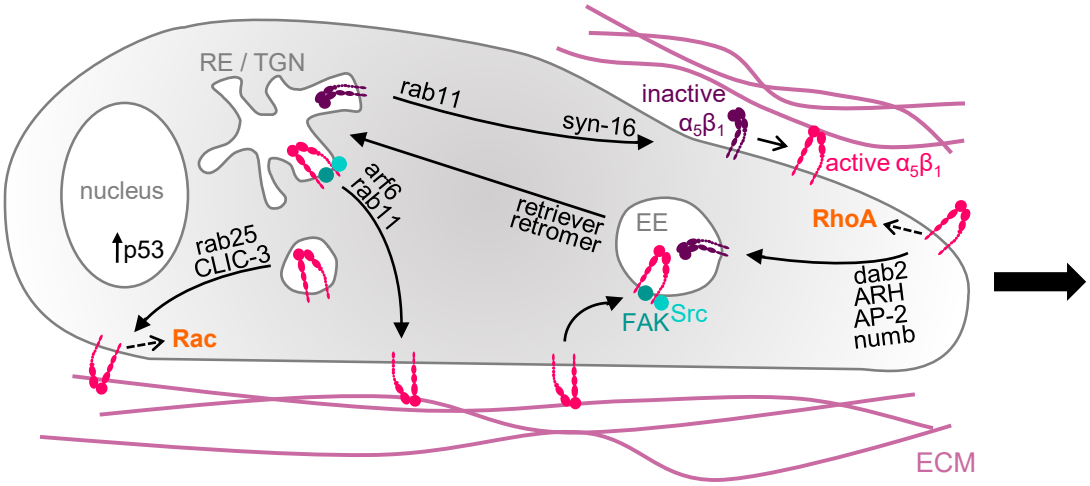

Figure 1.24. Integrin trafficking in cell migration. The internalisation and recycling pathways of $\alpha_5\beta_1$ integrin are shown in a cell that migrates through the ECM. Integrins activate in contact with their ligands in the ECM. Active $\alpha_5\beta_1$ integrin activates rhoA at the cell front to promote invasion. The internalisation of $\alpha_5\beta_1$ integrin can depend on clathrin adaptors like dab2, ARH, AP-2 and numb, and usually involves the inactivation of the integrin. It is recognised at EEs by retriever or the retromer and trafficked to the RE of the TGN, from which it is recycled to the plasma membrane in an arf6 and rab11-dependent way. Some $\alpha_5\beta_1$ integrin can retain their active conformation along their intracellular trafficking by maintaining their interaction with FAK and src. Finally, $\alpha_5\beta_1$ integrin can also be transported to the rear of the cell in rab25 and CLIC3-positive endosomes or lysosomes in order to activate rac. The recycling of $\alpha_5\beta_1$ integrin is promoted when the expression of the oncogene p53 is high.

The importance of the regulation of actin polymerisation in cell migration is highlighted by the effect that Arp2/3 inhibitors have on it. Indeed, gadkin inhibits Arp2/3 in endosomal vesicles and enhances its presence in the PM, thus promoting migration and cell spreading (Maritzen *et al.*, 2012). Arpin is important for cell migration as well, as it is found in WAVE-dependent lamellipodia. In that context, rac activates both WAVE and arpin to maintain a controlled migration speed and to induce turning (Gorelik and Gautreau, 2015). The actin cytoskeleton often responds to extracellular signals mediated by RTKs. Thus, the recycling of RTKs is also used by the cell to modulate migration. For example, leading cells in *Drosophila melanogaster* collective migration of border cells traffic EGFR and PVR through rab5, rab11 and exocyst to the PM. Interestingly, 'adaptative CME' has recently been described as a fast CME route for the EGFR that is mediated by dynamin-1 and the CLC-b to promote migration and invasion in cancer cells, without affecting TfnR trafficking (Sasaki, Hiroki and Yamashita, 2013). Additionally, the RTK c-Met activates rac during its recycling process, thus promoting migration and invasion. c-Met is recruited to lamellipodia through microtubules in rab4 and GGA3-positive endosomes (Parachoniak *et al.*, 2011). Often, the endosomal signalling of RTKs is coupled to the recycling of cadherins or integrins (Wilson, Allen and Caswell, 2018).

In addition to integrins, the regulation of cadherin recycling is important in collective migration and in migration linked to EMT. For example, during collective migration of astrocytes, N-cadherin is continuously recycled from the rear to the leading edge of each cell (Peglion, Llense and Etienne-Manneville, 2014). EMT implicates a change in the cell phenotype that leads to its detachment from the surrounding tissue. It enhances invasiveness and is a common process in cancer metastasis. Rab11-dependent recycling of N-cadherin promotes invasion of lung cancer cells (Lindsay and McCaffrey, 2017). On the other hand, trafficking of the cadherins to the PM in a rab35-dependent manner is downregulated to enhance cell motility (Allaire *et al.*, 2013).

Mesenchymal migration in 3D matrices also relies in protease activity that degrades the matrix. Increased recycling of the transmembrane MT1-MMP (Membrane-Type-1 MetalloProtease) is known to promote invasion. Many endosomal players have been shown to mediate its recycling: rab4, rab5, rab8, KIF5B, WASH and the exocyst, among others (Monteiro *et al.*, 2013; Frittoli *et al.*, 2014; Wang *et al.*, 2017). MTM1-MMP can also be retrieved from LEs or lysosomes for recycling. In fact, in *Caenorhabditis elegans*, MMP-enriched lysosomes are targeted to invadopodia during cell migration (Macpherson *et al.*, 2014). Overall, dynamic endosomal trafficking and recycling of adhesion molecules, small GTPases, RTKs and metalloproteases is well established in promoting migration and invasion.

1.5.3 Endosomal traffic in cytokinesis

Endosomal trafficking is required for membrane remodelling and for the transport of the necessary machinery during cell division. The rate of CME and recycling is diminished during metaphase and anaphase, and recovered during cytokinesis. In fact, membrane trafficking is of great importance to complete cytokinesis. Whereas the initial furrow contraction requires acto-myosin forces, late cytokinesis strongly depends on membrane trafficking (Pollard and O'Shaughnessy, 2019; Rizzelli *et al.*, 2020). There is an accumulation of endosomes and a variety of rabs at the intercellular bridge prior to abscission. These probably come from two prior endosomal clusters at the poles of the mitotic spindle. Interestingly, Golgi stacks adopt the same localisation (Montagnac, Echard and Chavrier, 2008).

The best characterised in cytokinesis is the rab11 recycling route, required for a constriction of the bridge termed 'secondary furrow ingression'. Activation by the rab11 GEF REI-1 induces the delivery of endosomes containing rab11 and its effector FIP3 to the intercellular bridge. FIP3-positive endosomes also contain arf6. These endosomes come back and forth along the bridge until they become stable at the end of abscission, a movement mediated by the microtubule motors dynein and KIF5B (Wilson *et al.*, 2005; Wilson, Allen and Caswell, 2018). One of the cargoes identified for rab11-FIP3 endosomes is p50rhoGAP, which inhibits rhoA at the abscission site, thus reducing actin polymerisation. The loss of actin at the abscission site, next to the midbody, is a requirement for ESCRT-III recruitment and abscission (Schiel *et al.*, 2012). Previous to rab11 endosomes, rab8-containing endosomes stabilise the intercellular bridge. They bind MICAL3, which docks them to the centralspindlin complex (Liu *et al.*, 2016). Recycling through rab35-containing endosomes is also required in cytokinesis, probably through PIP metabolism regulation. An enrichment in $PI(4,5)P_2$ allows recruitment of proteins that are essential for furrow stability. $PI(4,5)P_2$ inhibits cofilin and promotes actin polymerisation. However, as constriction progresses, rab35 mediates the trafficking of OCRL, which catalyses the hydrolysis of $PI(4,5)P_2$, required to decrease actin polymerisation and complete abscission (Dambournet *et al.*, 2011). In addition, rab35 endosomes transport MICAL1, which oxidises and induces actin depolymerisation and ESCRT-III recruitment (Frémont *et al.*, 2017).

The exocyst complex mediates tethering of REs. Since abscission is dependent on the SNARE proteins VAMP3 and VAMP7, they are likely to mediate the fusion of endosomes to the PM at the cleavage furrow (Boucrot and Kirchhausen, 2007). The final constriction of the intercellular bridge involves the ESCRT machinery. ESCRT-III subunits are delivered in rab5 and exocyst-containing endosomes (Kumar *et al.*, 2019). Interestingly, syntaxin-16 links rab11-FIP3 endosomes, the exocyst and ESCRT together and to the midbody. The function of ESCRT-III in abscission is regulated by TTC19, a protein recruited by FYVE-CENT. FYVE-CENT, in turn, is delivered in PI3P and VPS34-containing endosomes (Sagona *et al.*, 2010). While ESCRT-III filaments remodel the membrane, VPS4 produces the force to complete abscission (Mierzwa *et al.*, 2017).

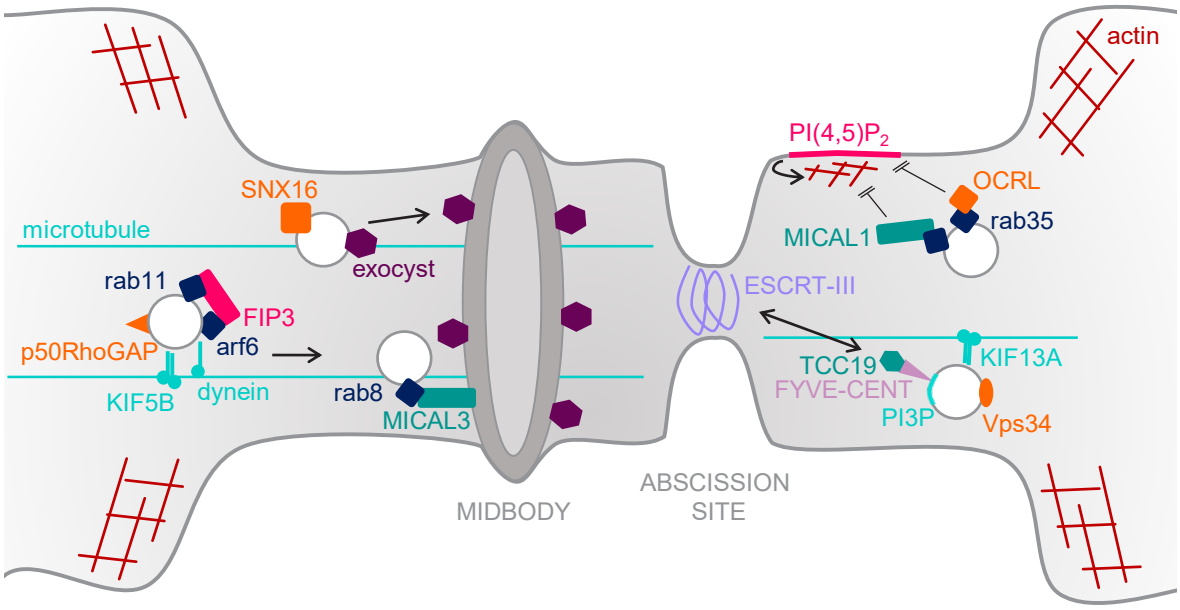

Figure 1.25. Endosomal traffic in late cytokinesis. The figure shows the intercellular bridge between the two daughter cells in mitosis. Constriction of the midbody requires the delivery of rab11, arf6 and FIP3-containing endosomes towards the plus end of microtubules by dynein and KIF5B motors. These and other vesicles carry p50rhoGAP, SNX16, exocyst and MICAL3. The fusion of the vesicles is mediated by the exocyst. In order to complete abscission, F-actin depolymerises at the intercellular bridge. Depolymerisation is promoted by MICAL1 and hydrolysis of $PI(4,5)P_2$, in turn catalysed by OCRL. Both OCRL and MICAL1 are transported in rab35-positive vesicles. The ESCRT-III complex further constricts the abscission site. ESCRT-III is regulated by TCC19, which is carried to the site in vesicles with PI3P, VPS34 and FYVE-CENT along microtubules.

1.6 Kazrin

Kazrin cDNA was first found in a screening looking for human brain genes and named KIAA1026 (Kikuno *et al.*, 1999). This cDNA corresponded to the later named kazrin K isoform (Cho *et al.*, 2011). The kazrin gene (Kazn) is located in chromosome 1 in human and chromosome 4 in mouse. Kazrin is only present in Animalia, and it is highly conserved in mammals. For instance, human kazrin C is 98% identical at the protein level to the amino acid sequence of mouse kazrin (Groot *et al.*, 2004). Kazrin mRNA is found in most tissues and its expression is specifically high in the central nervous system (Bgee and EMBL Expression Atlas data bases).

Kazrin pre-mRNA is alternatively-spliced in up to seven human variants with experimental protein evidence. These isoforms and their mouse equivalents are listed in **Table 1.5**. Exons 2 to 8 of human kazrin are spliced together, whereas four different first exons can be formed by alternative splicing. mRNAs including exons 1c or 1d contain a start codon at the beginning of exon 2 and encode for kazrin C and D, which have an identical amino

acid sequence and are referred to as kazrin C from now on. Different combinations of the remaining exons produce proteins with extra N or C-terminal sequences. Therefore, all isoforms bear most of the sequence of kazrin C as their core, supplemented with additional functional fragments (**Figure 1.26A**).

Splice variant	Nucleotide reference	Protein length (aa)	Predicted molecular mass (kDa)	Equivalent mouse variant
Kazrin A	NM_015209.2	421	46.7	Kazrin 2
Kazrin B	NM_001018000.3	415	37.0	Kazrin 3
Kazrin C/D	NM_001018001.2	327	37.0	9030409G11Rik
Kazrin E	NM_201628.3	775	86.3	Kazrin 1
Kazrin F	NM_001370229.1	412	46.2	-
Kazrin G	NM_001370230.1	304	41.6	-
Kazrin H	NM_001370231.1	420	54.6	-

Table 1.5. Kazrin isoforms. For each isoform, the nucleotide reference in the RefSec format, the length of the resulting protein and the equivalent mouse variant are shown.

Although there is no resolved structure of kazrin and it shows little homology to other protein families, secondary-structure predictions allow the identification of several domains (**Figure 1.26A**). Importantly, all kazrin isoforms contain a coiled-coil region (Lupas, Van Dyke and Stock, 1991; Cho *et al.*, 2010). Coiled-coils are formed by two or three α-helices that wind around each other due to the combination of charged and hydrophobic residues. This region is similar to regions found in other protein families, such as FERM, SMC, HOOK, the myosin tale and SbcC (Cho *et al.*, 2010). The coiled-coil region mediates homo and heterotypical interactions (Cho *et al.*, 2010). Indeed, all tested kazrin isoforms can interact with each other (Nachat *et al.*, 2009). Most isoforms contain a sequence of positively charged amino acids, from now on referred to as the poly-K sequence (**Figure 1.26B**). This sequence resembles those that might interact with lipids (Chapman *et al.*, 1998), although it has also been proposed to be a nuclear localisation signal (Groot *et al.*, 2004). Finally, most kazrin isoforms also contain a cluster of acidic residues that this laboratory has found to be similar to those found in NPFs such as N-WASP or WASH that are required for the interaction with the Arp2/3 complex (**Figure 1.26B**).

Despite their similarities, kazrin isoforms vary in their N and C-terminal regions (**Figure 1.26A**). Kazrin F, for instance, contains 97 extra amino acids at its N-terminus (Wang *et al.*, 2009). On the other hand, kazrin E contains seven extra exons inserted in exon 8, which encode for three SAM motifs (sterile α motifs) that conform a LHD domain (Liprin-Homology Domain; Nachat et al. 2009). This similarity to the liprin protein family has led to the proposal of liprin α and β as evolutionary-related genes (Nachat *et al.*, 2009).

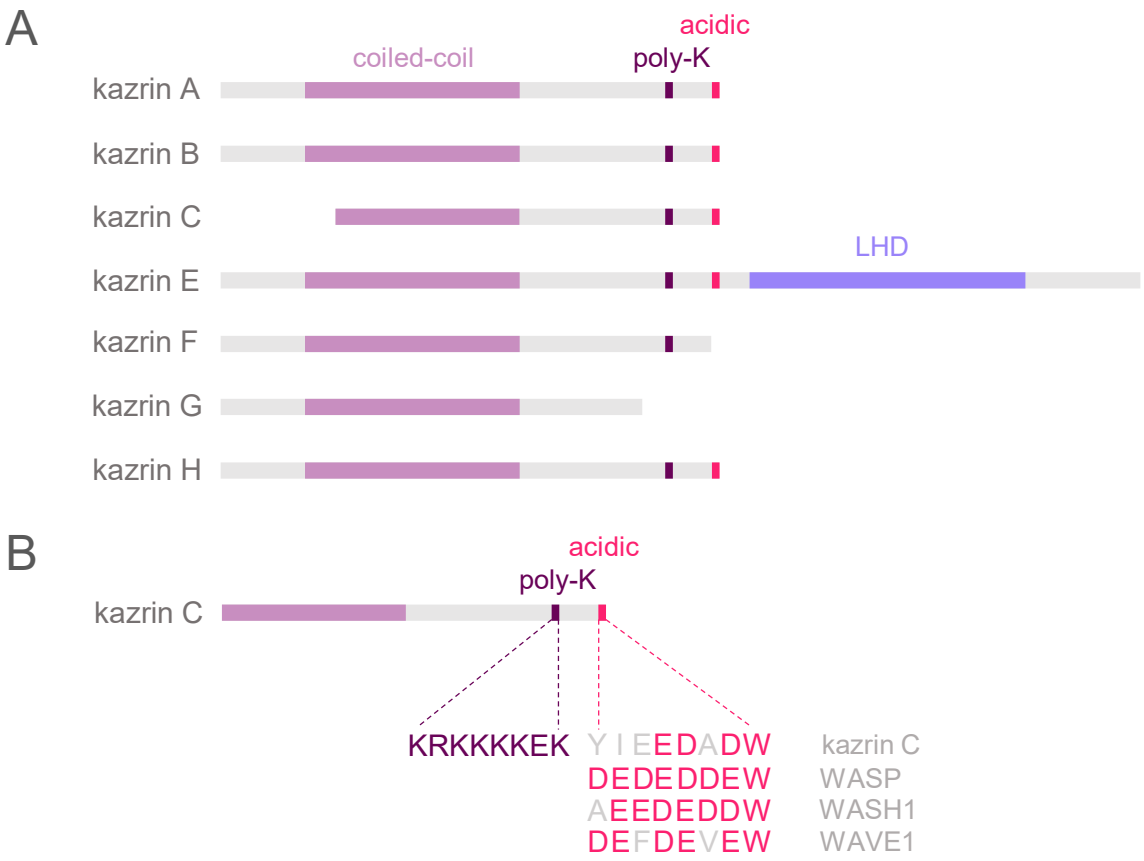

Figure 1.26. Domain structure in kazrin variants. A. Kazrin human isoforms and their domains. All isoforms contain a coiled-coil domain. Most isoforms contain a poly-K and an acidic domain. Kazrin E contains, in addition, a C-terminal LHD. **B.** Detailed domain structure of kazrin C, where the amino acid sequence of the poly-K and the acidic regions is shown. The latter is compared to similar sequences found in NPFs and the acidic residues are highlighted in pink.

Regarding its subcellular localisation, most tested kazrin isoforms have been shown to localise to the nucleus, cell membrane, desmosomes and adherens junctions (Groot *et al.*, 2004; Gallicano *et al.*, 2005; Nachat *et al.*, 2009; Cho *et al.*, 2010). Kazrin K does not contain the proposed NLS domain and is indeed found to be excluded from the nucleus in MCF7 cells (Cho *et al.*, 2010). The localisation of kazrin has extensively been studied in the mouse embryo (Gallicano *et al.*, 2005). In unfertilised mouse eggs, kazrin shows a dotted pattern along spindle microtubules. However, it is excluded from the spindle right after egg activation, and acquires a perispindle localisation where the cytokinetic ring is forming (Gallicano *et al.*, 2005). This data suggests a role for kazrin during cell cycle and division. At the four-cells stage, kazrin co-localises with actin, suggesting that kazrin is in association with both the tubulin and the actin cytoskeleton (Gallicano *et al.*, 2005). As development progresses, kazrin is found at the nuclei when these start to form. Finally, kazrin is located in cell-cell junctions in differentiated cells, as shown by its co-localisation with desmoplakin (Groot *et al.*, 2004; Gallicano *et al.*, 2005), a core desmosomal component, and with E-cadherin ARVCF-catenin (Gallicano *et al.*, 2005; Cho *et al.*, 2010), both adherens

junction components. Interestingly, kazrin localisation varies between cell types, being more prominent in the nucleus, the cytoplasm, or cell-cell junctions depending on the tissue (Gallicano *et al.*, 2005). Moderately overexpressed kazrin shows a similar localisation to that of endogenous kazrin (Groot *et al.*, 2004; Sevilla *et al.*, 2008). Also, both N and C-terminal tagged kazrin produce similar phenotypes when overexpressed (Sevilla *et al.*, 2008).

1.6.1 Kazrin in endocytosis

Most literature about kazrin refers to its role in cell-cell junctions and epidermal differentiation. Notably, a screening performed in this laboratory linked kazrin to endocytosis (Schmelzl and Geli, 2002). The screening was designed to identify proteins involved in CME in humans. Specifically, they looked for human brain cDNAs that would block TfnR endocytosis when overexpressed. To that end, an expression library with partial cDNAs from human brain, with an average size of 1.2 kb, was cloned in a vector bearing the SV40 origin of replication, which can be amplified in COS-7 cells. One day upon transfection, cells were exposed to a fluorescently-labelled antibody against the Tfn receptor. In intact COS7 cells, TfnR is continuously internalised by CME and recycled back to the PM from EEs and REs following different pathways. Because internalisation of the Tfn receptor is very efficient, most of the receptor accumulates in the RE at steady state. However, impairment of the uptake step of CME results in the accumulation of the receptor at the cell surface. Cells expressing human cDNAs that caused accumulation of the TfnR at the PM were detected and selected by Fluorescence-Activated Cell Sorting (FACS) and the plasmids encoding such cDNAs were recovered by extraction and electroporation in *E. coli* (**Figure 1.27**). The individual cDNAs were further analysed and one of the encoded proteins was the thus far uncharacterized KIAA102, nowadays known as kazrin C.

Bioformatic analysis of the polypeptide showed, as already mentioned, a coiled-coil region, a poly-K sequence and an acidic sequence at the C-terminus (**Figure 1.26B**). Possibly, the poly-K sequence could interact with lipids, whereas the acidic sequence could interact with the actin polymerisation machinery. Therefore, both could potentially mediate a role for kazrin C in endocytosis.

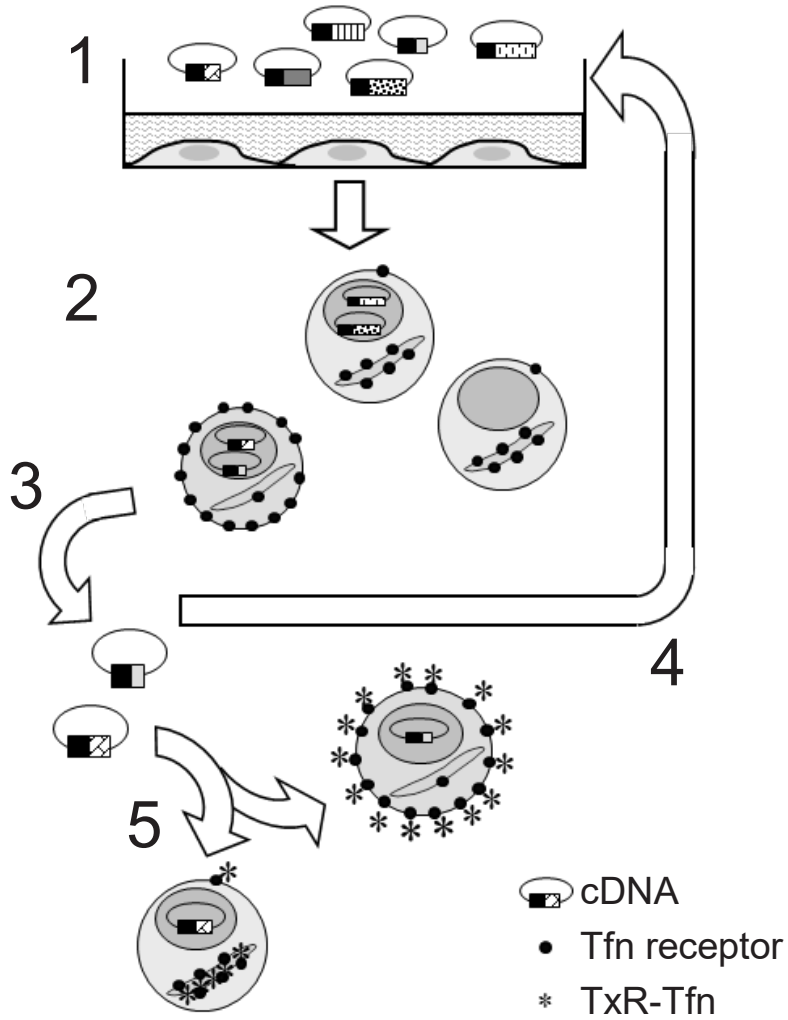

Figure 1.27. Procedure of the genetic screening in search for human proteins involved in CME. COS-7 cells were transfected with a library of partial cDNAs fused to GFP (1). One day after transfection, cells accumulating TfnR at the cell surface were selected. Either TfnR was detected by incubation with an antibody on secondary antibody-coated dishes, or the cells were labelled with CY5-Tfn and subjected to FACS (2). Selected cells were lysed and plasmids recovered by electroporation into *E. coli* (3). Plasmids from individual colonies were pooled and subjected to a new round of selection (4). After a second round of selection with individual plasmids, these were purified in order to analyse the effect of their overexpression under the fluorescence microscope using TxR-Tfn (5).

1.6.2 Kazrin in cell-cell junctions

Several studies have reported an association of kazrin with the cytoskeleton, most of which refer to a role for kazrin in cell-cell contacts. Kazrin is both associated to desmosomes (Groot *et al.*, 2004) and to adherens junctions (Cho *et al.*, 2010) depending on the cell type under analysis. Kazrin C is located in desmosomes in keratinocytes and forms part of the epidermal cornified envelope (Groot *et al.*, 2004), which is a layer of insoluble cross-linked

proteins in the inner surface of the PM of keratinocytes (Kalinin, Kajava and Steinert, 2002). Interestingly, kazrin overexpression prevents the recruitment of desmoplakin to cell-cell borders, although it does not alter E-cadherin recruitment (Sevilla, Nachat, et al. 2008). In fact, kazrin has been found to directly interact with envoplakin and periplakin (Groot *et al.*, 2004). Specifically, there is a direct interaction between aminoacids 89 to 239 in kazrin C and the N-terminal region of periplakin (Groot *et al.*, 2004). Desmoplakin, envoplakin and periplakin are all members of the plakin protein family and act as a link between cytoskeletal networks and adhesive sites. Plakins contain an N-terminal region that binds desmosomes and the actin cytoskeleton, a C-terminal region that binds microtubules and intermediate filaments, and an intermediate region with a coiled-coil domain that mediates homo and heterodimerisation (Boczonadi and Määttä, 2016). Kazrin is proposed to be mediating the function of periplakin with the actin cytoskeleton, thus far unknown. This idea is supported by the observation that kazrin localises at actin-based structures such as microvilli (Groot *et al.*, 2004).

A functional link between kazrin and the actin cytoskeleton has also been discovered. As demonstrated by Sevilla, Nachat, et al. (2008), kazrin A, B or C overexpression in keratinocytes causes the disappearance of the cortical actin band that is usually present in these cells, as well as a loss in their characteristic cuboidal shape. This phenotype was also observed upon kazrin E overexpression (Nachat *et al.*, 2009) and a similar one upon kazrin F overexpression (Liu *et al.*, 2017). In addition, kazrin overexpressing keratinocytes have less actin stress fibres, which is further confirmed by a decrease in the F-actin/G-actin ratio (Sevilla *et al.*, 2008). Importantly, these phenotypes were shown to be mediated by inhibition of rhoA. Overexpression of dominant-active rhoA (V14rhoA) rescued the effects of kazrin overexpression in cortical actin, cell shape and desmoplakin localisation (Sevilla *et al.*, 2008). Conversely, kazrin knock-down did not affect rho activity or desmoplakin recruitment. It is worth noting that the microtubule network was not visibly affected in this study (Sevilla *et al.*, 2008).

In addition to the study of Sevilla, Nachat, et al. (2008), the work by Cho et al. (2010) in *Xenopus laevis* also links kazrin to cell junctions and rhoA. In particular, they exhibit direct binding of *X. laevis* kazrin A (xkazrinA) to xARVCF-catenin and other members of the p120-catenin family, as well as their co-localisation in cultured cells and in the blastula. The interaction with xARVCF-catenin occurs through the coiled-coil domain of xkazrinA (amino acids 70 to 354). Importantly, they did not find a direct interaction with xβ-catenin, xC-cadherin or desmoglein1 (Cho *et al.*, 2010), suggesting kazrin might not be a core component of adherens or desmosomal junctions. xKazrinA and xARVCF are proposed to be recruited to cell-cell borders through their binding to spectrin, which forms a cytoskeletal web that is closely associated to the PM. The three proteins have been demonstrated to form a complex, and the xkazrinA-spectrin interaction in particular occurs through spectrin domains that are similar to the coiled-coil domains in kazrin (Cho *et al.*, 2010).

Cho et al. (2010) also demonstrated a direct interaction of xkazrinA with the Xp190B rho GAP. With respect to its physiological function, xkazrinA works with xARVCF-catenin and Xp190B rho GAP to maintain ectodermal integrity. xkazrinA seems to promote Xp190B rho GAP association with xARVCF-catenin in order to maintain the actin cytoskeleton and cell-cell junctions (Cho *et al.*, 2010). In fact, xkazrin depletion causes an ectodermal shedding caused by the loss of integrity of the cortical actin cytoskeleton and of cell-cell junctions. The phenotype is rescued by the injection of a dominant negative rhoA or of 190B rho GAP (Cho *et al.*, 2010), in accordance with the results from Sevilla, Nachat, et al. (2008).

Previously mentioned studies showed co-localisation of kazrin with microtubules (Gallicano *et al.*, 2005) and interactions with the microtubule-binding family of plakins (Groot *et al.*, 2004). Additional data by Nachat et al. (2009) reinforces the link between kazrin and the microtubule cytoskeleton. Kazrin E localises to perinuclear filaments identified as acetylated microtubules (Nachat et al. 2009), a particular pool of stable, long-lived microtubules (Janke and Montagnac 2017). Kazrin E is recruited to microtubules through its LHD, and is even able to recruit kazrin A in turn when overexpressed (Nachat et al. 2009).

1.6.3 Kazrin in differentiation and development

Given the effects of kazrin overexpression and depletion in the cytoskeleton and cell-cell contacts, it is not surprising that it plays a role in cell differentiation and development. Kazrin E silencing in the *X. tropicalis* or *X. laevis* embryos impedes gastrula elongation and causes defects in the head, eye, notochord and somites (Sevilla *et al.*, 2008; Cho *et al.*, 2011). Most efforts have been centred in the effect of kazrin knock-down in the development of epidermis and in craniofacial development.

The epidermis becomes disorganised and separated from the underlying mesoderm in *X. tropicalis* (Cho *et al.*, 2011). Interestingly, Sevilla, Nachat, et al. (2008) demonstrate changes in the differentiation state of cultured primary keratinocytes upon overexpression and silencing of kazrin A. Indeed, although kazrin is present in all epidermal layers, its expression is higher in the suprabasal layer, where differentiating cells are. Kazrin expression increases as primary undifferentiated keratinocytes remodel their cytoskeleton in response to Ca^{2+} (Sevilla *et al.*, 2008). While this study uses different approaches to show how kazrin A overexpression promotes differentiation, a later one demonstrates the same phenotypes for kazrin E overexpressing cells (Nachat *et al.*, 2009). First, they observe morphological changes in HA-kazrin A-overexpressing cells, which stretch and extend processes similar to those of differentiated keratinocytes. Also, they find an increase in differentiation markers. Kazrin overexpressing cells show a decrease in their proliferation capacity that is characteristic of terminally-differentiated cells. Finally, these cells have a different behaviour in a flow cytometry analysis due to their smaller size and increased granularity (Sevilla *et al.*, 2008). Importantly, an increased proportion of kazrin siRNA transfected cells have a non-differentiated-like phenotype compared to control cells.

This is shown by their different behaviour in flow cytometry and by the decrease in the expression of differentiation markers, both phenotypes being rescued by the expression of kazrin A (Sevilla *et al.*, 2008). The changes in keratinocyte shape in mice seem to be mediated by the coiled-coil region in kazrin and to be independent of its function in the nucleus (Chhatriwala *et al.*, 2012). The importance of kazrin in epidermal differentiation is highlighted by its altered expression in Lichen planus patients (Danielsson *et al.*, 2017). These patients have a chronic inflammation of oral or genital mucosa that is caused by a defective differentiation in the epithelial barrier. Interestingly, their biopsies show low kazrin expression when compared to controls (Danielsson *et al.*, 2017).

The defects in ectoderm caused by kazrin depletion affect craniofacial development in addition to epidermal development. Cho et al. (2011) demonstrate in *X. laevis* that xkazrin morpholino depletion causes ectodermal shedding and impedes normal neural tube closure. The same phenotype is produced by the depletion of the kazrin interactors xARVCF and xδ-catenin. In fact, xARVCF exogenous overexpression rescues the effects in head and eyes caused by xkazrin depletion (Cho *et al.*, 2011). Importantly, these phenotypes are caused by an incomplete establishment of neural crest cells, which leave the neural tube to develop the craniofacial cartilage and bone, among others. In addition to their defective induction and maintenance, neural crest cells are not able to migrate properly in xkazrin-depleted embryos (Cho *et al.*, 2011).

In the already exposed studies, the molecular mechanisms by which kazrin controls epithelial differentiation have been suggested to involve its role in regulating the actin cytoskeleton and adherens junctions (Sevilla *et al.*, 2008; Cho *et al.*, 2011). However, others have argued that it is rather due to its interaction with microtubules and desmosomes (Sevilla *et al.*, 2008; Nachat *et al.*, 2009). Muscle and notochord defects in *X. tropicalis* embryo are rescued by full-length kazrin A injection. Strikingly, they are also rescued by the injection of a kazrin A mutant that does not bind periplakin (depletion of amino acids 188 to 366), suggesting that this interaction is not required for the development of at least some tissues in *X. tropicalis* (Sevilla *et al.*, 2008). With regards to epidermis development, kazrin depletion is reported to cause an increase in desmoplakin (Sevilla *et al.*, 2008). Consistent with this observation, the association of kazrin E to microtubules has been shown to vary depending on the differentiation state (Nachat *et al.*, 2009). In basal keratinocytes, where microtubules are mainly associated to the centrosome, kazrin E is mostly at desmosomes. As keratinocytes differentiate, kazrin E co-localises with microtubules and is less present at cell-cell borders (Nachat *et al.*, 2009). During differentiation, microtubules form thick layers and coils in a process that is dependent on the kazrin interactor desmoplakin (Lechler and Fuchs, 2007). Desmoplakin recruits centrosomal protein ninein to desmosomes in order to rearrange the microtubule network and kazrin is thought to mediate in this process (Nachat *et al.*, 2009).

1.6.4 Kazrin in EMT

The isoform kazrin F has been linked to apoptosis and EMT. Kazrin depletion increases caspase-3 activity and apoptosis (Wang *et al.*, 2009; Liu *et al.*, 2017), whereas kazrin F overexpression diminishes apoptosis (Liu *et al.*, 2017). Moreover, kazrin F interacts and co-localises with the apoptosis-related proteins ARC and Bax (Q. Wang et al. 2009).

Notably, kazrin F overexpression promotes migration (2D) and invasion (in a 3D matrix) in HeLa and in cervical cancer cells. It also induces a morphological change from cuboidal to spindle-like (Liu *et al.*, 2017). Ultimately, kazrin F promotes the acquisition of EMT-related phenotypes. The opposing phenotypes are caused by kazrin silencing (Liu et al. 2017). In fact, there is a post-transcriptional deregulation of kazrin F mediated by miR-186 that decreases proliferation, migration and invasion (Liu *et al.*, 2017). It also increases E-cadherin while decreases vimentin expression, both characteristic signs of epithelial cells. All these effects are restored by ectopic kazrin F (Liu et al. 2017).

Endogenous kazrin F forms a perinuclear mesh in HeLa cells (Wang *et al.*, 2009), a different localisation to that observed for other isoforms. This might reflect different roles in the cell, but it is also likely that the effects of kazrin F in apoptosis and EMT are connected to its role in cell-cell contacts and differentiation observed for other isoforms. For instance, the effect on neural crest cells establishment and migration in *X. laevis* (Cho *et al.*, 2011) is equivalent to the EMT-related phenotypes produced by kazrin F in HeLa and cervical cancer cells (Liu *et al.*, 2017). The cuboidal shape lost upon overexpression of kazrin is also common for isoforms A, B, C in keratinocytes (Sevilla *et al.*, 2008) and F in HeLa and cervical cancer cells (Liu *et al.*, 2017).

Taken together, kazrin is a protein that is proven to be implicated in cell-cell junctions and in differentiation, and to have important physiological roles that derive from these. However, its role in endocytosis has not yet been explored.

2 Objectives

Objectives

Based on the preliminary results from Geli's group, the objectives of this thesis are:

1. to create cell lines for the study of the molecular function of kazrin,
2. to confirm and further study the role of kazrin on endocytosis,
3. to study the role of kazrin in endosomal recycling and its impact in cellular processes that depend on endosomal recycling,
4. to study the molecular mechanism by which kazrin affects endosomal trafficking, including the effects on the cytoskeleton and on phosphoinositides.

3 Results

Results

3.1 Previous results: kazrin C overexpression blocks endocytosis in COS7 cells

Kazrin C was originally identified in our laboratory in a screen performed with COS7 cells to select human brain cDNAs that inhibit CME when overexpressed (Schmelzl and Geli, 2002). In order to confirm that overexpression of kazrin C inhibited CME, COS7 cells were transfected with GFP, GFP-kazrin C or GFP-eps15-Δ95/295 and incubated with Texas Red-labelled Tfn (TxR-Tfn) for 15 min. GFP-eps15-Δ95/295 is a dominant negative eps15 (EGFR Pathway Substrate Clone 15) known to block endocytosis (Benmerah *et al.*, 1999) and it was used as a positive control. GFP was used as a negative control. As expected, cells overexpressing GFP-kazrin C and GFP-eps15-Δ95/295 accumulated less internalised Tfn than GFP-overexpressing cells (**Figure 3.1A,B**). A biotin-Tfn uptake assay demonstrated that the observed defect was caused by a block in endocytic budding from the PM. In this assay, the kinetics of biotin-Tfn internalisation is followed by assessing the amount of internalized biotin-Tfn (after stripping surface-bound Tfn with an acidic buffer) versus the amount of total biotin-Tfn (after an incubation in the physiological buffer PBS) at different times upon addition of biotin-Tfn to the media. Cells were recovered and proteins were analysed by SDS-PAGE followed by a peroxidase-conjugated Streptavidin overlay. As shown in **Figure 3.1C and D**, the uptake in GFP-kazrin C and GFP-eps15-Δ95/295-overexpressing cells was slower than in GFP-expressing cells.

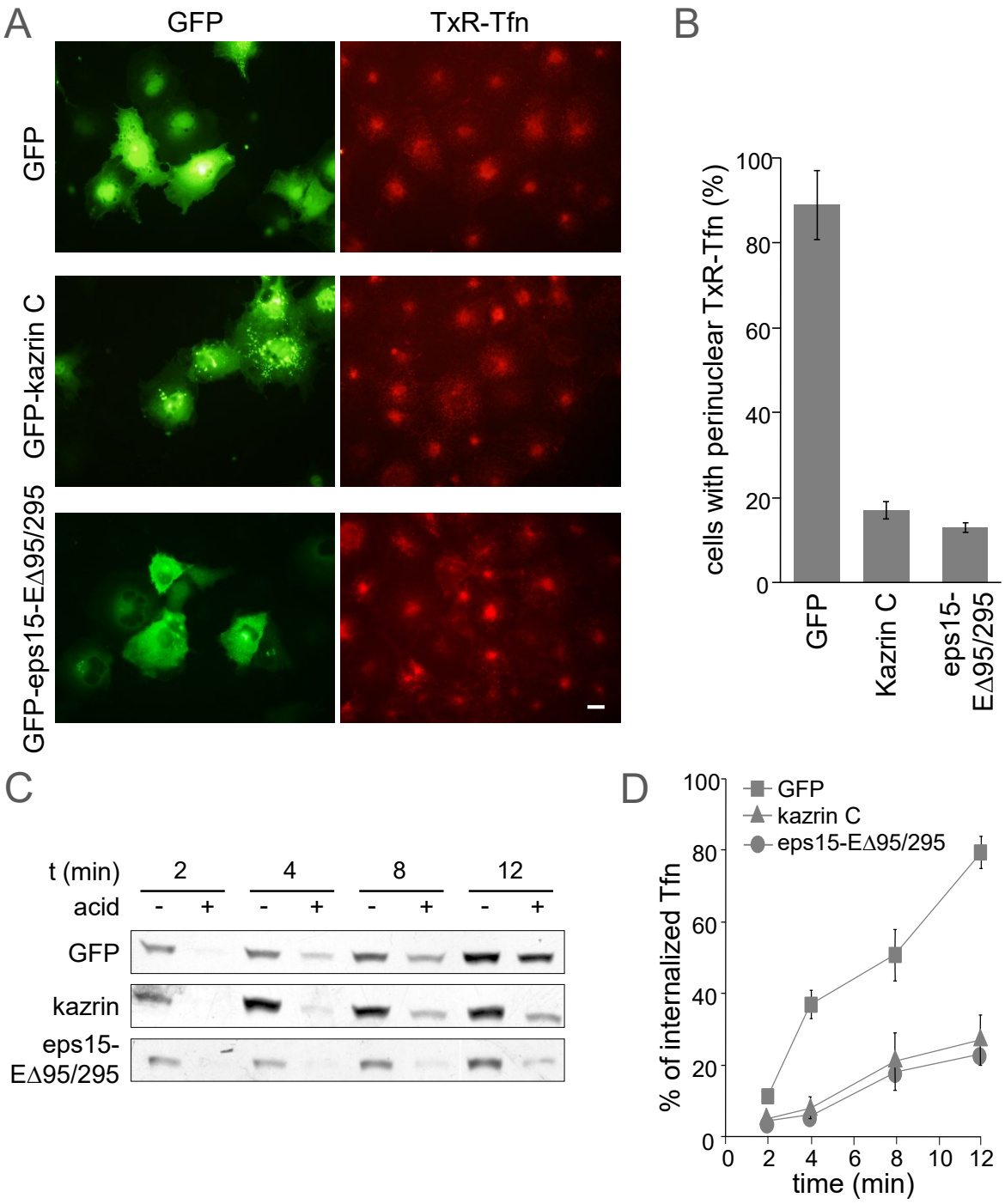
A
GFP
TxR-Tfn
GFP
GFP-kazrin C
GFP-eps15-EΔ95/295
B
cells with perinuclear TxR-Tfn (%)
100
80
60
40
20
0
GFP
Kazrin C
eps15-EΔ95/295
C
t (min)
2
4
8
12
acid
- + - + - + - +
GFP
kazrin
eps15-EΔ95/295
D
GFP
kazrin C
eps15-EΔ95/295
% of internalized Tfn
100
80
60
40
20
0
0 2 4 6 8 10 12
time (min)

Figure 3.1. Previous results: kazrin overexpression inhibits CME in COS7 cells. A. Confocal images of COS7 cells transfected with plasmids encoding GFP only or with GFP fused to kazrin C or eps15-Δ95/295. Cells were incubated in 20 μg/ml of TxR-Tfn for 15 min and fixed. Scale bar = 10 μm. **B.** Graph showing the mean ± SEM of the percentage of transfected cells with a perinuclear staining of TxR-Tfn for the experiment shown in A. **C.** Peroxidase-Streptavidin overlay of a biotin-Tfn uptake experiment in cells expressing GFP only or GFP fused to kazrin C or eps15-Δ95/295. The cells were incubated in biotin-Tfn for the indicated times and they were washed in PBS (-), to detect all bound Tfn, or in an acidic buffer (+), to detect internalised Tfn only. The membrane was blotted with Streptavidin fused to peroxidase**. D.** Graph of mean ± SEM internalized biotin-Tfn normalised to the total bound biotin-Tfn for each time point. The data is the mean of three independent experiments.

3.2 Establishment of kazrin KO and GFP-kazrin C expressing MEF cell lines

To study the cellular function of kazrin, we decided to create kazrin knock-out (KO) cell lines using the CRISPR-cas9 technology. Over the completely deleted background, we would introduce an inducible gene encoding GFP-tagged kazrin C through retroviral infection, allowing the control of the protein expression levels. These tools would allow us to perform experiments under more reproducible conditions, as compared to overexpression experiments with transiently transfected plasmids. Mouse Embryonic Fibroblasts (MEFs) were chosen as the experimental model in this thesis because they are easy to grow and manipulate in cell culture and because they are often used to study cell migration (Weaver *et al.*, 1997; Missirlis *et al.*, 2017), a process that might be altered by kazrin depletion. The process of cell line generation is schematised in **Figure 3.2A**.

The KO cell line was generated by using the CRISPR-cas9 technology on wild-type (WT) MEF cells. As opposed to siRNA and shRNA-mediated gene silencing, CRISPR-cas9 can completely abolish the expression of the targeted gene. For generation of a KO cell line, the cas9 nuclease is directed by the guide RNA (gRNA) to a specific site at the start of the gene, introducing a double strand break. The gRNA was designed to efficiently recognise a sequence after the start codon of the kazrin gene, as well as to minimize its binding to off-target sites. The gRNA also needs to precede a PAM site (AGG) that allows cas9 binding to the DNA (**Figure 3.2A**). After the double strand break is produced, the cellular repair mechanism often leads to frameshift mutations or premature stop codons that block the expression of the gene. The plasmid used in this study contained the cas9 and the gRNA sequence, as well as a gene encoding GFP that allowed identification of transfected cells by FACS. Upon selection of those expressing GFP, cells were seeded individually to create clones, which were analysed by IB. Several positive clones in which no kazrin was detected were amplified and subsequently used in this study (**Figure 3.2B**).

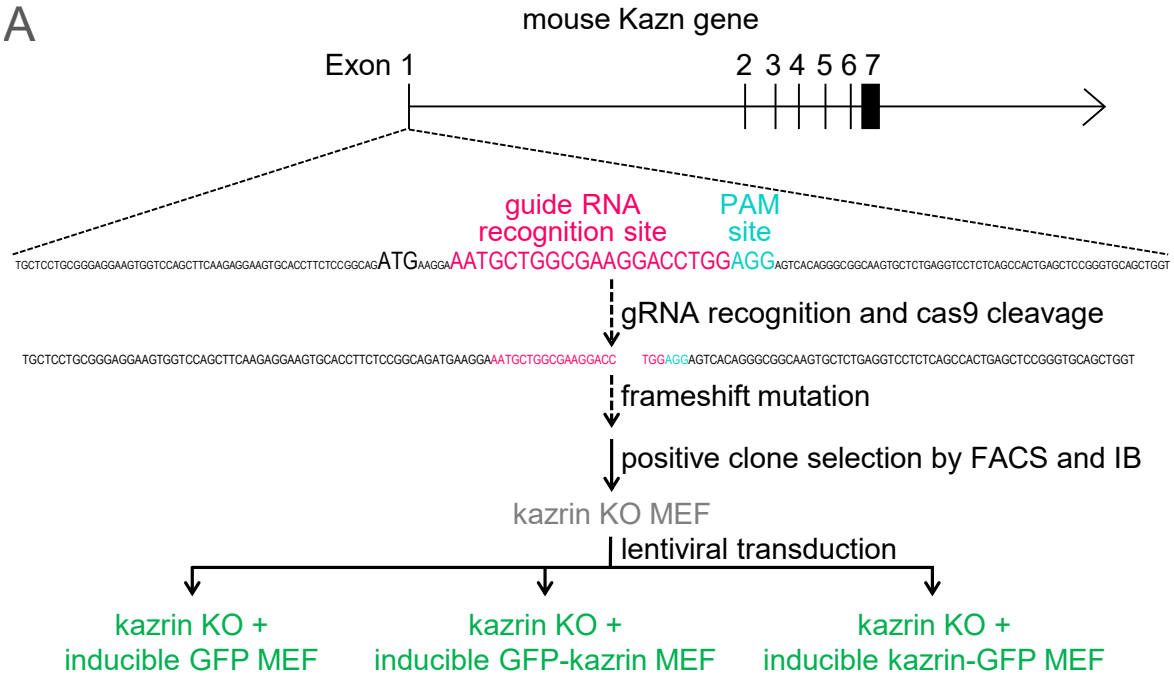
A
mouse Kazn gene
Exon 1
2 3 4 5 6 7
guide RNA recognition site
PAM site
gRNA recognition and cas9 cleavage
frameshift mutation
positive clone selection by FACS and IB
kazrin KO MEF
lentiviral transduction
kazrin KO + inducible GFP MEF
kazrin KO + inducible GFP-kazrin MEF
kazrin KO + inducible kazrin-GFP MEF

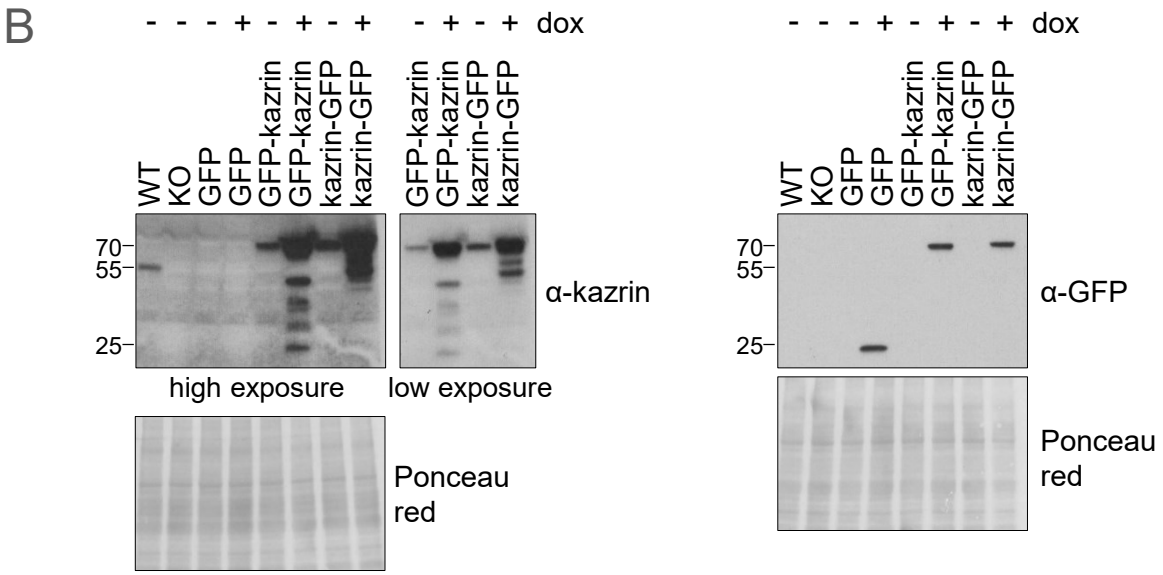
B
- - - + - + - + - + - + dox
WT
KO
GFP
GFP
GFP-kazrin
GFP-kazrin
kazrin-GFP
kazrin-GFP
70
55
25
α-kazrin
high exposure
low exposure
Ponceau red
α-GFP

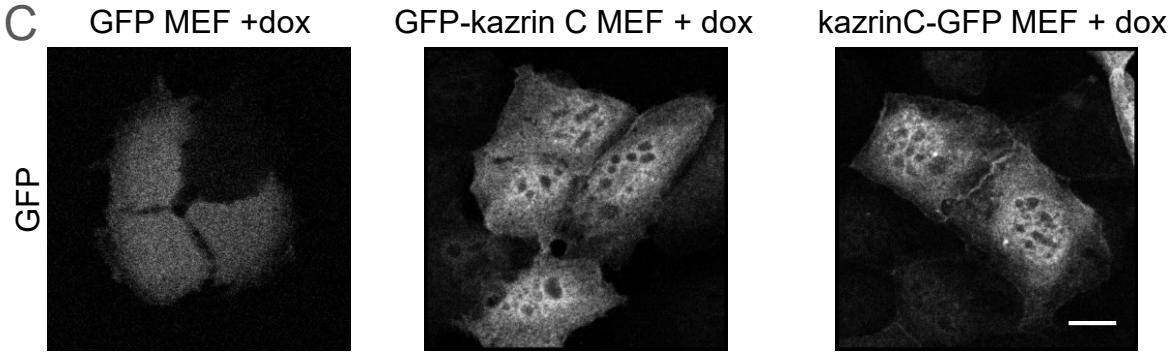
C
GFP MEF +dox
GFP-kazrin C MEF + dox
kazrinC-GFP MEF + dox
GFP

Figure 3.2. Establishment of a kazrin KO cell line and kazrin KO cell lines expressing doxycycline-inducible GFP-kazrin C and kazrin C-GFP. A. Strategy for the establishment of the MEF cell lines. Kazrin KO MEFs were created with the CRISPR-cas9 technology. The gRNA was designed to recognize a sequence at the beginning of exon 1 of the mouse Kazn gene. This sequence is followed by a PAM site. The cas9 nuclease was transfected in a plasmid into the cells, together with the gRNA. The cas9 specifically cleaves three nucleotides before the PAM sequence, leaving a gap in the DNA sequence. In some of the cells, the DNA repair is not correct and leads to a frameshift mutation that impedes the expression of the gene. The plasmid containing the gRNA and the cas9 also contains GFP, which allows sorting and isolation of transfected cells by FACS. The resulting clones were analysed by IB, and those with no kazrin expression were selected. One of them was used as the base for another three cell lines in which genes encoding GFP, GFP-kazrin C or kazrin C-GFP were inserted in the genome. The inserted constructs were preceded by a tetracycline-response element. The constructs were delivered by lentiviral transduction and cell selection by FACS. Thus, none of these cell lines have endogenous kazrin expression but express GFP, GFP-kazrin C or kazrin C-GFP upon doxycycline addition. **B.** IBs of non-denaturing lysates from WT, kazrin KO, GFP, GFP-kazrin C and kazrin C-GFP cells. The cells were treated with 5 μg/ml doxycycline for 24 h where indicated. The membranes were blotted with an α-kazrin serum raised against the N-terminal domain of kazrin (EMBL Heidelberg) or an α-GFP antibody (Living Colors 632380), followed by the adequate peroxidase-conjugated secondary antibody. Ponceau red was used to stain the proteins to control for equal loading and correct transference to the membrane. A high and a low exposure are shown for the lanes corresponding to GFP-expressing cells in the α-kazrin-blotted membrane. **C.** Confocal images of GFP-kazrin **C** and kazrin C-GFP MEFs, treated with 5 μg/ml doxycycline for 24 h before fixation. Images were taken with a TCS-SP5 confocal microscope. Scale bar = 10 μm.

On the KO cell line, we reintroduced inducible versions of a gene expressing GFP-tagged kazrin (**Figure 3.2A**). We decided to use a GFP-tagged version because we could not identify or generate kazrin antibodies that worked in immunofluorescence under the physiological kazrin expression levels in fibroblast. We decided against transient transfection because it would lead to variable kazrin overexpression at much higher levels than the endogenous protein. As an alternative, we used lentiviral vectors encoding either N or C-terminal-tagged kazrin C (GFP-kazrin C and kazrin C-GFP), under the control of a tetracycline-response element that promotes expression of the gene in the presence of doxycycline. We decided to use both N and C-terminal GFP tagged version to minimize the risk of interfering with kazrin functionality. In addition to cell lines expressing GFP-kazrin C and kazrin C-GFP, we generated a control cell line expressing GFP only. Surprisingly, as observed by IB analysis, the levels of GFP-kazrin C and kazrin C-GFP in non-induced cells were similar to those of endogenous kazrin (**Figure 3.2B**). On the other hand, incubation with doxycycline led to the overexpression of kazrin C (**Figure 3.2B**). GFP, GFP-kazrin C and kazrin C-GFP were visualised by fluorescence microscopy upon doxycycline incubation for 24 h (**Figure 3.2C**). Unfortunately, no GFP signal could be detected in the absence of doxycycline, in cells expressing GFP-kazrin C or kazrin C-GFP at levels close to physiological.

The four cell lines created were used in the subsequent experiments to study the localisation and cellular function of kazrin.

3.3 Kazrin depletion and kazrin C overexpression inhibit endocytosis in MEF cells

Kazrin C had been shown to inhibit CME when overexpressed in COS7. In order to investigate the role of kazrin in endocytosis in the new experimental model system, we performed microscopy-based Tfn uptake assays in WT and kazrin KO cells, as well as in cells expressing or overexpressing GFP-kazrin C or kazrin C-GFP. To that end, we incubated the cells in the presence of Alexa647-conjugated Tfn (A647-Tfn) for 8 min, fixed them, and observed them under the microscope (**Figure 3.3A**, quantified in **Figure 3.3B**). When compared to WT cells, kazrin KO cells accumulated 33% less internalised Tfn (**Figure 3.3B**), suggesting that kazrin is required for efficient CME. On the other hand, physiological expression levels of GFP-kazrin C (in the absence of doxycycline) on the KO background partially complemented the endocytic defect, as compared to cells expressing GFP. Physiological levels of kazrin C-GFP also partially recovered endocytic uptake, although to a lesser extent than GFP-kazrin C (**Figure 3.3B**), indicating that the N-terminal tag might interfere with the functionality of kazrin C more than the C-terminal tag.

We also analysed A647-Tfn internalisation in GFP, GFP-kazrin C or kazrin C-GFP overexpressing cells that had been incubated with 5 µg/ml doxycycline for 24 h and that showed a mean GFP expression over 10 a.u. (high GFP, high GFP-kazrin C and high kazrin C-GFP). The experiment demonstrated that, similar to what was observed in COS7 cells, overexpression of GFP-kazrin C or kazrin C-GFP potently inhibited Tfn uptake (**Figure 3.3A,B,C**), regardless of the position of the tag.

Finally, an uptake experiment with TxR-Tfn was performed in WT and KO cells to measure internalisation at different time points. Consistent with the previous results, uptake in kazrin KO cells was slower (**Figure 3.3D**). Overall, these results proved that both kazrin depletion and overexpression block CME in MEF cells. Whereas highly overexpressed kazrin C seems to work as a dominant negative, low kazrin levels can rescue the phenotype of the KO. Since GFP-kazrin C seemed to complement the endocytic defect better than kazrin C-GFP, it was the construct used in subsequent functional complementation assays.

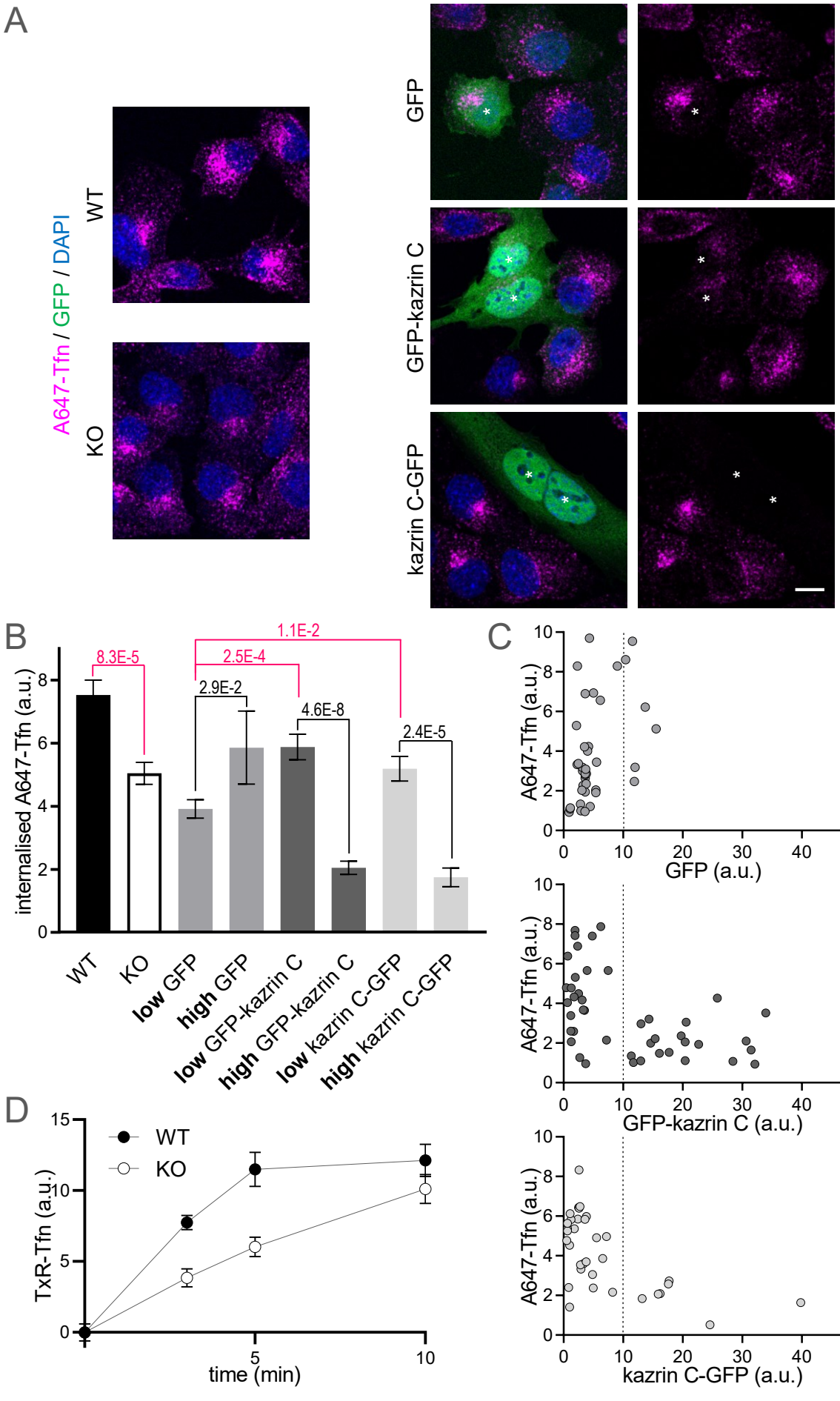
A
A647-Tfn / GFP / DAPI
WT
KO
GFP
GFP-kazrin C
kazrin C-GFP
B
internalised A647-Tfn (a.u.)
8.3E-5
1.1E-2
2.5E-4
2.9E-2
4.6E-8
2.4E-5
WT
KO
low GFP
high GFP
low GFP-kazrin C
high GFP-kazrin C
low kazrin C-GFP
high kazrin C-GFP
C
A647-Tfn (a.u.)
GFP (a.u.)
GFP-kazrin C (a.u.)
kazrin C-GFP (a.u.)
D
TxR-Tfn (a.u.)
WT
KO
time (min)

Figure 3.3. Overexpression and depletion of kazrin inhibit CME. A. Merged confocal images of WT, kazrin KO, GFP and GFP-kazrin C MEF cells, incubated in 20 µg/ml of A647-Tfn for 8 min before fixation and stained with DAPI. The overexpression of the GFP constructs was induced with 5 µg/ml doxycycline for 24 h. Images were taken with a TCS-SP5 confocal microscope. The individual channel corresponding to A647-Tfn is shown for GFP-expressing cell lines. The asterisks mark cells with a high GFP or GFP-kazrin C expression. Scale bar = 10 µm. **B.** Quantification of the experiment described in A. The graph shows the mean ± SEM of the A647-Tfn fluorescence intensity per cell for the indicated cell lines. In the case of cells expressing a GFP construct, the data is shown separately for cells without doxycycline induction (low GFP expression) and cells with a GFP expression higher than 10 a.u. (high). The p values from an unpaired two-tailed t test are shown. P values in pink account for the differences between each cell line (only shown for the low GFP expression cells) with its control cell line. P values in black account for the differences between low and high GFP expressing cells within each cell line. **C.** Quantification of the experiment described in A. The three graphs represent the amount of A647-Tfn as a function of the expression of GFP, GFP-kazrin C and kazrin C-GFP, respectively. The line at x = 10 marks a threshold from which the overexpression of kazrin correlates with low amounts of Tfn internalization. **D.** Graph of the mean ± SEM of the fluorescence intensity of TxR-Tfn internalized in WT and kazrin KO MEF cells at the indicated time points.

3.4 Kazrin intracellular localisation

The study of the localisation of kazrin was a first approach to understand its role in endocytosis. Since neither the commercially available antibodies or the antibodies produced in Geli's laboratory recognised endogenous kazrin in immunofluorescence experiments under physiological expression levels, we analysed the localisation of GFP-kazrin C at the minimal expression levels that allowed visualization. We also performed subcellular fractionation experiments followed by IB to assess the localisation of endogenous kazrin.

3.4.1 GFP-kazrin C is localised in the PM and intracellular structures

Fluorescence microscopy analysis of cells expressing GFP or GFP-kazrin C one day upon induction with 5 µg/ml doxycycline demonstrated that slightly overexpressed GFP-kazrin C was present at the PM in a patch-like pattern, mostly at intercellular contacts (**Figure 3.4**). GFP-kazrin C-positive structures at the PM were dynamic. They transiently assembled with life-spans in the range of seconds to minutes, or they moved along the PM (**Figure 3.4B**). In addition to the PM staining, GFP-kazrin C was present in cytoplasmic structures mostly at the cell periphery (**Figure 3.4A**). We also observed some nuclear signal, which is consistent with previous reports showing kazrin at the nucleus (Groot *et al.*, 2004; Gallicano *et al.*, 2005; Nachat *et al.*, 2009). Finally, a bright GFP-kazrin C dot-like structure next to the nucleus was evident in most cells. This structure was reminiscent of the centrosome because of its localisation and the fact that it sometimes appeared as a double dot (**Figure 3.4**).

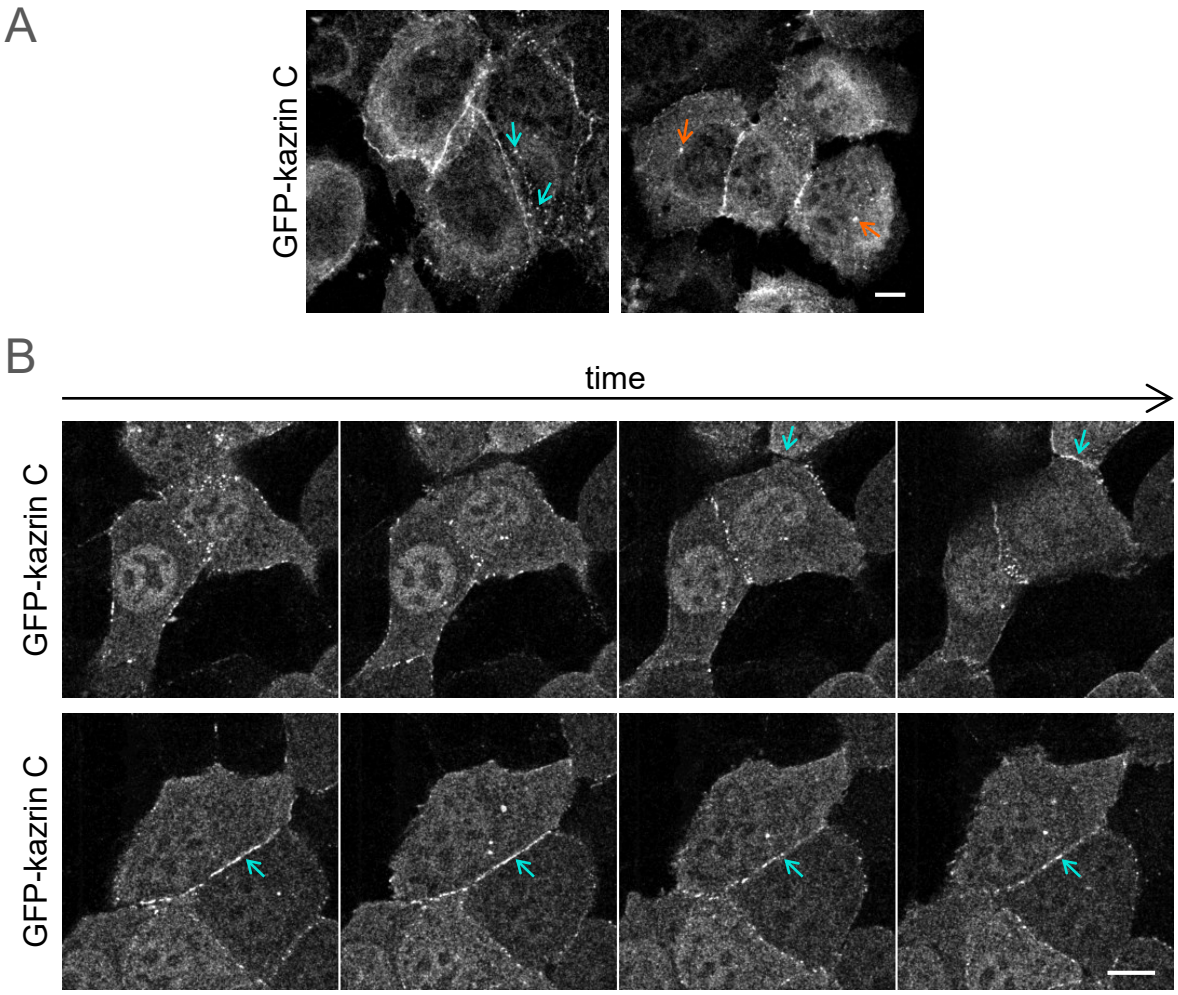

Figure 3.4. GFP-kazrin C localizes to the PM and intracellular structures. **A.** Confocal images of GFP-kazrin C MEFs treated with 5 µg/ml of doxycycline for 24 h before fixation. Images were taken with a SP5 confocal. Blue arrows in the image on the left indicate GFP-kazrin C localisation at intracellular structures. Orange arrows in the image on the right indicate GFP-kazrin C localisation at centrosomal-like structures. Scale bar = 10 µm. **B.** Time lapse confocal images of GFP-kazrin C MEFs treated with 5 µg/ml of doxycycline for 24 h. Images of life cells were taken every 5 min with a Zeiss LSM-780 confocal microscope. Scale bar = 10 µm.

3.4.2 GFP-kazrin C co-localises with markers of adherens junctions at the PM and cytoplasmic structures

Given the clear GFP-kazrin C signal at the intercellular contacts at the PM in MEF cells, and the previous literature describing the localisation and function of kazrin in desmosomes and adherent junctions, we looked for a possible co-localisation of GFP-kazrin C with components of these structures in MEF cells (Groot *et al.*, 2004; Cho *et al.*, 2010). N-cadherin is the main component of adherens junctions in fibroblasts. Indeed, it co-localised with GFP-kazrin C in the PM and, interestingly, also in the cytoplasmic structures (**Figure 3.5**). As a negative control, we looked at E-cadherin, which was present in cytoplasmic structures but did not seem to be part of adherens junctions. Of note, E-cadherin containing structures did not

contain GFP-kazrin C. Similar to N-cadherin, the cytoplasmic components of adherens junctions β-catenin and p120-catenin co-localised with GFP-kazrin C at the PM and in intracellular structures. We also looked at the p120-catenin family member ARVCF-catenin, known to interact with kazrin in *X. laevis* embryonic cells. In MEF cells, we did not observe localisation of ARVCF-catenin at the PM or co-localisation with GFP-kazrin C (**Figure 3.5**).

Kazrin has been shown to be part of desmosomes in keratinocytes and to be important for their differentiation (Groot *et al.*, 2004). However, we did not found co-localisation of GFP-Kazrin C with the desmosomal marker desmoglein. In fact, the cells did not have desmoglein in the PM, suggesting that MEF cells lack desmosomes (**Figure 3.5**). Therefore, kazrin seemed to be a component of the adherens junctions in MEF cells.

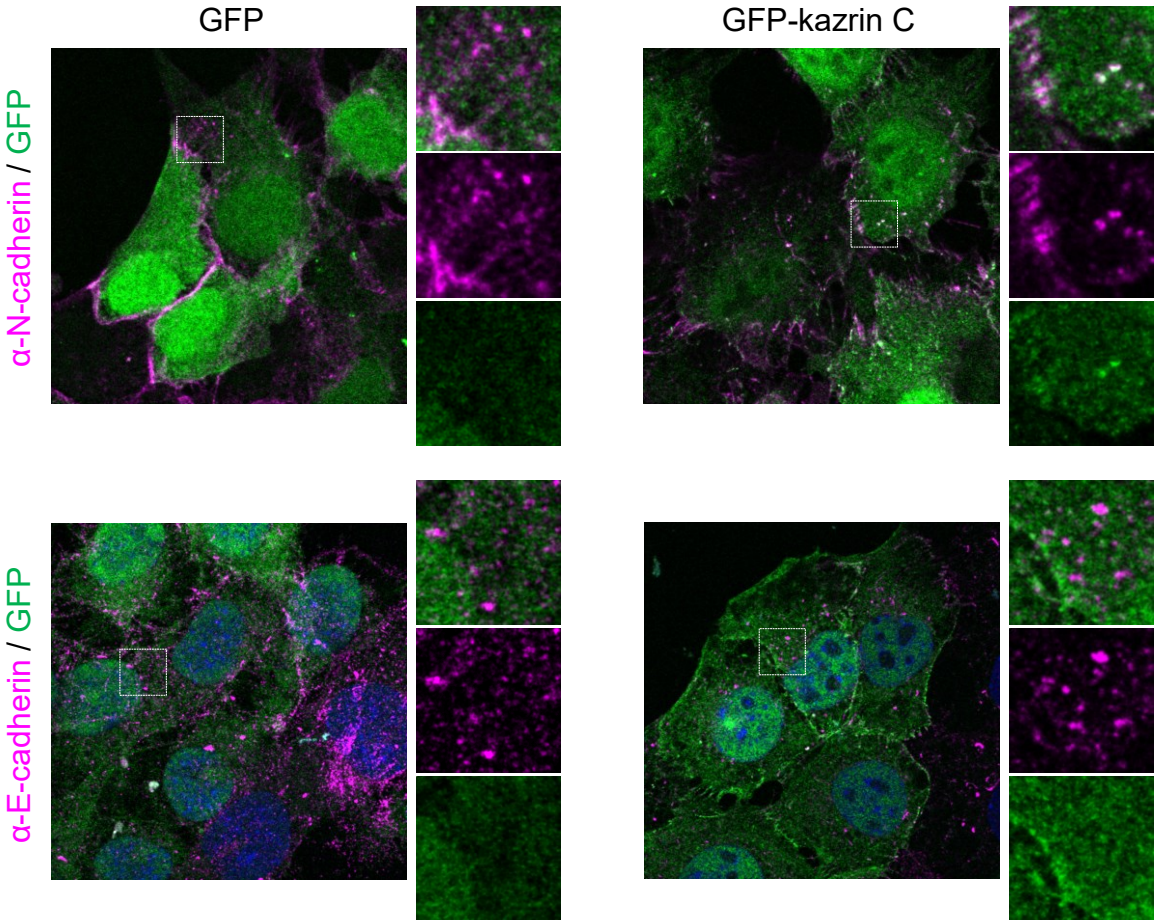

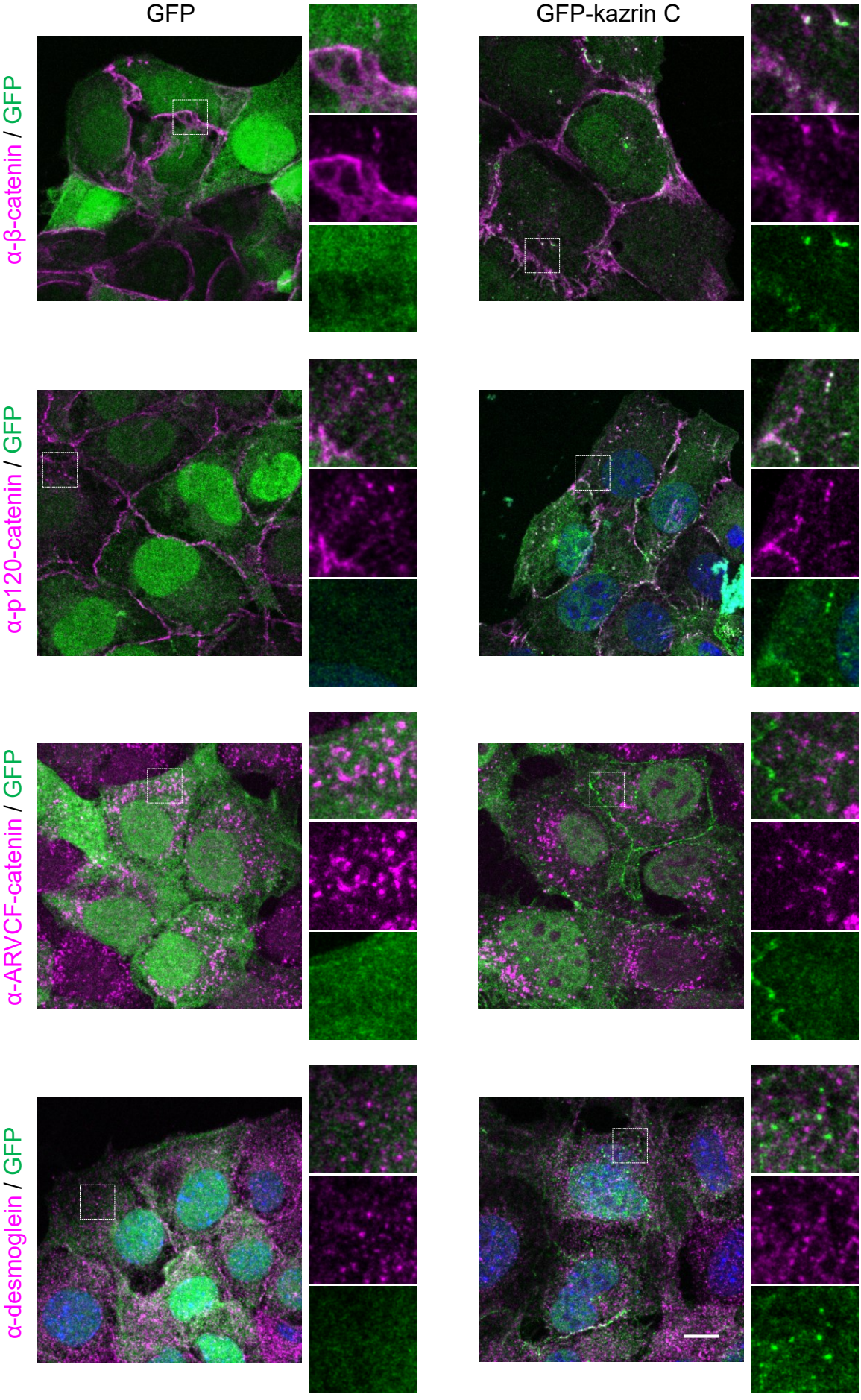
GFP
GFP-kazrin C
α-β-catenin / GFP
α-p120-catenin / GFP
α-ARVCF-catenin / GFP
α-desmoglein / GFP

Figure 3.5. GFP-kazrin C co-localizes with markers of adherens junctions at the PM and internal structures. Merged confocal images of GFP or GFP-kazrin C expressing MEFs, treated with 5 µg/ml doxycycline for 24 h before fixation and stained with α-N-cadherin (BD 51-9001943), α-E-cadherin (BD 610181), α-β-catenin (BD 610153), α-p120-catenin (BD 51-9002040), α-ARVCF-catenin (Santa Cruz 23874) or α-desmoglein (BD 51-9001952) antibodies, the adequate A647-conjugated secondary antibody and DAPI. Images were taken with a SP5 confocal microscope. Individual channels and merged images of 8 times zoomed-up sections of the indicated areas are shown. Scale bar = 10 µm.

3.4.3 Endogenous kazrin is localised on EEs

To identify the nature of the cytoplasmic structures, we carried out a subcellular fractionation analysis. We created a 10 to 32 % Optiprep gradient that could discriminate cellular structures such as EE, RE, lysosomes and the Golgi, according to their density. The nucleus and the PM were mostly pelleted at 3,000 g and they were excluded from the lysates before performing the gradient. Endogenous kazrin was present in three fractions of very low density in the Optiprep gradient (**Figure 3.6**). The bands did not appear in the gradient from kazrin KO cells, which confirmed their nature. Kazrin-containing fractions were also highly enriched in the EE marker EEA1. Conversely, kazrin did not co-fractionate with markers of other subcellular compartments, such as rab11 (REs), GM130 (*trans*-Golgi) and VPS35 (EE-LE transition), which were present in heavier fractions (**Figure 3.6**). This experiment pointed to a very specific localisation of the endogenous kazrin in EEs.

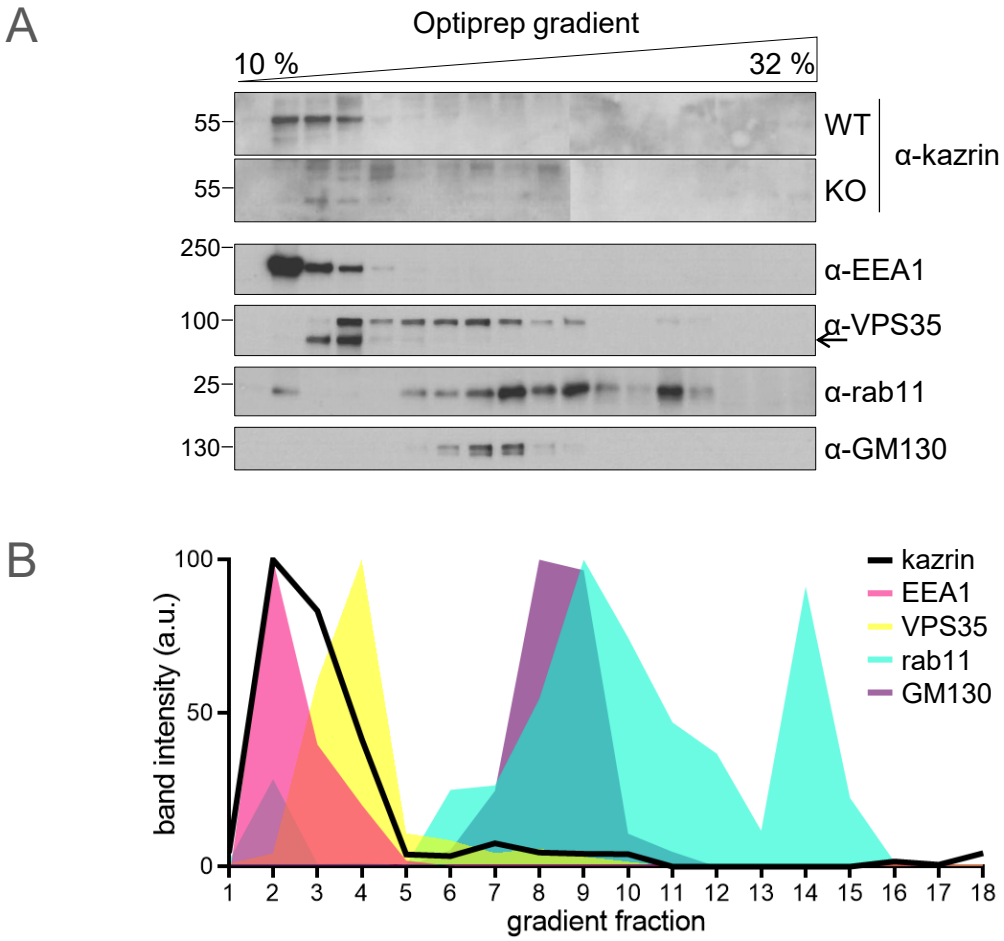

Figure 3.6. Subcellular fractionation indicates that endogenous kazrin is at EEs. **A.** IB of a subcellular fractionation assay of WT and kazrin KO MEFs. An Optiprep gradient from 10 % to 32 % was used to separate membranous subcellular compartments according to their density. Each lane corresponds to a gradient fraction. The IB membranes were blotted with antibodies raised against kazrin (EMBL Heidelberg) or markers of subcellular compartments, and with the adequate peroxidase-conjugated secondary antibodies. EEA1 (Cell Signaling 3288) marks EEs, VPS35 (Santa Cruz 374372) marks membranes with the retromer complex that are most likely found in the rab5/rab7 transition, rab11 (BD 610656) marks recycling endosomes and GM130 (BD 610822), the Golgi. **B.** Quantification of the experiments described in A. The band intensity for each fraction of the gradient is plotted for each antibody. The maximum intensities of each antibody were normalized. The areas under the curves for the markers allow visualization of the separation and overlap of the different cell subcomparments.

3.5 Kazrin depletion affects N-cadherin trafficking

Cadherins are trafficked continuously in cells as a way to modulate cell-cell adhesion (Cadwell, Su and Kowalczyk, 2016). The fact that GFP-kazrin C and adherens junction components were present in the same structures at the PM and within the cytoplasm, together with the implication of kazrin in CME, made us wonder if kazrin had a role controlling the trafficking of cadherins. Again, we did a subcellular fractionation experiment

to analyse specific intracellular compartments. In accordance with the immunofluorescence experiments, kazrin and N-cadherin co-fractionated in EE (**Figure 3.7A**). Therefore, the major part of cytoplasmic cadherin seemed to be contained within EEs together with the endogenous kazrin.

Based on the Tfn CME defect we expected kazrin KO cells to accumulate N-cadherin at the PM and reduce the presence of N-cadherin at EEs. However, the amount of endosomal N-cadherin was 10 times higher in kazrin KO than in WT cells. This phenotype was rescued by the expression of GFP-kazrin C but not GFP (**Figure 3.7**). This result indicated that the exit of N-cadherin from EE or the maturation of EE was defective in kazrin KO cells. This defect dominated over the uptake defect described for the KO cells in **Figure 3.1**, which would rather tend to reduce the EE fraction.

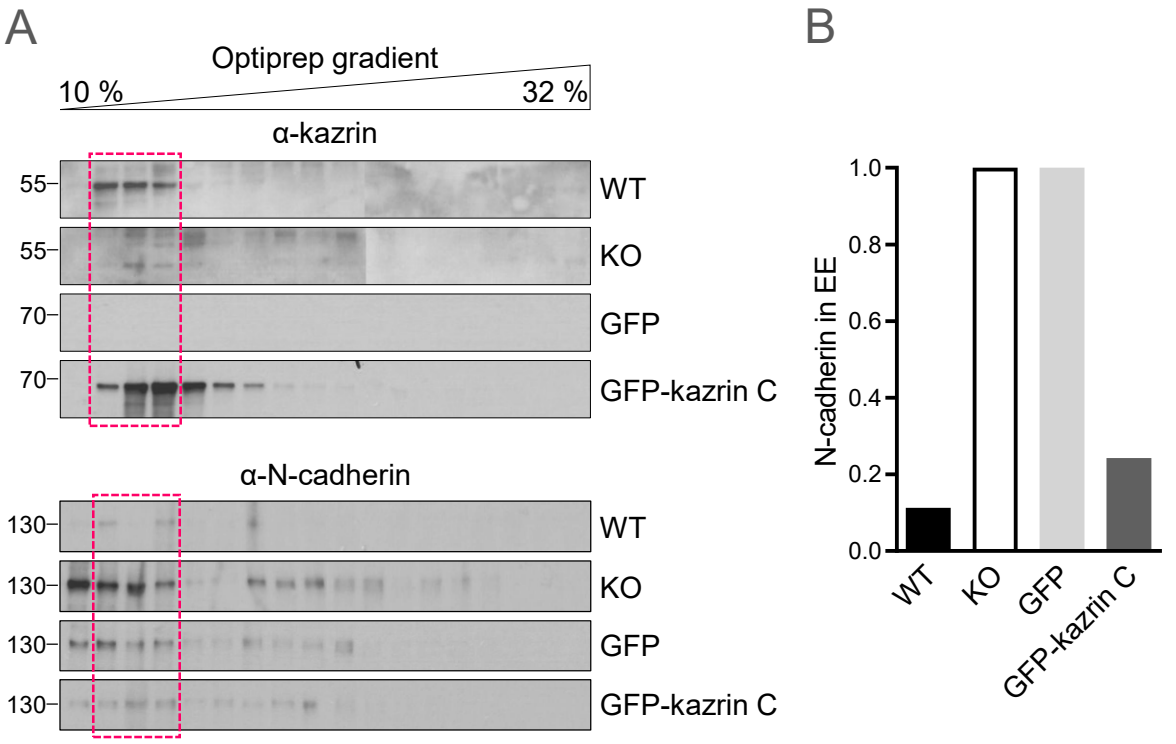

Figure 3.7. Depletion of kazrin causes the accumulation of N-cadherin at EEs. **A.** IB of a subcellular fractionation assay of WT, kazrin KO, GFP and GFP-kazrin C expressing MEFs. GFP and GFP-kazrin C cells were incubated in 5 µg/ml doxycycline for 24 h before starting the assay. An Optiprep gradient from 10 to 32 % was used to separate membranous subcellular compartments according to their density. Each lane corresponds to a gradient fraction. The IB membranes were blotted with α-kazrin (EMBL Heidelberg) or α-N-cadherin (BD 51-9001943) antibodies and the appropriate peroxidase-conjugated secondary antibodies. The rectangles in pink indicate the lanes that correspond to EEs, according to the localisation of EEA1 (shown in Figure 4.6). **B.** Quantification of the experiment described in A. The graph shows the intensity of the N-cadherin bands in the lanes of the IB that correspond to early endosomal fractions. The values were normalised to the corresponding control.

3.6 Kazrin depletion delays transport, maturation or exit from EEs

3.6.1 EEs are bigger and more dispersed in kazrin-depleted cells

Despite the Tfn uptake defects observed in the kazrin KO cells, we observed enlarged TxR-Tfn-containing peripheral endosomes. The structures were EEA1-positive and therefore mostly corresponded to EEs (**Figure 3.8A**). This result is consistent with the accumulation of endosomal N-cadherin (**Figure 3.7**) and points to an additional role of kazrin in membrane trafficking. Kazrin might promote exit of cargo from EEs and/or the transport of EEs to the perinuclear compartment and their concomitant maturation.

A thorough analysis revealed an accumulation of EEA1-positive organelles in kazrin KO cells when compared to WT cells, which was accompanied by a more dispersed distribution. The bigger and more dispersed EE distribution was also evident in KO cells expressing GFP. Expression of GFP-kazrin C partially corrected the EE dispersal phenotype and their accumulation (**Figure 3.8B,C**). We then checked the distribution of REs. Although kazrin KO cells had slightly more dispersed rab11-positive organelles, these were affected to a much lesser extent than EEA1-positive organelles (**Figure 3.8D,E**). Consistent with the accumulation of EEA1 upon kazrin depletion, we observed a 25% increase in EEA1 in the fractionations of an Optiprep gradient that corresponded to EEs in KO cells compared to WT cells. The phenotype was again rescued by GFP-kazrin C expression but not by expression of GFP alone (**Figure 3.8F,G**).

These results clearly suggest a defect in EE maturation and transport towards the perinuclear region.

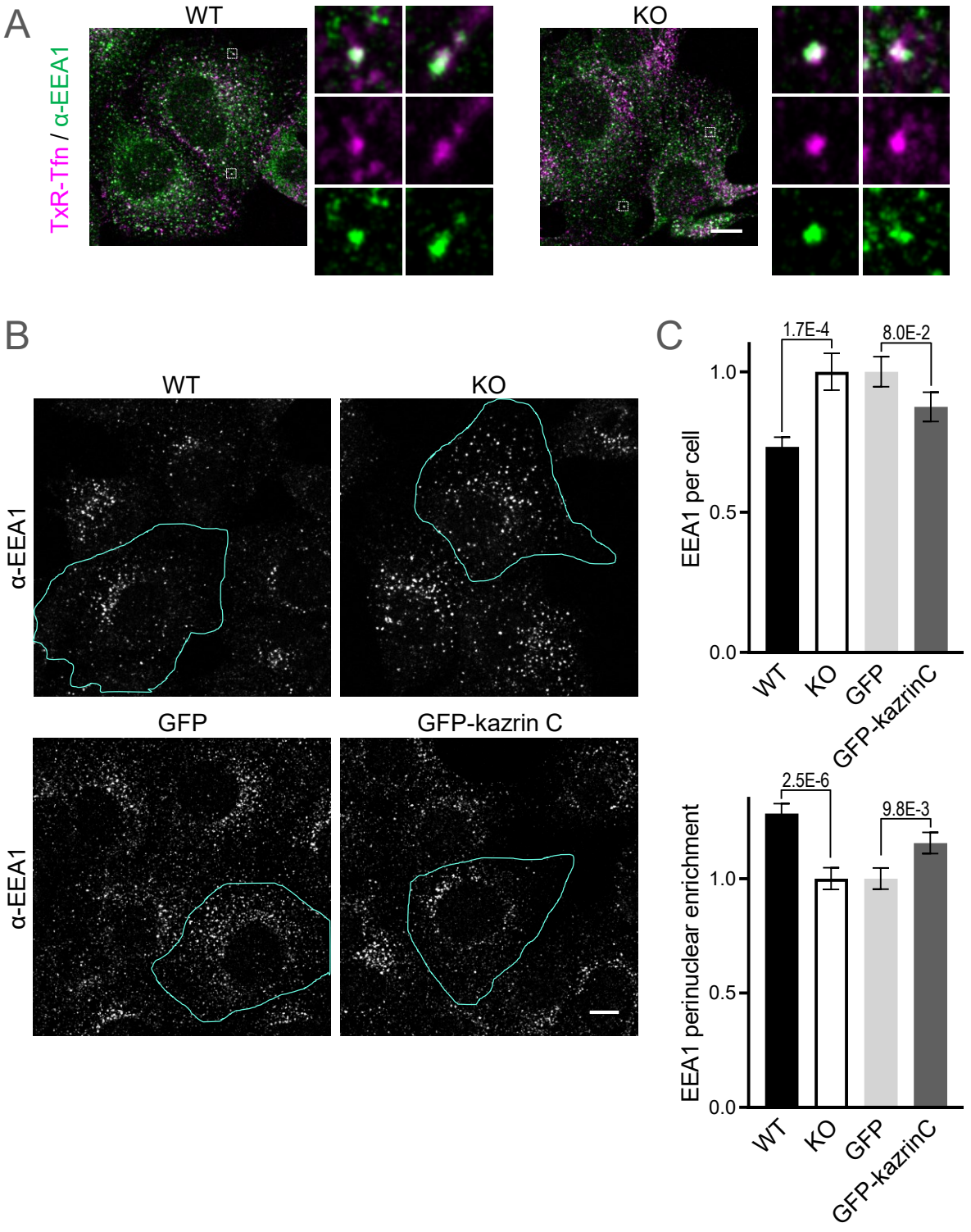
A
WT
KO
TxR-Tfn / α-EEA1
B
WT
KO
α-EEA1
GFP
GFP-kazrin C
α-EEA1
C
1.7E-4
8.0E-2
EEA1 per cell
1.0
0.5
0.0
WT
KO
GFP
GFP-kazrinC
2.5E-6
9.8E-3
EEA1 perinuclear enrichment
1.0
0.5
0.0
WT
KO
GFP
GFP-kazrinC

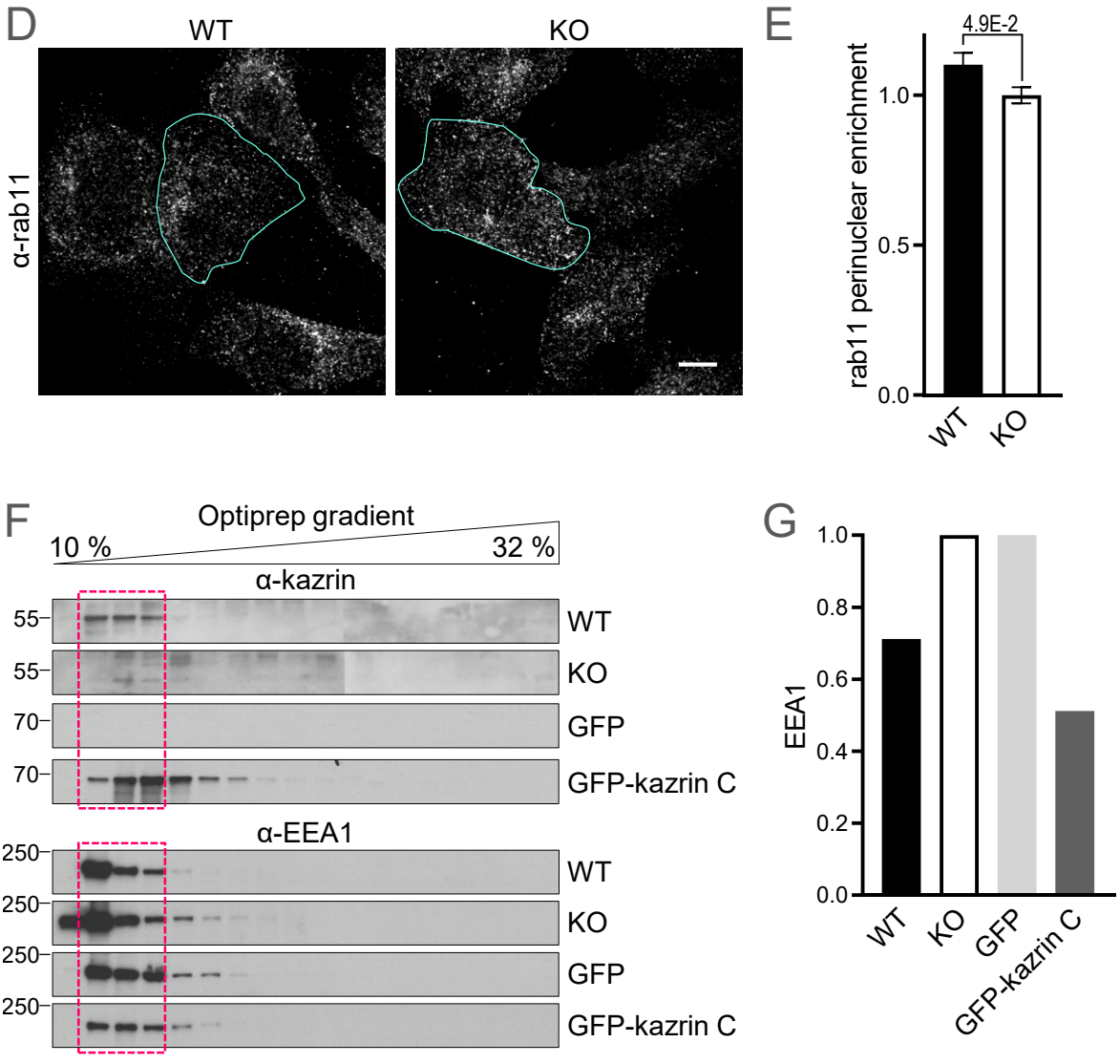
D
WT
KO
α-rab11
E
4.9E-2
rab11 perinuclear enrichment
1.0
0.5
0.0
WT
KO
F
Optiprep gradient
10 %
32 %
α-kazrin
55
55
70
70
WT
KO
GFP
GFP-kazrin C
α-EEA1
250
250
250
250
WT
KO
GFP
GFP-kazrin C
G
EEA1
1.0
0.8
0.6
0.4
0.2
0.0
WT
KO
GFP
GFP-kazrin C

Figure 3.8. Kazrin depletion causes an increase in EEA1 and dispersal of EEs. A. Merged confocal images of WT and kazrin KO MEFs incubated with 20 µ/ml TxR-Tfn for 20 min, fixed and stained with an α-EEA1 antibody (Cell Signaling 3288) and a A647-conjugated secondary antibody. Images were taken with a Zeiss LSM-780 confocal microscope. Merge images and individual channels of 24 times amplifications of the indicated areas are shown. Scale bar = 10 µm. **B.** Confocal images of WT, kazrin KO, GFP and GFP-kazrin C expressing MEFs. GFP and GFP-kazrin C MEFs were treated with 5 µg/ml of doxycycline for 24 h. Cells were fixed and stained with an α-EEA1 antibody (Cell Signaling 3288) and a A647-conjugated secondary antibody. Only the channel to visualize EEA1 is shown. Images were taken with a TCS-SP5 confocal microscope. Scale bar = 10 µm. **C.** Quantification of the amount and the dispersal of endosomes marked with EEA1 as described in B. The data in the upper graph is the mean ± SEM signal intensity per cell. The lower graph shows the mean ± SEM signal within a circle of 10 µm in the perinuclear region divided by the total EEA1 signal in the cell. The values were normalised to the corresponding control. The p values of a two-tailed Mann-Whitney test are shown. **D.** Confocal images of WT and kazrin KO MEFs. Cells were fixed and stained with an α-rab11 antibody (BD 610656) and a A488-conjugated secondary antibody. Images were taken with a TCS-SP5 confocal microscope. Scale bar = 10 µm. **E.** Quantification of the amount and the dispersal of endosomes marked with rab11 as described in D. The data is the mean ± SEM signal within a circle of 10 µm in the perinuclear region divided by the total rab11 signal in the cell. The values were normalised to the KO. The p values of a two-tailed Mann-Whitney test are shown. **F.** IB of a subcellular fractionation assay of WT, kazrin KO, GFP and GFP-kazrin C expressing MEFs. An Optiprep gradient from 10 to 32 % was used to separate membranous subcellular compartments according to their density. Each lane corresponds to a gradient fraction. The IB membranes were blotted with α-kazrin (EMBL Heidelberg) or α-EEA1 (Cell Signaling 3288) antibodies and the adequate peroxidase-conjugated secondary antibodies. The rectangles in pink indicate the lanes that correspond to EEs, according to the EEA1 localisation (shown in Figure 4.6A). **G.** Quantification of D. The graph shows the band intensity for N-cadherin in the lanes of the IB indicated by the pink rectangle, which corresponds to EEs. The values were normalised to the corresponding control.

3.6.2 Tfn transport to the perinuclear region is delayed in kazrin depleted cells

To test the hypothesis that kazrin was involved in the transport of EEs and/or their cargoes to the perinuclear region, we performed a TxR-Tfn recycling experiment. TxR-Tfn was loaded in EEs by incubating the cells at 16 ºC. A shift to 37 ºC in the presence of unlabelled Tfn triggered progression of TxR-Tfn to REs in the perinuclear region. Cells were fixed 10 min after the shift to 37 ºC. A control was added in which cells were fixed immediately after the 16 ºC incubation. In WT cells, Tfn accumulated at the perinuclear region 10 minutes after the shift to 37 ºC. Specifically, the signal was 1.75 times more intense in a perinuclear region of 10 µm than in the cell as a whole. However, this process was perturbed in kazrin KO cells, where most Tfn labelling was still dispersed after 10 min (**Figure 3.9**). Importantly, kazrin KO cells that expressed GFP-kazrin C reverted the phenotype and showed an accumulation of Tfn at the perinuclear region. Expression of GFP alone did not revert the

phenotype (**Figure 3.9B**). Overall, our experiments demonstrated that kazrin had a role in the transport of EEs and its cargo Tfn towards the centre of the cell. This type of transport is essential for endosomal maturation and endosomal recycling to regions of polarized cell growth (Neefjes, Jongsma and Berlin, 2017).

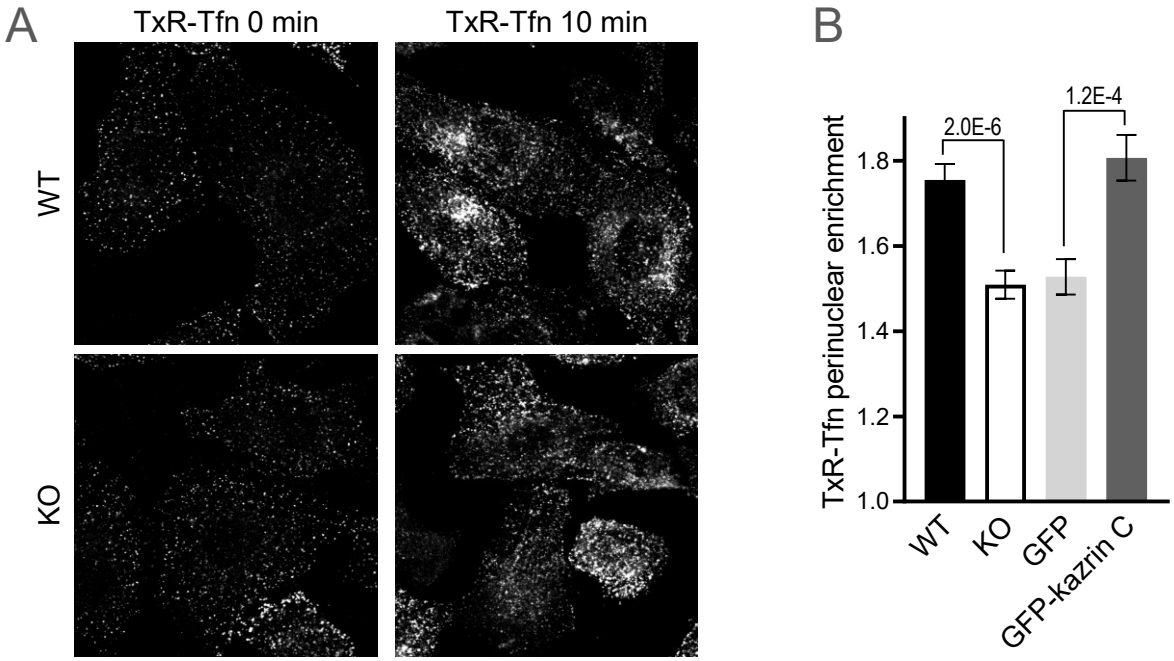

Figure 3.9. Transport of Tfn to the perinuclear region is defective in kazrin depleted cells. A. Confocal images of a TxR-Tfn recycling experiment in WT and kazrin KO MEFs. Cells were incubated with TxR-Tfn at 16 ºC to allow accumulation of cargo at EEs, washed and incubated with non-labeled Tfn at 37 ºC to allow recycling. Recycling was stopped after 0 or 10 min by transferring the cells to ice. Images were taken with a Zeiss LSM-780 confocal microscope. Scale bar = 10 µm. **B.** Quantification of TxR-Tfn perinuclear enrichment of the experiment described in A, after 10 min of recycling. The graph shows the mean ± SEM TxR-Tfn fluorescence intensity within a circle of 10 µm in the perinuclear region divided by the total TxR-Tfn intensity in the cell.

3.6.3 Tfn recycling is delayed in kazrin depleted cells

A more detailed TxR-Tfn recycling experiment revealed differences in the kinetics of WT and kazrin KO cells. At longer time points, labelled-Tfn progressively disappeared from cells, as it reached the cell surface saturated with unlabelled Tfn. Kazrin KO cells showed a slight delay in the recycling to Tfn to the cell surface, which could be recovered by re-expression of GFP-kazrin C but not GFP. Recycling was not completely inhibited, presumably because the portion of Tfn that is directly recycled from EEs, without traversing the RE, was not affected in the KO cells (**Figure 3.10**).

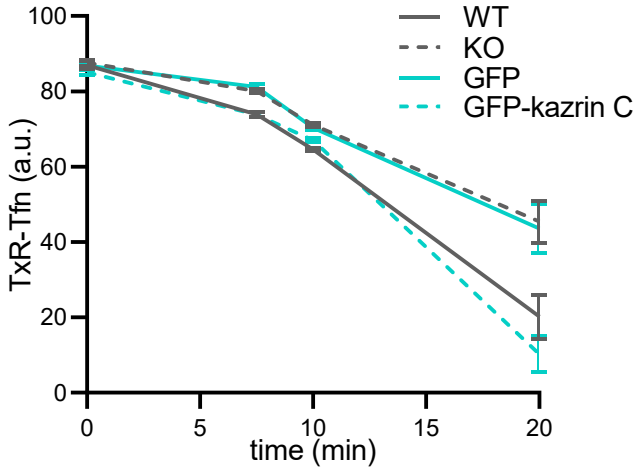

Figure 3.10. Recycling of Tfn is slightly delayed in kazrin depleted cells. Graph showing the dynamics of TxR-Tfn recycling in WT, kazrin KO, GFP and GFP-kazrin C expressing MEFs. Cells were incubated 30 min with TxR-Tfn at 16 ºC to allow accumulation of cargo in EEs, washed and incubated with non-labelled Tfn at 37 ºC to allow recycling. The cells were transferred to ice to stop recycling at different time points. The mean ± SEM TxR-Tfn per cell in each condition is shown for each time point.

3.7 Kazrin depletion affects cellular processes that rely on endosomal trafficking through the RE

According to our results, kazrin was important for the transfer of endocytosed material to the perinuclear region, and therefore for the rab11-dependent recycling pathway. The Tfn recycling assay was not the most adequate assay to assess the impact of kazrin depletion in this process because, similar to most recycling cargoes, Tfn can be transported directly from EE to the PM. Thus, to better grasp the role of kazrin in recycling through the perinuclear compartment, we investigated its impact in cellular processes that strongly rely on polarized secretion of endocytosed material. In these processes, cargoes are transported to the perinuclear region, where endosomes acquire rab11 and their competence to meet the exocyst. Such processes include cell migration and invasion though a 3D matrix and abscission after cytokinesis.

3.7.1 Kazrin depletion slows cell migration

To test the involvement of kazrin in cell migration, we analysed the movement of individual cells in a 3D matrix. In order to progress through the matrix, cells must regulate adhesions by the internalisation and polarized recycling of integrins (Paul, Jacquemet and Caswell, 2015; McNally *et al.*, 2017). They also need to recycle metalloproteases to digest the matrix. Specifically, defects in $\alpha_5\beta_1$ integrin recycling through the perinuclear region diminish migration speed (Paul, Jacquemet and Caswell, 2015) and increases the directionality of the movement (White, Caswell and Norman, 2007). In our experiment, we seeded the cells

on a Matrigel-coated plate and covered them with another layer of Matrigel, so that they would be embedded. We then recorded the cells for 9 h and tracked their migration.

The plot of migration tracks of individual cells is shown in **Figure 3.11A** and **Videos 1, 2, 3 and 4**. At first glance, the plots already revealed a defect in the migration speed of kazrin KO cells, since WT cells were able to cover a wider surface in a set time frame (**Figure 3.11A**). Careful analysis of the migration speed indeed revealed a 54 % reduction upon kazrin depletion. Similar to the endosomal trafficking defects, the phenotype was partially rescued by the expression of GFP-kazrin C (**Figure 3.11B**). Kazrin depleted cells also appeared to have straighter tracks than WT cells, suggesting a difference in the directionality of migration (**Figure 3.11A**). We initially quantified the end-point directionality, which is the distance between the start and final point, divided by the length of the total track covered by the cell. The higher the value, the more directional the migration is. As observed, kazrin KO cells were slightly more directional than WT cells. This was however not rescued by GFP-kazrin C expression (**Figure 3.11C**). The end-point directionality is not a good way to measure persistence, since its value can be influenced by the speed of the cell. In shorter tracks, there is less probability of turning and therefore they tend to show higher end-point directionality values. Because KO cells are slower, we decided to use an additional test of directionality: direction autocorrelation. The direction autocorrelation of a migration track is the mean turn angle in a specific time frame. When plotted, it describes an exponential curve because the probability of turning increases if the frame of time is wider. Consistent with the end-point directionality values, kazrin KO cells described wider angles in their tracks, which reflects a higher persistency. Again, the phenotype was not rescued by the expression of GFP-kazrin C (**Figure 3.11D**).

We concluded that depletion of kazrin affected the speed of cell migration within a 3D matrix, which is consistent with a role of kazrin in endosomal traffic through the perinuclear compartment.

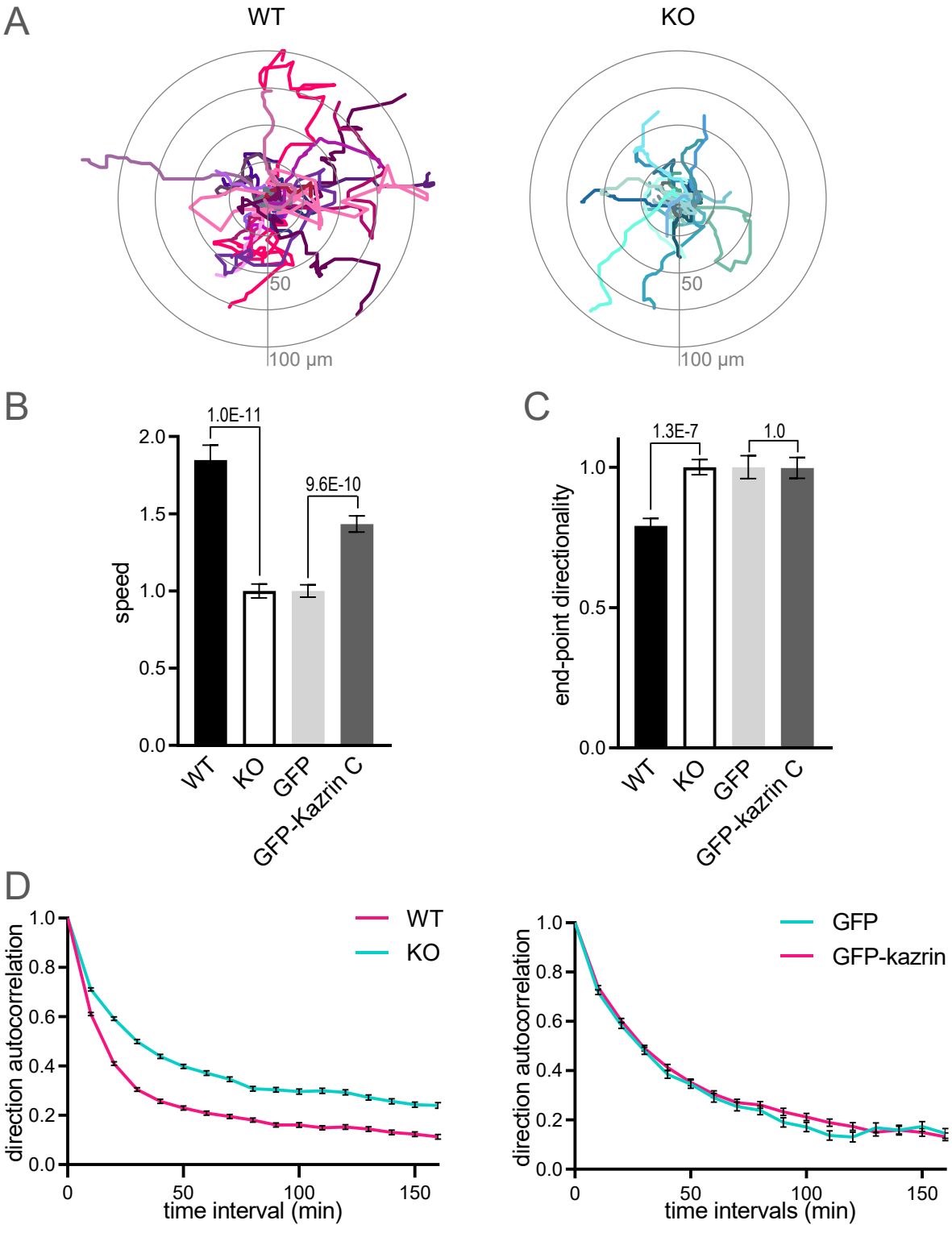
A
WT
KO
50
100 µm
50
100 µm
B
1.0E-11
9.6E-10
speed
2.0
1.5
1.0
0.5
0.0
WT
KO
GFP
GFP-Kazrin C
C
1.3E-7
1.0
end-point directionality
1.0
0.5
0.0
WT
KO
GFP
GFP-kazrin C
D
direction autocorrelation
1.0
0.8
0.6
0.4
0.2
0.0
0
50
100
150
time interval (min)
WT
KO
direction autocorrelation
time intervals (min)
GFP
GFP-kazrin

Figure 3.11. Migration and invasion are altered in kazrin depleted cells. A. Plots of the paths described by individually migrating WT or kazrin KO MEFs. The cells were embedded in Matrigel and tracked for 9 h. All tracks start at the (0,0) coordinate in the graph. **B.** Quantification of the speed of WT, kazrin KO, GFP and GFP-kazrin C expressing MEFs, from the experiment described in A. GFP and GFP-kazrin C expressing MEFs were treated with 5 μg/ml doxycycline for 24 h before the start of the experiment. The data is the mean ± SEM speed of the cells in each condition normalised to the corresponding control. The p values of two-tailed Mann-Whitney tests are shown. **C.** Quantification of the end-point directionality of cells in the experiment described in A and B. The end-point directionality corresponds to the ratio of the total distance covered by a cell and the track it described. The data is the mean ± SEM directionality of the cells in each condition normalized to the corresponding control. The p values of two-tailed Mann-Whitney tests are shown. **D.** Quantification of the direction autocorrelation of cells in the experiment described in A and B. The direction autocorrelation is the mean turning angle of cells as they migrate. The data is the mean ± SEM angle for each condition, as a function of the time interval.

3.7.2 Kazrin depletion impedes correct abscission during mitosis

Recycling through REs is also essential for mitosis, specifically for the secondary ingression of the cleavage furrow during cytokinesis. Rab11-positive REs are transported to the cleavage furrow to deliver abscission machinery and to deliver membrane to increase PM surface. These mechanisms are needed for the completion of late stage abscission and complete cytokinesis (Wilson *et al.*, 2005; Schiel *et al.*, 2012).

In order to investigate the potential implication of kazrin in mitosis, we analysed dividing cells embedded in 3D Matrigel. We identified mitotic cells by their characteristic rounding and detachment from the matrix. We measured the time from the formation of two distinguishable cells to their complete separation. Kazrin KO cells remained attached for more than double the time than WT cells (**Figure 3.12**). These cells were not able to correctly break the cytoplasmic bridge connecting the two daughter cells. Importantly, GFP-kazrin C cells showed much shorter abscission timing then GFP cells, which demonstrates that the cytokinetic defect was indeed caused by kazrin depletion (**Figure 3.12**).

Overall, cell migration and cytokinetic defects upon kazrin depletion support the idea that kazrin is important for cargo recycling through the RE and for the cellular processes that depend on it.

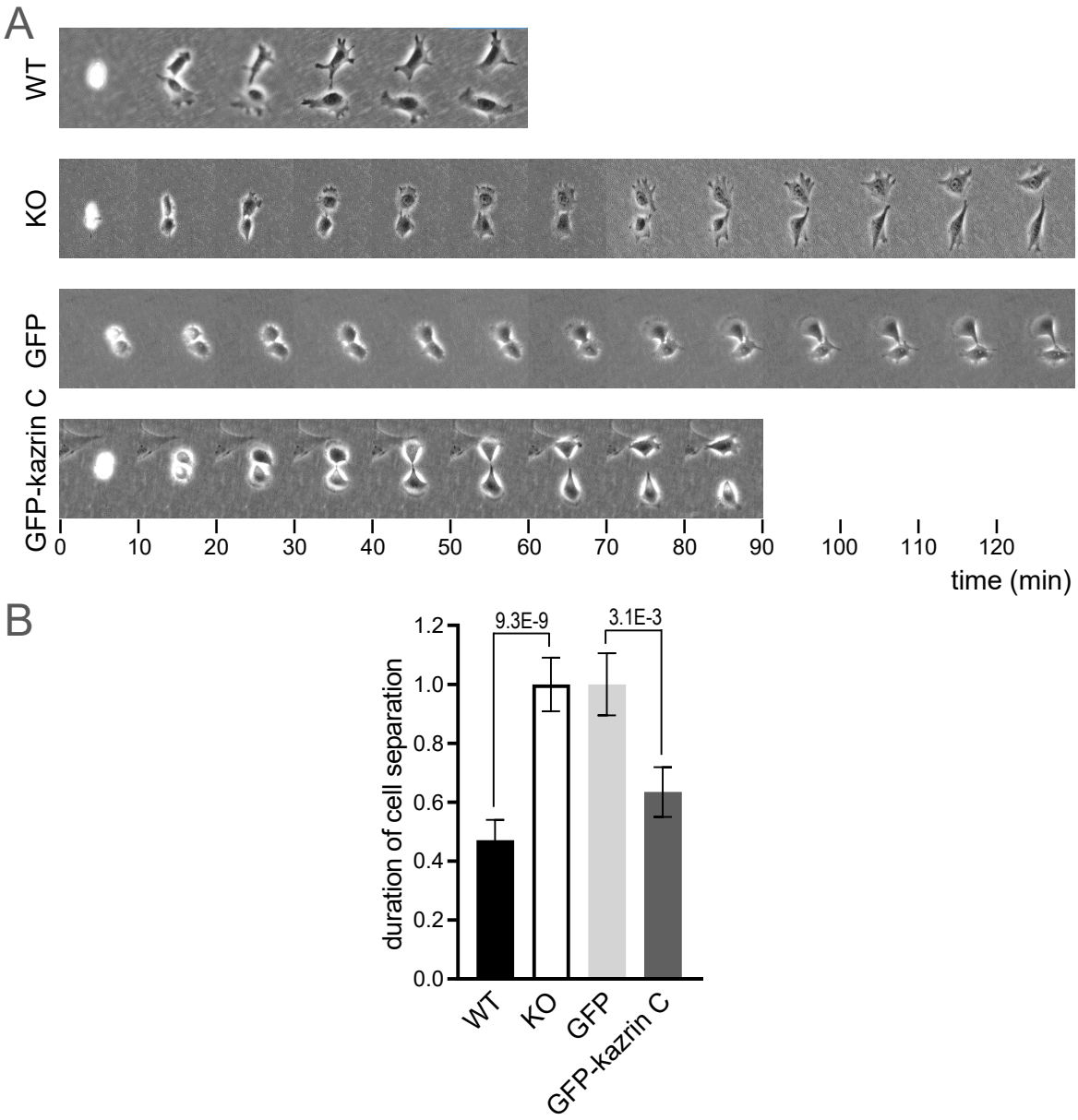

Figure 3.12. Cytokinesis is delayed by kazrin depletion. A. Time lapse epifluorescence images of WT, kazrin KO, GFP and GFP-kazrin C expressing MEFs that were embedded in Matrigel, as they divide. Images were taken with a Leica AF7000 wide-field microscope. Cell division is timed from the reattachment to the substrate until the complete separation of the two daughter cells. **B.** Graph of the mean ± SEM time lapse between substrate attachment and complete cell separation in WT, KO, GFP or GFP-kazrin C expressing MEFs, treated as described in A. GFP and GFP-kazrin C MEFs were treated with 5 μg/ml doxycycline for 24 h before the start of the experiment. The data was normalized to the corresponding control. The p values of two-tailed Mann-Whitney tests are shown.

3.8 Sequence analysis of kazrin C reveals putative functional domains and motifs

Given the evidence for a role of kazrin C in CME and recycling, we started to investigate the molecular mechanisms that supported it. Our approach was to first analyse the sequence of kazrin C in search for homologies to other proteins or conserved motifs. The structure of kazrin is currently unknown. As previously demonstrated, secondary structure predictions using the ExPASy program COILS showed a coiled-coil domain in the N-terminal half of the protein (Cho *et al.*, 2010). Using the 'SWISS-MODEL' tool from ExPASy to detect structural homologies, we identified a protein with a 21.94 % sequence identity with full-length kazrin that could be used to produce a secondary structure model for the N-terminus (**Figure 3.13A**). The protein used as a template was the dynein adaptor BICD-related protein 1 (BICDR1; Urnavicius *et al.*, 2018), a dynactin and kinesin adaptor involved in the transport of rab6-positive secretory vesicles (Schlager *et al.*, 2010). Since we had identified a function of kazrin in endosomal transport, the link with a microtubule motor adaptor seemed relevant.

No structural homology was found for the C-terminal part of kazrin C. Indeed, analysis of the kazrin sequence using the IUPred2A software (Mészáros, Erdös and Dosztányi, 2018) predicted the C-terminus to be an Intrinsically Unstructured Regions (IDRs). IUPred2A assigns each residue a IUPred score that is the probability of it being part of a IDR. We found that amino acids 191 to 301 showed a consistent IUPred score over 0.5 (**Figure 3.13B**). IDRs are a common feature of proteins that work as scaffolds of transiently-assembling macromolecular complexes. These complexes are frequently associated to membrane traffic, the assembly of cytoskeleton structures, transcription and RNA splicing (Haynes *et al.*, 2006). IDRs often weakly bind to several components of the complexes and are thought to promote molecular crowding, possibly through phase separation mechanisms (Miao *et al.*, 2018). Within the putative IDR of kazrin C, we found several short motifs which point to functional implications in membrane traffic and the control of the actin cytoskeleton (**Figure 3.13C**). First, a 'LEDLED' motif (amino acids 274 to 279) could constitute a 'clathrin box' that would mediate an interaction with the terminal domain of CHC (Kirchhausen, Owen and Harrison, 2014). Second, a poly-K sequence (amino acids 281 to 288) could mediate an interaction with PIPs (Chapman *et al.*, 1998). Third, an acidic domain at the very C-terminal end (amino acids 320 to 327) is highly conserved in activators and inhibitors of the Arp2/3 complex (**Figure 3.13C**).

In summary, the structure of kazrin C can be divided in an N-terminal coiled-coil domain with a low homology to the microtubule motor adaptor BICDR1, and a C-terminal IDR that could be involved in molecular crowding during the assembly of endocytic complexes and actin based structures. In the following sections, we investigated these potential interactions.

A

kazrin C N-terminus structure prediction

B

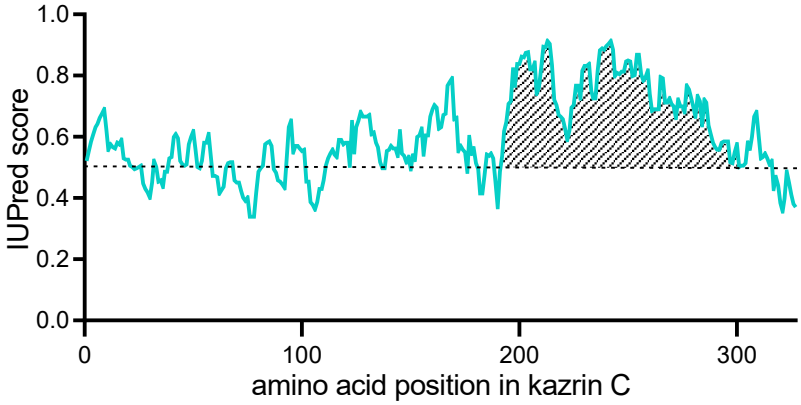

C

M K E M L A K D L E E S Q G G K S S E V L S A T E L R V Q L A Q K E Q E L A R A K E A L
Q A M K A D R K R L K G E K T D L V S Q M Q Q L Y A T L E S R E E Q L R D F I R N Y E Q
H R K E S E D A V K A L A K E K D L L E R E K W E L R R Q A K E A T D H A T A L R S Q L
D L K D N R M K E L E A E L A M A K Q S L A T L T K D V P K R H S L A M P G E T V L N G
N Q E W V V Q A D L P L T A A I R Q S Q Q T L Y H S H P P H P A D R Q A V R V S P C H S
R Q P S V I S D A S A A E G D R S S T P S D I N S P R H R T H S L C N G D S P G P V Q K
N L H N P I V Q S L E D L E D Q K R K K K K E K M G F G S I S R V F A R G K Q R K S L D
P G L F D G T A P D Y Y I E E D A D W

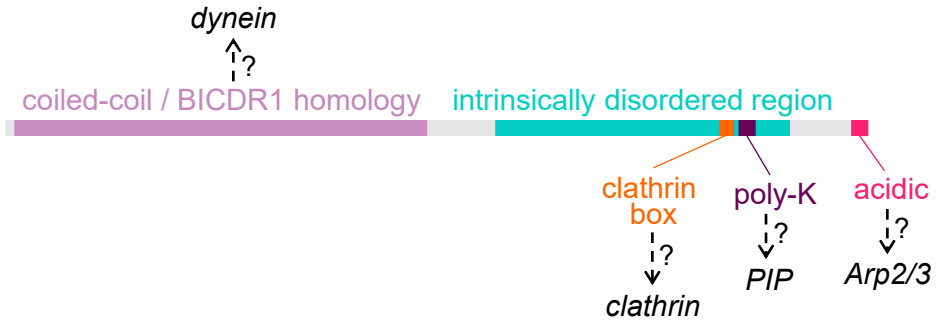

Figure 3.13. Sequence analysis of kazrin C. A. Structural model of the N-terminal half of kazrin C, from amino acid 3 to 164. The model was created with the ExPASy tool 'SWISS-MODEL', which identifies a 21.94 % sequence identity between kazrin C and BICDR1. The structure of BICDR1 was resolved by cryo-EM and was used as a template (Urnavicius *et al.*, 2018). **B.** Prediction of IDRs in kazrin C. The graph shows the probability of each residue of being part of an IDR, according to the IUPred2A software. The shaded area indicates a predicted IDR. **C.** Predicted functional domains and sequences in kazrin C, represented by the one letter amino acid code (above) or a schematic view of the sequence (below). The hypothesised interactions are indicated for each region.

3.9 Kazrin might be implicated in microtubule-mediated transport

A series of evidence led us to investigate a role of kazrin in microtubule-dependent transport. Previous results in this thesis showed a role for kazrin in the transport of endosomes to the perinuclear region, which is microtubule-dependent (Goodson and Jonasson, 2018). In addition, the N-terminus of kazrin C showed slight sequence identity and a potential structural homology with the dynein adaptor BICDR1. And finally, similar to BICDR1 and other dynein adaptors such as HOOK2 and HOOK3 (Szebenyi *et al.*, 2007; Ge *et al.*, 2010; Schlager *et al.*, 2010), GFP-kazrin C showed what seemed a prominent centrosomal localisation (**Figure 3.4A**).

3.9.1 Kazrin interacts with microtubule motors

To investigate the possible role of kazrin as an adaptor for microtubule-dependent molecular motors, we performed an immunoprecipitation experiment from lysates of GFP and GFP-kazrin C expressing cells. Immunoprecipitates were analysed by IB in search of components of the microtubule transport machinery. We detected specific interactions of GFP-kazrin C with the dynactin component p150-glued and with kinesin-1 heavy chain (HC). We did not detect tubulin in the IP, suggesting a direct interplay of kazrin with the motors dynein-dynactin and kinesin, or with their adaptors (**Figure 3.14A**). The BICDR1 region that shows homology with kazrin binds to dynein Intermediate Light Chain isoforms LIC1 and LIC2 (Lee *et al.*, 2018). To investigate if kazrin might behave as a *bona fide* dynein adaptor, we tested its capacity to interact with these proteins in pull-down assays with purified components. To this end, LIC1 and LIC2 fused to Glutathione S-Transferases (GST) were expressed in *E. coli*, immobilized on glutathione-Sepharose beads, and subsequently incubated with 6-Histidine (6xHis)-kazrin C, also expressed and purified from *E.coli*. IB analysis was then used to detect pulled-down kazrin. GST-covered beads were used as a negative control. Indeed, we detected a direct interaction of 6xHis-kazrin C with GST-LIC1, but not with GST. The interaction seemed isoform-specific, as no detectable kazrin was pulled-down with GST-LIC2 (**Figure 3.14B**). These results are consistent with a possible role of kazrin as a dynein/kinesin adaptor that could transport endosomes towards the perinuclear region.

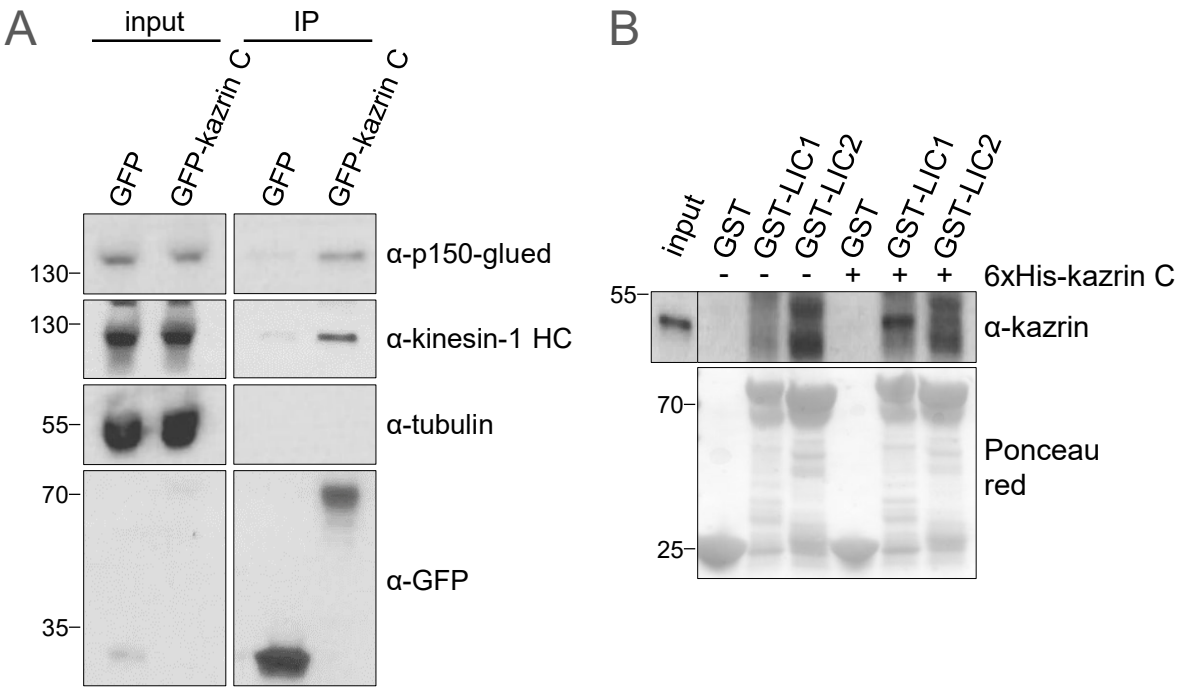

Figure 3.14. GFP-kazrin C interacts with kinesin and dynein. A. IB of immunoprecipitations from GFP or GFP-kazrin C MEF cells treated with 5 µg/ml of doxycycline for 24 h. From 3 mg of total non-denaturing cell lysate, 0.5% was loaded as input and the rest was immunoprecipitated with GFP-trap beads and loaded (IP). The membranes were incubated with α-p150-glued (BD 610473), α-kinesin-1 HC (Santa Cruz 133184), α-tubulin (Sigma-Aldrich T-6557) and α-GFP (Living Colors 632380) as an expression control. **B.** IBs of pull-down experiments with purified 6xHis-kazrin C and GST or GST fused to LIC1 or LIC2. 500 ng of 6xHis-kazrin were added to approximately 500 ng of each GST construct and incubated with glutathione-Sepharose beads. 0.5 ng of 6xHis-kazrin were loaded as input. The membranes were stained with Ponceau red to detect GST and GST fusion constructs and with an α-kazrin antibody (Abcam 88752) and the appropriate peroxidase-conjugated secondary antibody to detect pulled-down kazrin.

3.9.2 GFP-kazrin C is at the centrosome and pericentrosomal structures

We suspected that GFP-kazrin C localised at the centrosome. To confirm this hypothesis, we checked its co-localisation with pericentrin, a component of the PCM that surrounds centrioles. The co-localisation was clear (**Figure 3.15A**). GFP-kazrin C seemed to form a more complex structure than that immediately surrounding the centrioles. Smaller dots of GFP-kazrin C could be observed in the centrosomal area. These dots were dynamic and seemed to travel to or from the centrioles, consistent with the detected interaction of kazrin C with centripetal and centrifugal microtubule-dependent motors (**Figure 3.15B**; **Video 5**). We hypothesised that the GFP-kazrin C structures corresponded to centrosomal satellite structures, which are membrane-less compartments that transport material to and from the centrosome. Indeed, we observed a partial co-localisation of GFP-kazrin C with the satellite scaffolding protein PCM-1 (**Figure 3.15C**). These findings prove that GFP-kazrin C localises at the centrosome and the PMC, similar to other kinesin and dynein adaptors.

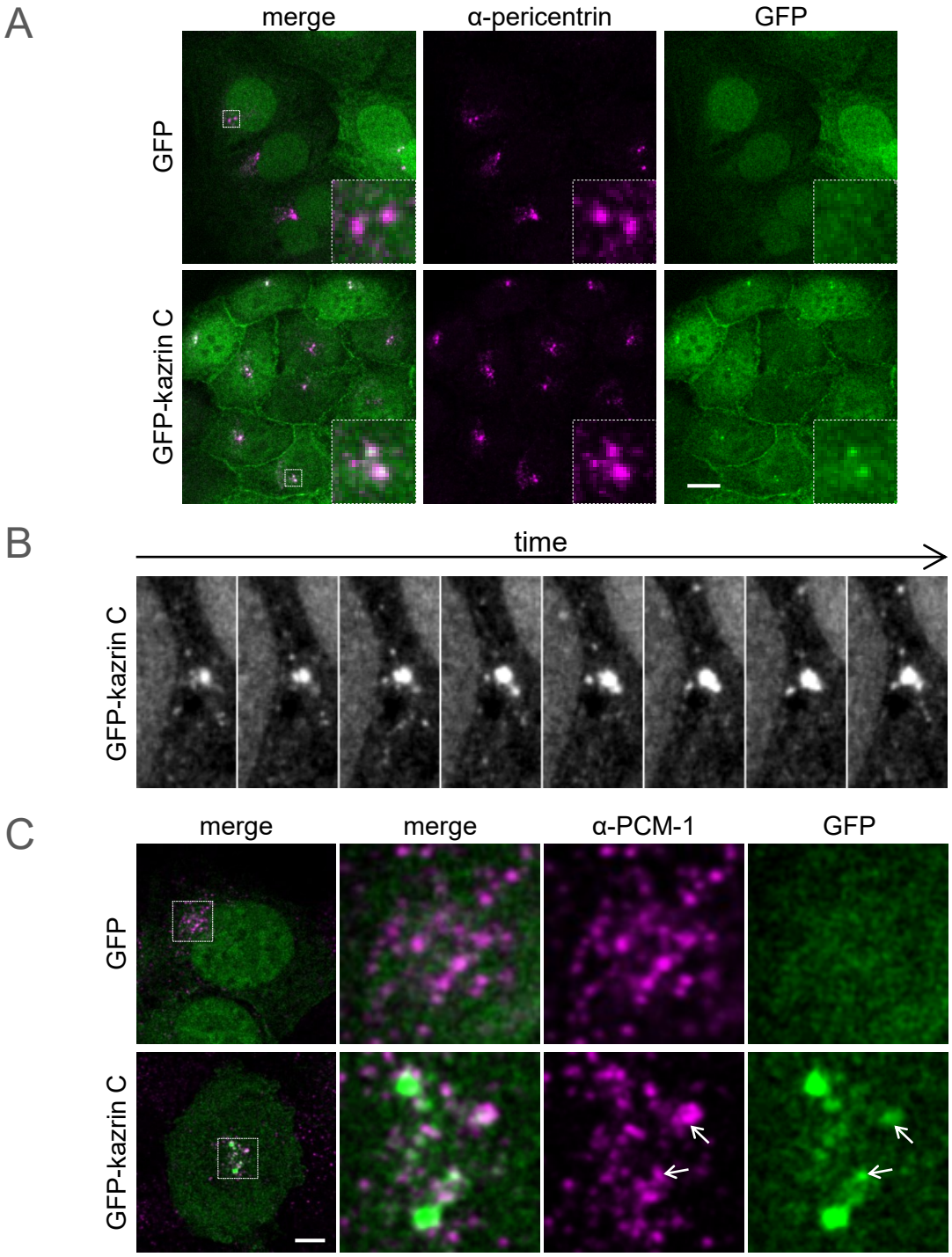

Figure 3.15. GFP-Kazrin C localises at the pericentriolar region. A. Merged and individual channels of confocal images of GFP and GFP-kazrin C expressing MEFs treated with 5 µg/ml doxycycline for 24 h, fixed and stained with an α-pericentrin antibody and a A568-conjugated secondary antibody. The images were taken with a Zeiss LSM-780 confocal microscope. 3.5 times amplifications of the indicated areas are shown. Scale bar = 10 µm. **B.** Time lapse fluorescence micrographs of GFP-kazrin C expressing MEF imaged every 2.65 s. The centrosomal area is shown. Scale bar = 2 µm. **C.** Merge fluorescence micrographs of GFP or GFP-kazrin C expressing cells, fixed and stained with an α-PCM-1 antibody and a A568-conjugated secondary antibody. Merged images and individual channels of 5 times amplifications of the indicated areas are shown. The arrows point to sites of co-localisation. Scale bar = 5 µm.

3.9.3 GFP-kazrin C entraps endosomes in the pericentrosomal area

We next decided to study the link between the localisation of kazrin in the centrosome and its function in the transport of endosomes. We had previously observed co-fractionation of endogenous kazrin and EEs. We also knew that kazrin depletion caused the dispersal of EEs, whereas GFP-kazrin C expression rescued the phenotype. That is, GFP-kazrin C was able to promote EE transport to the centrosomal region or entrap these organelles in the vicinity of the centrioles. This idea was supported by an immunofluorescence observation of EEA1-marked endosomes that seemed to be entrapped by a pericentriolar GFP-kazrin C network (**Figure 3.16**).w

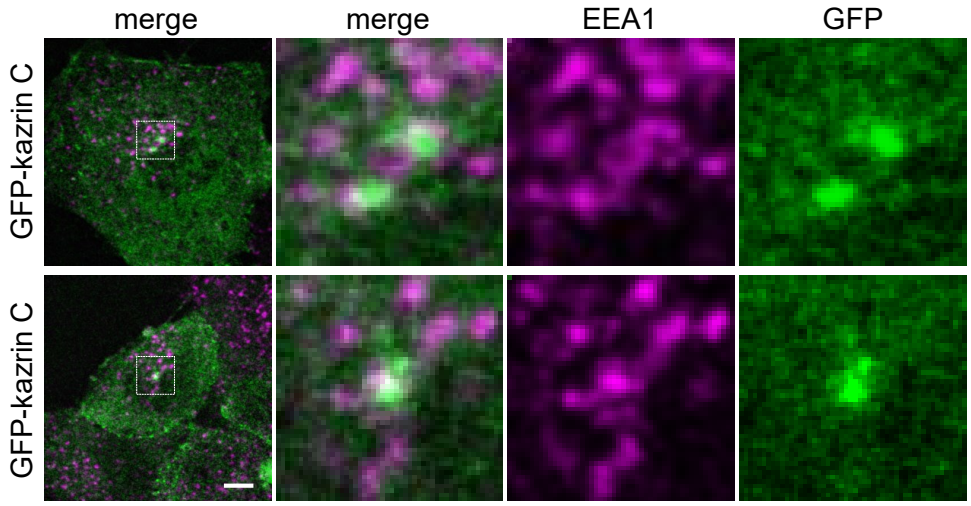

Figure 3.16. GFP-kazrin C traps endosomes in a pericentriolar network. Merged confocal images of GFP and GFP-kazrin C expressing MEFs treated with 5 µg/ml doxycycline for 24 h, fixed and stained with an α-EEA1 antibody (Cell Signaling 3288) and a A568-conjugated secondary antibody. The images were taken with a Zeiss LSM-780 confocal microscope. Individual channels and merged images of 6 times amplifications of the indicated areas are shown. Scale bar = 2 µm.

Altogether, our results strongly suggest a role for kazrin in the microtubule-dependent transport or pericentriolar retention of EEs, possibly contributing to endosomal maturation and cargo recycling.

3.10 Kazrin interacts with endosomal components

In order for kazrin to be a dynein or kinesin adaptor for endosomal compartments, its C-terminal portion should be capable of interacting with some surface components of these organelles. Accordingly, the subcellular fractionation experiments demonstrated that endogenous kazrin was indeed localised at EEs (**Figure 3.6**). Thus, we decided to investigate the interaction of kazrin with different types of endosomal components.

3.10.1 Kazrin interacts with clathrin, clathrin adaptors and EHD1/3

Previous data from A. Baumann and B. Schmelzl in the laboratory have shown that endogenous clathrin and γ-adaptin co-immunoprecipitated with endogenous kazrin in COS7 cells. Furthermore, pull-down assays with purified components demonstrated direct interactions between the region containing the LELELD motif in kazrin and the terminal domain of CHC. Pull-down assays with purified components also showed an interaction of the ear of γ-adaptin with a region of kazrin comprised between amino acids 161 and 250. A GFP-trap immunoprecipitation from GFP or GFP-kazrin C expressing cells confirmed specific interactions between GFP-kazrin C with CHC, as well as with the endosomal and Golgi clathrin adaptor AP-1. However, no interaction was detected with α-adaptin from the AP-2 complex or with another clathrin adaptor, GGA2 (**Figure 3.17A**). In addition, we detected weak but specific interactions of kazrin C with the endogenous GTPases EHD1/3. Both kazrin interactors γ-adaptin and EHD1/3 are implicated in EE to RE transport. We failed to detect interactions between GFP-kazrin C and the tether EEA1, the retromer component VPS35, rab4 or the rab5 adaptor rabaptin-5 (**Figure 3.17A**). These are all endosomal components not directly involved in EE to RE transport.

Consistent with the co-immunoprecipitation results, kazrin co-fractionated with EHD1/3 in an Optiprep gradient. A partial overlap with γ-adaptin could be observed in the subcellular fractionation, although γ-adaptin had a spread pattern that most likely reflected its presence in endosomes and the Golgi (**Figure 3.17B**). We performed immunofluorescence experiments in GFP or GFP-kazrin C expressing cells to further investigate the possible co-localisation of kazrin with its interactors. γ-Adaptin was mainly observed in the perinuclear region, most likely associated with the Golgi, but it was also found in peripheral structures, some of which contained GFP-kazrin C. EHD1/3 was observed, as expected, on tubules. Similar to γ-adaptin, some co-localisation sites with GFP-kazrin C were detected (**Figure 3.17C**).

To support the immunoprecipitation results, we checked the interactions in a yeast-two-hybrid experiment, in which we detected a weak but significant interaction of kazrin with the γ-adaptin ear but not the α-adaptin ear. We failed to demonstrate binding to EHD1, EHD3 or the EH domains of EHD1 and EHD3 in this type of experiment (**Figure 3.17D**). However, pull-down experiments with purified 6xHis-Kazrin C and GST-EHD1 or GST-EHD3 confirmed a direct interaction of kazrin C with the dynamin-related GTPases (**Figure 3.17E**). Consistent with negative results previously obtained in immunoprecipitation and pull-down experiments performed in the laboratory, no interactions were observed between kazrin C and the small GTPases rab4a, rab4b, a rab4b dominant positive mutant or a rab4b dominant negative mutant (**Figure 3.17D**).

Altogether the data indicated that the C-terminal portion of kazrin C weakly interacted with several components of EEs, with a preference for those involved in the transport or

maturation processes between EEs and REs, further reinforcing the hypothesis that kazrin plays a specific role in this transport step.

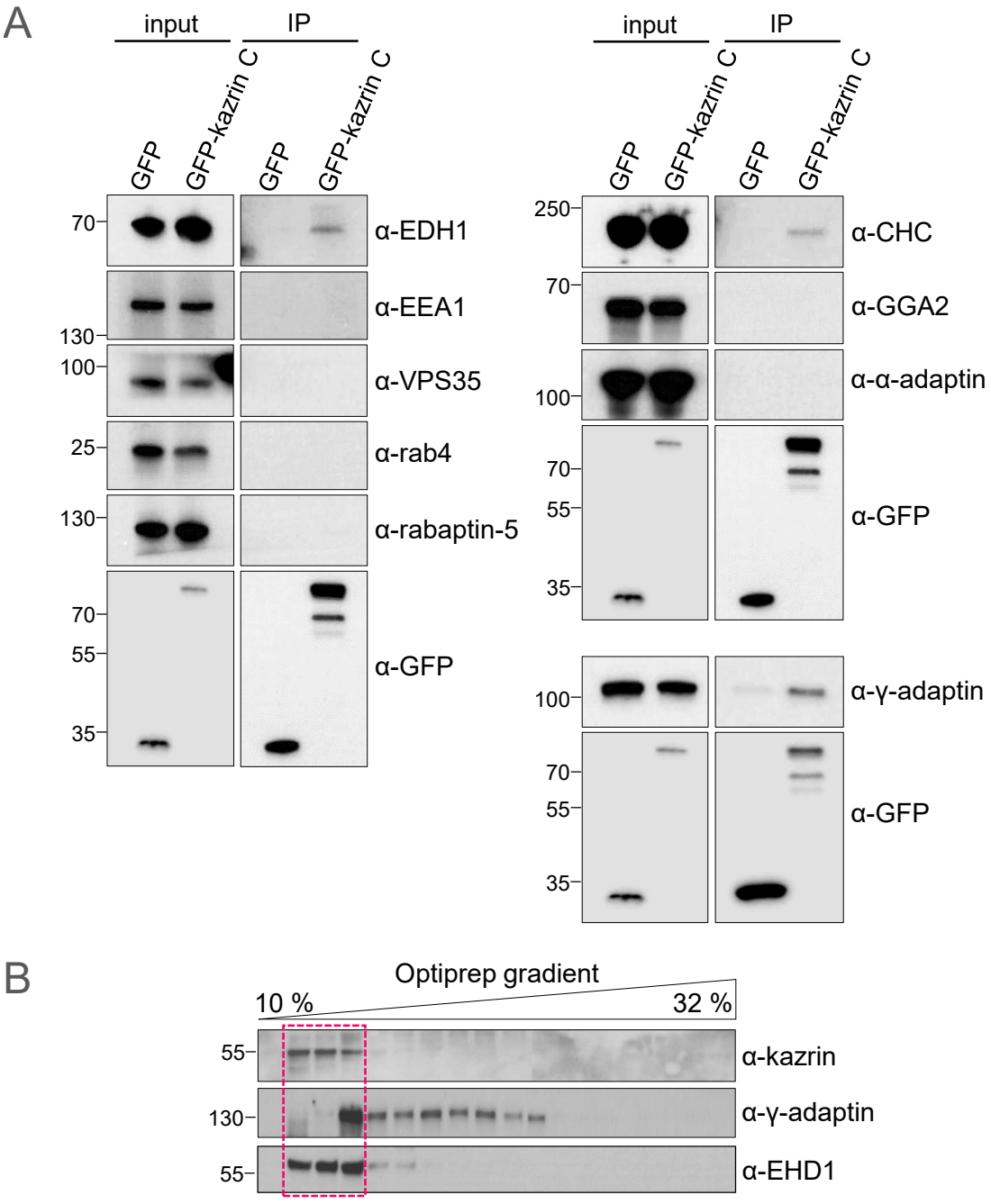

C

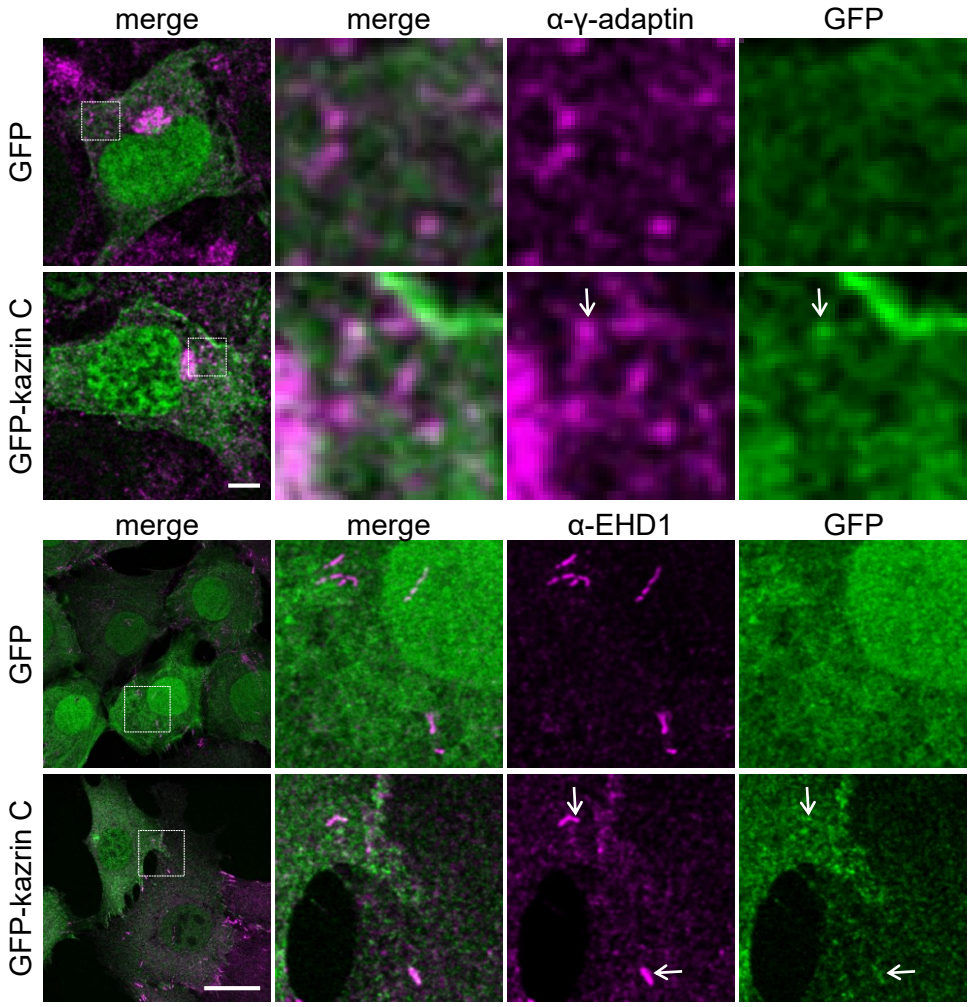
merge
merge
α-γ-adaptin
GFP
GFP
GFP-kazrin C
merge
merge
α-EHD1
GFP
GFP
GFP-kazrin C

D

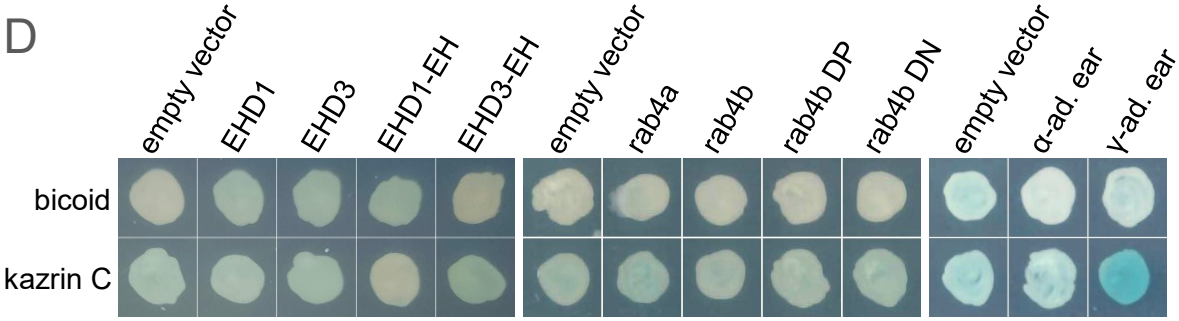
empty vector
EHD1
EHD3
EHD1-EH
EHD3-EH
empty vector
rab4a
rab4b
rab4b DP
rab4b DN
empty vector
α-ad. ear
γ-ad. ear
bicoid
kazrin C

E

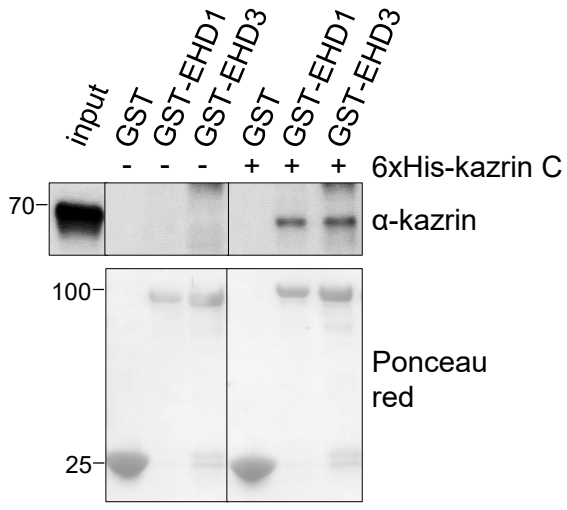
input
GST
GST-EHD1
GST-EHD3
GST
GST-EHD1
GST-EHD3
- - - + + +
6xHis-kazrin C
70
α-kazrin
100
25
Ponceau red

Figure 3.17. Kazrin interacts with EEs components. A. IB of immunoprecipitations from GFP or GFP-kazrin C expressing MEFs treated with 5 µg/ml doxycycline for 24 h. Immunoprecipitations were performed from non-denaturing cell lysates containing 2-4 mg of total protein. 0.5 % was loaded as input, except for the case of γ-adaptin, in which 1.25 % of lysate was used as input. The rest was immunoprecipitated with GFP-trap beads and loaded (IP). The membranes were incubated with α-EHD1 (Abcam 109311), α-EEA1 (Cell Signaling 3288), α-VPS35 (Santa Cruz 374372), α-rab4 (BD 610888), α-rabaptin-5 (BD 610676), α-CHC (BD 610499), α-GGA2 (BD 612612), α-γ-adaptin (BD 610386) and α-GFP (Living Colors 632380) antibodies and the adequate peroxidase-conjugated secondary antibody. **B.** IB of a subcellular fractionation assay of WT MEFs. An Optiprep gradient from 10 to 32 % was used to separate membranous subcellular compartments according to their density. Each lane corresponds to a gradient fraction. The IB membranes were blotted with α-kazrin (EMBL Heidelberg), α-γ-adaptin (BD 610386) and α-EHD1 (Abcam 109311) antibodies and the adequate peroxidase-conjugated secondary antibodies. Of note, the α-EHD1 antibody also recognised EHD3. The rectangle in pink indicates the lanes that correspond to EEs. **C.** Merged confocal images of GFP and GFP-kazrin C expressing MEFs treated with 5 µg/ml doxycycline for 24 h. The cells were fixed and stained with an α-γ-adaptin (BD 610386) or α-EHD1 (Abcam 109311) antibody and the adequate A568-conjugated secondary antibodies. Merged and individual channel images of 3.5 times amplifications of the indicated areas are shown. The images were taken with a Zeiss LSM-780 confocal microscope. The arrows point to sites of co-localisation. Scale bar = 5 µm. **D.** Yeast-two-hybrid assay in which the negative control protein bicoid or kazrin C were used as baits, and EHD1, EHD3, EHD1 EH domain, EHD3 EH domain, rab4a, rab4b, rab4b dominant positive (DP), rab4b dominant negative (DN), α-adaptin ear or γ-adaptin ear were used as preys. Blue indicates interaction. **E.** IBs of pull-down experiments with purified 6xHis-kazrin C and GST or GST fused to EHD1 or EHD3. 200 ng of 6xHis-kazrin were added to approximately 500 ng of each GST construct and incubated with glutathione-Sepharose beads. 0.5 ng of 6xHis-kazrin C were loaded as input. The membranes were stained with Ponceau red to detect GST and GST fusion constructs and with an α-kazrin antibody (Abcam 88752) and the appropriate peroxidase-conjugated secondary antibody.

3.10.2 Kazrin depletion does not affect EHD1/3-mediated tubulation

Since two of the kazrin interactors detected by immunoprecipitation and pull-down were EHD1 and EHD3, we speculated a role for kazrin in endosomal tubulation. It could constitute a molecular mechanism for the regulation of recycling by kazrin. The detection of endogenous EHD1/3 by immunofluorescence allowed the visualisation of endosomal tubules that could be quantified (**Figure 3.18A**). We did not detect any differences in the number or the length of EHD1/3 tubules between WT and kazrin KO cells (**Figure 3.18B**). We therefore discarded a major role of kazrin in endosomal tubulation. The result further supported the view that kazrin rather works in the transport or maturation of EHD1/3-containing organelles.

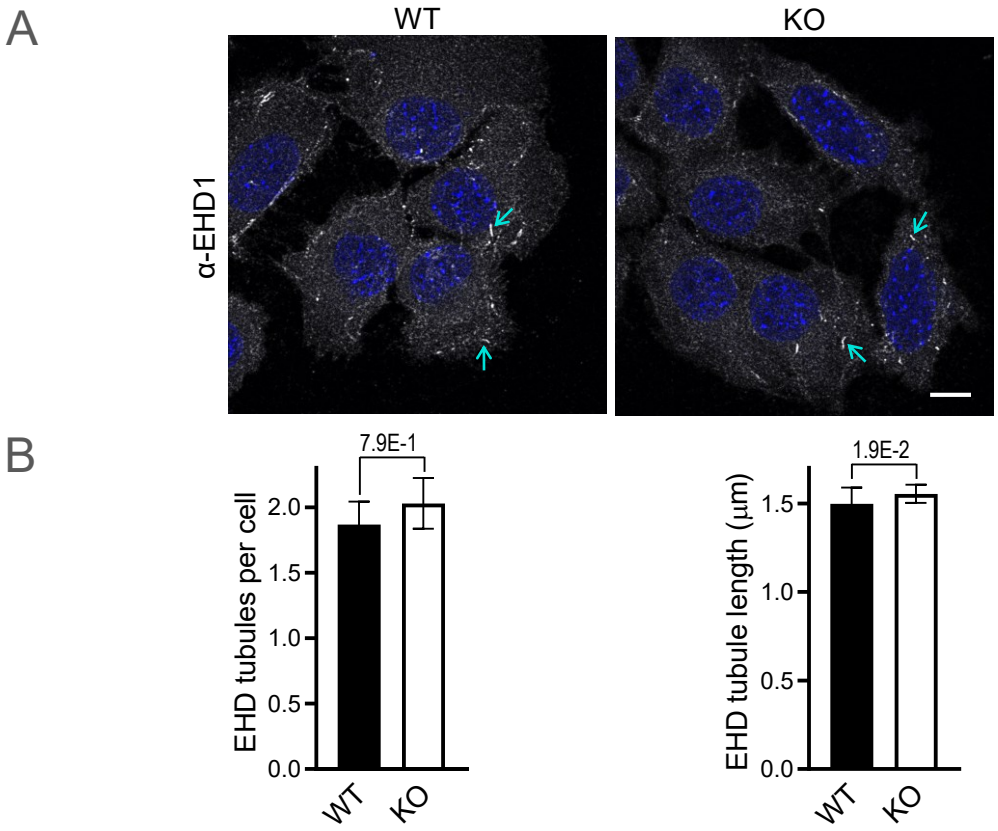

Figure 3.18. Kazrin depletion does not affect the number or length of EHD1/3-marked tubules. A. Confocal images of WT and kazrin KO MEFs fixed and stained with an α-EHD1 antibody (Abcam 109311) and a A488-conjugated secondary antibody. Images were taken with a Zeiss LSM-780 confocal microscope. The arrows indicate EHD1/3 tubules. Scale bar = 10 µm. **B.** Quantification of the mean ± SEM number per cell or length of EHD1/3 elongated structures in WT and kazrin KO MEFs. The p values of a two-tailed Mann-Whitney test are shown.

3.10.3 GST-kazrin C interacts with PI3P

As mentioned above, there is a poly-K motif at the C-terminus of kazrin C, similar to that described for PIP-binding sequences (Chapman *et al.*, 1998). PIP are important players in membrane trafficking that serve as identity markers of subcellular membranes and recruit specialised machinery.

To analyse kazrin-lipid interactions, we purified a series of GST-tagged kazrin C constructs (**Figure 3.19A**) and used them to overlay lipid strip membranes. The commercially-available lipid strip membranes were spotted with sphingosine-1-phosphate and the following phosphoinositides: PI, PI3P, PI4P, PI5P, PI(3,4)P_2, PI(3,5)P_2, PI(4,5)P_2, PI(3,4,5)P_3, PA, PS, PE, PC, LPA and LPC (**Figure 3.19B**). Upon immunodetection of the GST constructs bound to the lipids we could demonstrate specific binding of amino acids 251 to 327 in the C-terminal part of kazrin with PI3P. The binding of this region was abolished when the poly-K stretch was deleted (ΔCt) or mutated to alanines (polyK→A). Conversely, binding was not

prevented when the acidic peptide was mutated into to a stretch of alanines, a mutation previously shown to disrupt binding to the Arp2/3 complex (Ct acidic→A; **Figure 3.19C**). We did not observe any binding of the GST-only control. To confirm the specificity of the kazrin binding to PI3P, we used a variant of lipid strips that contained a concentration gradient of PIPs. Again, we detected a concentration-dependent interaction of the kazrin C-terminus (amino acids 161 to 327) with PI3P. The interaction did not occur when the poly-K mutant was used in the assay (Ct polyK→A; **Figure 3.19D**).

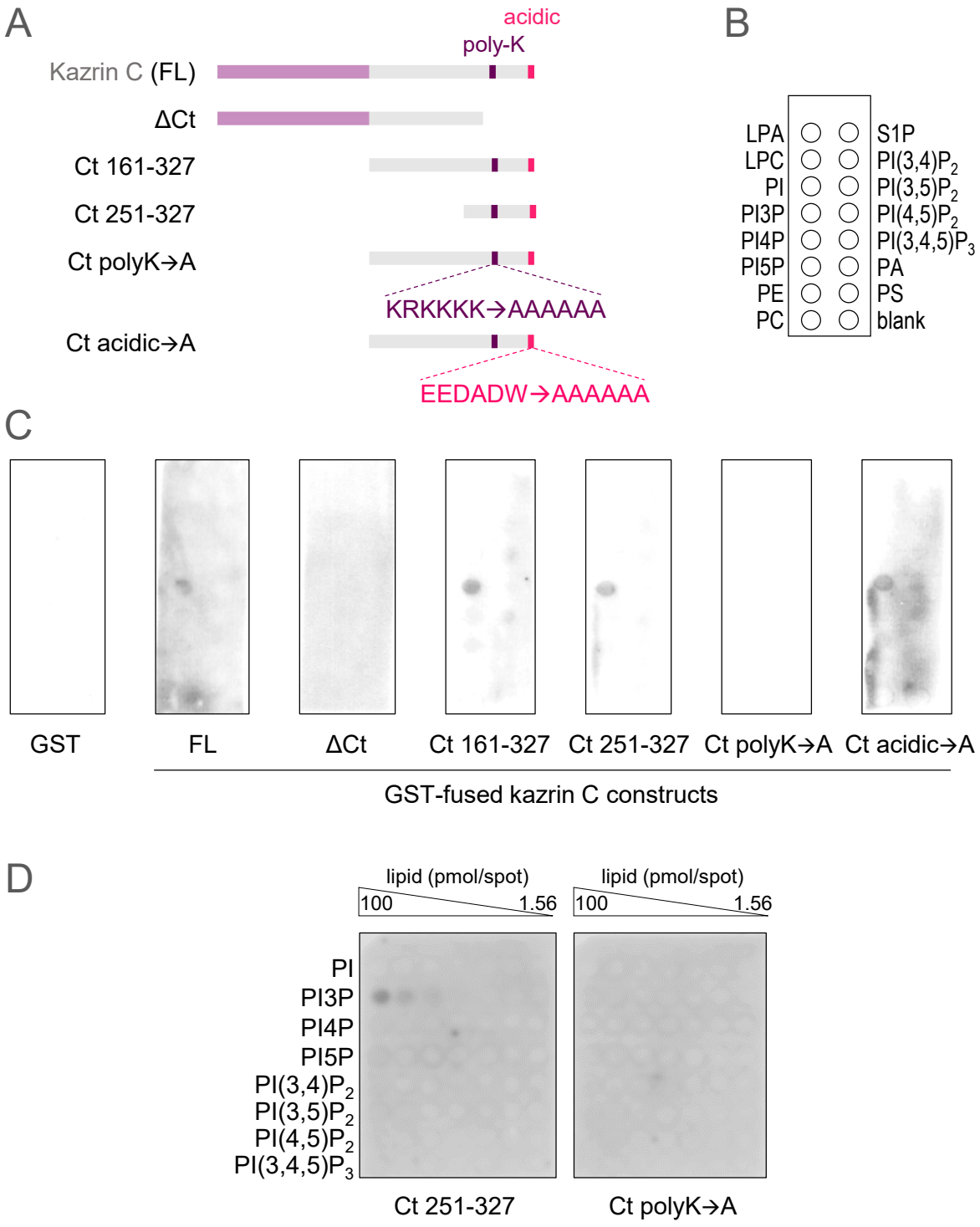

Figure 3.19. Kazrin C interacts with PI3P through a poly-K region in its C-terminus. **A.** Representation of the kazrin constructs used to overlay the lipid strips. The poly-K and acidic regions are highlighted. **B.** Representation of a lipid strip spotted with: lysophosphatidic acid (LPA), lysophosphatidylcoline (LPC), sphingosine-1-phosphate (S1P), phosphatidic acid (PA), phosphatidylethanolamine (PE), phosphatidylserine (PS), phosphatidylcholine (PC), PI, the indicated PIPs and a blank spot. **C.** Lipid binding assay performed with purified GST protein and the kazrin constructs described in A, fused to GST. The purified proteins were incubated with the membranes, which were washed and overlaid with an α-GST antibody (Amersham 27-57701) and the adequate peroxidase-conjugated secondary antibody. The representation of a lipid strip in B allows the identification of the spots showing an interaction. **D.** Lipid binding assay performed with purified GST fused to the C-terminus of kazrin C or the poly-K mutant, which was used as a control. The membranes used in this assay contain a concentration gradient of the indicated PIPs.

Since PI3P is enriched in EEs, this result supports a role for the C-terminus of kazrin C as a scaffold entrapping EEs and is consistent with the idea that kazrin works as an adaptor for the centripetal transport of these organelles.

3.10.4 GFP-kazrin C interacts with the class III PI3K and might inhibit its activity

Once a direct link between kazrin and PI3P was established, we contemplated the possibility of kazrin regulating the metabolism of this lipid. We transfected WT and kazrin KO cells with a GFP-fused FYVE domain to detect PI3P. As a negative control, we treated cells with the VPS34 inhibitor IN1, which completely abolished GFP-FYVE recruitment to EE (Bago *et al.*, 2014). Interestingly, kazrin KO cells exhibited more endosomal GFP-FYVE than WT cells (**Figure 3.20A**). The experiment was quantified using the signal of the IN1 control as background. We observed a 2.3-fold increase of endosomal PI3P signal in kazrin depleted cells in comparison to WT cells (**Figure 3.20B**).

The increase in endosomal PI3P could be a cause or a consequence of the accumulation EE observed in kazrin depleted cells. To investigate this matter, we decided to test if kazrin interacted with VPS34, the main class III PI-3-kinase generating PI3P in EEs (Backer, 2016). In an immunoprecipitation experiment, we saw a strong interaction of GFP-kazrin C with VPS34, the catalytic component of the kinase. Weaker interactions were detected for other components of the core complex, VPS15 and beclin, but not with the endosomal adaptor UVRAG (**Figure 3.20C**). These results opened the possibility that kazrin might negatively regulate the formation of PI3P by competing out the interaction of the PI-3 kinase core complex (VPS34, beclin and VPS15) with its endosomal adaptor UVRAG, which would undoubtedly affect endosomal trafficking and/or maturation.

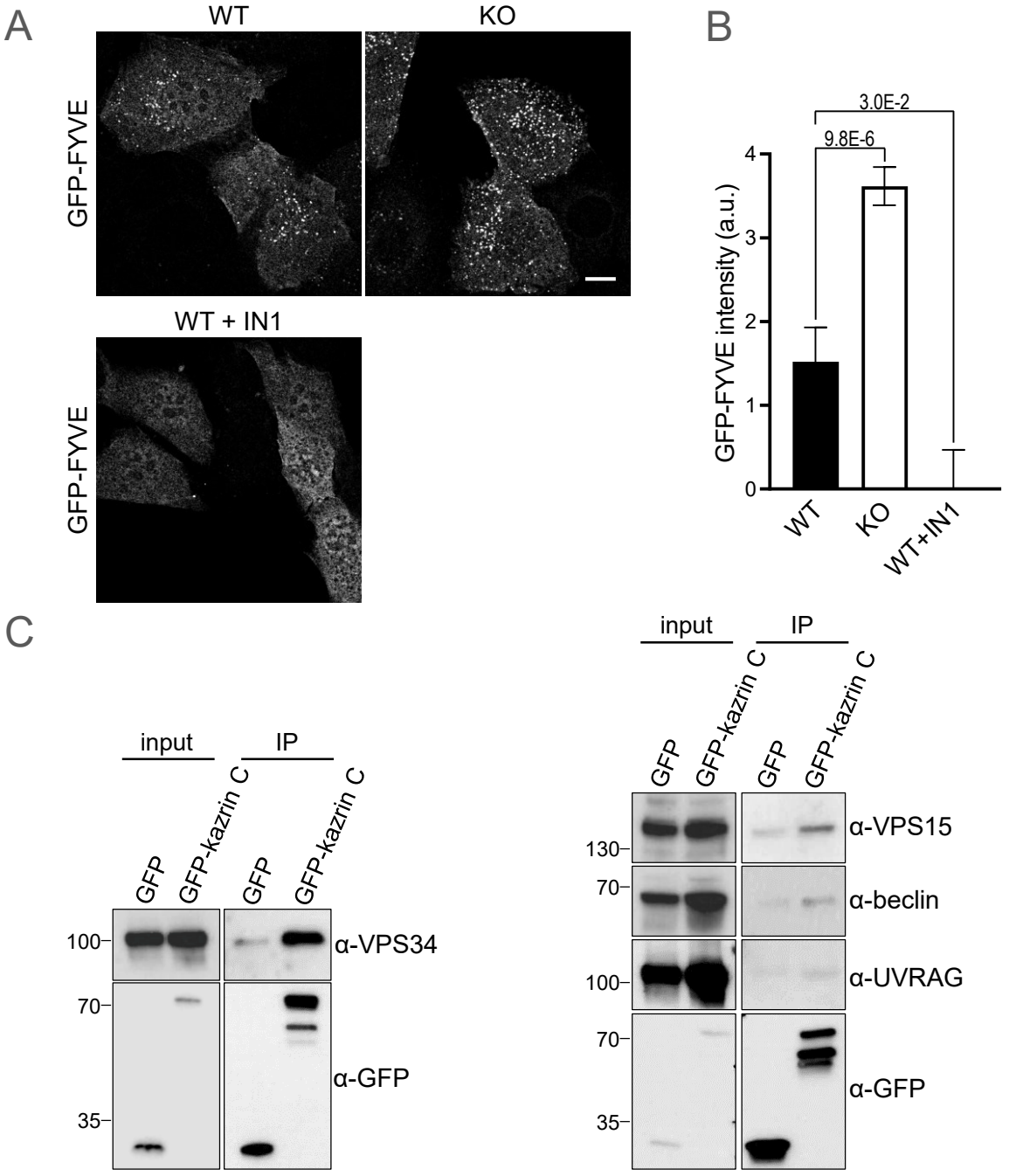

Figure 3.20. Kazrin C interacts with VPS34 and it might inhibit its activity. A. Confocal images of WT and KO cells transfected with a plasmid encoding the PI3P probe GFP-FYVE. 24 h after transfection, cells were treated with the VPS34 inhibitor IN1 (1 μM) o with DMSO for 2 h before fixation. Images were taken with a Zeiss LSM-780 confocal microscope. Scale bar = 10 μm. **B.** Quantification of the experiment described in A. The mean ± SEM fluorescence intensity for the GFP-FYVE probe over the cytosolic signal per cells is plotted. The p values of a two-tailed t test are shown. **C.** IB of immunoprecipitations from GFP or GFP-kazrin C expressing MEFs treated with 5 μg/ml of doxycycline for 24 h. the IPs were performed from non-denaturing cell lysates containing 1.5 mg of total protein. 0.5% was loaded as input. The rest was immunoprecipitated with GFP-trap beads and loaded (IP). The membranes were incubated with α-VPS34 (Cell Signaling 4263), α-VPS15 (Abcam 124817), α-beclin (Cell Signaling 3738), α-UVRAG (MBL M160-3) and α-GFP (Living Colors 632380) antibodies and the adequate peroxidase-conjugated secondary antibodies.

3.11 Kazrin regulates Arp2/3-mediated actin polymerisation

So far, we had linked kazrin to microtubule transport, the machinery involved in EE to RE transport (γ-adaptin and the GTPases EHD1 and 3) and PI3P metabolism, all of which are regulators of endocytosis and endosomal trafficking. In this section, we describe a relationship between kazrin and the Arp2/3-dependent actin polymerisation machinery. Initially, the link was suggested by the presence of an acidic peptide at the C-terminus of kazrin that resembled that present in activators and inhibitors of the Arp2/3 complex. Previous data from A. Baumann demonstrated that GFP-kazrin C interacted with the Arp2/3 complex in immunoprecipitation experiments performed in COS7 cells. Moreover, the acidic peptide was indeed required to mediate direct binding of kazrin C to the Arp2/3 complex, as shown in pull-down experiments with purified components. Further, he also demonstrated an interaction between kazrin and WASH, a major endosomal activator of the Arp2/3 complex. However, pyrene actin polymerisation assays failed to demonstrate an effect of kazrin C on Arp2/3-dependent actin polymerisation either alone or in the presence of the PVCA domain of WASH, posing a doubt on the physiological relevance of the described interaction. In the present thesis, we deepened in the analysis of kazrin and the endosomal actin polymerisation machinery and we found that endosomal N-WASP and cortactin, rather that WASH, are the relevant physiological partners of kazrin.

3.11.1 Kazrin interacts with the Arp2/3 polymerisation machinery

In order to study the interaction of kazrin with complexes that regulate actin polymerisation on endosomal membranes, we performed a GFP-trap immunoprecipitation experiment from GFP and GFP-kazrin C MEF lysates. We looked for the presence not only of WASH but also N-WASP and cortactin, which have been shown to modulate actin polymerisation in the PM in the context of endocytic uptake (Kaksonen and Roux, 2018), and in early endosomal membranes (Taunton *et al.*, 2000; Puthenveedu *et al.*, 2010). Interestingly, we recapitulated in MEF the interaction of kazrin with WASH, previously described in COS7 cells, but we detected a much stronger interaction with N-WASP and cortactin. We did not detect an interaction of kazrin with the endosomal WASH complex component fam21, questioning the functional significance of their binding (**Figure 3.21A**). A subcellular fractionation analysis showed a sharp co-fractionation of endogenous kazrin with cortactin and N-WASP in EEs. Strikingly, WASH was detected in heavier fractions but not in EEs (**Figure 3.21B**). This result reinforced the possible physiological link between kazrin and N-WASP and cortactin rather than WASH in MEF cells. The co-localisation of GFP-kazrin C in internal structures with cortactin was particularly evident by immunofluorescence experiments. Some co-localisation was also obvious at the PM (**Figure 3.21C**).

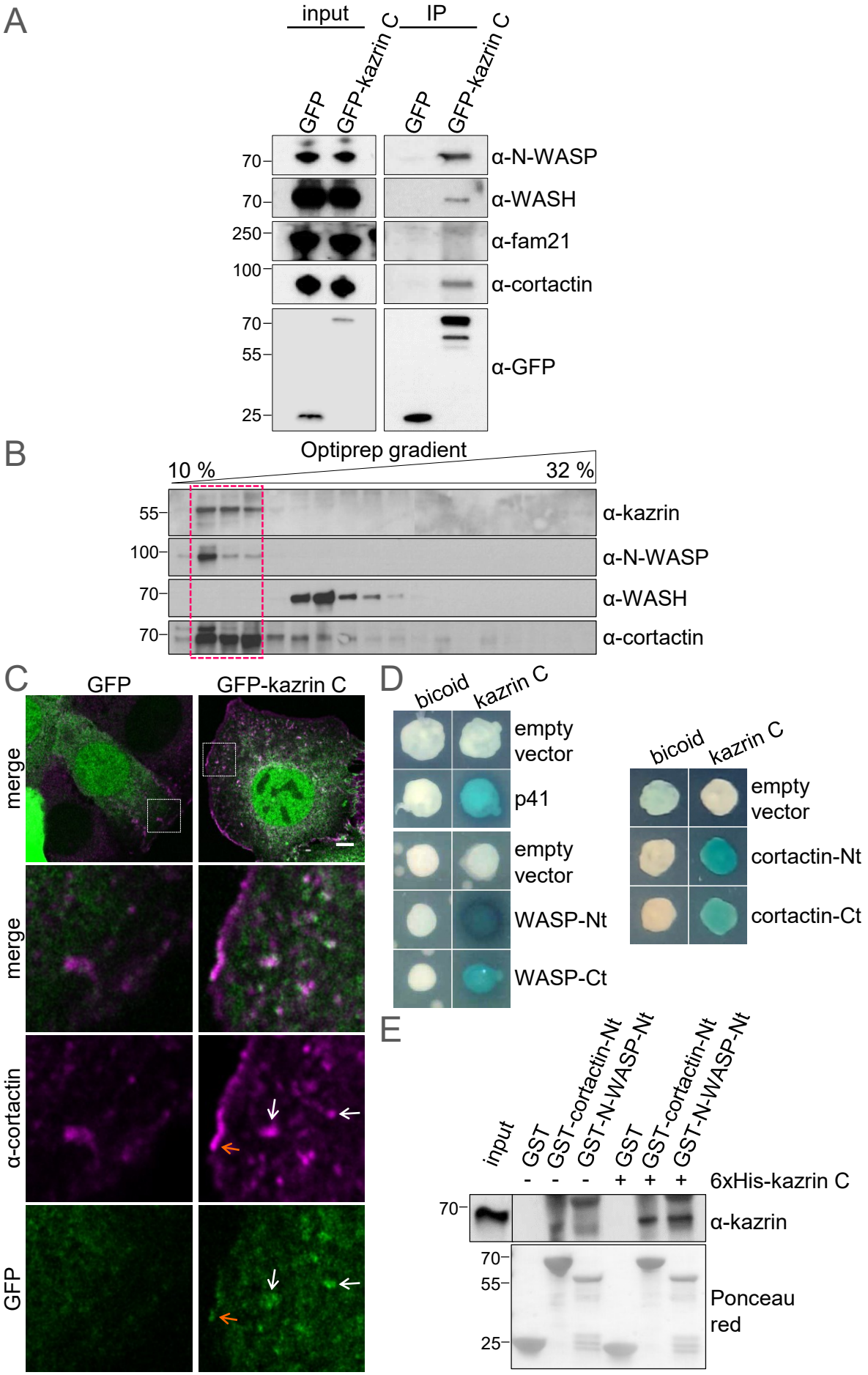
A
input
IP
GFP
GFP-kazrin C
GFP
GFP-kazrin C
70
70
250
100
70
55
25
α-N-WASP
α-WASH
α-fam21
α-cortactin
α-GFP
B
Optiprep gradient
10 %
32 %
55
100
70
70
α-kazrin
α-N-WASP
α-WASH
α-cortactin
C
GFP
GFP-kazrin C
merge
merge
α-cortactin
GFP
D
bicoid
kazrin C
empty vector
p41
empty vector
WASP-Nt
WASP-Ct
bicoid
kazrin C
empty vector
cortactin-Nt
cortactin-Ct
E
input
GST
GST-cortactin-Nt
GST-N-WASP-Nt
GST
GST-cortactin-Nt
GST-N-WASP-Nt
- - - + + +
6xHis-kazrin C
70
α-kazrin
70
55
25
Ponceau red

Figure 3.21. Kazrin interacts with N-WASP and cortactin. A. IB of immunoprecipitations from GFP or GFP-kazrin C expressing MEFs treated with 5 µg/ml doxycycline for 24 h. Immunoprecipitations were performed from non-denaturing protein extracts bearing 1.5 mg of total protein. 0.5% was loaded as input. The rest was immunoprecipitated with GFP-trap beads and loaded (IP). The membranes were incubated with α-WASP (Santa Cruz 20770), α-WASH (A. Gautreu), α-fam21 (WASH complex component; Millipore ABT79), α-cortactin (Millipore 05-180) or α-GFP (Living Colors 632380) antibodies and the appropriate peroxidase-conjugated secondary antibody. **B.** IB of a subcellular fractionation assay of WT MEFs. An Optiprep gradient from 10% to 32% was used to separate membranous subcellular compartments according to their density. Each lane corresponds to a gradient fraction. The IB membranes were blotted with α-kazrin (EMBL Heidelberg), α-WASP (Santa Cruz 20770), α-WASH (A. Gautreu) or α-cortactin (Millipore 05-180) antibodies and the appropriate peroxidase-conjugated secondary antibody. The rectangle in pink indicates the lanes that correspond to EEs. **C.** Merged confocal images of GFP and GFP-kazrin C expressing MEFs treated with 5 µg/ml doxycycline for 24 h. The cells were fixed and stained with an α-cortactin antibody (Millipore 05-180) and the adequate A568-conjugated secondary antibody. Merged and individual channel confocal images of 3.5 times amplifications of the indicated areas are shown. The images were taken with a Zeiss LSM-780 confocal microscope. The white arrows point to sites of co-localisation in intracellular structures and the orange arrows point to co-localisation at the PM. Scale bar = 5 µm. **D.** Yeast-two-hybrid assay in which the negative control protein bicoid or kazrin were used as baits and p41 (Arp2/3 component), WASP-Nt, WASP-Ct, cortactin-Nt or cortactin-Ct were used as preys. Blue indicates interaction. **E.** IBs of pull-down experiments with purified 6xHis-kazrin and GST or GST fused to the N- or C-terminal domains of N-WASP or cortactin. 50 ng of 6xHis-kazrin C were added to approximately 500 ng of each GST construct and incubated with glutathione-Sepharose beads. 0.5 ng of 6xHis-kazrin C were loaded as input. The membranes were stained with Ponceau red to detect GST and GST fusion constructs and with α-kazrin (Abcam 88752) and the appropriate peroxidase-conjugated secondary antibody to detect pulled-down kazrin.

Yeast-two-hybrid assays confirmed the interactions of kazrin with the actin polymerisation machinery. The Arp2/3 complex component p41, known to interact with the acidic peptide of NPFs, interacted with kazrin as previously shown. Further, we detected specific interactions of kazrin with the N- and C-terminus of N-WASP and cortactin. In both cases, the interaction was stronger with the N-terminal half of the protein (**Figure 3.21D**). Pull-down assays with purified 6xHis-kazrin C and GST fusion constructs also confirmed a very strong interaction of kazrin with the N-terminus of N-WASP and the N-terminus of cortactin (**Figure 3.21E**).

3.11.2 Kazrin depletion increases endosomal branched actin

Given the previous results, we decided to investigate a functional relationship between kazrin and Arp2/3-induced actin polymerisation. We used cortactin as a marker to analyse cortical actin in WT and kazrin KO cells by immunofluorescence. Kazrin depletion caused a 35 % decrease in cortical cortactin (**Figure 3.22**). However, the phenotype was not rescued by the expression of GFP-kazrin C, suggesting that it might be indirect (**Figure 3.22**).

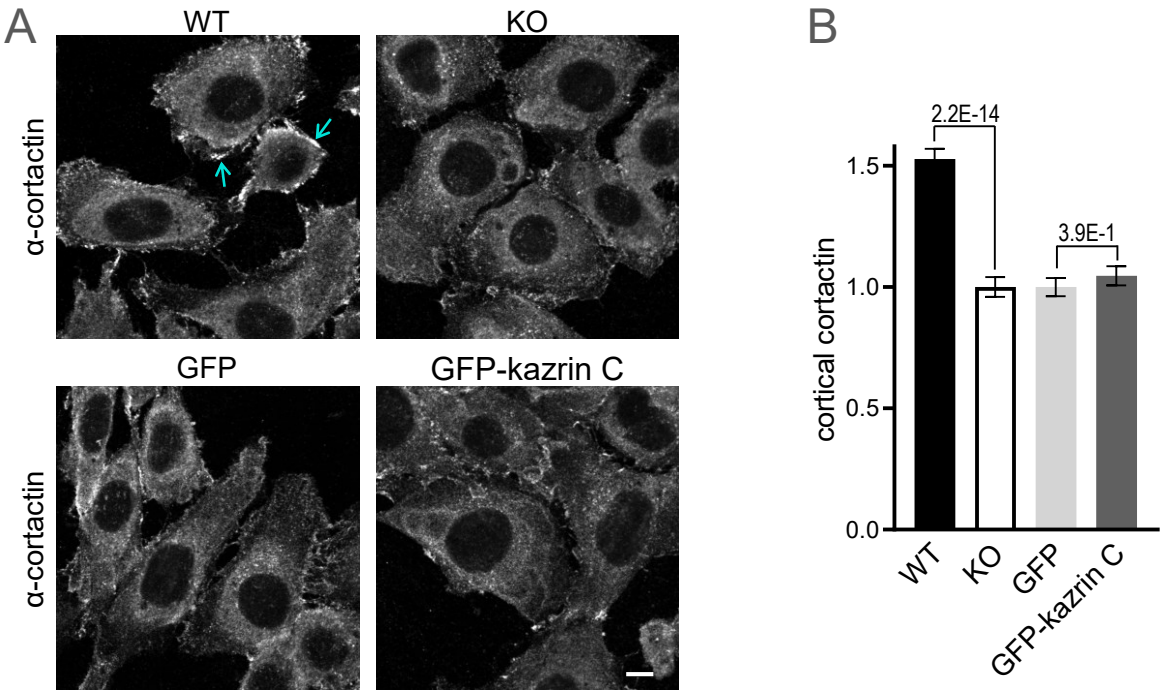

Figure 3.22. Kazrin depletion diminishes cortical actin. A. Confocal images of WT and kazrin KO MEFs, fixed and stained with an α-cortactin antibody (Millipore 05-180) and a A568-conjugated secondary antibody. The images were taken with a Zeiss LSM-780 confocal microscope. The arrows indicate areas of cortactin accumulation at the PM in WT cells. Scale bar = 10 μm. **B.** Quantification of cortical branched actin marked by cortactin as described in A, for WT, kazrin KO, GFP and GFP-Kazrin C expressing MEFs. GFP and GFP-kazrin C MEFs were treated with 5 μg/ml doxycycline for 24 h. The data is the mean ± SEM cortactin fluorescence intensity along the PM normalized to the cell perimeter. The values were normalised to the corresponding controls. The p values of an unpaired two-tailed t test are shown.

Besides the PM, we had shown co-localisation of kazrin and cortactin in EEs by fluorescence microscopy and co-fractionation. For that reason, we analysed endosomal cortactin in WT and kazrin KO cells. We selected areas of the cytoplasm of WT and kazrin depleted cells with similar amounts of EEA1 and compared the associated cortactin. There was more cortactin in kazrin KO cells (**Figure 3.23A**). The quantification of these images was challenging. E. Rebollo created a macro for ImageJ in which only those cortactin patches that were closely-associated to EEA1 patches were selected. The ratio between cortactin and EEA1 was 1.67 times higher in kazrin KO versus WT cells (**Figure 3.23B**), suggesting that kazrin might inhibit N-WASP and cortactin-induced actin polymerisation on endosomal membranes. The expression of GFP-kazrin C could not revert the observed phenotype in kazrin KO MEF, as the cortactin-to-EEA1 ratio was similar to that in GFP only expressing cells (**Figure 3.23B**).

Altogether, our results show a physical and functional interaction of kazrin with branched actin polymerisation in the PM and in endosomes.

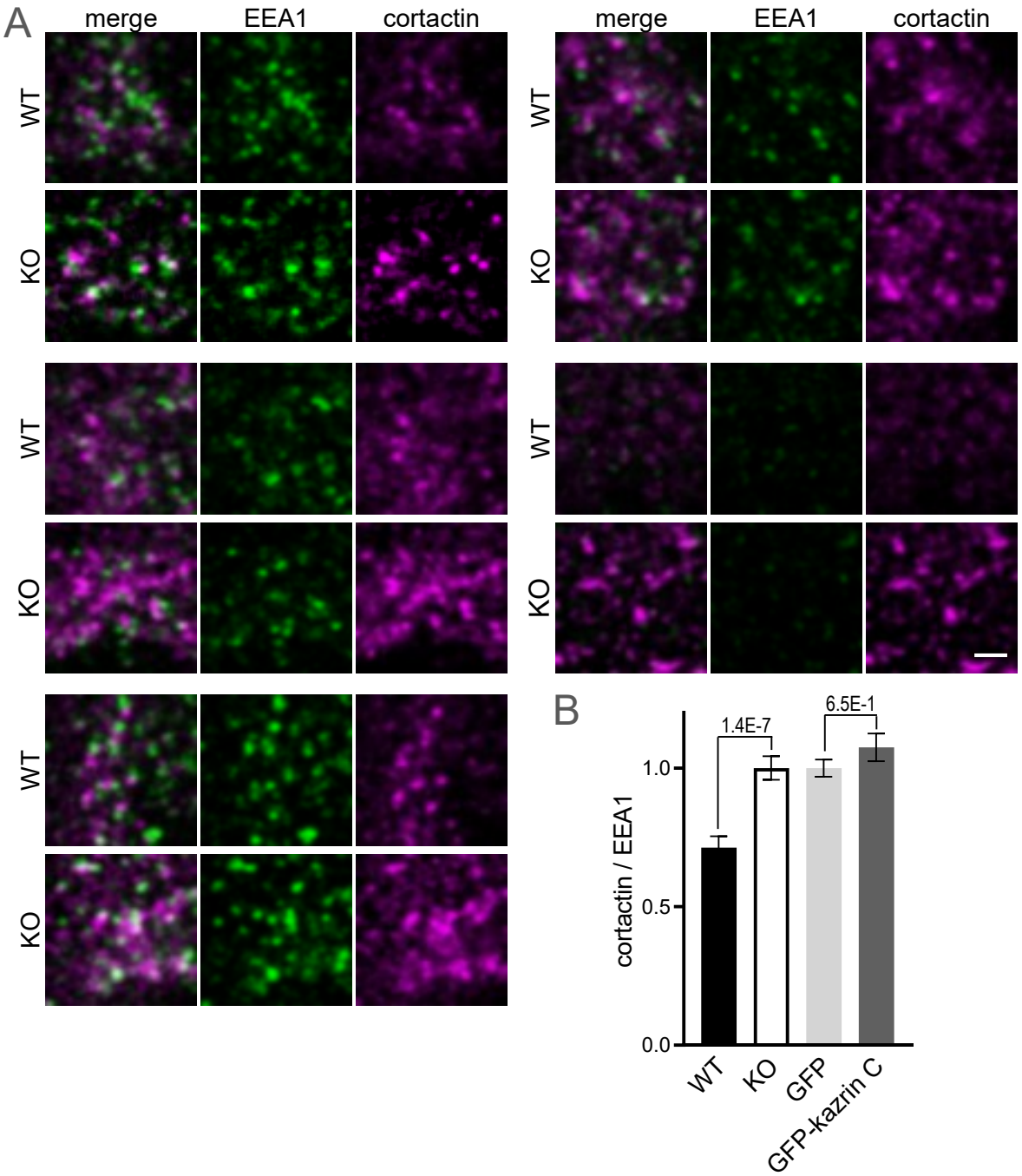

Figure 3.23. Kazrin depletion increases endosomal actin. A. Merged and individual confocal images of WT and kazrin KO MEFs fixed and stained with α-EEA1 (Cell Signaling 3288) and α-cortactin (Millipore 05-180) antibodies and the adequate A647-conjugated or A568-conjugated secondary antibodies, respectively. Images were taken with a Zeiss LSM-780 confocal microscope. Regions with a similar number and intensity of EEA1-marked endosomes were selected in WT and KO cells, in order to compare cortactin levels. Scale bar = 2 μm. **B.** Quantification of the cortactin/EEA1 ratio from the experiment described in A in WT, kazrin KO, GFP and GFP-kazrin C expressing MEFs. GFP and GFP-kazrin C MEFs were treated with 5 μg/ml of doxycycline for 24 h before fixation. The graph indicates mean ± SEM of the fluorescence intensity of the cortactin signal associated to EEA1-positive structures, divided by the area of the corresponding EEA1 signal. Measurements were performed with an ImageJ macro developed by E. Rebollo. The p values of an unpaired two-tailed t test are shown.

4 Discussion

Discussion

In the present thesis we have deepened into the analysis of the cellular and molecular functions of kazrin, a protein that is only expressed in vertebrates. Kazrin was originally identified in our laboratory as a cDNA that potently inhibits CME when overexpressed. Subsequent articles from other laboratories identified kazrin as a protein that interacted with components of desmosomes and adherens junctions, and suggested a role for kazrin in stabilizing cell-cell contacts. However, its direct role in endocytic traffic remained to be demonstrated, as well as the molecular mechanisms by which kazrin exerts its potential functions in endocytosis and the stabilisation of cell-cell contacts. Whether its potential roles in cell adhesion and endocytic traffic were related was also unknown.

To address these issues, we decided to generate a stable kazrin KO MEF cell line. We used the CRISPR-cas9 technology, which had clear advantages over other gene silencing methods like siRNA or shRNA. The direct modification of the DNA allowed complete and stable depletion, and therefore better reproducibility of the results. Kazrin KO cells provided a genetic background to generate GFP and GFP-kazrin C expressing stable cell lines through lentiviral transduction. As a result, we obtained kazrin KO cells that expressed GFP or GFP-kazrin C in similar levels to those of endogenous kazrin in WT cells. Moreover, the expression could be increased by the addition of doxycycline to the cell media in order to study kazrin localisation and perform biochemical analysis. Several antibodies detected by IB a kazrin isoform expressed in WT but not in KO MEFs. Unfortunately, none of the available kazrin antibodies we tested detected a specific kazrin signal in WT MEFs in immunofluorescence experiments. Indeed, expression of GFP-kazrin C at physiological levels (as assessed by IB) did not allowed visualization of the protein with any of our fluorescence microscopy settings. Previous studies had shown that moderate kazrin overexpression has the same localisation pattern as endogenous kazrin in keratynocytes, where the kazrin expression level must be higher than in MEFs (Sevilla *et al.*, 2008; Nachat *et al.*, 2009).

We also used the expression of GFP-kazrin C to evaluate the capacity of this isoform to complement the defects observed in KO MEFs. In this context, strong overexpression of GFP-kazrin C installed the same phenotype as kazrin depletion in CME, indicating that the construct has a potent dominant negative effect. We also observed a dominant negative effect when the GFP tag was positioned at the C-terminus, suggesting that it was not merely caused by the interference of the N-terminal tag with the molecular functions of kazrin. At low or moderate expression levels, we observed a variable capacity of the GFP-kazrin C protein to complement the phenotypes caused by depletion of kazrin. There was almost complete complementation of the defects in Tfn perinuclear enrichment and recycling, N-cadherin accumulation at EEs, migration speed and cytokinetic abscission. Uptake defects were partially complemented, whereas there was no complementation of migration directionality or cortical and endosomal actin levels. We speculated several possibilities to explain the variable complementation capacity of GFP-kazrin C for the different phenotypes described for the KO cells. First, the GFP tag may affect the kazrin interactome and therefore, its

different cellular functions. Second, some of the phenotypes may not be directly caused by depletion of kazrin. Third, the different molecular and cellular functions of kazrin may be differentially sensitive to kazrin expression levels. Fourth, some of the phenotypes installed upon kazrin depletion in MEFs may not be complemented by the human kazrin C isoform. In fact, the molecular weight of the kazrin isoform expressed in MEF cells is higher than that of kazrin C, and would likely correspond to isoforms A, B, F or H. These isoforms contain the kazrin C core plus a small N-terminal extension, which might be important for some functions but not others. Thus, those phenotypes complemented by kazrin C were dependent on the function of the core of kazrin.

Finally, we analysed the sequence and structural features of kazrin C and used the GFP and GFP-kazrin C expressing MEFs to investigate its interactome and define possible molecular mechanisms by which kazrin exerts its functions.

The experiments performed along this thesis project confirmed the presence of kazrin in adherens junctions and a possible role of kazrin inducing or stabilizing cortical actin, possibly through the regulation of cortactin and N-WASP. We have also unveiled a possible role of kazrin in CME uptake, which might also be related to its capacity to link clathrin to the actin polymerisation machinery. Most strikingly, we provide robust evidence demonstrating that kazrin is recruited to EEs, possibly via its interaction with PI3P and several endosomal components. There, kazrin contributes to the transfer of endocytosed material to perinuclear REs, contributing to cell processes that strongly rely on endosomal recycling through pericentriolar compartments. The molecular analysis of the kazrin interactome revealed three different mechanisms by which kazrin might exercise its function in endosomal traffic: by acting as a dynein adaptor for EEs, by downregulating the levels of PI3P and by lowering endosomal actin polymerisation. The possible cellular and molecular functions of kazrin are discussed in detail below.

4.1 Possible roles of kazrin at the PM

Previous results showed that kazrin C overexpression blocks endocytosis of Tfn in COS7 transformed monkey fibroblasts (Schmelzl and Geli, 2002). We obtained similar results on MEF mouse fibroblasts. The overexpression of GFP-kazrin C above a certain threshold harshly diminishes the amount of internalised Tfn. We interpret this as a dominant negative effect, since the same defect was observed upon kazrin depletion. Importantly, low expression of GFP-kazrin C or kazrin C-GFP in kazrin KO cells partially restored WT Tfn uptake kinetics, indicating that the human kazrin C isoform can at least partially complement kazrin function in CME in MEFs. Consistent with its possible role in endocytic uptake, GFP-kazrin C localised to the PM, as previously shown for endogenous kazrin and several overexpressed isoforms (Groot *et al.*, 2004; Gallicano *et al.*, 2005). We observed kazrin as part of dynamic structures that appeared and disappeared in the range of seconds and minutes, perhaps

due to cycles of assembly and disassembly or internalisation and recycling. This behaviour would be compatible with kazrin being a component of clathrin-coated pits at the PM and therefore, with kazrin directly participating in endocytic uptake. We detected a specific interaction between kazrin and clathrin in immunoprecipitation experiments, and previous data from the laboratory indicated that kazrin can directly interact with the terminal domain of the clathrin heavy chain. However, we failed to demonstrate co-localisation of kazrin with clathrin at the PM by immunofluorescence (data not shown) or co-immunoprecipitation or co-fractionation of kazrin with the main PM clathrin adaptor, AP-2. These negative results pose a doubt on the direct role of kazrin in endocytic uptake.

The localisation of GFP-kazrin C at the PM seemed to be restricted to cell-cell contacts. In fact, we saw a striking co-localisation of GFP-kazrin C with the components of adherens junctions N-cadherin, β-catenin and p120-catenin. This is in agreement with the data from Cho *et al.* (2010) in *X. laevis*, which includes co-localisation and biochemical interactions with p120-catenin family members. They demonstrated an interaction of the N-terminus of xkaxrin A with xARVCF-catenin, xδ-catenin and xp0071-catenin, but not with p120-catenin itself. Our immunofluorescence experiments on MEF cells do not show ARVCF-catenin at the PM or co-localising with GFP-kazrin C. These variances might be due to the prevalence of different cell-cell contact components in different cell models. In addition to adherens junctions, kazrin is essential for the formation of desmosomes in keratinocytes and it interacts with several members of the plakin family (Groot *et al.*, 2004). We do not see localisation of the desmosomal marker desmoglein at the PM in MEF cells. In fact, fibroblasts are not tightly attached to each other with desmosomes like epithelial or endothelial cells are (Green and Simpson, 2007). Therefore, kazrin appears to be part of different cell-cell contact structures, depending on the cell type, and is likely to fulfil a role that is common to all of them.

The members of p120-catenin family are known to stabilise adherens junctions and promote tight cell-cell contacts. At least in part, they do so by inhibiting CME of cadherins. Binding of p120-catenins to E-cadherins masks their AP-2 binding motif, preventing recruitment of cadherins into CCVs (Davis, Ireton and Reynolds, 2003; Xiao *et al.*, 2005; Miyashita and Ozawa, 2007; Gu *et al.*, 2009). In addition, p120-catenins link adherens junction to N-WASP, cortactin and the Arp2/3 complex to promote and stabilise actin polymerisation at cell-cell contacts (Boguslavsky *et al.*, 2007; Rajput *et al.*, 2013). Cho et al. (2010) demonstrated that depletion of kazrin using morpholinos resulted in low levels of E-cadherin at the PM, which could be recovered by inhibition of endocytosis. These evidences suggest that kazrin inhibits E-cadherin endocytosis, similar to p120-catenins. Consistent with this view, we observed a strong increase in the intracellular accumulation of N-cadherin, a major component of adherens junctions in fibroblasts, in kazrin KO cells as compared to WT. However, we failed to detect any differences in the levels of N-cadherin at the PM by immunofluorescence (data not shown). Moreover, as discussed below, kazrin depletion causes an additional strong

endocytic recycling defect that would also explain N-cadherin accumulation in EEs. A more detailed study of the internalisation kinetics of N-cadherin in WT and kazrin KO cells would be required to conclude if kazrin has a general role inhibiting cadherin internalisation.

On the other hand, we have demonstrated a clear, direct interaction of kazrin with cortactin, N-WASP and the Arp2/3 complex, and the co-localisation of kazrin with cortactin at the PM. Further, knocking-down of kazrin in MEFs significantly lowered the levels of cortical cortactin (this thesis) and actin (A. Baumann's thesis). Earlier publications have described an interaction of xkazrin A with cortical actin, with the protein spectrin acting as a link (Cho *et al.*, 2010). In agreement with our results, the overexpression of several kazrin isoforms, including kazrin C, has previously been shown to inhibit cortical actin formation in keratinocytes (Sevilla *et al.*, 2008). In light of our results in kazrin KO MEFs, we speculate that this is due to a dominant negative effect. Also kazrin depletion alters cortical actin in *X. laevis* blastula. As a consequence, kazrin depletion has an impact on the shape of the keratinocytes and causes ectodermal shedding (Cho *et al.*, 2010). Together with the localisation of kazrin at adherens junctions in MEFs, the data suggested that kazrin might work together with p120-catenin members to stabilise cortical actin and cell-cell contacts at the PM.

We can hypothesise a link between the functions of kazrin on CME, actin polymerisation and adherens junction stabilisation. The role of actin in CME in mammalian cells is controversial and seems to depend on the nature of the membrane subdomain where endocytic internalisation occurs, on the internalised cargo and on membrane tension (Cureton *et al.*, 2010; Boulant *et al.*, 2011). When required, Arp2/3 and N-WASP aid membrane bending by inducing actin polymerisation at the rim of the invagination. They also provide pulling forces for the scission of the clathrin-coated pit and possibly for the propulsion of the CCVs through the cytoplasm (Kaksonen and Roux, 2018). Specific functions of Arp2/3-dependent actin polymerisation have been described in cadherin endocytosis. The cdc42-par6-aPKC polarity complex promotes E-cadherin endocytosis by recruiting the cip4-WASP-Arp2/3 actin machinery (Leibfried *et al.*, 2008). F-BAR proteins such as cip4 facilitate scission by recruiting dynamin to the neck of the nascent vesicle. This recruitment requires the cip4 SH3 domain to bind to proline-rich motifs in dynamin and N-WASP. The GTPase rho seems to suppress cadherin endocytosis by antagonizing cdc42–par6–aPKC functions (Warner and Longmore, 2009). Super-resolution microscopy and a finer analysis of the kazrin interactome at the PM would aid to define if the kazrin-N-WASP-cortactin-Arp2/3 axes at the PM is directly linked to CME and/or adherens junctions.

4.2 The role of kazrin in endosomal traffic

Although we originally observed that depletion of kazrin inhibits CME of Tfn, we noticed that peripheral Tfn-loaded endosomes accumulated in kazrin KO cells, compared to WT, in our Tfn uptake experiments. These peripheral compartments could be labelled with antibodies against EEA1, the EE tethering factor. Subsequent experiments demonstrated the accumulation of EEA1 and PI3P on intracellular membranes at the cell periphery in kazrin KO cells by fluorescence microscopy. Accumulation of EEA1 in light membranous fractions in KO cells could also be demonstrated using density gradients. The accumulation of EEs was accompanied by a significant delay in the transfer of endocytosed Tfn to the perinuclear region, as well as a slight defect in the recycling of Tfn to the PM. All phenotypes in the KO cells were recovered by the expression of GFP-kazrin C but not GFP, indicating that they were directly caused by the absence of kazrin. The data strongly indicated that kazrin was specifically required for the maturation or transport of EE to RE, or for the generation of transport intermediates that effect endocytic transport between these two compartments. Additional observations supported the first option. On one hand, EEs are more dispersed in kazrin KO cells, whereas REs are affected to a lesser extent. On the other hand, kazrin depletion did not affect the generation of EHD1/3 tubules, suggesting that the main function of kazrin in endosomal trafficking was related to the microtubule-dependent centripetal transport of EEs rather than to the formation of transport intermediates. EEs might mature into REs as they are transported to the perinuclear region or they might transfer cargoes to the REs once at the perinuclear region, via a ‘kiss-and-run’ mechanism or the generation of transport intermediates.

Key to proving a direct role of kazrin in endosomal trafficking was the demonstration of its localisation on endosomes and of its physical interaction with cellular factors involved in endosomal trafficking. Since we failed to detect endogenous kazrin at physiological levels by immunofluorescence in MEFs, we attempted the analysis of its subcellular localisation by subcellular fractionation in a density gradient followed by IB using different organelle markers. Strikingly, we observed a sharp co-fractionation of kazrin with the EE markers EEA1 and EHD1/3 in light density fractions, whereas it did not overlap significantly with resident proteins of the Golgi or recycling endosomes. Moderately expressed GFP-kazrin C also appeared to be recruited to EEs, although it slightly distributed to heavier membranes, as compared to endogenous kazrin. Besides the evident localisation of GFP-kazrin C at cell-cell contacts, kazrin C could also be observed in peripheral intracellular structures that co-localised with components of the adherens junctions and partially co-localized with the endosomal components EHD1/3 and the endosomal/TGN marker γ-adaptin. Interestingly, we observed a very clear co-localisation of GFP-kazrin C and N-cadherin in these intracellular structures. Together with the observation that N-cadherin accumulates in EEs in kazrin KO cells, the data suggested that kazrin might have a particular role in the recycling of adherens junction components. The internalisation and recycling of cadherins

is key to controlling the number and distribution of adherence junctions (Cadwell, Su and Kowalczyk, 2016). Therefore, some of the effects observed in the establishment of cell-cell contacts upon depletion of kazrin, might directly derive from alterations in the intracellular trafficking of cadherins.

Analysis of the kazrin interactome in immunoprecipitation experiments using MEFs that express GFP-kazrin C or GFP as a negative control, evidenced a preference of kazrin C binding for proteins specifically implicated in the transport of EE to RE, including the EHD1/3 GTPases and γ-adaptin, as compared to other components of EEs involved in the tethering of incoming endocytic vesicles (EEA1) or other recycling pathways (VPS35 and fam21). Likewise, no interaction was detected between GFP-kazrin C and other Golgi or PM clathrin adaptors such as GGA2 and AP-2, respectively. Endogenous kazrin sharply co-fractionated with the EHD1/3 GTPases in Optiprep density gradients and it overlapped with γ-adaptin, although this clathrin adaptor appeared more spread towards heavier fractions in accordance with its more ubiquitous localisation also in RE and the TGN (Ling *et al.*, 2007; Perrin *et al.*, 2013). Pull-down experiments confirmed a direct but weak interaction of the γ-adaptin ear (A. Baumann's thesis) and the EHD GTPases with kazrin. The interplay of clathrin with other sorting machineries in recycling pathways is not well understood. Our results support the notion of a clathrin, AP-1 and EHD1/3-dependent recycling pathway that does not involve retromer or commander. This idea agrees with the study by McGough and Cullen (2013), which shows that carrier formation that depends on SNX-BARs does not require clathrin.

Furthermore, we found that kazrin C interacted with PI3P in a concentration-dependent manner on lipid strip overlay experiments. PI3P is a landmark of EEs, where it facilitates fusion of incoming CCVs and sorting. Maturation from EEs to REs, or the formation of transport intermediates from EEs to REs, involves the conversion of PI3P to PI and then to PI4P (Marat and Haucke, 2016; Campa *et al.*, 2018), whereas maturation of EEs to LEs implicates the conversion of PI3P to $PI(3,5)P_2$ by PIK-FYVE. The interaction occurred through the poly-K sequence on the C-terminal portion of kazrin, as the deletion or mutation of the lysines to alanines completely blocked the interaction. Importantly, PI3P was the only out of a phosphoinositide collection showing affinity for kazrin. Kazrin did not interact with the lipid species that accumulate in REs and the Golgi (PI4P), late endosomes/lysosomes ($PI(3,5)P_2$), the PM (PI4P and $PI(4,5)P_2$) or endocytic vesicles ($PI(4,5)P_2$ and $PI(3,4)P_2$). All the data reinforced the idea that kazrin was specifically localised at EEs, where it promoted EE to RE transport.

4.3 Kazrin is required in processes that strongly depend on recycling through the RE

Endocytic recycling through the perinuclear compartment is essential to those cellular functions that need to redirect endocytosed material to sites of polarised secretion, labelled by the exocyst, such as migration or cytokinesis (Jones, Caswell and Norman, 2006; Frémont and Echard, 2018). Our data indicated that kazrin played an important role in the transfer of endocytosed material from EEs to REs. A prediction of our hypothesis was that kazrin depletion would also cause defects in migration and cytokinesis and that these would be recovered by the expression of GFP-kazrin C. This was indeed the case. A more detailed discussion on the role of kazrin in cell migration and cytokinesis are discussed below.

4.3.1 Kazrin in cell migration

The analysis of migrating kazrin KO MEFs in a 3D Matrigel matrix demonstrated shorter paths than those of WT cells. In detail analysis revealed a decrease in the migration speed and a higher directionality of kazrin depleted cells.

Integrins are dynamically internalised, mostly through CME, and recycled through REs in order to create new focal adhesions as the cell migrates. $\alpha_5\beta_1$ integrin, in particular, is recycled in a rab11-dependent manner to the leading edge of the cell, where it promotes the formation of ruffles and fast invasion. This function is aided by the co-recycling of RTKs (Paul *et al.*, 2015; Nader, Ezratty and Gundersen, 2016). Because kazrin is involved in both CME and recycling through the rab11 compartment, the observed reduction in invasion speed fit the data described in the literature. In addition to speed, recycling pathways modulate migration directionality. Inhibition of $\alpha_5\beta_1$ integrin recycling enhances the recycling of $\alpha_V\beta_3$ integrin through the fast route, which promotes Arp2/3-induced polarisation at the leading edge, lamellipodia formation and directional migration in NIH3T3 fibroblasts (White, Caswell and Norman, 2007). β_1 integrin free chains can also traffic in a retromer-dependent manner to promote directionality in epithelial RPE-1 cells (Shafaq-Zadah *et al.*, 2016). Our observation that kazrin KO cells are slower but more directional is consistent with the hypothesis that kazrin depletion impedes $\alpha_5\beta_1$ integrin recycling through the RE compartment, without affecting (or even accelerating) $\alpha_v\beta_3$ or β_1 integrin recycling directly from EE. In light of the described literature, the data reinforces the idea that kazrin C specifically promotes EE to RE transport as opposed to other recycling routes.

The decreased speed but not the increased directionality of kazrin KO cells was recovered by the expression of GFP-kazrin C but not GFP. The expression levels of GFP-kazrin C in our doxycycline-induced cell line were very variable between cells. Kazrin levels might need to be finely tuned in order to control directionality. The GFP tag or the absence of other kazrin isoforms could also be affecting molecular interactions required for inhibition of short recycling routes.

Interestingly, Cho *et al.* (2011) previously demonstrated that depletion of kazrin in *X. laevis* results in a defect in the migration of neural crest cells, which cause eye and craniofacial defects similar to depletion of ARVCF. This suggests that kazrin plays an important role in cell migration also *in vivo*, which might at least partially derive from its primary function in membrane traffic.

4.3.2 Kazrin in cytokinesis

In the present thesis, we also provided data pointing to a role of kazrin C in cell abscission during cytokinesis, since daughter kazrin KO MEFs remained bridged for longer periods of time than WT MEFs. The phenotype was rescued by the moderate overexpression of GFP-kazrin C but not GFP. It is well-established that the transport of a set of cargoes and machinery to the cleavage furrow is essential for secondary furrow ingression, including the exocyst, FIP3, MICAL1 and 3, OCRL and SNX16 (Rizzelli *et al.*, 2020). Consistent with the role of kazrin in microtubule-mediated transport (discussed in the next section), the delivery of transport intermediates to the abscission site occurs through dynein and kinesin motors (Wilson, Allen and Caswell, 2018).

The effect of kazrin on cytokinesis could also be due to its impact on the PI3P abundance (discussed in the next section). The delivery of the PI3P-binding protein FYVE-CENT is necessary for the recruitment of TTC19 and the activation of ESCRT-III, which leads to the final constriction (Sagona *et al.*, 2010). Kazrin depletion increased endosomal PI3P, which would lead to an activation of ESCRT-III and enhance constriction. This is opposite to the phenotype we observed. We therefore conclude that, either the inhibition of PI3P by kazrin is not involved in regulating cytokinesis, or it is involved in a different pathway than that described by Sagona *et al.* (2010). In fact, we do not detect kazrin at rab11-containing REs, suggesting that kazrin is involved in recycling from EEs to REs, rather than in the transport of machinery in rab11-containing REs to the abscission site.

4.4 Molecular mechanisms supporting the role of kazrin in EE to RE transport

In order to investigate the molecular mechanisms explaining the roles of kazrin in endocytic traffic, we analysed its sequence in search of structural similarities and to define domains or putative interacting motifs that would provide some hints. This kind of analysis led us to investigate three different molecular mechanisms that might cooperatively work to promote EE to RE transport: kazrin might be an endosomal dynein adaptor, an inhibitor of the class II PI3 kinase VPS34, and an inhibitor of endosomal actin polymerisation. The results that support these molecular functions of kazrin and their role in the context of endocytic traffic are discussed below.

4.4.1 Kazrin might be an EE dynein adaptor

In search for structural homologies of kazrin with other proteins, we identified the dynein adaptor BICDR1 showing a 21.94 % sequence identity. BICDR1 is a dynein-dynactin adaptor that promotes perinuclear enrichment of secretory vesicles (Schlager *et al.*, 2010). The similarity lies at the coiled-coil region in the N-terminal portion of kazrin C. Since EEs travel towards the cell centre along microtubules (Neefjes, Jongsma and Berlin, 2017), the function of kazrin as an endosomal dynein adaptor would explain its function in endosomal trafficking at the molecular level. Several pieces of evidence indicated that this might indeed be the case.

Dynein adaptors bear long coiled-coil regions that promote dimerisation and extend along the dynactin filament in the dynein-dynactin complex. Immunoprecipitation experiments with MEF expressing GFP-kazrin C or GFP as a negative control, demonstrated a specific interaction of kazrin C and the dynactin component p150-glued. On the other hand, most studied dynein adaptors bind the LIC (Light Intermediate Chain) subunits of dynein and we could indeed demonstrate a specific interaction of kazrin C with LIC1 in pull-down assays with purified components. LIC binding sites greatly vary among adaptors. Kazrin does not contain any of the previously-described LIC-binding sequences, such as the CC1-box or the HOOK domain (Reck-Peterson *et al.*, 2018), indicating that a new LIC binding motif is present in this protein. Further, dynein adaptors form or are predicted to form dimers, and kazrin isoforms have been shown to be able to interact with each other (Nachat *et al.*, 2009). Another characteristic of dynein adaptors is the presence of a cargo binding site that does not overlap with the dynein and dynactin interacting surfaces (Reck-Peterson *et al.*, 2018). Moreover, dynein adaptors often bind a kinesin protein (Schlager *et al.*, 2010), and we could demonstrate an interaction of GFP-kazrin C with the heavy chain of kinesin-1 in immunoprecipitations assays. We did not see co-immunoprecipitation of tubulin, suggesting that the interaction occurs directly with microtubule motors or adaptors.

On the other hand, consistent with the view that kazrin is an endosomal adaptor for dynein, we found that the C-terminus of kazrin interacts with components of EE, including γ-adaptin and PI3P. Finally, similar to other dynein adaptors such as BICDR1, HOOK2 and HOOK3, GFP-kazrin C prominently localized in the vicinity of the centrosome. Kazrin co-localised with the centriolar marker pericentrin and partially co-localised with the PCM marker PCM-1. GFP-kazrin C corpuscles could be observed moving in and out from the pericentriolar material, in agreement with its possible association with microtubule molecular motors. Consistent with the contribution of kazrin to the transport of EEs towards the ERC, we observed EEA1-positive endosomes entrapped in the pericentrosomal GFP-kazrin C matrix.

Taken together, these results point towards a function of kazrin as a dynein adaptor, promoting the transport of EEs to the ERC or entrapping endosomes in this region. *In vitro* motility assays are now required to confirm the role of kazrin as a microtubule motor adaptor.

Interestingly, an opposite role has been reported for the protein gadkin. This Arp2/3 inhibitor is an AP-1 binding protein that works as a kinesin-1 adaptor in order to direct the transport of endosomes towards the periphery of the cell. Reciprocally to kazrin, gadkin overexpression causes the accumulation of AP-1-containing endosomes at the cell periphery, whereas gadkin depletion accelerates Tfn recycling (Schmidt *et al.*, 2009). Kazrin and gadkin could have complementary roles.

Earlier studies have shown an association of kazrin with the microtubule cytoskeleton. Nachat *et al.* (2009) showed that the LHD (Liprin-Homology Domain) of kazrin E binds to acetylated tubulin, which is present in centrioles. Since all isoforms of kazrin can form dimers with each other, it is possible that kazrin E binds to centrioles and attracts kazrin C to them. However, GFP-kazrin C localizes at the centrosome in the absence of any other kazrin isoform, suggesting that centrosomal localisation might be a feature of all kazrin isoforms. As mentioned above, the localisation of overexpressed kazrin in the perinuclear region is not restricted to the immediate surroundings of centrioles. We have also observed partial co-localisation of GFP-kazrin C with PCM-1, a marker of centriolar satellites. Since PCM-1 is required for the localisation of many centrosomal proteins, we speculate that PCM-1 might participate the recruitment or retrieval of kazrin to or from the centrosome (Dammermann and Merdes, 2002).

The functions of kazrin at cell-cell junctions and at the centrosome might be linked. It has been shown that desmoplakin is able to recruit ninein from centrosomes to desmosomes in order to promote epidermal differentiation. Ninein is a centrosomal protein that promotes microtubule nucleation, the anchoring of the minus end of microtubules, and that works as a dynein adaptor (Delgehyr, Sillibourne and Bornens, 2005; Redwine *et al.*, 2017). Kazrin E has been proposed to coordinate the transfer of ninein from the centrosome to the desmosomes (Nachat *et al.*, 2009). Given the functional analogies between ninein and kazrin, we hypothesise that they both work together in coordinating microtubule-mediated transport, and cell-cell junction formation.

4.4.2 Kazrin might downregulate endosomal PI3P levels

Phosphoinositides are master controllers of the progression of endosomal trafficking. Together with rab GTPases, phosphoinositides recruit downstream effectors that promote positive and negative feedback loops that result in endosomal maturation, cargo recruitment and membrane budding or fusion. Since we detected a very specific interaction between kazrin and the EE phosphoinositide PI3P, we wondered if kazrin could regulate the endosomal levels of this lipid. To analyse this, we used a GFP-tagged FYVE domain as a probe to detect PI3P by microscopy, and ensured its specificity by showing no GFP-FYVE signal in cells treated with the VPS34 inhibitor IN1. We observed a highly significant increase in the GFP-FYVE signal associated to intracellular structures in kazrin KO cells. The increase in PI3P levels could be a consequence of the EE accumulation observed in kazrin KO cells.

However, we detected an interaction of GFP-kazrin C with the main kinase responsible for the production of endosomal PI3P, the class III PI3K VPS34, which suggested a possible role of kazrin as an inhibitor of this enzyme (Backer, 2016). Immunoprecipitation experiments showed interactions of GFP-kazrin C with the catalytic subunit VPS34 as well as with the core regulatory proteins VPS15 and beclin. We did not detect an interaction with the fourth subunit of the complex, UVRAG, which targets the VPS34 core complex to endosomes. Because the interaction with VPS34 seemed strong, we speculate that kazrin acts as an inhibitor of VPS34 by impeding UVRAG binding and EE targeting.

PI3P dephosphorylation and conversion to PI4P is required for the maturation of endosomal membranes and recycling of cargoes through the RE (Wang, Lo and Haucke, 2019). VPS34 inhibition would lead to a decrease in PI3P and a consequent increase in PI, which might be converted to PI4P for endocytic recycling through the ERC. On the other hand, PI3P is key in the initial steps of the recruitment of the ESCRT complex, in the recruitment of the PI3P-5 kinase (PIKfyve) that promotes maturation of EE to LE, and in the recruitment of retromer and SNXs (Sbrissa, Ikonomov and Shisheva, 2002; Cullen and Steinberg, 2018). Therefore, by inhibiting VPS34, kazrin would strongly favour the transport from EE to RE versus the degradative pathway or other recycling mechanisms.

4.4.3 Kazrin downregulates actin polymerisation on endosomal membranes

Previous work in the laboratory showed a direct interaction of kazrin C with the Arp2/3 complex by immunoprecipitation and pull-down experiments. The interaction was found to require the acidic motif at the C-terminus of kazrin, analogous to that present in activators and inhibitors of the Arp2/3 complex. Previous data in COS7 cells indicated that kazrin might also interact with WASH (A. Baumann's thesis), a major factor orchestrating actin polymerisation on endosomal membranes. In this study, we confirmed that GFP-kazrin C co-immunoprecipitated with WASH in MEFs, but we could not detect an interaction with the WASH complex member fam21, key to the function of WASH at endosomal membranes. Further, our immunoprecipitations experiments showed a stronger binding of kazrin C with other components of the branched actin polymerisation machinery, N-WASP and cortactin, which have functions both at the PM and endosomal compartments (Tanabe *et al.*, 2011; Kaksonen and Roux, 2018). In line with these observations, we observed co-localisation of kazrin C and cortactin both at the PM and intracellular structures and a sharp co-fractionation of kazrin with N-WASP and cortactin in light fractions of density gradients, corresponding to EEs. WASH was instead present in heavier fractions. It is possible that WASH-induced actin polymerisation occurs at a later stage of endosomal maturation, when EEA1 is no longer present, as suggested by its recruitment by the rab7 GTPase (Balderhaar *et al.*, 2010).

We confirmed the direct interactions of kazrin with the Arp2/3 complex (A. Baumann's thesis), N-WASP and cortactin by yeast-two-hybrid experiments and pull-down assays

with purified components. These experiments also allowed us to demonstrate a strong interaction of kazrin with the N-terminus of N-WASP and cortactin. We concluded that kazrin might regulate N-WASP and cortactin-induced actin polymerisation, not only at the PM but also on EE membranes. Strikingly, the effects observed upon kazrin depletion on EEs were opposite to those described for cortical actin. Kazrin depletion in MEFs using shRNAs caused an increase in the endosomal versus PM actin ratio (A. Baumann's thesis). In this thesis, we also showed an increase of endosomal versus PM cortactin ratio upon kazrin depletion, suggesting that kazrin modulates the balance of endosome and PM Arp2/3 branched networks. The expression of GFP-kazrin C did not rescue any of the actin related phenotypes on endosomes, again suggesting that the expression levels of kazrin need to be fine-tuned, that the GFP tag interferes with kazrin function or that other isoforms are required. In our experimental set up, cells were doxycycline-induced and expressed different amounts of GFP-kazrin C. Hence, another possibility is that the observed phenotypes might be a combination of rescue and dominant negative effects.

In vitro actin polymerisation assays are required to prove a direct function of kazrin in the regulation of actin polymerisation and to understand why kazrin upregulates actin polymerisation at the PM, whereas it downregulates it on endosomal membranes. We favour the idea that kazrin directly functions as an inhibitor of cortactin on endosomes by preventing binding of its N-terminus to the Arp2/3 complex. The role of kazrin in promoting actin polymerisation at the PM might be indirect, as a consequence of the stabilisation of adherens junctions.

Actin is required for EE exit (Ohashi *et al.*, 2011). Arp2/3 and cortactin, in particular, are known to establish endosomal subdomains that allow sorting and recycling through the fast route (Puthenveedu *et al.*, 2010). It is possible that kazrin inhibits endosomal actin polymerisation in order to regulate sorting of a specialised pool of cargoes or to promote a specific recycling pathway. We speculate that kazrin promotes recycling through the RE by inhibiting recycling through other routes that depend on actin polymerisation, such as retromer and commander-dependent routes. In addition to cortactin, WASH has been the NPF found to activate the Arp2/3 complex to modulate endosomal sorting (Gomez and Billadeau, 2009). In our cellular system WASH was not enriched in EEs or co-fractionate with cortactin. We thus propose that kazrin might function in endosomal sorting through the inhibition of N-WASP-dependent rather than WASH-dependent polymerisation. Since N-WASP is involved in endosomal tubule formation and fission of transport intermediates (Bu *et al.*, 2010), this could potentially be a process that kazrin is interfering with.

In summary, kazrin seems to regulate the balance between cortical and endosomal branched actin. Its depletion decreases cortical whereas increases endosomal cortactin. Surprisingly, gadkin also has opposite effects to kazrin on actin polymerisation, as gadkin depletion causes a redistribution of Arp2/3 from endosomes to the PM. As a consequence,

migration speed is increased (Maritzen *et al.*, 2012), opposite to what we observe in kazrin depleted cells.

4.5 Kazrin as a hub

Our data confirms previous hypothesis of kazrin being an interactor of both the actin and tubulin cytoskeletons. A study by Gallicano *et al.* (2005) already showed co-localisation of kazrin with both tubulin and actin, depending on the cell cycle phase and developmental stage. In addition, the plakin family of kazrin interactors contain an N-terminal domain for the binding to actin and a C-terminal domain for the binding to microtubules (Boczonadi and Määttä, 2016). Plakins interact with kazrin E at desmosomes, where they work as cytoskeletal linkers (Groot *et al.*, 2004). Whether this role is related to the role of kazrin in CME and whether a parallel mechanism applies to endosomal kazrin is still unknown.

Notably, this study presents multiple interactors of kazrin that belong to a variety of functional groups. The branched actin polymerisation machinery, microtubule motors, GTPases EHD1 and EHD3, PI3P and the class III PI3K, CHC and AP-1, all of them participating in membrane traffic at EE membranes. Kazrin C could work as a hub that brings sets of proteins together. This ability might be related to the presence of an IDR in the C-terminal region of kazrin C. IDRs are significantly enriched in hub proteins (Haynes *et al.*, 2006) and they are particularly enriched in proteins controlling the dynamics of the actin cytoskeleton and membrane traffic (Miao *et al.*, 2018). The mechanism is not understood but IDR-containing proteins can induce molecular crowding that sometimes leads to phase transition and the formation of liquid droplets (Li *et al.*, 2012). The intrinsic structural flexibility of IDRs confers them the ability to adapt to different contexts and change their molecular interactions as a specific cellular process progresses. In the context of CME and endosomal recycling, a number of machineries concentrate at transient membrane subdomains in order to produce a transport intermediate that contains the appropriate cargoes and is delivered to the appropriate organelle. We propose kazrin C is a scaffold for the formation of these subdomains in specific CME and endosomal recycling routes.

4.6 Integrating model

Taking together the results presented here and previous work from our and other laboratories, we propose a model in which kazrin C works at two types of cellular membranes: the PM and EEs. Kazrin C is present in the PM, particularly in cell-cell contact sites or in their very close vicinity. There, it could interact with the Arp2/3 complex, N-WASP and cortactin to enhance branched actin polymerisation. There are two possible outcomes based on our and previous data. Kazrin might link endocytic sites to N-WASP and cortactin to promote fission of CCVs or to allow propulsion of endocytic vesicles into the cytosol. This option is supported by the observation that GFP-kazrin C co-localises with N-cadherin at the PM and

also in internal structures, together with previous observations that N-WASP is particularly important for the internalisation of E-cadherins (Leibfried *et al.*, 2008).

On the other hand, kazrin might increase cortical actin in order to stabilise cell-cell contacts, rather than to induce their internalisation. This second option is supported by evidences showing that xkazrin A depletion decreases E-cadherin levels and that this phenotype is restored by CME inhibition (Cho *et al.*, 2010). In this case, kazrin expression would stabilise N-cadherin at the PM by preventing its internalisation, by favouring actin polymerisation at adherens junctions or by favouring its recycling back to the PM. Since adherens junctions play an important role in mechanosensing (Charras and Yap, 2018), their stabilisation could have a strong impact in membrane tension and influence CME dynamics (Ferguson *et al.*, 2017). This would explain the general defect in CME that we observed in kazrin KO cells. Several experiments would be required to discriminate between the two models. Cell adhesion assays and analysis on N-cadherin internalisation dynamics in the presence or absence of kazrin, as well as a finer study of kazrin localisation at the PM would be reveal the function of kazrin at the PM.

This thesis also shows that Kazrin is present on EE membranes, where it might be recruited through its multiple interactions with endosomal components such as EHD1/3, γ-adaptin, VPS34 or PI3P. There, it would promote the transport from EE to RE via different molecular mechanisms. Its interaction with the Arp2/3 complex, N-WASP and cortactin would reduce endosomal actin. This would impede the formation of endosomal subdomains leading to recycling through actin-dependent routes that directly transport cargo to the PM. Kazrin C would also inhibit the function of the class III PI3K VPS34, thus inhibiting PI3P formation, promoting PI accumulation and PI4P formation. As a consequence, kazrin would inhibit PI3P-dependent recycling and degradative routes, while favouring PI4P-dependent recycling routes through REs. Finally, kazrin C would work as a dynein adaptor for EEs and allow microtubule-dependent transport of these organelles towards the ERC or their trapping in the vicinity of the centrosome. Overall, kazrin C would promote cargo recycling through REs, having an impact on the regulation of cell migration speed and the completion of cytokinetic abscission (**Figure 4.1**).

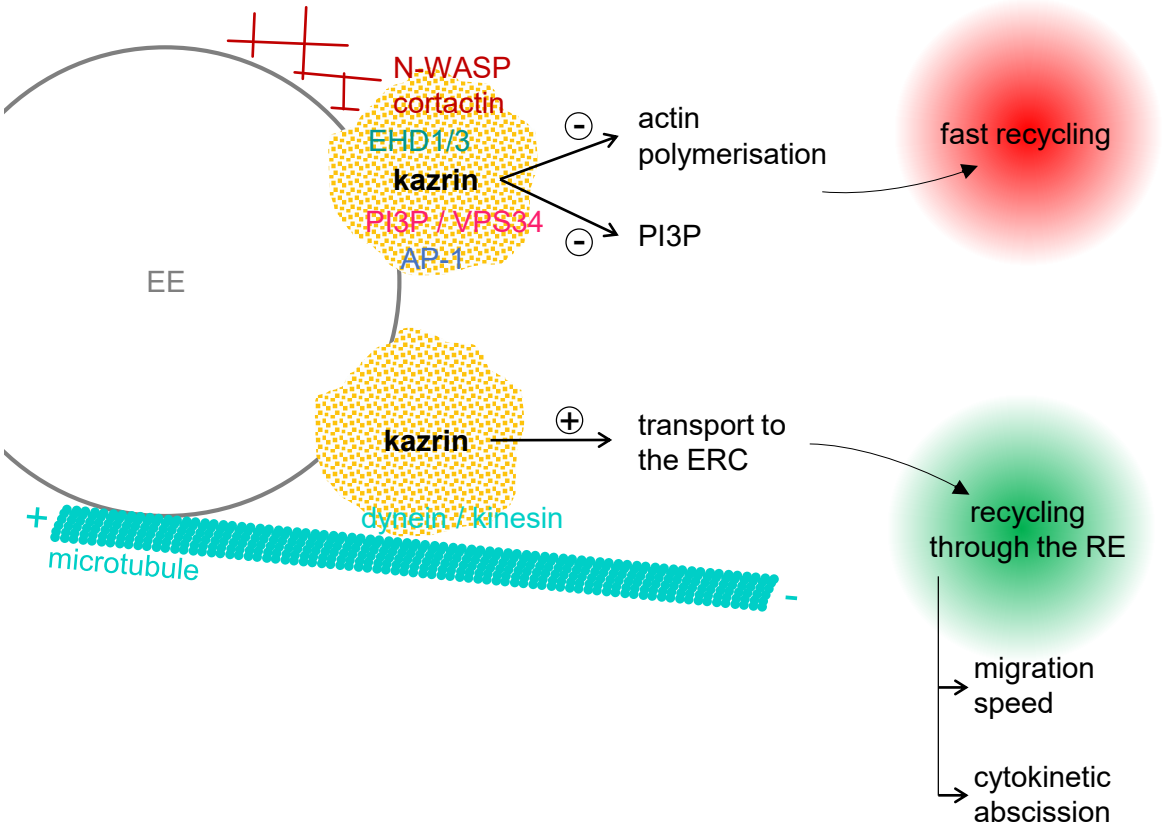

Figure 4.1. Model of the molecular functions of kazrin C in endosomal recycling. We propose that kazrin localises to EE subdomains, possibly recruited by EHD1 or the AP-1 complex. Kazrin might interact with N-WASP and cortactin to inhibit actin polymerisation. It might also interact with PI3P and VPS34 to inhibit PI3P formation. As a consequence, fast recycling pathways depending on PI3P and/or actin polymerisation would be blocked. On the other hand, kazrin might act as a dynein adaptor for the transport of EEs towards the perinuclear region and favour recycling through REs. As a consequence, it might allow cellular processes such as migration and cytokinetic abscission.

5 Conclusions

Conclusions

The conclusions of this thesis are the following:

- Kazrin depletion and overexpression block CME in MEF cells.
- Kazrin C co-localises with markers of adherens junctions at the PM and EEs.
- Kazrin depletion causes an increase in EEA1 and in EE dispersal.
- Kazrin depletion impedes the transport of Tfn towards the ERC and delays its recycling.
- Kazrin depleted cells migrate slower.
- Kazrin depletion delays cytokinetic abscission.
- Kazrin C contains a C-terminal IDR.
- Kazrin C interacts with dynein and kinesin-1 and directly interacts with the LIC1 and LIC2 dynein subunits.
- Kazrin C localises at the pericentriolar region, where it entraps EEs.
- Kazrin directly interacts and partially co-localises with EHD1/3 and γ-adaptin at EEs.
- Kazrin interacts with PI3P and the class III PI3K.
- Kazrin depletion causes an increase in PI3P.
- Kazrin C directly interacts with the N-terminus of N-WASP and cortactin and co-localises with cortactin at the PM and EEs.
- Kazrin depletion decreases cortical cortactin and increases endosomal cortactin.

6 Materials and methods

Mat. and methods

6.1 Cell culture

6.1.1 Handling of *Escherichia coli* cells

E. coli cell culture was done according to standard protocols (J. Sambrook, D.W. Russell 2001). *E. coli* cells were grown in LB media (0.5 % (w/v) yeast extract, 1 % (w/v) bacto-tryptone and 0.5 % (w/v) NaCl) supplemented with 50 mg/l ampicillin or kanamycin (Sigma-Aldrich) at 37 ºC with shaking. The *E. coli* strain DH5α was used for molecular cloning, whereas the strain BL21 was used for protein expression (see section 6.3.2).

6.1.2 Handling of *Saccharomyces cerevisiae* cells

S. cerevisiae cell culture was performed as described (J. Sambrook, D.W. Russell 2001). Yeast cells we grown in agitation at 28 ºC in Synthetic Dextrose minimal media (SDC), which is composed of of 2 % (w/v) glucose (Duchefa), 0.67 % (w/v) yeast nitrogen base (Difco) and 0.075 % (w/v) complete synthetic mix (CSM; Qbiogene). SDC also contained all required amino acids, purine and pyrimidine bases except those required for auxotrophic marker selection, in the following concentrations: 10 mg/l adenine, 50 mg/l L-arginine, 80 mg/l L-aspartate, 20 mg/l L-histidine-HCl, 50 mg/l L-leucine, 50 mg/l L-lysine, 20 mg/l L-methionine, 50 mg/l L-phenylalanine, 100 mg/l L-threonine, 50 mg/l tryptophan, 50 mg/l L-tyrosine, 20 mg/l uracil and 140 mg/l valine. Solid media also contained 2 % (w/v) agar. *S. cerevisie* was stored in 20 % (v/v) glycerol in cell culture medium at -80 ºC.

6.1.3 Handling of mammalian cell lines

The cell lines that were used in this study were the following: MEF are Mouse Embryonic Fibroblasts (ATCC SCRC-1040) and HEK293T (ATCC CRL-11268) are Human Embryonic Kidney cells that constitutively express the simian virus 40 (SV40) large T antigen. MEF and HEK293T cells were provided by A. Aragay, IBMB-CSIC.

All cell lines were grown in 10 cm culture plates (Nunc, Sigma-Aldrich) at 37 ºC and 5 % CO_2. MEF and HEK293T cells were grown in DMEM (Thermo Fisher) supplemented with 10 % (v/v) FCS, 100 µ/ml penicillin, 100 µg/ml streptaminicin and 2 mM L-glutamine (Thermo Fisher). Cells were passaged every 2 to 4 days by trypsinization. Briefly, cells were washed with PBS (137 mM NaCl, 2.7 mM KCl, 10 mM Na_2HPO_4, 2 mM KH_2PO_4, pH 7.4) and incubated in PBS with 0.05 % (v/w) trypsin and 0.02 % (v/w) EDTA (Thermo Fisher) until detached from the plate, then resuspended in the corresponding medium and transferred to a new plate in a convenient dilution. In order to plate cells for an immediate experiment, an automated cell counter (Thermo Fisher) was used to plate an adequate number of cells.

In order to freeze the cells for long-term storage, a confluent 10 cm plate was trypsinised as usual and centrifuged at 300 g for 5 min. The pellet was resuspended in 1.5 ml of medium with 10 % DMSO (Sigma-Aldrich), of which each 0.5 ml were transferred to cryogenic vials

(Nunc CryoTubes, Sigma-Aldrich). Cells were slowly frozen down to -80 ºC in a freezing container (Mr. Frosty, Sigma-Aldrich), and transferred to liquid N_2 within a month. When thawing cells, the vials were placed in a 37 ºC water bath and the cells pipetted into a 10 cm plate with medium. The medium was replaced the day after.

6.2 Genetic techniques

6.2.1 Transformation of *E. coli*

When plasmids were transformed into BL21 or DH5α *E. coli* cells, the protocol used was the $CaCl_2$ method (J. Sambrook, D.W. Russell 2001). Briefly, to create $CaCl_2$ competent cells they were grown to an $O.D._{600}$ of 0.7, harvested and washed in ice-cold 0.1 M $CaCl_2$. They were aliquoted and stored in 0.1 M $CaCl_2$ and 10 % glycerol at -80 ºC. 50 µl of competent cells were incubated with 2 µl of DNA for 2 min on ice, heat-shocked at 42 ºC for 90 s, and incubated 10 min on ice. They were grown in liquid LB medium for 20 min before plating on LB-agar plates containing the appropriate antibiotic.

Ligations were transformed into DH5α cells by electroporation for a greater efficiency (J. Sambrook, D.W. Russell 2001). Component cells for electroporation were formed by growing them to a $O.D._{600}$ of 0.7, chilled on ice for 30 min and harvested. They were washed in cold water twice before resuspending them in H_2O with 10 % glycerol and making aliquots to store at -80 ºC. Competent cells mixed with the DNA were transferred to pre-cooled 2.5 mm cuvettes (Cell Projects) and electroporated at 2.5 KV using a Gene Pulser Xcell system (BioRad). They were allowed to grow in liquid LB medium for 20 min before plating on LB-agar plates containing the appropriate antibiotic.

6.2.2 Transformation of *S. cerevisiae*

The protocol for *S. cerevisiae* transformation was adapted from Ito et al. (1983). Cells were grown to an $O.D._{600}$ of 0.4. Cells were harvested, washed three times with 1 ml LiAc-TE (100 mM lithium acetate, 10 mM EDTA, 100 mM Tris HCl, pH 7.5) and resuspended in 0.5 ml of LiAc-TE 2x. 3 µl of carrier DNA (herring sperm DNA) were mixed with 2 µl of plasmid DNA, 50 µl of cells and 150 µl of PEG 50 % (Fluka) and vortexed. Cells were incubated 30 min at room temperature and then 15 min at 42 ºC. Finally, cells were harvested, resuspended in 100 µl of TE (100 mM Tris HCl, 19 mM EDTA, pH 7.5) and plated on the appropriate media.

6.2.3 Molecular cloning techniques

Standard DNA manipulations were performed as described in J. Sambrook, D.W. Russell (2001). The construction of most plasmids was performed with standard cloning techniques (J. Sambrook, D.W. Russell 2001), except for those DNA constructs intended for protein overexpression by lentivirus production, which were cloned using the Getaway cloning system (see section 6.2.3.1; Life Technologies).

Standard Polymerase Chain Reactions (PCRs) were performed in a TRIO-thermoblock (Biometra GmbH) using the Expand High Fidelity polymerase (Roche). Oligonucleotides were synthesized by Fisher Scientific or Sigma-Aldrich. DNA restriction digestions were done with enzymes from New England Biolabs in the suggested conditions. DNA was purified using PCR or gel extraction kits from Macherey-Nagel. Analytical agarose gel electrophoresis was performed using Sub-Cell cells (Bio-Rad). Ligation of DNA fragments with plasmid vectors was performed for 2 h at room temperature using T4 DNA ligase (New England Biolabs). Plasmids were amplified and purified from *E. coli* with a Nucleospin plasmid purification kit according to the manufacturers protocol (Macherey-Nagel). The correct construction of the plasmids was confirmed by sequencing (Macrogen).

6.2.3.1 Getaway cloning system

In the Getaway cloning system (Thermo Fisher), flanking regions called attB1 and attB2 are added to the DNA to be cloned by PCR (ACAAGTTTGTACAAAAAAGCAGGCT and ACCACTTTGTACAAGAAAGCTGGGT, respectively). These regions recombine with the attP1 and attP2 regions present in the donor vector (pDONR221) in a reaction catalysed by the BP clonase. The product of this reaction is a donor vector that contains the DNA of interest flanked by attL1 and attL2 regions. A second reaction catalysed by the LR clonase induces the recombination with the attR1 and attR2 regions present in the destination vector (pINDUCER20 in our case), which results in a destination vector containing the gene of interest. The manufacturer's instructions were followed.

6.2.3.2 Plasmid constructs used in this thesis

The plasmids that were used in this study and their description are listed in **Table 6.1**. The cloning of those plasmids made during the course of this study is explained below, and the oligonucleotides used are listed in **Table 6.2**.

Plasmid	Insert	Backbone	Source	Ref.
pEGFP-N2	EGFP	pEGFP-N2	Clontech	740
pEGFP-kazrin	EGFP + kazrin C, human gene KIAA1026	pEGFP-C2	M. I. Geli (Schmelzl and Geli 2002)	746
pKazrin-EGFP	Kazrin C + EGFP	pEGFP-N2	This study	1268
pGFP-FYVE	EGFP + 2xFYVE (Hrs)	pEGFP-C3	F. Martín-Belmonte	-
pGEX-5X-3	GST	pGEX-5X-3	GE (#28-9545-55)	25
pGST-hB24	GST + kazrin C human gene KIAA1026	pGEX-4T-2	B. Schmelzl thesis	747

Plasmid	Insert	Backbone	Source	Ref.
pGST-KazrinC-Nt	GST + kazrin C-Ct minus polyK and acidic (aa 161-250)	pGEX-5X-3	A. Baumann thesis	1186
pGST-kaz-Ct	GST + kazrin C Ct (aa 161-327)	pGEX-5X-3	A. Baumann thesis	694
pGST-kaz-Ct251	GST + kazrin C Ct (aa 251-327)	pGEX-5X-3	A. Baumann thesis	695
pGST-kaz-Ct-EA	GST + kazrin C Ct (aa 161-327) - (322-EEDADW-327, AAAAAA)	pGEX-5X-3	A. Baumann thesis	1198
pGST-kaz-Ct-KA	GST + kazrin C Ct (aa 161-327) - (281-KRKKKK-286, AAAAAA)	pGEX-5X-3	A. Baumann thesis	1201
pQE11-kazrin	6xHis + kazrin C	pQE11	A. Baumann thesis	1168
pGST-LIC1	GST + dynein light intermediate chain 1	pGEX-6P-1	M. Mapelli	1357
pGST-LIC2	GST + dynein light intermediate chain 1	pGEX-6P-1	M. Mapelli	1358
pGST-N-WASP-Nt	GST + WASP Nt (aa 1-242)	pGEX-5X-3	M. I. Geli	1341
pGST-cortactin-Nt	GST + WASP Ct (aa 1-350)	pGEX-5X-3	M. I. Geli	1343
pGST-EHD1	GST + EHD1	pGEX-5X-3	M. I. Geli	1349
pGST-EHD3	GST +EHD3	pGEX-5X-3	M. I. Geli	1350
pSpCas9(BB)-2A-GFP pX458)	Cas9	pSpCas9(BB)-2A-GFP (pX458)	J. Roig	1337
pX458-kaz KO 1	Cas9 and cas9 target sequence 1	pSpCas9(BB)-2A-GFP (pX458)	This study	1338
pX458-kaz KO 2	Cas9 and cas9 target sequence 2	pSpCas9(BB)-2A-GFP (pX458)	This study	1339
pVSV-G	Lentivirus envelope protein	pCMV	M. Martínez	1264
pAX8	Lentivirus packaging protein	n.a.	M. Martínez	1265
pDONR221	Donor vector	pDONR221	M. Martínez	1266
pINDUCER20	-	pINDUCER20	M. Martínez	1267
pINDUCER-EGFP	EGFP	pINDUCER20	This study	1269

Plasmid	Insert	Backbone	Source	Ref.
pINDUCER-EGFP-kazrin	EGFP + kazrin C	pINDUCER20	This study	1271
pINDUCER-kazrin-EGFP	Kazrin C + EGFP	pINDUCER20	This study	1272
pSH18-34	LacZ	pSH18-34	R. Brent (Golemis et al. 2011)	183
LexA-BCD1	LexA + BCD1	pEG202	R. Brent (Golemis et al. 2011)	187
LexA-kazrin	LexA + kazrin C	pEG202	M. I. Geli	824
B42	B42	pJG4-5	R. Brent (Golemis et al. 2011)	182
pJG4-5-Rn.AP2.A2.ear	B42 + α-adaptin ear (aa 710-940)	pJG4-5	M. I. Geli	717
pJG4-5Hs-gamma-adaptin	B42 + γ-adaptin ear (aa 712-826)	pJG4-5	M. I. Geli	1291
pJG4-5ARC40	B42 + Arp2/3 p41	pJG4-5	M. I. Geli	418
pJG4-5-N-WASP-Nt	B42 + N-WASP Nt (aa 1-245)	pJG4-5	M. I. Geli	1287
pJG4-5-N-WASP-Ct	B42 + N-WASP Ct (aa 243-505)	pJG4-5	M. I. Geli	1288
pJG4-5-cortactin-Nt	B42 + Cortactin Nt (aa 1-350)	pJG4-5	M. I. Geli	1346
pJG4-5-cortactin-Ct	B42 + Cortactin Ct (aa 351-547)	pJG4-5	M. I. Geli	1297
pJG4-5-EHD1	B42 + EHD1	pJG4-5	M. I. Geli	1349
pJG4-5-EHD3	B42 + EHD3	pJG4-5	M. I. Geli	1350
pJG4-5-EHD1-EH	B42 + EHD1 EH (aa 438-535)	pJG4-5	M. I. Geli	1347
pJG4-5-EHD3-EH	B42 + EHD3 EH (aa 438-536)	pJG4-5	M. I. Geli	1348
pJG4-5-rab4a	B42 + rab4a	pJG4-5	M. I. Geli	1293
pJG4-5-rab4b	B42 + rab4b	pJG4-5	M. I. Geli	1294
pJG4-5-rab4b Q67L	B42 + rab4b-Q76L active form	pJG4-5	M. I. Geli	1295
pJG4-5-rab4b DS22N	B42 + rab4b-S22N negative form	pJG4-5	M. I. Geli	1296

Table 6.1. Plasmids. The plasmids used in the experiments presented in this thesis are listed together with the proteins encoded in them, their backbone, their source and their reference number in Geli's laboratory plasmid collection.

During the course of this study, plasmids were cloned as follows, using the oligonucleotides from **Table 6.2**:

- pKazrin-EGFP

The kazrin C gene was amplified by PCR from a pEGFP-kazrin plasmid using oligonucleotides hB24.BamHI.EcoRI.1D and hB24.XhoI.SmaI.984U. Vector pEGFP-N2 and the PCR product were digested with EcoRI and SmaI and ligated.

- pX458-Kaz KO 1 and pX458-Kaz KO 2

The plasmid pSpCas9(BB)-2A-GFP (pX458) was cut with BbsI and dephosphorylated with shrimp alkaline phosphatase (rSAP; New England Biolabs). Oligos mouse.kazrin. KO.1.FWD and mouse.kazrin.KO.1.REV, or mouse.kazrin.KO.2.FWD and mouse.kazrin. KO.2.REV, were hybridised by incubating 10 min and 70 ºC and letting to slowly cool, and then phosphorylated with T4 polynucleotide kinase (New England Biolabs). Oligonucleotides and vector were ligated.

- pINDUCER-EGFP

EGFP was amplified from pEGFP-N2 by PCR with the oligonucleotides attB1.GFP.FWD and attB2.GFP.STOP.REV. The resulting fragment, flanked by attB sequences, was inserted in pDONOR221 by the BP clonase. The GFP sequence was finally transferred from the resulting vector into pINDUCER20 with the LR clonase.

- pINDUCER-EGFP-kazrin

EGFP was amplified from pEGFP-kazrin by PCR with the oligonucleotides attB1.GFP.FWD and attB2.KAZ.STOP.REV. The resulting fragment, flanked by attB sequences, was inserted in pDONOR221 by the BP clonase. The EGFP sequence was finally transferred from the resulting vector into pINDUCER20 with the LR clonase.

- pINDUCER-kazrin-EGFP

EGFP was amplified from kazrin-pEGFP by PCR with the oligonucleotides attB1.KAZ.FWD and attB2.GFP.STOP.REV. The resulting fragment, flanked by attB sequences, was inserted in pDONOR221 by the BP clonase. The EGFP sequence was finally transferred from the resulting vector into pINDUCER20 with the LR clonase.

Name, restriction sites	Sequence
hB24.BamHI.EcoRI.1D	AACCAAGGATCCCCGAATTCATGAAGGAGATGTTG GCGAAGG
hB24.XhoI.SmaI.984U	AACCAACCCGGGCCAGTCCGCGTCCGCGTCCTCC
mouse.kazrin.KO.1.FWD	CACCGAATGCTGGCGAAGGACCTGG
mouse.kazrin.KO.1.REV	AAACCCAGGTCCTTCGCCAGCATTC
mouse.kazrin.KO.2.FWD	CACCGCCTTCTGTACCAGCTGCACC
mouse.kazrin.KO.2.REV	AAACGGTGCAGCTGGTACAGAAGGC
attB1.KAZ.FWD	GGGGACAAGTTTGTACAAAAAAGCAGGCTTCACCA TGAAGGAGATGTTGGCGAAG
attB2.KAZ.STOP.REV	GGGGACCACTTTGTACAAGAAAGCTGGGTTTCACC AGTCCGCGTCCTCCTCTAT
attB1.GFP.FWD	GGGGACAAGTTTGTACAAAAAAGCAGGCTTCACCA TGGTGAGCAAGGGCGAGGAGC
attB2.GFP.STOP.REV	GGGGACCACTTTGTACAAGAAAGCTGGGTTTTACTT GTACAGCTCGTCCATGCC

Table 6.2. Oligonucleotides. The names of the oligonucleotides used for the construction of plasmids during the course of this study are listed with their nucleotide sequence.

6.2.4 Manipulation of mammalian cells: protein overexpression and depletion

6.2.4.1 DNA transfection

HEK293 cells were transfected with calcium phosphate. $2.2 \cdot 10^6$ cells were seeded on three 10 cm plates the day before transfection. 10 µg of total DNA were added to 500 µl of 250 mM $CaCl_2$. This transfection mix was added to 500 µl of Hebbs 2x (280 mM NaCl, 10 mM KC, 1.5 mM Na_2HPO_4 (+$2H_2O$), 12 mM Glucose, 50 mM Hepes, pH 7.12) dropwise under agitation by vortexing. The mix was incubated for 15 min at room temperature. The precipitate was added dropwise to the plate and the media was changed after 5 h.

Due to the low efficiency of liposome-mediated transfection in MEF cells, these cells were electroporated for transient protein overexpression and for the delivery of CRISPR-cas9 plasmids, or lentiviral transduced for the generation of stable cell lines (see 1.2.4.4). For electroporation, cells were plated the day before on a 10 cm plate to reach 50 to 60 % confluency on the transfection day. They were trypsinized, resuspended in media and counted. $2 \cdot 10^6$ cells were transferred to an Eppendorf tube and spun at 250 g. The pellet was resuspended in 100 ul of MEF 2 Nucleofector solution (Lonza), 5 µg of total DNA was added, and the mix was electroporated in an Amaxa cuvette using program A-23 in an

Amaxa Nucleofector (Lonza). Immediately after electroporation, cells were transferred into a pre-warmed 35 mm plate. The media was changed the day after.

6.2.4.2 Cell sorting by flow cytometry

Cells were trypsinised and counted. $2 \cdot 10^6$ cells were transferred to an Eppendorf tube, spun at 250 g and resuspended in 1 ml of DMEM without phenol red with serum. They were sorted using an Aria FUSION (Becton Dikinson) cell sorter in sterile conditions. After stablishing a threshold with a WT control, positive cells with a GFP signal were transferred to a 10 cm plate with pre-warmed medium. If clonal selection was needed, individual positive cells were sorted into a 96-well plate.

6.2.4.3 CRISPR-cas9 system and establishment of KO cell lines

MEF cells were genetically modified to produce kazrin KO cell lines using the CRISPR-cas9 system (Cong et al. 2013; Mojica, F. J., Diez-Villasenor, C., Soria, E. & Juez 2000). Briefly, this system consists on targeting a cas9 nuclease to a specific DNA sequence using a guide RNA (gRNA) that is complementary to that sequence. The cas9 produces a double-strand break that is repaired by the cells. However, the repair is often not perfect and results in a frame shift. If cas9 is targeted to the start of the gene, protein expression will be disrupted in some clones (**Figure 6.1A**).

A protocol from Moyer and Holland (2015) was followed (**Figure 6.1B**). The gRNA was designed to contain a region that is complementary to the target sequence, in this case to the start of exon 1 in kazrin C. It also precedes a Protospacer Adjacent Motif (PAM) that is necessary for the cleavage. In addition, the gRNA was designed to have a high affinity for the target sequence and also to show specificity for that sequence and thus minimise off-target effects. Online resources were used for the design of gRNAs: Benchling (https://www.benchling.com/) and the Broad Institute tool GPP (https://portals.broadinstitute.org/gpp/public/analysis-tools/sgrna-design). Two gRNAs were selected to maximise the chances of depletion. Cells were transfected with a pX458-kaz KO plasmid containing a template for the gRNA, the sequence for the cas9 nuclease and a EGFP sequence in order to visualise transfected cells. Transfected cells were sorted by FACS and plated in individual wells. Those forming colonies were cultured and amplified until they covered two 35 mm plates. The cells in one of the plates were trypsinised and kept at -80 ºC, while the cells from the other plate were lysed for testing. The clones were tested by IB with antibodies against the N-terminal or the C-terminal part of kazrin, and those with no kazrin expression were selected and amplified from the -80 ºC stock (**Figure 6.1B**).

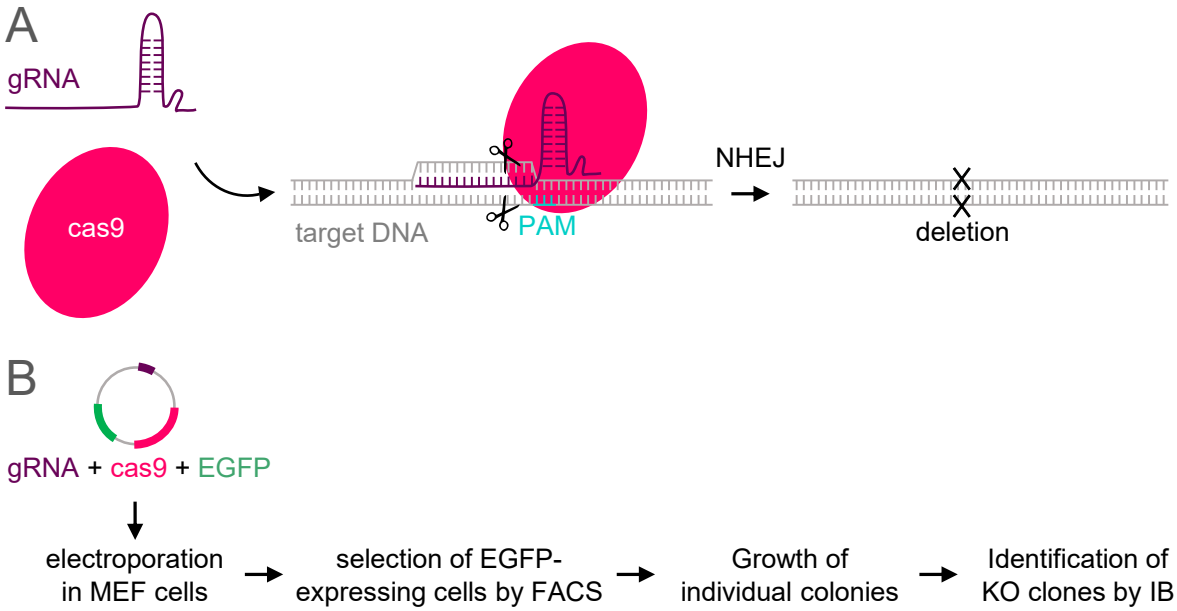

Figure 6.1. CRISPR-cas9 system for the establishment of KO cell lines. A. The molecular bases for the formation of KO cells rely on the expression of a gRNA and a cas9 nuclease in the cell. The gRNA recognises a specific sequence in the target DNA, adjacent to a PAM sequence. Cas9 binds to the gRNA and cuts both DNA strands three nucleotides upstream of the PAM sequence. The cell activates the Non-Homologous End Joining (NHEJ) program for DNA reparation, with often results in a deletion. This deletion impedes the expression of the gene. **B.** A plasmid containing the sequences of the gRNA, the cas9 nuclease and EGFP are electroporated into WT MEF cells. Successfully electroporated cells will express EGFP and can be selected by FACS, which is also used to isolate individual cells. Once colonies are formed, they are analysed by IB with an α-kazrin antibody to identify KO clones.

6.2.4.4 Lentivirus production and establishment of overexpressing cell lines

Lentiviral particles were produced in HEK 293T cells. Three 10 cm plates were transfected with the packaging plasmid pAX8, the envelope plasmid pVSV-G and the pINDUCER20 vector containing the gene of interest, which in our case is fused to GFP. The supernatant was collected the morning after and replaced by new media. A second recovery of lentiviral particles was done after 6 h. The virus-containing media was filtered with a 0.45 mm filter and stored at -80˚C.

MEF cells were plated on a 10 cm plate to reach 90 % confluence on the day of transduction. 4 ml of lentivirus-containing medium and 6 ml of medium were added to each plate. The medium was changed after 24 h. The cells were passaged during a week so that the plasmid would either integrate in their genome or be lost during cell division. Since the vector used in all cases was pINDUCER20, the expression of the construct could be induced with doxycycline. Cells were incubated for 24 h with 5 µg/ml doxycycline hyclate (Millipore) to induce the expression of the construct. All the constructions used in this study for overexpression through lentiviral transduction contain GFP, and therefore they could be

selected by flow cytometry (see 6.2.4.2). Positive cells were pooled and expanded in order to make as much stocks of an early passage as possible.

6.3 Biochemistry techniques

6.3.1 SDS-PAGE and IB

SDS-PAGE was performed as described in Laemmli (1970), using a Minigel system (BioRad). PageRuler prestained molecular weight standars (BioRad) were used. Laemmli sample buffer 2x (4 % (w/v) SDS, 200 mM DTT, 20 % (v/v) glycerol, 120 mM Tris-HCl pH 6.8, bromophenol blue) was added to the samples, which were incubated at 95°C for 8 min, quickly spun at room temperature and run in a 4-20 % polyacrylamide gradient SDS-PAGE gel (BioRad). Gels were then analysed by either IB or by Coomassie Blue (0.25 % (w/v) Coomassie brilliant blue, 7.5 % (v/v) acetic acid, 50 % (v/v) methanol) for the detection of total proteins.

IBs were performed as described in Geli, Wesp, & Riezman (1998). Before blocking, membranes were incubated in Ponceau red (0.3 % (v/v) Ponceau red, 3 % (w/v) trichloroacetic acid; Sigma-Aldrich) to detect total proteins in the membrane. After rising with distilled water, membranes were blocked for 30 min in blocking buffer (PBS, 3 % (w/v) non-fat lyophilized milk, 0.1 % (v/v) Nonidet P-40). They were then incubated for 1 h with the primary antibody, dissolved in blocking buffer, washed with blocking buffer three times for 10 min, and incubated with the peroxidase-conjugated secondary antibody for 1 h in blocking buffer. Finally, membranes were washed three times for 10 min with blocking buffer and 10 min with PBS (137 mM NaCl, 2.7 mM KCl, 10 mM Na_2HPO_4, 2 mM KH_2PO_4, pH 7.4). The antibodies used for the detection of each protein and their dilution are listed in **Table 6.5**. The peroxidase attached to the secondary antibody was detected using an enhanced chemoluminiscence (ECL) detection kit (Amersham Biosciences), together with Super RX radiograph films (Fujifilm).

6.3.2 Protein purification from *E. coli*

Recombinant proteins for pull-down and lipid strip experiments were expressed and purified from BL21 *E. coli* cells (M.I. Geli 2000). The bacteria were transformed with plasmids encoding GST or 6xHis-tagged protein constructs and a single colony was inoculated into LB with 50 mg/l of ampicillin (Sigma-Aldrich). A 1/100 dilution of an overnight culture was grown at 37 ºC until an optical density at 600 nm (OD_{600}) of 0.4 was reached. The culture was then incubated at 24 ºC until it reached a OD_{600} of 0.6-0.8, at which expression of recombinant proteins was induced with 0.1 mM of Isopropyl-β-D-ThioGalactoside (IPTG; Sigma-Aldrich) in the case of GST constructs and 1 mM of IPTG in the case of 6xHis constructs. The induction was conducted at 24 ºC for 2-4 h. Cells were then recovered by centrifuging at 5,000 g for 30 min. The resulting pellets were stored at -20 ºC.

To purify GST-tagged proteins, pellets of BL21 culture were lysed in PBS with 0.5 % (v/v) Tween-20 (PBS-Tween) and one tablet of Complete protease inhibitors cocktail (Roche) per 50 ml of buffer for GST fusion proteins or Complete protease inhibitors cocktail without EDTA (Roche) for 6xHis-fusion proteins. They were lysed by sonication in a Branson ultrasonic microtip sonifier at 30 % amplitude for 2 min. The cells were kept on ice and rested for 20 s every 20 s of sonication to avoid overheating of the sample and protein degradation. The lysate was centrifuged at 15,000 g for 30 min and the supernatant recovered. The appropriate amount of 50 % (v/v) Glutathione-Sepharose (GSH)-beads (GE Healthcare), according to the manufacturer, were added to the cleared lysate. The beads had been previously equilibrated in PBS-Tween. The lysate was incubated with the beads in 15 ml of buffer with protease inhibitors for 1 h at 4 ºC in head-over-shoulder rotation. Beads we recovered by a short spin at 500 g. For GST-kazrin purification for lipid strip experiments, the beads were washed three times with 15 ml of PBS-Tween and twice with 15 ml of PBS containing protease inhibitors, and resuspended in the appropriate buffer (see section 6.3.3). In the case of GST constructs for pull-down experiments, the beads were washed three times with 10 ml of PBS-Tween, twice with 1 ml of PBS with 0.1 % (v/v) Triton X-100 (PBS-Triton) and once with 1 ml of PBS-Triton with 0.5 % (w/v) BSA. The beads were then drained and resuspended in the appropriate buffer (see section 6.3.6.1).

Purification of 6xHis-tagged kazrin C was carried out in denaturing conditions. A 2 L pellet of BL21 was lysed in 30 ml of lysis buffer (8 M urea, 100 mM NaH_2PO_4, 10 mM Tris pH 8.0) at room temperature. The lysate was clarified by centrifugation at 9,500 g for 30 min. The supernatant was incubated with 600 µl of 50 % (v/v) nickel-charged beads (Ni-NTA Superflow from Qiagen). Beads were then washed twice with 10 ml of lysis buffer. They were transferred to 15 ml disposable column bearing 35 µm pore filters. Beads were washed twice with 1 ml of each renaturing buffer (400 mM NaCl, 10 % (v/v) glycerol, 10 mM NaH_2PO_4, 10 mM Tris pH 7.7) containing the following decreasing concentrations of urea: 8 M, 7 M, 6 M, 5 M, 4 M, 3 M, 2 M, 1 M, 0 M for 1 h. The elution was performed in 300 µl elution buffer (400 mM NaCl, 10 % glycerol (v/v), 10 mM NaH_2PO_4, 10 mM Tris pH7.7, 250 mM imidazol, pH 8.0) containing protease inhibitors without EDTA (Complete Roche). The elution was aliquoted, snap-frozen in liquid N_2 and stored at -80 ºC. After thawing, the day of the experiment, the protein was centrifuged at 18,000 g for 30 min to eliminate aggregates.

6.3.3 Lipid strip assays

Lipid strip (Echelon) assays were performed to detect possible interactions between GST-kazrin C constructs and the different lipids and concentrations embedded in the strips. GST-fused constructs were purified as explained in section 1.3.2. Lipid strips were incubated in blocking buffer of 1 % (w/v) skimmed milk in PBS for 1 h at room temperature. Once blocked, the corresponding GST fusion protein was added to a final concentration of 15 µg/ml in incubation buffer 10 mM Tris pH 8.0, 150 mM NaCl, 0.1 % (v/v) Tween-20, 3 %

(w/v) BSA (fatty acid free, Sigma), with protease inhibitors (1 mM PMSF, 1 µg/ml pepstatin, 1 µg/ml aprotinin, 2.5 µg/ml antipain, 5 µg/ml leupeptin) overnight at 4 ºC. The strips were washed three times for 10 min in the incubation buffer and blotted with and anti-GST goat antibody, washed three times and incubated with the appropriate peroxidase-conjugated anti-goat IgG a secondary antibody (see **Table 6.5**). After three washes with the incubation buffer and another three with the incubation buffer without BSA, the peroxidase attached to the secondary antibody was detected using an enhanced chemoluminiscence (ECL) detection kit (Amersham Biosciences), together with Super RX radiograph films (Fujifilm).

6.3.4 Optiprep density gradient

The subcellular fractionation of MEF cells using Optiprep density gradients was performed as described in Li and Donowitz (2014). For each cell type, ten 10 cm plates of cells grown to confluency in complete DMEM, seeded 24 h beforehand. They were placed on ice, rinsed with cold PBS and scraped in 1 ml of cold PBS. Cells were harvested by centrifugation at 700 g for 10 min and resuspended in 1 ml of ice cold Lysis buffer (LB: 25 mM Hepes pH 7.4, 150 mM NaCl, 1 mM DTT, 2 mM EGTA) containing protease inhibitors with a 25 cm cell scraper (Sarstedt). 1 ml of the cell suspension was then passed 10 times through a 27 G needle using a 1 ml syringe to lyse the cells. The lysate was then cleared by centrifuging twice at 3,000 g for 15 min. The supernatant was subsequently centrifuged in a TLA-55 rotor in a table-top Beckman Coulter Optima MAX-XP ultracentrifuge at 186,000 g for 1 h at 4 ºC to fractionate cellular membranes from cytosol. The membrane pellet was then carefully resuspended in 300 µl of LB with protease inhibitors by passing them 10 times though a 27 G needle using a 1 ml syringe, and carefully laid on a 12 x 1 ml, 2 % (v/v) Optiprep step gradient, prepared beforehand in Ultra-Clear tubes (Beckman Coulter 344059, thin wall, 13.2 ml, 14 x 89 mm) for the Beckman Coulter SW41Ti rotor. 32 % to 10 % Optiprep mixtures were prepared by mixing the amounts of Optiprep (60 %, Sigma), LB x 3 and double distilled water stated in **Table 6.3.**

Mixtures were prepared and left overnight at 4 ºC in 15 ml polypropylene tubes. Before cell lysis, the Optiprep gradient was prepared by mixing 1 ml of each solution with 10 µl of protease inhibitors x 100, and by laying each mixture carefully with a Pasteur pipette starting from the heavier solution (32 %) at the bottom to the lightest (10 %) at the top. The step gradient was carefully deposited on ice and stored until the membrane fraction was laid.

Once the membranes were laid on the top of the gradient, the tube was filled (if necessary) with LB and samples were spun for 16 h at 100,000 g at 4 ºC, in a SW41Ti rotor in an Optima L-90K ultracentrifuge. The gradient was carefully placed on ice and 0.6 ml fractions were carefully collected from the top into 1.5 ml polypropylene tubes. Samples were then precipitated by adding 66 µl of 100 % (w/v) trichloroacetic acid, incubating on ice for 1 h and centrifuging at 4 ºC for 30 min at 20,000 g. Pellets were rinse once with 1 ml of 10 %

(w/v) trichloroacetic acid, spun for 20 min, and rinsed again with 1 ml of -20 ºC pre-cooled acetone. After centrifuging for 20 min at 4 ºC, the supernatant was removed and the pellets were air-dried and resuspended in 30 µl of SDS-PAGE sample buffer. After boiling, 10 µl were loaded for IB analysis (see section 6.3.1).

Optiprep mixture (%)	60 % Optiprep (ml)	LB x 3 (ml)	ddWater (ml)
10	2	4	6
12	2.4	4	5.6
14	2.8	4	5.2
16	3.2	4	4.8
18	3.6	4	4.4
20	4	4	4
22	4.4	4	3.6
24	4.8	4	3.2
26	5.2	4	2.8
28	5.6	4	2.4
30	6	4	2
32	6.4	4	1.6

Table 6.3. Mixtures for an Optiprep gradient. The table shows the volumes of the components for the preparation of the Optiprep mixtures necessary to create a gradient.

6.3.5 Total protein extraction from mammalian cells

Cells from a confluent 60 mm plate were washed with cold PBS and harvested with a cell scraper in 1 ml of PBS. After 10 min of centrifugation at 500 g at 4°C, the supernatant was discarded, the cell pellet was resuspended in 50 µl of PBS with 1 % (v/v) Triton X-100 (Merck) containing protease inhibitors and left 10 min on ice for cell lysis. The lysate was centrifuged at 4°C for 10 min with 5,000 g to remove cell debris. The supernatant was recovered and protein concentration was determined with the BioRad Protein assay. Briefly, 1 µl of protein sample was diluted in 800 µl of H_2O and 200 µl of Bradford Reagent (BioRad) and the OD_{595} of the solution was measured. The protein concentration corresponding to the observed OD_{595} was calculated from a calibration curve that had previously been established using BSA solutions of known concentration. The sample was diluted 1/2 in Laemmli sample buffer (2 % (w/v) SDS, 200 mM DTT, 20 % (v/v) glycerol, 120 mM Tris-HCl pH 6.8, bromophenol blue) and usually 20 µg of protein were analysed by SDS-PAGE and IB (see chapter 6.3.1).

6.3.6 Analysis of protein-protein interactions

6.3.6.1 Pull-down assays

Pull-down experiments were performed with GSH beads coated with 0.5 µg of GST-tagged proteins and 50 ng of 6xHis-kazrin C (purified as described in section 6.3.2). The coated beads were transferred to a siliconized Eppendorf tube and suspended in 1 ml of binding buffer containing PBS, 0.1 % (v/v) Triton-X100 and 0.5 % (w/v) BSA with protease inhibitors (Complete Roche). 50 ng of 6xHis-kazrin C was added and the mixture was incubated 1 h at 4 ºC in a head-over-shoulder rotation. Beads were washed three times with 10 ml of PBS-Tween, twice with 1 ml of PBS with 0.1 % (v/v) Triton X-100 (PBS-Triton) and once with 1 ml of PBS-Triton with 0.5 % (w/v) BSA. A 30 s spin at 500 g was performed between washes to recover the beads. The beads were drained, resuspended in 40 µl of 1x Laemmli buffer and incubated 5 min at 90 ºC. The supernatant was recovered. Input and pull-down samples were loaded in an SDS-PAGE gel and analysed by IB (see section 6.3.1).

6.3.6.2 Immunoprecipitation assays

For immunoprecipitations from GFP and GFP-kazrin C overexpressing MEFs, 15 confluent 10 cm plates were needed for each immunoprecipitation condition. The cells were seeded in complete DMEM with 5 µg/ml of doxycycline on the day before the experiment. Samples were handled at 4 ºC at all times. Cells were washed with PBS and harvested from the plate in 1 ml of PBS with a cell scraper (Sarstedt), pooled and centrifuged at 100 g. The pellet was resuspended in 500 µl of IP buffer (20 mM Hepes, 50 mM KAc, 2 mM EDTA, 200 mM sorbitol, 0.1 % (v/v) Triton X-100, pH 7.2) containing protease inhibitors and passed 30 times through a 27 G needle. The lysate was centrifuged 5 min at 10,000 g to remove whole cells and nuclei. The pellet was resuspended in 100 µl of IP buffer and the resulting supernatant was mixed with the first one and then subjected to a final centrifugation of 5 min at 10,000 g. The protein concentration of the supernatant was measured and adjusted to the lowest sample, and the total volume was increased up to 1 ml with IP buffer. 5 % of each sample was kept as the input, the same volume of 2x Laemmli buffer was added, and the samples were incubated 5 min at 90 ºC.

10 µl of GFP-binding agarose beads (Chromotek) were equilibrated in IP buffer, beads were recovered by centrifugation and subsequently incubated with the protein extract for 1 h at 4 ºC in head-over-shoulder rotation. Beads were washed six times with 1 ml of IP buffer, spinning 30 s at 500 g between washes. The beads were drained, resuspended in 30 µl of Laemmli buffer and incubated 5 min at 90 ºC. Input and IP samples were loaded in an SDS-PAGE gel and analysed by IB (see section 6.3.1).

6.3.6.3 Yeast-two-hybrid assay

The interaction trap two-hybrid system was used (Gyuris et al. 1993; **Figure 6.2**). The strain EGY48 containing the *lacZ* reporter plasmid pSH18-34 was transformed with a pEG202 plasmid encoding the DNA binding protein lexA fused to a kazrin C construct (bait), together with the pJG4-5 plasmid encoding the B42 transcriptional activator fused to another protein of interest (prey; see **Table 6.1**). Yeast were selected in SCD-Ura-His-Trp plates. To test the possible interactions, co-transformants were spotted on plates containing 80 mg/l X-gal (5-bromo-4-cloro-3-indolil-β-D-galactopiranoside), 1 % (w/v) raffinose (Sigma), 2 % (w/v) galactose (Sigma), 0.67 % (w/v) yeast nitrogen base, 0.054 % (w/v) of CSM-Ura-His-Trp, 20 mM Na_2HPO_4, 25 mM NaH_2PO_4, and 100 mg/l leucine, at pH 7.0 (**Figure 6.2A**).

The binding of a kazrin C construct with the corresponding protein under study would bring lexA and B42 in close proximity, thus allowing the transcription of the *lacZ* gene and the expression of β-galactosidase. Hydrolysis of the X-Gal in the plates by the β-galactosidase would produce a blue precipitate (**Figure 6.2B**).

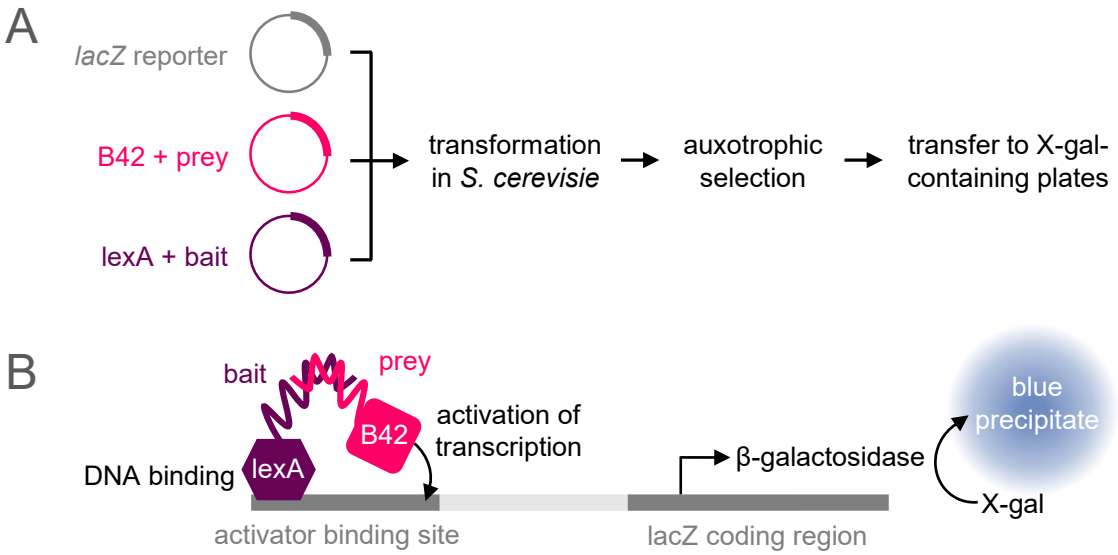

Figure 6.2. Yeast-two-hybrid system for the analysis of protein-protein interactions. A. *S. cerevisie* cells are transformed with plasmids containing a *lacZ* reporter, the sequence of B42 fused to a protein of interest or prey, and the sequence of lexA fused to another protein of interest or bait, respectively. The objective is to detect a possible interaction between the prey and the bait. The plasmids contain auxotrophic markers that allow the selection of transformed cells. These are then transferred to plates that contain X-gal. **B.** If there is an interaction between bait and prey, the proteins lexA and B41 will also come together. LexA binds the activator binding site of the *lacZ* operon, whereas B42 activates the transcription of the operon and the expression of β-galactosidase. β-Galactosidase catalyses the transformation of X-gal into an insoluble blue compound that can be identified by sight.

6.4 Imaging techniques

6.4.1 Live cell epifluorescence imaging

Migration and cell division were observed on individual MEFs by epifluorescence microscopy. 0.5 ml of 400 µg/ml Matrigel in serum-free DMEM were evenly distributed on a 35 mm plate, incubated for 30 min at 37 ºC, after which the Matrigel excess was removed. 10^4 cells were then plated in 1 ml of complete DMEM and let to attach for 5 h, after which the medium was replaced by 0.5 ml of 400 µg/ml Matrigel in serum-free DMEM for 30 min at 37 ºC. Matrigel excess was removed and 1 ml of complete DMEM was added to the cells. Cells were kept at 37 °C with 5 % CO_2 during imaging. Phase contrast images were taken every 10 min for a total of 13 h in a Leica AF700 microscope with a 10x objective (see section 6.4.5).

6.4.2 Live cell fluorescence confocal imaging

Cells were seeded on 35 mm plates with polymer coverslips for high-end microscopy (Ibidi). Cells were treated with 5 µg/ml of doxycycline for 24 h before imaging for visualization of GFP-kazrin C, when the medium was renewed with pre-warmed culture medium. Cells were kept at 37°C with 5 % CO_2 during the imaging. Images were taken every 2.65 s on a Zeiss LSM780 confocal microscope.

6.4.3 Fluorescent-based assays with fixed cells

Cells were plated approximately 20 h before fixation on glass coverslips of 1.5 thickness (Karl Hech Assistent) and grown up to a convenient confluence. Cells were fixed with 4 % (w/v) paraformaldehyde (PFA; Merck) in PBS* (0.02 % (w/v) sodium azide, 0.02 % (w/v) BSA, PBS pH 7.4) for 10 min at room temperature. Fixation in uptake and recycling experiments was performed on ice for 20 min instead. If no antibody staining was needed, coverslips were mounted on microscope slides (Waldemar Knittel) using Prolong that included DAPI for nuclear staining (Thermo Fisher). Slides were let to dry overnight at room temperature, then stored at 4 ºC.

For immunofluorescence experiments, cells were then permeabilized in 0.25 % (v/v) Triton X-100 in PBS* for 10 min. Blocking was performed in PBS* with 1 % (v/v) BSA for 30 min. Coverslips were washed between each step with PBS. Primary and secondary antibodies were incubated sequentially for 1 h at room temperature in PBS*. For details about dilutions and references of antibodies see **Table 6.5**. Between each step, the coverslips were washed three times in PBS*. Three final washes of 5 min in PBS were done before mounting. In experiments of VPS34 inhibition, a 1/500 dilution of IN1 (Selleckchem) in DMSO was added to the cells to reach a 1 µM concentration of the inhibitor for 3 h before fixation. An equal volume of DMSO was added to control cells.

6.4.4 Uptake and recycling assays

For Tfn uptake or recycling experiments, 10^5 MEF cells were plated on collagen-coated coverslips in a 12-well plate the day before the experiment. The coating was achieved by adding 300 µl of 200 µg/ml of collagen IV in 0.25 % (v/v) acetic acid on each coverslip and incubating for 2 h at 37 ºC. The coverslips were then thoroughly washed twice with PBS before plating the cells. For uptake experiments, the cells were starved for 30 min in DMEM without FBS or BSA. 0.5 ml of pre-warmed DMEM containing 20 µg/ml of 647-Tfn or TxR-Tfn (from human serum, Molecular Probes) and 0.1 % (v/v) BSA was added to each well. Tfn was added to different wells at different time points, except to control wells without Tfn (0 min), and the plate was quickly transferred back to the 37 ºC incubator to avoid temperature change. All cells were then transferred to ice at the same time, and washed in ice-cold PBS once and immediately fixed in 4 % (v/v) PFA for 20 min on ice.

In the case of recycling experiments, cells were starved for 30 min in DMEM without FBS or BSA. Plates were transferred to ice, where 0.5 ml of 20 µg/ml of TxR-Tfn in DMEM with 0.1 % (v/v) BSA was added to all wells. Plates were incubated at 16 ºC for 30 min to allow accumulation at sorting endosomes, then washed once in ice-cold PBS with 25 mM acetic acid pH 4.2 and once in PBS. 500 µg/ml unlabelled Tfn (Sigma) in DMEM with 0.1 % (v/v) BSA was added to all wells and the plates were placed in a 37 ºC incubator. Plates were sequentially transferred to ice at different time points, washed once in ice-cold PBS with 25 mM acetic acid pH 4.2 and once with PBS. They were immediately fixed in 4 % (v/v) PFA for 20 min on ice.

6.4.5 Microscopes specifications

Images were acquired in the Molecular Imaging Platform of the IBMB. The basic specifications of the hardware are summarised below. The specific laser and filter used depended on the fluorophore to be visualised (**Table 6.4**).

The Leica AF7000 wide field microscope was equipped with a solid state excitation white light led and an emission filter BP520/28 for GFP, among others. The objective used was a dry 0.3 10x objective. A Digital CCD camera ORCA-R2 was used. This microscope contained a motorised XY stage, as well as temperature control system (Pecon) and a CO_2 incubator (OKO-lab). The system was controlled by the Leica LAS_X software.

The Leica TCS-SP5 confocal microscope was equipped with a diode laser (405 nm), multiline argon laser (458 nm, 476 nm, 488 nm, 496 nm, 514 nm), solid state DPSS laser (561 nm) and HeNe laser (633 nm). Emission filters were LP425, BP525/50 optimized for GFP, LP515 (450-490,510), LP590 (BP515-560,580). A 63x/1.4NA Oil HCX Plan-Apochromat was the objective used. The spectral detection system was composed of an Acousto Optical Beam

Splitter, a Spectral Detector SP and with three PMTs (photomultiplier tubes). The system was controlled with the Leica Application Suite Advanced Fluorescence (LAS AF).

The Zeiss LSM-780 confocal microscope system was equipped with a diode laser (405 nm), multiline argon laser (458/488/514 nm), solide state DPSS Laser (561 nm), HeNe laser (594 nm) and HeNe laser (633 nm). The objective used was a 63x/1.4NA oil DIC Plan-Apochromat objective. The internal detectors of the LSM-780 system had three channels, two usual PMTs (photomultiplier tubes) and a 32 PMT GaAsP array, all PMTs usable for fluorescence and reflection and an additional PMT for transmitted light, allowing simultaneously detection of fluorescence and bright field images. The system was controlled with the LSM software Zen2.1.

Microscope	Fluorophore	Laser	Filter
Zeiss LSM-780	DAPI	Diode (405 nm)	Zeiss 49 set
Zeiss LSM-780	GFP / A488	Multiline argon (458/488/514 nm)	Zeiss 38 set
Zeiss LSM-780	A568	Solide state DPSS (561 nm)	Zeiss 43 set
Zeiss LSM-780	A647	HeNe (633 nm)	Zeiss 43 set
Leica TCS-SP5	DAPI	Diode (405 nm)	Leica A cube
Leica TCS-SP5	GFP / A488	Multiline argon (458/476/488/496/514 nm)	Leica GFP cube
Leica TCS-SP5	A568	Multiline argon (458/476/488/496/514 nm)	Leica N2.1 cube
Leica TCS-SP5	A647	HeNe (633 nm)	Leica N2.1 cube

Table 6.4. Image acquisition specifications. The laser and filter used in the acquisition of each fluorophore in each microscope are detailed.

6.5 Image and data analysis

6.5.1 Analysis of IBs

Quantification of blots was performed with the FIJI distribution of the ImageJ software (NIH). Briefly, the radiograph films of the IBs were scanned and converted with ImageJ into an 8-bit gray-scale image. Each band was delimited by an area, whose integrated density was measured. The integrated density of a background area was subtracted to that of the band.

6.5.2 Analysis of microscopy images

6.5.2.1 Processing of confocal images

All images were processed and analysed using the FIJI distribution of the ImageJ software (NIH). The histograms of the images were adjusted, the background was substracted and a mild Gauss filter was applied to facilitate quantification and visualisation. Images were

modified equally in all conditions. Analysis was performed on a single z-layer, except for the quantification of cortactin on EEA1 endosomes, in which z-projections were analysed. The data shown is the mean of the values of the individual cells quantified in each condition.

To quantify uptake experiments, the area of each cell was delimited and the mean intensity of Tfn or GFP was measured within the cell. The mean cytosolic background in each cell was subtracted to that value. In the case of recycling experiments, the threshold of the images was adjusted to create a mask in which only endosomal Tfn was included, excluding the cytosolic signal. The mean intensity per cell was measured. In order to quantify the amount of GFP-FYVE, the mean intensity of the whole cell was divided by the mean intensity of the nucleus. The average value of the WT+IN1 condition, which was used as a negative control, was subtracted to the average of each condition. Cortical cortactin was quantified as the mean intensity in a line along the PM of 0.6 µm width. The perinuclear enrichment of EEA1 was determined by the integrated density within a 10 µm diameter circle in the perinuclear region divided by the integrated density of the whole cell, minus the background intensity in the coverslip. To quantify the amount of EEA1 per cell, the area of each cell was delimited and the integrated density of EEA1 was measured within the cell. The mean signal form the coverslip in each condition was taken as background and subtracted to the EEA1 value.

Finally, a semi-automated macro for ImageJ was developed by E. Rebollo and used to measure the amount of endosomal cortactin in relation to the amount of EEA1. Briefly, areas of 70 um diameter were selected in a z-projected image. The macro identified EEA1 endosomes and those cortactin patches that were in contact with them in a manually thresholded image. The ratio between the integrated densities of cortactin around the endosome and the EEA1 in it was calculated.

6.5.2.2 Analysis of migration and cell division assays

Images of living cells were taken as described in 6.4.1. Only isolated cells were taken into account. Cells were tracked along their migratory path using the Fiji plugin MTrackJ to obtain the position of the cell for every time point. The data was transferred to Microsoft Excel and further analysed with the program DiPer (Gorelik and Gautreau 2014), which calculates cell speed, directionality ratio and the direction autocorrelation. It also gives an arbitrary common starting point to all cell tracks and plots them in one graph per condition. The duration of late telophase and cytokinesis during cell division was measured from the moment daughter cells attach to the substrate until they completely detach from each other.

6.5.3 Data presentation and statistics

The data acquired with ImageJ were analysed in Microsoft Excel and the graphs designed in Graphpad Prism. The figures in this thesis were assembled in Microsoft Power Point.

Prism was also used for statistics. The D'Agostino-Pearson test was applied to data sets to assess normality. If the data followed a normal distribution or the result of the normality test was not significant, an unpaired two-tailed t test was performed to assess significance. If the distribution was not normal, a two-tailed Mann-Whitney test was used. A difference with a p value of 0.05 or less was considered significant.

6.6 Antibodies

The antibodies used in this thesis are listed in **Table 6.5**, together with their specifications.

Antigen	Host	Source, reference	IB dilution	IF dilution
Kazrin Nt (aa1-147)	Rabbit	EMBL Heidelberg	1:6,000	-
Kazrin Ct (aa148-327)	Rabbit	EMBL Heidelberg	1:8,000	-
Kazrin	Mouse	Abcam 88752	1:500	-
GFP	Mouse	Living Colors 632380	1:1,000	-
GST	Goat	Amersham 27-57701	1:2,000	-
EEA1	Rabbit	Cell Signaling 3288	1:1,000	1:100
EHD1	Rabbit	Abcam 109311	1:200	1:100
GM130	Mouse	BD 610822	1:100	-
Rab4	Mouse	BD 610888	1:200	-
Rab11	Mouse	BD 610656	1:500	1:20
Rabaptin 5	Mouse	BD 610676	1:1,000	-
CHC	Mouse	BD 610499	1:1,000	-
GGA2	Mouse	BD 612612	1:100	
α-adaptin	Mouse	BD 610501	1:100	
γ-adaptin	Mouse	BD 610386	1:5,000	1:500
N-cadherin	Mouse	BD 51-9001943	1:1,000	1:1,000
E-cadherin	Mouse	BD 610181	-	1:1,000
β-catenin	Mouse	BD 610153	-	1:1,000
p120-catenin	Mouse	BD 51-9002040	-	1:1,000
ARVCF-catenin	Mouse	Santa Cruz 23874	-	1:1,000
Desmoglein	Mouse	BD 51-9001952	-	1:1,000
VPS35	Mouse	Santa Cruz 374372	1:500	-
PCM-1	Rabbit	Cell Signaling 5213	-	1:200
Pericentrin	Rabbit	Abcam 4448	-	1:1,000
p150-glued	Mouse	BD 610473	1:1,000	-
Kinesin-1 heavy chain	Mouse	Santa Cruz 133184	1:1,000	-
Tubulin	Mouse	Sigma-Aldrich T-6557	1:1,000	-
VPS34	Rabbit	Cell Signaling 4263	1:1,000	-

Antigen	Host	Source, reference	IB dilution	IF dilution
VPS15	Rabbit	Abcam 124817	1:1,000	-
Beclin	Rabbit	Cell Signaling 3738	1:1,000	-
UVRAG	Mouse	MBL M160-3	1:1,000	-
N-WASP	Rabbit	Santa Cruz 20770	1:100	-
WASH	Rabbit	A. Gautreu (Derivery et al. 2009)	1:100	-
Fam21	Rabbit	Millipore ABT79	1:1,000	-
Cortactin	Mouse	Millipore 05-180	1:1,000	1:100
Rabbit IgG (HRP)	Goat	Sigma-Aldrich A0545	1:8,000	-
Mouse IgG (HRP)	Goat	Sigma-Aldrich A2554	1:4,000	-
Goat IgG (HRP)	Rabbit	Sigma-Aldrich A4174	1:2,000	-
Mouse IgG (A568)	Donkey	Thermo Fisher A11037	-	1:2,000
Rabbit IgG (A488)	Donkey	Thermo Fisher A21206	-	1:2,000
Rabbit IgG (A568)	Goat	Thermo Fisher A11036	-	1:2,000
Rabbit IgG (A647)	Goat	Thermo Fisher A21245	-	1:2,000

Table 6.5. Antibodies. This table shows the antigen of each antibody used in this study, along with the host animal in which it was produced, the source (laboratory or brand of production), the dilution used in immunoblot (IB) experiments and the dilution used in immunofluorescence (IF) experiments.

References

- Ahmed, S. M., Nishida-Fukuda, H., Li, Y., McDonald, W. H., Gradinaru, C. C., & Macara, I. G. (2018). Exocyst dynamics during vesicle tethering and fusion. Nature Communications. https://doi.org/10.1038/s41467-018-07467-5
- Alberts, B., Johnson, A., Lewis, J., Raff, M., Roberts, K., & Walter, P. (2019). Cell Junctions, Cell Adhesion, and the Extracellular Matrix. In Molecular Biology of the Cell (pp. 1131–1204). Garland Science. https://doi.org/10.1201/9780203833445-19
- Albertson, R., Riggs, B., & Sullivan, W. (2005). Membrane traffic: A driving force in cytokinesis. Trends in Cell Biology. article. https://doi.org/10.1016/j.tcb.2004.12.008
- Alekhina, O., Burstein, E., & Billadeau, D. D. (2017). Cellular functions of WASP family proteins at a glance. Journal of Cell Science, 130(14), 2235–2241. https://doi.org/10.1242/jcs.199570
- Allaire, P. D., Sadr, M. S., Chaineau, M., Sadr, E. S., Konefal, S., Fotouhi, M., … McPherson, P. S. (2013). Interplay between Rab35 and Arf6 controls cargo recycling to coordinate cell adhesion and migration. Journal of Cell Science, 126(3), 722–731. https://doi.org/10.1242/jcs.112375
- Allgood, S., & Neunuebel, M. (2018). The recycling endosome and bacterial pathogens. Cell Microbilogy, 176(1), 139–148. https://doi.org/10.1016/j.physbeh.2017.03.040
- Almeida, C. G., Yamada, A., Tenza, D., Louvard, D., Raposo, G., & Coudrier, E. (2011). Myosin 1b promotes the formation of post-Golgi carriers by regulating actin assembly and membrane remodelling at the trans-Golgi network. Nature Cell Biology, 13(7). https://doi.org/10.1038/ncb2262
- Andres, D. A., Seabra, M. C., Brown, M. S., Armstrong, S. A., Smeland, T. E., Cremers, F. P. M., & Goldstein, J. L. (1993). cDNA cloning of component A of Rab geranylgeranyl transferase and demonstration of its role as a Rab escort protein. Cell. https://doi.org/10.1016/0092-8674(93)90639-8
- Antonny, B., Burd, C., De Camilli, P., Chen, E., Daumke, O., Faelber, K., … Schmid, S. (2016). Membrane fission by dynamin: what we know and what we need to know. The EMBO Journal, 35(21), 2270–2284. https://doi.org/10.15252/embj.201694613
- Arighi, C. N., Harmell, L. M., Aguilar, R. C., Haft, C. R., & Bonifacino, J. S. (2004). Role of the mammalian retromer in sorting of the cation-independent mannose 6-phosphate receptor. Journal of Cell Biology, 165(1), 123–133. https://doi.org/10.1083/jcb.200312055
- Arjonen, A., Alanko, J., Veltel, S., & Ivaska, J. (2012). Distinct Recycling of Active and Inactive b1 Integrins. Traffic, 13(4), 610–625. https://doi.org/10.1111/j.1600-0854.2012.01327.x
- Austin, C. D., De Mazière, A. M., Pisacane, P. I., Van Dijk, S. M., Eigenbrot, C., Sliwkowski, M. X., … Scheller, R. H. (2004). Endocytosis and sorting of ErbB2 and the site of action of cancer therapeutics trastuzumab and geldanamycin. Molecular Biology of the Cell, 15(12), 5268–5282. https://doi.org/10.1091/mbc.E04-07-0591
- Bachir, A. I., Horwitz, A. R., Nelson, W. J., & Bianchini, J. M. (2017). Actin-based adhesion modules mediate cell interactions with the extracellular matrix and neighboring cells. Cold Spring Harbor Perspectives in Biology, 9(7). https://doi.org/10.1101/cshperspect.a023234

- Backer, J. M. (2016). The intricate regulation and complex functions of the Class III phosphoinositide 3-kinase Vps34. Biochemical Journal, 473(15), 2251–2271. https://doi.org/10.1042/bcj20160170
- Bago, R., Malik, N., Munson, M. J., Prescott, A. R., Davies, P., Sommer, E., … Alessi, D. R. (2014). Characterization of VPS34-IN1, a selective inhibitor of Vps34, reveals that the phosphatidylinositol 3-phosphate-binding SGK3 protein kinase is a downstream target of class III phosphoinositide 3-kinase. Biochemical Journal, 463(3), 413–427. https://doi.org/10.1042/BJ20140889
- Bahl, K., Xie, S., Spagnol, G., Sorgen, P., Naslavsky, N., & Caplan, S. (2016). EHD3 protein is required for tubular recycling endosome stabilization, and an asparagine-glutamic acid residue pair within its Eps15 Homology (EH) domain dictates its selective binding to NPF peptides. Journal of Biological Chemistry. https://doi.org/10.1074/jbc.M116.716407
- Balderhaar, H. J. K., Arlt, H., Ostrowicz, C., Bröcker, C., Sündermann, F., Brandt, R., … Ungermann, C. (2010). The Rab GTPase Ypt7 is linked to retromer-mediated receptor recycling and fusion at the yeast late endosome. Journal of Cell Science. https://doi.org/10.1242/jcs.071977
- Barr, F. A. (2013). Rab GTPases and membrane identity: Causal or inconsequential? Journal of Cell Biology, 202(2), 191–199. https://doi.org/10.1083/jcb.201306010
- Bartles, J. R. (2000). Parallel actin bundles and their multiple actin-bundling proteins. Current Opinion in Cell Biology. https://doi.org/10.1016/S0955-0674(99)00059-9
- Beacham, G. M., Partlow, E. A., & Hollopeter, G. (2019). Conformational regulation of AP1 and AP2 clathrin adaptor complexes. Traffic, 20(10), 741–751. https://doi.org/10.1111/tra.12677
- Behnia, R., & Munro, S. (2005). Organelle identity and the signposts for membrane traffic. Nature. https://doi.org/10.1038/nature04397
- Beltzner, C. C., & Pollard, T. D. (2004). Identification of Functionally Important Residues of Arp2/3 Complex by Analysis of Homology Models from Diverse Species. Journal of Molecular Biology. https://doi.org/10.1016/j.jmb.2003.12.017
- Benesch, S., Lommel, S., Steffen, A., Stradal, T. E. B., Scaplehorn, N., Way, M., … Rottner, K. (2002). Phosphatidylinositol 4,5-biphosphate (PIP2)-induced vesicle movement depends on N-WASP and involves Nck, WIP, and Grb2. Journal of Biological Chemistry, 277(40), 37771–37776. https://doi.org/10.1074/jbc.M204145200
- Benesch, S., Polo, S., Lai, F. P., Anderson, K. I., Stradal, T. E. B., Wehland, J., & Rottner, K. (2005). N-WASP deficiency impairs EGF internalization and actin assembly at clathrin-coated pits. Journal of Cell Science, 118(14), 3103–3115. https://doi.org/10.1242/jcs.02444
- Benmerah, A., Bayrou, M., Cerf-Bensussan, N., & Dautry-Varsat, A. (1999). Inhibition of clathrin-coated pit assembly by an Eps15 mutant. Journal of Cell Science, 112(9), 1303–1311.

- Blackburn, J. B., D'Souza, Z., & Lupashin, V. V. (2019). Maintaining order: COG complex controls Golgi trafficking, processing, and sorting. FEBS Letters. https://doi.org/10.1002/1873-3468.13570
- Boczonadi, V., & Määttä, A. (2016). Functional Analysis of Periplakin and Envoplakin, Cytoskeletal Linkers, and Cornified Envelope Precursor Proteins. Methods in Enzymology (1st ed., Vol. 569). Elsevier Inc. https://doi.org/10.1016/bs.mie.2015.06.019
- Boguslavsky, S., Grosheva, I., Landau, E., Shtutman, M., Cohen, M., Arnold, K., … Bershadsky, A. (2007). p120 catenin regulates lamellipodial dynamics and cell adhesion in cooperation with cortactin. Proceedings of the National Academy of Sciences of the United States of America, 104(26). https://doi.org/10.1073/pnas.0702731104
- Bonazzi, M., Kühbacher, A., Toledo-Arana, A., Mallet, A., Vasudevan, L., Pizarro-Cerda, J., … Cossart, P. (2012). A common clathrin-mediated machinery co-ordinates cell-cell adhesion and bacterial internalization. Traffic. https://doi.org/10.1111/tra.12009
- Bonifacino, J. S., & Glick, B. S. (2004, January 23). The Mechanisms of Vesicle Budding and Fusion. Cell. Elsevier. https://doi.org/10.1016/S0092-8674(03)01079-1
- Bonifacino, J. S., & Neefjes, J. (2017). Moving and positioning the endolysosomal system. Current Opinion in Cell Biology, 47, 1–8. https://doi.org/10.1016/j.ceb.2017.01.008
- Boucrot, E., & Kirchhausen, T. (2007). Endosomal recycling controls plasma membrane area during mitosis. Proceedings of the National Academy of Sciences of the United States of America, 104(19), 7939–7944. https://doi.org/10.1073/pnas.0702511104
- Boulant, S., Kural, C., Zeeh, J., Ubelmann, F., & Kirchhausen, T. (2011). Actin dynamics counteract membrane tension during clathrin-mediated endocytosis. Nature Cell Biology, 13(9). https://doi.org/10.1038/ncb2307
- Brandstaetter, H., Kishi-Itakura, C., Tumbarello, D. A., Manstein, D. J., & Buss, F. (2014). Loss of functional MYO1C/myosin 1c, a motor protein involved in lipid raft trafficking, disrupts autophagosome-lysosome fusion. Autophagy, 10(12). https://doi.org/10.4161/15548627.2014.984272
- Bright, N. A., Gratian, M. J., & Luzio, J. P. (2005). Endocytic delivery to lysosomes mediated by concurrent fusion and kissing events in living cells. Current Biology, 15(4), 360–365. https://doi.org/10.1016/j.cub.2005.01.049
- Brodsky, F. M. (2012). Diversity of Clathrin Function: New Tricks for an Old Protein. Annual Review of Cell and Developmental Biology, 28(1), 309–336. https://doi.org/10.1146/annurev-cellbio-101011-155716
- Bryce, N. S., Clark, E. S., Leysath, J. L., Currie, J. D., Webb, D. J., & Weaver, A. M. (2005). Cortactin promotes cell motility by enhancing lamellipodial persistence. Current Biology, 15(14). https://doi.org/10.1016/j.cub.2005.06.043
- Bu, W., Lim, K. B., Yu, Y. H., Chou, A. M., Sudhaharan, T., & Ahmed, S. (2010). Cdc42 interaction with N-WASP and Toca-1 regulates membrane tubulation, vesicle formation and vesicle motility: Implications for endocytosis. PLoS ONE, 5(8). https://doi.org/10.1371/journal.pone.0012153

- Burd, C., & Cullen, P. J. (2016). Retromer : A Master Conductor of Endosome Sorting. https://doi.org/10.1101/cshperspect.a016774
- Buss, F., Arden, S. D., Lindsay, M., Luzio, J. P., & Kendrick-Jones, J. (2001). Myosin VI isoform localized to clathrin-coated vesicles with a role in clathrin-mediated endocytosis. EMBO Journal, 20(14), 3676–3684. https://doi.org/10.1093/emboj/20.14.3676
- Cadwell, C. M., Su, W., & Kowalczyk, A. P. (2016). Cadherin tales: Regulation of cadherin function by endocytic membrane trafficking. Traffic, 17(12), 1262–1271. https://doi.org/10.1111/tra.12448
- Cai, B., Xie, S., Caplan, S., & Naslavsky, N. (2014). GRAF1 forms a complex with MICAL-L1 and EHD1 to cooperate in tubular recycling endosome vesiculation. Frontiers in Cell and Developmental Biology, 2(May), 1–14. https://doi.org/10.3389/fcell.2014.00022
- Campa, C. C., Margaria, J. P., Derle, A., Del Giudice, M., De Santis, M. C., Gozzelino, L., Hirsch, E. (2018). Rab11 activity and PtdIns(3)P turnover removes recycling cargo from endosomes. Nature Chemical Biology, 14(8), 801–810. https://doi.org/10.1038/s41589-018-0086-4
- Campellone, K., & Welch, M. (2010). A Nucleator Arms Race: Cellular Control of Actin Assembly. Nat Rev Mol Cell Biol (Vol. 23). https://doi.org/10.1038/jid.2014.371
- Cao, C., Backer, J. M., Laporte, J., Bedrick, E. J., & Wandinger-Ness, A. (2008). Sequential actions of myotubularin lipid phosphatases regulate endosomal PI(3)P and growth factor receptor trafficking. Molecular Biology of the Cell, 19(8), 3334–3346. https://doi.org/10.1091/mbc.E08-04-0367
- Cao, H., Weller, S., Orth, J. D., Chen, J., Huang, B., Chen, J. L., … McNiven, M. A. (2005). Actin and Arf1-dependent recruitment of a cortactin-dynamin complex to the Golgi regulates post-Golgi transport. Nature Cell Biology, 7(5). https://doi.org/10.1038/ncb1246
- Caplan, S., Naslavsky, N., Hartnell, L. M., Lodge, R., Polishchuk, R. S., Donaldson, J. G., & Bonifacino, J. S. (2002). A tubular EHD1-containing compartment involved in the recycling of major histocompatibility complex class I molecules to the plasma membrane. EMBO Journal, 21(11), 2557–2567. https://doi.org/10.1093/emboj/21.11.2557
- Carlier, M. F., Nioche, P., Broutin-L'hermite, I., Boujemaa, R., Le Clainche, C., Egile, C., … Pantaloni, D. (2000). GRB2 links signaling to actin assembly by enhancing interaction of neural wiskott-aldrich syndrome protein (N-WASp) with actin-related protein (ARP2/3) complex. Journal of Biological Chemistry. https://doi.org/10.1074/jbc.M000687200
- Caswell, P., & Norman, J. (2008). Endocytic transport of integrins during cell migration and invasion. Trends in Cell Biology, 18(6), 257–263. https://doi.org/10.1016/j.tcb.2008.03.004
- Chánez-Paredes, S., Montoya-García, A., & Schnoor, M. (2019). Cellular and pathophysiological consequences of Arp2/3 complex inhibition: role of inhibitory proteins and pharmacological compounds. Cellular and Molecular Life Sciences, 76(17), 3349–3361. https://doi.org/10.1007/s00018-019-03128-y

- Chapman, E. R., Desai, R. C., Davis, A. F., & Tornehl, C. K. (1998). Delineation of the oligomerization, AP-2 binding, and synprint binding region of the C2B domain of synaptotagmin. Journal of Biological Chemistry, 273(49), 32966–32972. https://doi.org/10.1074/jbc.273.49.32966
- Charras, G., & Yap, A. S. (2018). Tensile Forces and Mechanotransduction at Cell–Cell Junctions. Current Biology. https://doi.org/10.1016/j.cub.2018.02.003
- Chavrier, P., Gorvel, J. P., Stelzer, E., Simons, K., Gruenberg, J., & Zerial, M. (1991). Hypervariable C-termmal domain of rab proteins acts as a targeting signal. Nature. https://doi.org/10.1038/353769a0
- Chavrier, P., Parton, R. G., Hauri, H. P., Simons, K., & Zerial, M. (1990). Localization of low molecular weight GTP binding proteins to exocytic and endocytic compartments. Cell. https://doi.org/10.1016/0092-8674(90)90369-P
- Chen, K. E., Healy, M. D., & Collins, B. M. (2019). Towards a molecular understanding of endosomal trafficking by Retromer and Retriever. Traffic. https://doi.org/10.1111/tra.12649
- Chen, W., Feng, Y., Chen, D., & Wandinger-Ness, A. (1998). Rab11 is required for trans-Golgi network-to-plasma membrane transport and a preferential target for GDP dissociation inhibitor. Molecular Biology of the Cell, 9(11). https://doi.org/10.1091/mbc.9.11.3241
- Cherfils, J. (2014). Arf GTPases and their effectors: Assembling multivalent membrane-binding platforms. Current Opinion in Structural Biology, 29, 67–76. https://doi.org/10.1016/j.sbi.2014.09.007
- Chhatriwala, M. K., Cipolat, S., Sevilla, L. M., Nachat, R., & Watt, F. M. (2012). Exons 5-15 of kazrin are dispensable for murine epidermal morphogenesis and homeostasis. Journal of Investigative Dermatology, 132(8), 1977–1987. https://doi.org/10.1038/jid.2012.110
- Chi, R. J., Liu, J., West, M., Wang, J., Odorizzi, G., & Burd, C. G. (2014). Fission of SNX-BAR-coated endosomal retrograde transport carriers is promoted by the dynamin-related protein Vps1. Journal of Cell Biology, 204(5). https://doi.org/10.1083/jcb.201309084
- Cho, K, Vaught, T. G., Ji, H., Gu, D., Papasakelariou-Yared, C., Horstmann, N., … McCrea, P. D. (2010). Xenopus Kazrin interacts with ARVCF-catenin, spectrin and p190B RhoGAP, and modulates RhoA activity and epithelial integrity. Journal of Cell Science, 123(Pt 23), 4128–4144. https://doi.org/10.1242/jcs.072041
- Cho, K, Lee, M., Gu, D., Munoz, W. A., Ji, H., Kloc, M., & McCrea, P. D. (2011). Kazrin, and its binding partners ARVCF- and delta-catenin, are required for Xenopus laevis craniofacial development. Developmental Dynamics, 240(12), 2601–2612. https://doi.org/10.1002/dvdy.22721
- Christoforidis, S., McBride, H. M., Burgoyne, R. D., & Zerial, M. (1999). The rab5 effector EEA1 is a core component of endosome docking. Nature, 397(6720). https://doi.org/10.1038/17618
- Collins, A., Warrington, A., Taylor, K. A., & Svitkina, T. (2011). Structural organization of the actin cytoskeleton at sites of clathrin-mediated endocytosis. Current Biology. https://doi.org/10.1016/j.cub.2011.05.048

- Cong, L., Ran, F. A., Cox, D., Lin, S., Barretto, R., Habib, N., … Zhang, F. (2013). Multiplex genome engineering using CRISPR/Cas systems. Science, 339(6121), 819–823. https://doi.org/10.1126/science.1231143
- Cui, Y., Carosi, J. M., Yang, Z., Ariotti, N., Kerr, M. C., Parton, R. G., … Teasdale, R. D. (2019). Retromer has a selective function in cargo sorting via endosome transport carriers. Journal of Cell Biology. https://doi.org/10.1083/jcb.201806153
- Cullen, P. J., & Steinberg, F. (2018). To degrade or not to degrade: mechanisms and significance of endocytic recycling. Nature Reviews Molecular Cell Biology, 19(11), 679–696. https://doi.org/10.1038/s41580-018-0053-7
- Cureton, D. K., Massol, R. H., Whelan, S. P. J., & Kirchhausen, T. (2010). The length of vesicular stomatitis virus particles dictates a need for actin assembly during clathrin-dependent endocytosis. PLoS Pathogens, 6(9). https://doi.org/10.1371/journal.ppat.1001127
- D'Angelo, G., Vicinanza, M., Di Campli, A., & De Matteis, M. A. (2008). The multiple roles of PtdIns(4)P - Not just the precursor of PtdIns(4,5)P2. Journal of Cell Science. https://doi.org/10.1242/jcs.023630
- D'Souza, R. S., Semus, R., Billings, E. A., Meyer, C. B., Conger, K., & Casanova, J. E. (2014). Rab4 orchestrates a small GTPase cascade for recruitment of adaptor proteins to early endosomes. Current Biology, 24(11), 1187–1198. https://doi.org/10.1016/j.cub.2014.04.003
- Daboussi, L., Costaguta, G., & Payne, G. S. (2012). Phosphoinositide-mediated clathrin adaptor progression at the trans-Golgi network. Nature Cell Biology, 14(3), 239–248. https://doi.org/10.1038/ncb2427
- Dai, J., Li, J., Bos, E., Porcionatto, M., Premont, R. T., Bourgoin, S., … Hsu, V. W. (2004). ACAP1 promotes endocytic recycling by recognizing recycling sorting signals. Developmental Cell. https://doi.org/10.1016/j.devcel.2004.10.002
- Dambournet, D., MacHicoane, M., Chesneau, L., Sachse, M., Rocancourt, M., El Marjou, A., Echard, A. (2011). Rab35 GTPase and OCRL phosphatase remodel lipids and F-actin for successful cytokinesis. Nature Cell Biology. https://doi.org/10.1038/ncb2279
- Dammermann, A., & Merdes, A. (2002). Assembly of centrosomal proteins and microtubule organization depends on PCM-1. Journal of Cell Biology, 159(2), 255–266. https://doi.org/10.1083/jcb.200204023
- Danielsson, K., Ebrahimi, M., Nylander, E., Wahlin, Y. B., & Nylander, K. (2017). Alterations in factors involved in differentiation and barrier function in the epithelium in oral and genital lichen planus. Acta Dermato-Venereologica, 97(2), 214–218. https://doi.org/10.2340/00015555-2533
- Danson, C., Brown, E., Hemmings, O. J., McGough, I. J., Yarwood, S., Heesom, K. J., … Cullen, P. J. (2013). SNX15 links clathrin endocytosis to the PtdIns3P early endosome independently of the APPL1 endosome. Journal of Cell Science, 126(21). https://doi.org/10.1242/jcs.125732

- Dart, A. E., Donnelly, S. K., Holden, D. W., Way, M., & Caron, E. (2012). Nck and Cdc42 co-operate to recruit N-WASP to promote FcγR-mediated phagocytosis. Journal of Cell Science, 125(12), 2825–2830. https://doi.org/10.1242/jcs.106583
- Daste, F., Walrant, A., Holst, M. R., Gadsby, J. R., Mason, J., Lee, J. E., … Gallop, J. L. (2017). Control of actin polymerization via the coincidence of phosphoinositides and high membrane curvature. Journal of Cell Biology, 216(11), 3745–3765. https://doi.org/10.1083/jcb.201704061
- Daumke, O., Lundmark, R., Vallis, Y., Martens, S., Butler, P. J. G., & McMahon, H. T. (2007). Architectural and mechanistic insights into an EHD ATPase involved in membrane remodelling. Nature. https://doi.org/10.1038/nature06173
- Davis, M. A., Ireton, R. C., & Reynolds, A. B. (2003). A core function for p120-catenin in cadherin turnover. Journal of Cell Biology, 163(3). https://doi.org/10.1083/jcb.200307111
- De Craene, J. O., Bertazzi, D. L., Bär, S., & Friant, S. (2017). Phosphoinositides, major actors in membrane trafficking and lipid signaling pathways. International Journal of Molecular Sciences, 18(3). https://doi.org/10.3390/ijms18030634
- De Graaf, P., Zwart, W. T., Van Dijken, R. A. J., Deneka, M., Schulz, T. K. F., Geijsen, N., Van Bergen En Henegouwen, P. M. P. (2004). Phosphatidylinositol 4-Kinaseβ Is Critical for Functional Association of rab11 with the Golgi Complex. Molecular Biology of the Cell, 15(4). https://doi.org/10.1091/mbc.E03-12-0862
- De Luca, M., Cogli, L., Progida, C., Nisi, V., Pascolutti, R., Sigismund, S., Bucci, C. (2014). RILP regulates vacuolar ATPase through interaction with the V1G1 subunit. Journal of Cell Science, 127(12), 2697–2708. https://doi.org/10.1242/jcs.142604
- Del Conte-Zerial, P., Brusch, L., Rink, J. C., Collinet, C., Kalaidzidis, Y., Zerial, M., & Deutsch, A. (2008). Membrane identity and GTPase cascades regulated by toggle and cut-out switches. Molecular Systems Biology, 4(206), 1–9. https://doi.org/10.1038/msb.2008.45
- Delevoye, C., Heiligenstein, X., Ripoll, L., Gilles-Marsens, F., Dennis, M. K., Linares, R. A., Raposo, G. (2016). BLOC-1 Brings Together the Actin and Microtubule Cytoskeletons to Generate Recycling Endosomes. Current Biology. https://doi.org/10.1016/j.cub.2015.11.020
- Delevoye, C., Miserey-Lenkei, S., Montagnac, G., Gilles-Marsens, F., Paul-Gilloteaux, P., Giordano, F., … Raposo, G. (2014). Recycling endosome tubule morphogenesis from sorting endosomes requires the kinesin motor KIF13A. Cell Reports, 6(3), 445–454. https://doi.org/10.1016/j.celrep.2014.01.002
- Delgehyr, N., Sillibourne, J., & Bornens, M. (2005). Microtubule nucleation and anchoring at the centrosome are independent processes linked by ninein function. Journal of Cell Science, 118(8). https://doi.org/10.1242/jcs.02302
- Delva, E., Jennings, J. M., Calkins, C. C., Kottke, M. D., Faundez, V., & Kowalczyk, A. P. (2008). Pemphigus vulgaris IgG-induced desmoglein-3 endocytosis and desmosomal disassembly are mediated by a clathrin- and dynamin-independent mechanism. Journal of Biological Chemistry, 283(26). https://doi.org/10.1074/jbc.M710046200

- Deneka, M., Neeft, M., Popa, I., Van Oort, M., Sprong, H., Oorschot, V., … Van der Sluijs, P. (2003). Rabaptin-5α/rabaptin-4 serves as a linker between rab4 and γ1-adaptin in membrane recycling from endosomes. EMBO Journal. https://doi.org/10.1093/emboj/cdg257
- Dengjel, J., Schoor, O., Fischer, R., Reich, M., Kraus, M., Müller, M., … Stevanovic, S. (2005). Autophagy promotes MHC class II presentation of peptides from intracellular source proteins. Proceedings of the National Academy of Sciences of the United States of America. https://doi.org/10.1073/pnas.0501190102
- Derivery, E., Sousa, C., Gautier, J. J., Lombard, B., Loew, D., & Gautreau, A. (2009). The Arp2/3 Activator WASH Controls the Fission of Endosomes through a Large Multiprotein Complex. Developmental Cell, 17(5), 712–723. https://doi.org/10.1016/j.devcel.2009.09.010
- Desclozeaux, M., Venturato, J., Wylie, F. G., Kay, J. G., Joseph, S. R., Le, H. T., & Stow, J. L. (2008). Active Rab11 and functional recycling endosome are required for E-cadherin trafficking and lumen formation during epithelial morphogenesis. American Journal of Physiology. Cell Physiology, 295(2), C545–C556. https://doi.org/10.1152/ajpcell.00097.2008
- Devereaux, K., Dall'Armi, C., Alcazar-Roman, A., Ogasawara, Y., Zhou, X., Wang, F., Di Paolo, G. (2013). Regulation of Mammalian Autophagy by Class II and III PI 3-Kinases through PI3P Synthesis. PLoS ONE, 8(10). https://doi.org/10.1371/journal.pone.0076405
- Di Fiore, P. P., & Zastrow, M. Von. (2014). Endocytosis, Signaling, and Beyond. Cold Spring Harbor Perspect Biol.
- Dionne, L. K., Wang, X. J., & Prekeris, R. (2015). Midbody: From cellular junk to regulator of cell polarity and cell fate. Current Opinion in Cell Biology. https://doi.org/10.1016/j.ceb.2015.04.010
- Donaldson, J. G., & Jackson, C. L. (2011). ARF family G proteins and their regulators: roles in membrane transport, development and disease. Nature Reviews Molecular Cell Biology, 12(6), 362–375. https://doi.org/10.1038/nrm3117
- Doray, B., Lee, I., Knisely, J., Bu, G., & Kornfeld, S. (2007). The γ/σ1 and α/σ2 hemicomplexes of clathrin adaptors AP-1 and AP-2 Harbor the dileucine recognition site. Molecular Biology of the Cell. https://doi.org/10.1091/mbc.E07-01-0012
- Dozynkiewicz, M. A., Jamieson, N. B., Macpherson, I., Grindlay, J., van den Berghe, P. V. E., von Thun, A., Norman, J. C. (2012). Rab25 and CLIC3 collaborate to promote integrin recycling from late endosomes/lysosomes and drive cancer progression. Developmental Cell, 22(1), 131–145. https://doi.org/10.1016/j.devcel.2011.11.008
- Dugina, V., Zwaenepoel, I., Gabbiani, G., Clément, S., & Chaponnier, C. (2009). β- and γ-cytoplasmic actins display distinct distribution and functional diversity. Journal of Cell Science. https://doi.org/10.1242/jcs.041970

- Dyve, A. B., Bergan, J., Utskarpen, A., & Sandvig, K. (2009). Sorting nexin 8 regulates endosome-to-Golgi transport. Biochemical and Biophysical Research Communications, 390(1), 109–114. https://doi.org/10.1016/j.bbrc.2009.09.076
- Eichel, K., & von Zastrow, M. (2018). Subcellular Organization of GPCR Signaling. Trends in Pharmacological Sciences. https://doi.org/10.1016/j.tips.2017.11.009
- Engqvist-Goldstein, Å. E. Y., Warren, R. A., Kessels, M. M., Keen, J. H., Heuser, J., & Drubin, D. G. (2001). The actin-binding protein Hip1R associates with clathrin during early stages of endocytosis and promotes clathrin assembly in vitro. Journal of Cell Biology, 154(6). https://doi.org/10.1083/jcb.200106089
- Fan, J., Hu, Z., Zeng, L., Lu, W., Tang, X., Zhang, J., & Li, T. (2008). Golgi apparatus and neurodegenerative diseases. International Journal of Developmental Neuroscience. https://doi.org/10.1016/j.ijdevneu.2008.05.006
- Farina, F., Gaillard, J., Guérin, C., Couté, Y., Sillibourne, J., Blanchoin, L., & Théry, M. (2016). The centrosome is an actin-organizing centre. Nature Cell Biology, 18(1), 65–75. https://doi.org/10.1038/ncb3285
- Ferguson, J. P., Huber, S. D., Willy, N. M., Aygün, E., Goker, S., Atabey, T., & Kural, C. (2017). Mechanoregulation of clathrin-mediated endocytosis. Journal of Cell Science, 130(21). https://doi.org/10.1242/jcs.205930
- Ferguson, S., Raimondi, A., Paradise, S., Shen, H., Mesaki, K., Ferguson, A., … De Camilli, P. (2009). Coordinated Actions of Actin and BAR Proteins Upstream of Dynamin at Endocytic Clathrin-Coated Pits. Developmental Cell, 17(6). https://doi.org/10.1016/j.devcel.2009.11.005
- Fili, N., & Toseland, C. P. (2020). Unconventional myosins: How regulation meets function. International Journal of Molecular Sciences, 21(1), 1–25. https://doi.org/10.3390/ijms21010067
- Ford, M. G. J., & Chappie, J. S. (2019). The structural biology of the dynamin-related proteins: New insights into a diverse, multitalented family. Traffic, 20(10), 717–740. https://doi.org/10.1111/tra.12676
- Fotin, A., Cheng, Y., Sliz, P., Grigorieff, N., Harrison, S. C., Kirchhausen, T., & Walz, T. (2004). Molecular model for a complete clathrin lattice from electron cryomicroscopy. Nature. https://doi.org/10.1038/nature03079
- Frankel, E. B., & Audhya, A. (2018). ESCRT-dependent cargo sorting at multivesicular endosomes. Seminars in Cell and Developmental Biology. https://doi.org/10.1016/j.semcdb.2017.08.020
- Frémont, Stéphane, & Echard, A. (2018, April 23). Membrane Traffic in the Late Steps of Cytokinesis. Current Biology. Cell Press. https://doi.org/10.1016/j.cub.2018.01.019
- Frémont, Stephane, Hammich, H., Bai, J., Wioland, H., Klinkert, K., Rocancourt, M., … Echard, A. (2017). Oxidation of F-actin controls the terminal steps of cytokinesis. Nature Communications. https://doi.org/10.1038/ncomms14528

– Fried, S., Reicher, B., Pauker, M. H., Eliyahu, S., Matalon, O., Noy, E., … Barda-Saad, M. (2014). Triple-color FRET analysis reveals conformational changes in the WIP-WASp actin-regulating complex. Science Signaling. https://doi.org/10.1126/scisignal.2005198

– Frittoli, E., Palamidessi, A., Marighetti, P., Confalonieri, S., Bianchi, F., Malinverno, C., … Scita, G. (2014). A RAB5/RAB4 recycling circuitry induces a proteolytic invasive program and promotes tumor dissemination. Journal of Cell Biology, 206(2), 307–328. https://doi.org/10.1083/jcb.201403127

– Fujii, S., Kurokawa, K., Inaba, R., Hiramatsu, N., Tago, T., Nakamura, Y., … Satoh, A. K. (2020). Recycling endosomes attach to the trans-side of Golgi stacks in Drosophila and mammalian cells. Journal of Cell Science, 133(4). https://doi.org/10.1242/jcs.236935

– Fujiwara, I., Vavylonis, D., & Pollard, T. D. (2007). Polymerization kinetics of ADP- and ADP-Pi-actin determined by fluorescence microscopy. Proceedings of the National Academy of Sciences of the United States of America. https://doi.org/10.1073/pnas.0702510104

– Funato, K., Riezman, H., & Muñiz, M. (2020). Vesicular and non-vesicular lipid export from the ER to the secretory pathway. Biochimica et Biophysica Acta - Molecular and Cell Biology of Lipids. https://doi.org/10.1016/j.bbalip.2019.04.013

– Gaidarov, I., & Keen, J. H. (1999). Phosphoinositide-AP-2 interactions required for targeting to plasma membrane clathrin-coated pits. Journal of Cell Biology, 146(4), 755–764. https://doi.org/10.1083/jcb.146.4.755

– Gallicano, G. I., Foshay, K., Pengetnze, Y., & Zhou, X. (2005). Dynamics and unexpected localization of the plakin binding protein, kazrin, in mouse eggs and early embryos. Developmental Dynamics, 234(1), 201–214. https://doi.org/10.1002/dvdy.20519

– Gallon, M., Clairfeuille, T., Steinberg, F., Mas, C., Ghai, R., Sessions, R. B., … Cullen, P. J. (2014). A unique PDZ domain and arrestin-like fold interaction reveals mechanistic details of endocytic recycling by SNX27-retromer. Proceedings of the National Academy of Sciences of the United States of America. https://doi.org/10.1073/pnas.1410552111

– Gallon, M., & Cullen, P. J. (2015). Retromer and sorting nexins in endosomal sorting. Biochemical Society Transactions, 43(1), 33–47. https://doi.org/10.1042/BST20140290

– Garnham, C. P., & Roll-Mecak, A. (2012). The chemical complexity of cellular microtubules: Tubulin post-translational modification enzymes and their roles in tuning microtubule functions. Cytoskeleton. https://doi.org/10.1002/cm.21027

– Gatta, A. T., & Carlton, J. G. (2019). The ESCRT-machinery: closing holes and expanding roles. Current Opinion in Cell Biology, 59, 121–132. https://doi.org/10.1016/j.ceb.2019.04.005

– Gautreau, A., Oguievetskaia, K., & Ungermann, C. (2014). Function and regulation of the endosomal fusion and fission machineries. Cold Spring Harbor Perspectives in Biology, 6(3), 24591520. https://doi.org/10.1101/cshperspect.a016832.Function

– Ge, X., Frank, C. L., Calderon de Anda, F., & Tsai, L. H. (2010). Hook3 Interacts with PCM1 to Regulate Pericentriolar Material Assembly and the Timing of Neurogenesis. Neuron, 65(2). https://doi.org/10.1016/j.neuron.2010.01.011

- Geli, M.I., Wesp, A., & Riezman, H. (1998). Distinct functions of calmodulin are required for the uptake step of receptor-mediated endocytosis in yeast: The type I myosin Myo5p is one of the calmodulin targets. EMBO Journal, 17(3), 635–647. https://doi.org/10.1093/emboj/17.3.635
- Geli, M.I. (2000). An intact SH3 domain is required for myosin I-induced actin polymerization. The EMBO Journal, 19(16). https://doi.org/10.1093/emboj/19.16.4281
- Geuze, H. J., Slot, J. W., Strous, G. J. A. M., Lodish, H. F., & Schwartz, A. L. (1983). Intracellular site of asialoglycoprotein receptor-ligand uncoupling: Double-label immunoelectron microscopy during receptor-mediated endocytosis. Cell, 32(1), 277–287. https://doi.org/10.1016/0092-8674(83)90518-4
- Gilleron, J., Gerdes, J. M., & Zeigerer, A. (2019). Metabolic regulation through the endosomal system. Traffic. https://doi.org/10.1111/tra.12670
- Gillingham, A. K., & Munro, S. (2003). Long coiled-coil proteins and membrane traffic. Biochimica et Biophysica Acta - Molecular Cell Research, 1641(2–3), 71–85. https://doi.org/10.1016/S0167-4889(03)00088-0
- Girao, H., Geli, M.I., & Idrissi, F.Z. (2008). Actin in the endocytic pathway: from yeast to mammals. FEBS Letters, 582(14), 2112–2119. https://doi.org/10.1016/j.febslet.2008.04.011
- Golemis, E. A., Serebriiskii, I., Finley, R. L., Kolonin, M. G., Gyuris, J., & Brent, R. (2011). Interaction Trap/Two-hybrid system to identify interacting proteins. Current Protocols in Neuroscience. https://doi.org/10.1002/0471142301.ns0404s55
- Goley, E. D., Rodenbusch, S. E., Martin, A. C., & Welch, M. D. (2004). Critical conformational changes in the Arp2/3 complex are induced by nucleotide and nucleation promoting factor. Molecular Cell. https://doi.org/10.1016/j.molcel.2004.09.018
- Gomez, & Billadeau, D. (2009a). A FAM21-containing WASH complex regulates retromer-dependent sorting. Developmental Cell, 17(5), 699–711. https://doi.org/10.1016/j.devcel.2009.09.009
- Gomez, T. S., & Billadeau, D. D. (2009b). A FAM21-Containing WASH Complex Regulates Retromer-Dependent Sorting. Developmental Cell, 17(5), 699–711. https://doi.org/10.1016/j.devcel.2009.09.009
- González-Jamett, A. M., Guerra, M. J., Olivares, M. J., Haro-Acuña, V., Baéz-Matus, X., Vásquez-Navarrete, J., … Cárdenas, A. M. (2017). The F-actin binding protein cortactin regulates the dynamics of the exocytotic fusion pore through its SH3 domain. Frontiers in Cellular Neuroscience, 11. https://doi.org/10.3389/fncel.2017.00130
- Gooding, J. M., Yap, K. L., & Ikura, M. (2004). The cadherin-catenin complex as a focal point of cell adhesion and signalling: New insights from three-dimensional structures. BioEssays, 26(5), 497–511. https://doi.org/10.1002/bies.20033
- Goodson, H. V, & Jonasson, E. M. (2018). Microtubules and Microtubule-Associated Proteins. Cold Spring Harbor Perspect Biol.

- Gorelik, R., & Gautreau, A. (2014). Quantitative and unbiased analysis of directional persistence in cell migration. Nature Protocols, 9(8), 1931–1943. https://doi.org/10.1038/nprot.2014.131
- Gorelik, R., & Gautreau, A. (2015). The Arp2/3 inhibitory protein arpin induces cell turning by pausing cell migration. Cytoskeleton, 72(7), 362–371. https://doi.org/10.1002/cm.21233
- Grant, B. D., & Donaldson, J. G. (2009). Pathways and mechanisms of endocytic recycling. Nature Reviews Molecular Cell Biology, 10(9), 597–608. https://doi.org/10.1038/nrm2755
- Green, K. J., & Simpson, C. L. (2007). Desmosomes: New perspectives on a classic. Journal of Investigative Dermatology. https://doi.org/10.1038/sj.jid.5701015
- Groot, K. R., Sevilla, L. M., Nishi, K., DiColandrea, T., & Watt, F. M. (2004). Kazrin, a novel periplakin-interacting protein associated with desmosomes and the keratinocyte plasma membrane. The Journal of Cell Biology, 166(5), 653–659. https://doi.org/10.1083/jcb.200312123
- Gruenberg, J., & Van Der Goot, F. G. (2006). Mechanisms of pathogen entry through the endosomal compartments. Nature Reviews Molecular Cell Biology. https://doi.org/10.1038/nrm1959
- Gryaznova, T., Gubar, O., Burdyniuk, M., Kropyvko, S., & Rynditch, A. (2018). WIP/ITSN1 complex is involved in cellular vesicle trafficking and formation of filopodia-like protrusions. Gene, 674(June), 49–56. https://doi.org/10.1016/j.gene.2018.06.078
- Gu, D., Sater, A. K., Ji, H., Cho, K., Clark, M., Stratton, S. A., … McCrea, P. D. (2009). Xenopus δ-catenin is essential in early embryogenesis and is functionally linked to cadherins and small GTPases. Journal of Cell Science, 122(22). https://doi.org/10.1242/jcs.031948
- Guillet, V., Knibiehler, M., Gregory-Pauron, L., Remy, M. H., Chemin, C., Raynaud-Messina, B., … Mourey, L. (2011). Crystal structure of γ-tubulin complex protein GCP4 provides insight into microtubule nucleation. Nature Structural and Molecular Biology. https://doi.org/10.1038/nsmb.2083
- Gyuris, J., Golemis, E., Chertkov, H., & Brent, R. (1993). Cdi1, a human G1 and S phase protein phosphatase that associates with Cdk2. Cell, 75(4), 791–803. https://doi.org/10.1016/0092-8674(93)90498-F
- Håberg, K., Lundmark, R., & Carlsson, S. R. (2008). SNX18 is an SNX9 paralog that acts as a membrane tubulator in AP-1-positive endosomal trafficking. Journal of Cell Science. https://doi.org/10.1242/jcs.028530
- Han, S. P., Gambin, Y., Gomez, G. A., Verma, S., Giles, N., Michael, M., … Yap, A. S. (2014). Cortactin scaffolds Arp2/3 and WAVE2 at the epithelial zonula adherens. Journal of Biological Chemistry, 289(11), 7764–7775. https://doi.org/10.1074/jbc.M113.544478
- Hao, M., & Maxfield, F. R. (2000). Characterization of rapid membrane internalization and recycling. Journal of Biological Chemistry, 275(20), 15279–15286. https://doi.org/10.1074/jbc.275.20.15279

- Hao, Y.H., Doyle, J. M., Ramanathan, S., Gomez, T. S., Jia, D., Xu, M., … Potts, P. R. (2013). Regulation of WASH-dependent actin polymerization and protein trafficking by ubiquitination. Cell, 152(5), 1051–1064. https://doi.org/10.1016/j.cell.2013.01.051
- Harayama, T., & Riezman, H. (2018). Understanding the diversity of membrane lipid composition. Nature Reviews Molecular Cell Biology. https://doi.org/10.1038/nrm.2017.138
- Haynes, C., Oldfield, C. J., Ji, F., Klitgord, N., Cusick, M. E., Radivojac, P., … Iakoucheva, L. M. (2006). Intrinsic disorder is a common feature of hub proteins from four eukaryotic interactomes. PLoS Computational Biology, 2(8), 0890–0901. https://doi.org/10.1371/journal.pcbi.0020100
- Helgeson, L. A., & Nolen, B. J. (2013). Mechanism of synergistic activation of Arp2/3 complex by cortactin and N-WASP. ELife. https://doi.org/10.7554/eLife.00884
- Hemalatha, A., & Mayor, S. (2019). Recent advances in clathrin-independent endocytosis. F1000Research. https://doi.org/10.12688/f1000research.16549.1
- Hertzog, M., Van Heijenoort, C., Didry, D., Gaudier, M., Coutant, J., Gigant, B., … Carlier, M. F. (2004). The β-thymosin/WH2 domain: Structural basis for the switch from inhibition to promotion of actin assembly. Cell. https://doi.org/10.1016/S0092-8674(04)00403-9
- Heuser, J. (1989). Changes in lysosome shape and distribution correlated with changes in cytoplasmic pH. Journal of Cell Biology, 108(3). https://doi.org/10.1083/jcb.108.3.855
- Higgs, H. N., & Pollard, T. D. (2000). Activation by Cdc42 and PIP2 of Wiskott-Aldrich Syndrome protein (WASp) stimulates actin nucleation by Arp2/3 complex. Journal of Cell Biology, 150(6), 1311–1320. https://doi.org/10.1083/jcb.150.6.1311
- Hirst, J., Miller, S. E., Taylor, M. J., Von Mollard, G. F., & Robinson, M. S. (2004). EpsinR is an adaptor for the SNARE protein Vti1b. Molecular Biology of the Cell. https://doi.org/10.1091/mbc.E04-06-0468
- Hoepfner, S., Severin, F., Cabezas, A., Habermann, B., Runge, A., Gillooly, D., … Zerial, M. (2005). Modulation of receptor recycling and degradation by the endosomal kinesin KIF16B. Cell, 121(3), 437–450. https://doi.org/10.1016/j.cell.2005.02.017
- Hong, N. H., Qi, A., & Weaver, A. M. (2015). PI(3,5)P2 controls endosomal branched actin dynamics by regulating cortactin-actin interactions. The Journal of Cell Biology, 210(5), 753–769. https://doi.org/10.1083/jcb.201412127
- Horgan, C. P., Hanscom, S. R., Jolly, R. S., Futter, C. E., & McCaffrey, M. W. (2010). Rab11-FIP3 links the Rab11 GTPase and cytoplasmic dynein to mediate transport to the endosomal-recycling compartment. Journal of Cell Science, 123(2). https://doi.org/10.1242/jcs.052670
- Hori, A., & Toda, T. (2017). Regulation of centriolar satellite integrity and its physiology. Cellular and Molecular Life Sciences, 74(2), 213–229. https://doi.org/10.1007/s00018-016-2315-x

- Horiuchi, H., Lippé, R., McBride, H. M., Rubino, M., Woodman, P., Stenmark, H., … Zerial, M. (1997). A novel Rab5 GDP/GTP exchange factor complexed to Rabaptin-5 links nucleotide exchange to effector recruitment and function. Cell, 90(6). https://doi.org/10.1016/S0092-8674(00)80380-3
- Hu, Y. B., Dammer, E. B., Ren, R. J., & Wang, G. (2015). The endosomal-lysosomal system: From acidification and cargo sorting to neurodegeneration. Translational Neurodegeneration. https://doi.org/10.1186/s40035-015-0041-1
- Hunt, S. D., Townley, A. K., Danson, C. M., Cullen, P. J., & Stephens, D. J. (2013). Microtubule motors mediate endosomal sorting by maintaining functional domain organization. Journal of Cell Science, 126(11), 2493–2501. https://doi.org/10.1242/jcs.122317
- Huotari, J., & Helenius, A. (2011). Endosome maturation. EMBO Journal, 30(17), 3481–3500. https://doi.org/10.1038/emboj.2011.286
- Hurley, J. (2015). ESCRTs are everywhere. Embo J, 34(19), 2398–2407. Retrieved from http://dx.doi.org/10.15252/embj.201592484
- Huxley, H. E. (1963). Electron microscope studies on the structure of natural and synthetic protein filaments from striated muscle. Journal of Molecular Biology. https://doi.org/10.1016/S0022-2836(63)80008-X
- Idrissi, F.-Z., Blasco, A., Espinal, A., & Geli, M. I. (2012). Ultrastructural dynamics of proteins involved in endocytic budding. Proceedings of the National Academy of Sciences of the United States of America, 109(39), E2587-94. https://doi.org/10.1073/pnas.1202789109
- Ishiyama, N., & Ikura, M. (2012). Adherens Junctions: from Molecular Mechanisms to Tissue Development and Disease. Adherens Junctions: From Molecular Mechanisms to Tissue Development and Disease, Development and Disease - Subcellular Biochemistry, Vol 60, 60, 39–62. https://doi.org/10.1007/978-94-007-4186-7
- Ito, H., Fukuda, Y., Murata, K., & Kimura, A. (1983). Transformation of intact yeast cells treated with alkali cations. Journal of Bacteriology, 153(1), 163–168. https://doi.org/10.1271/bbb1961.48.341
- Itoh, T., Koshiba, S., Kigawa, T., Kikuchi, A., Yokoyama, S., & Takenawa, T. (2001). Role of the ENTH domain in phosphatidylinositol-4,5-bisphosphate binding and endocytosis. Science, 291(5506). https://doi.org/10.1126/science.291.5506.1047
- Jia, D., Gomez, T. S., Billadeau, D. D., & Rosen, M. K. (2012). Multiple repeat elements within the FAM21 tail link the WASH actin regulatory complex to the retromer. Molecular Biology of the Cell. https://doi.org/10.1091/mbc.E11-12-1059
- Jin, N., Lang, M. J., & Weisman, L. S. (2016). Phosphatidylinositol 3,5-bisphosphate: Regulation of cellular events in space and time. Biochemical Society Transactions, 44, 177–184. https://doi.org/10.1042/BST20150174
- Jones, M. C., Caswell, P. T., & Norman, J. C. (2006). Endocytic recycling pathways: emerging regulators of cell migration. Current Opinion in Cell Biology, 18(5), 549–557. https://doi.org/10.1016/j.ceb.2006.08.003

- Kabsch, W., Mannherz, H. G., Suck, D., Pai, E. F., & Holmes, K. C. (1990). Atomic structure of the actin: DNase I complex. Nature. https://doi.org/10.1038/347037a0
- Kachhap, S. K., Faith, D., Qian, D. Z., Shabbeer, S., Galloway, N. L., Pili, R., … Carducci, M. A. (2007). The N-Myc down regulated gene1 (NDRG1) is a Rab4a effector involved in vesicular recycling of E-cadherin. PLoS ONE, 2(9). https://doi.org/10.1371/journal.pone.0000844
- Kaksonen, M., Peng, H. B., & Rauvala, H. (2000). Association of cortactin with dynamic actin in lamellipodia and on endosomal vesicles. Journal of Cell Science, 113(24), 4421–4426.
- Kaksonen, M., & Roux, A. (2018). Mechanisms of clathrin-mediated endocytosis. Nature Reviews Molecular Cell Biology. Nature Publishing Group. https://doi.org/10.1038/nrm.2017.132
- Kälin, S., Hirschmann, D. T., Buser, D. P., & Spiess, M. (2015). Rabaptin5 is recruited to endosomes by Rab4 and Rabex5 to regulate endosome maturation. Journal of Cell Science, 128(22). https://doi.org/10.1242/jcs.174664
- Kalinin, A. E., Kajava, A. V., & Steinert, P. M. (2002). Epithelial barrier function: Assembly and structural features of the cornified cell envelope. BioEssays. article, New York: Wiley Subscription Services, Inc., A Wiley Company. https://doi.org/10.1002/bies.10144
- Katsuno-Kambe, H., & Yap, A. S. (2020). Endocytosis, cadherins and tissue dynamics. Traffic, 21(3), 268–273. https://doi.org/10.1111/tra.12721
- Kawauchi, T., Sekine, K., Shikanai, M., Chihama, K., Tomita, K., Kubo, K. ichiro, … Hoshino, M. (2010). Rab GTPases-dependent endocytic pathways regulate neuronal migration and maturation through N-cadherin trafficking. Neuron. https://doi.org/10.1016/j.neuron.2010.07.007
- Kelly, B. T., Graham, S. C., Liska, N., Dannhauser, P. N., Höning, S., Ungewickell, E. J., & Owen, D. J. (2014). AP2 controls clathrin polymerization with a membrane-activated switch. Science, 345(6195), 459–463. https://doi.org/10.1126/science.1254836.AP2
- Kendall, A. K., Xie, B., Xu, P., Wang, J., Burcham, R., Frazier, M. N., … Jackson, L. P. (2020). Mammalian Retromer Is an Adaptable Scaffold for Cargo Sorting from Endosomes. Structure. https://doi.org/10.1016/j.str.2020.01.009
- Ketel, K., Krauss, M., Nicot, A.-S., Puchkov, D., Wieffer, M., Müller, R., … Haucke, V. (2016). A phosphoinositide conversion mechanism for exit from endosomes. Nature, 529(7586), 408–412. https://doi.org/10.1038/nature16516
- Kihara, A., Noda, T., Ishihara, N., & Ohsumi, Y. (2001). Two distinct Vps34 phosphatidylinositol 3-kinase complexes function in autophagy and carboxypeptidase y sorting in Saccharomyces cerevisiae. Journal of Cell Biology, 153(3). https://doi.org/10.1083/jcb.152.3.519
- Kikuno, R., Nagase, T., Ishikawa, K., Hirosawa, M., Miyajima, N., Tanaka, A., … Ohara, O. (1999). Prediction of the coding sequences of unidentified human genes. XIV. The complete sequences of 100 new cDNA clones from brain which code for large proteins in

vitro. DNA Research : An International Journal for Rapid Publication of Reports on Genes and Genomes, 6(3), 197–205. http://www.ncbi.nlm.nih.gov/pubmed/10470851

– Kim, J. J., Lipatova, Z., & Segev, N. (2016). TRAPP complexes in secretion and autophagy. Frontiers in Cell and Developmental Biology, 4(MAR), 1–10. https://doi.org/10.3389/fcell.2016.00020

– Kirchhausen, T., Owen, D., & Harrison, S. C. (2014). Molecular structure, function, and dynamics of clathrin-mediated membrane traffic. Cold Spring Harbor Perspectives in Biology, 6(5). https://doi.org/10.1101/cshperspect.a016725

– Kirkbride, K. C., Hong, N. H., French, C. L., Clark, E. S., Jerome, W. G., & Weaver, A. M. (2012). Regulation of late endosomal/lysosomal maturation and trafficking by cortactin affects Golgi morphology. Cytoskeleton, 69(9). https://doi.org/10.1002/cm.21051

– Kitagawa, D., Vakonakis, I., Olieric, N., Hilbert, M., Keller, D., Olieric, V., … Steinmetz, M. O. (2011). Structural basis of the 9-fold symmetry of centrioles. Cell, 144(3), 364–375. https://doi.org/10.1016/j.cell.2011.01.008

– Kollman, J. M., Merdes, A., Mourey, L., & Agard, D. A. (2011). Microtubule nucleation by γ-tubulin complexes. Nature Reviews Molecular Cell Biology. https://doi.org/10.1038/nrm3209

– Kollmar, M., Lbik, D., & Enge, S. (2012). Evolution of the eukaryotic ARP2/3 activators of the WASP family: WASP, WAVE, WASH, and WHAMM, and the proposed new family members WAWH and WAML. BMC Research Notes. https://doi.org/10.1186/1756-0500-5-88

– Korolchuk, V., & Banting, G. (2003). Kinases in clathrin-mediated endocytosis. In Biochemical Society Transactions (Vol. 31, pp. 857–860). https://doi.org/10.1042/BST0310857

– Korolchuk, V., Saiki, S., Lichtenberg, M., Siddiqi, F. H., Roberts, E. A., Imarisio, S., … Rubinsztein, D. C. (2011). Lysosomal positioning coordinates cellular nutrient responses. Nature Cell Biology, 13(4). https://doi.org/10.1038/ncb2204

– Kouranti, I., Sachse, M., Arouche, N., Goud, B., & Echard, A. (2006). Rab35 Regulates an Endocytic Recycling Pathway Essential for the Terminal Steps of Cytokinesis. Current Biology, 16(17), 1719–1725. https://doi.org/10.1016/j.cub.2006.07.020

– Kovacs, G. G. (2018). Concepts and classification of neurodegenerative diseases. In Handbook of Clinical Neurology (Vol. 145, pp. 301–307). Elsevier. https://doi.org/10.1016/B978-0-12-802395-2.00021-3

– Kovtun, O., Leneva, N., Bykov, Y. S., Ariotti, N., Teasdale, R. D., Schaffer, M., … Collins, B. M. (2018). Structure of the membrane-assembled retromer coat determined by cryo-electron tomography. Nature, 561(7724), 561–564. https://doi.org/10.1038/s41586-018-0526-z

– Kowalski, J. R., Egile, C., Gil, S., Snapper, S. B., Li, R., & Thomas, S. M. (2005). Cortactin regulates cell migration through activation of N-WASP. Journal of Cell Science, 118(1). https://doi.org/10.1242/jcs.01586

- Kreishman-Deitrick, M., Goley, E. D., Burdine, L., Denison, C., Egile, C., Li, R., … Rosen, M. K. (2005). NMR analyses of the activation of the Arp2/3 complex by neuronal Wiskott-Aldrich syndrome protein. Biochemistry. https://doi.org/10.1021/bi051065n
- Kumar, H., Pushpa, K., Kumari, A., Verma, K., Pergu, R., & Mylavarapu, S. V. S. (2019). The exocyst complex and Rab5 are required for abscission by localizing ESCRT III subunits to the cytokinetic bridge. Journal of Cell Science, 132(14). https://doi.org/10.1242/jcs.226001
- Kural, C., & Kirchhausen, T. (2012). Live-cell imaging of clathrin coats. In Methods in Enzymology (Vol. 505, pp. 59–80). Academic Press Inc. https://doi.org/10.1016/B978-0-12-388448-0.00012-7
- Kvainickas, A., Jimenez-Orgaz, A., Nägele, H., Hu, Z., Dengjel, J., & Steinberg, F. (2017). Cargo-selective SNX-BAR proteins mediate retromer trimer independent retrograde transport. Journal of Cell Biology, 216(11), 3677–3693. https://doi.org/10.1083/jcb.201702137
- Lacy, M. M., Ma, R., Ravindra, N. G., & Berro, J. (2018). Molecular mechanisms of force production in clathrin-mediated endocytosis. FEBS Letters, 592(21), 3586–3605. https://doi.org/10.1002/1873-3468.13192
- Laemmli, U. K. (1970). Cleavage of structural proteins during the assembly of the head of bacteriophage T4. Nature, 227(5259), 680–685. https://doi.org/10.1038/227680a0
- Lamaze, C., & Prior, I. (2018). Endocytosis and Signaling. Springer.
- Lamber, E. P., Siedenburg, A. C., & Barr, F. A. (2019). Rab regulation by GEFs and GAPs during membrane traffic. Current Opinion in Cell Biology, 59, 34–39. https://doi.org/10.1016/j.ceb.2019.03.004
- Langevin, J., Morgan, M. J., Rossé, C., Racine, V., Sibarita, J. B., Aresta, S., … Bellaïche, Y. (2005). Drosophila exocyst components sec5, sec6, and Sec15 regulate DE-Cadherin trafficking from recycling endosomes to the plasma membrane. Developmental Cell. https://doi.org/10.1016/j.devcel.2005.07.013
- Lapierre, L. A., Kumar, R., Hales, C. M., Navarre, J., Bhartur, S. G., Burnette, J. O., … Goldenring, J. R. (2001). Myosin Vb is associated with plasma membrane recycling systems. Molecular Biology of the Cell, 12(6). https://doi.org/10.1091/mbc.12.6.1843
- Le Guennec, M., Klena, N., Gambarotto, D., Laporte, M. H., Tassin, A. M., van den Hoek, H., … Guichard, P. (2020). A helical inner scaffold provides a structural basis for centriole cohesion. Science Advances. https://doi.org/10.1126/sciadv.aaz4137
- Lechler, T., & Fuchs, E. (2007). Desmoplakin: An unexpected regulator of microtubule organization in the epidermis. Journal of Cell Biology, 176(2), 147–154. https://doi.org/10.1083/jcb.200609109
- Lecuit, T., & Pilot, F. (2003). Developmental control of cell morphogenesis: a focus on membrane growth. Nature Cell Biology, 5(2), 103–108. article. https://doi.org/10.1038/ncb0203-103

– Lee, I. G., Olenick, M. A., Boczkowska, M., Franzini-Armstrong, C., Holzbaur, E. L. F., & Dominguez, R. (2018). A conserved interaction of the dynein light intermediate chain with dynein-dynactin effectors necessary for processivity. Nature Communications, 9(1). https://doi.org/10.1038/s41467-018-03412-8

– Lee, S., Chang, J., & Blackstone, C. (2016). FAM21 directs SNX27-retromer cargoes to the plasma membrane by preventing transport to the Golgi apparatus. Nature Communications, 7, 10939. https://doi.org/10.1038/ncomms10939

– Lees-Miller, J. P., Henry, G., & Helfman, D. M. (1992). Identification of act2, an essential gene in the fission yeast Schizosaccharomyces pombe that encodes a protein related to actin. Proceedings of the National Academy of Sciences of the United States of America. https://doi.org/10.1073/pnas.89.1.80

– Leibfried, A., Fricke, R., Morgan, M. J., Bogdan, S., & Bellaiche, Y. (2008). Drosophila Cip4 and WASp Define a Branch of the Cdc42-Par6-aPKC Pathway Regulating E-Cadherin Endocytosis. Current Biology, 18(21). https://doi.org/10.1016/j.cub.2008.09.063

– Lemmon, M. A. (2008). Membrane recognition by phospholipid-binding domains. Nature Reviews Molecular Cell Biology, 9(2), 99–111. https://doi.org/10.1038/nrm2328

– Lewellyn, E. B., Pedersen, R. T. A., Hong, J., Lu, R., Morrison, H. M., & Drubin, D. G. (2015). An Engineered Minimal WASP-Myosin Fusion Protein Reveals Essential Functions for Endocytosis. Developmental Cell, 35(3), 281–294. https://doi.org/10.1016/j.devcel.2015.10.007

– Li, Jia, Mao, Z., Huang, J., & Xiaa, J. (2018). PICK1 is essential for insulin production and the maintenance of glucose homeostasis. Molecular Biology of the Cell, 29(5), 587–596. https://doi.org/10.1091/mbc.E17-03-0204

– Li, Jian, Peters, P. J., Bai, M., Dai, J., Bos, E., Kirchhausen, T., … Hsu, V. W. (2007). An ACAP1-containing clathrin coat complex for endocytic recycling. Journal of Cell Biology, 178(3), 453–464. https://doi.org/10.1083/jcb.200608033

– Li, P., Banjade, S., Cheng, H. C., Kim, S., Chen, B., Guo, L., … Rosen, M. K. (2012). Phase transitions in the assembly of multivalent signalling proteins. Nature, 483(7389), 336–340. https://doi.org/10.1038/nature10879

– Li, X., & Donowitz, M. (2014). Fractionation of subcellular membrane vesicles of epithelial and non-epithelial cells by OptiPrep??? density gradient ultracentrifugation. Methods in Molecular Biology, 1174, 85–99. https://doi.org/10.1007/978-1-4939-0944-5_6

– Linder, S., Nelson, D., Weiss, M., & Aepfelbacher, M. (1999). Wiskott-Aldrich syndrome protein regulates podosomes in primary human macrophages. Proceedings of the National Academy of Sciences of the United States of America, 96(17). https://doi.org/10.1073/pnas.96.17.9648

– Lindsay, A. J., & McCaffrey, M. W. (2017). Rab coupling protein mediated endosomal recycling of N-cadherin influences cell motility. Oncotarget, 8(62), 104717–104732. https://doi.org/10.18632/oncotarget.10513

- Linford, A., Yoshimura, S. I., Bastos, R. N., Langemeyer, L., Gerondopoulos, A., Rigden, D. J., & Barr, F. A. (2012). Rab14 and Its Exchange Factor FAM116 Link Endocytic Recycling and Adherens Junction Stability in Migrating Cells. Developmental Cell. https://doi.org/10.1016/j.devcel.2012.04.010
- Ling, K., Bairstow, S. F., Carbonara, C., Turbin, D. A., Huntsman, D. G., & Anderson, R. A. (2007). Type Iγ phosphatidylinositol phosphate kinase modulates adherens junction and E-cadherin trafficking via a direct interaction with μ 1B adaptin. Journal of Cell Biology, 176(3), 343–353. https://doi.org/10.1083/jcb.200606023
- Liu, C., Wang, J., Hu, Y., Xie, H., Liu, M., & Tang, H. (2017). Upregulation of kazrin F by miR-186 suppresses apoptosis but promotes epithelial-mesenchymal transition to contribute to malignancy in human cervical cancer cells. Chinese Journal of Cancer Research, 29(1), 45–56. https://doi.org/10.21147/j.issn.1000-9604.2017.01.06
- Liu, Q., Liu, F., Yu, K. Lou, Tas, R., Grigoriev, I., Remmelzwaal, S., … Akhmanova, A. (2016). MICAL3 flavoprotein monooxygenase forms a complex with centralspindlin and regulates cytokinesis. Journal of Biological Chemistry. https://doi.org/10.1074/jbc.M116.748186
- Liu, R., Abreu-Blanco, M. T., Barry, K. C., Linardopoulou, E. V., Osborn, G. E., & Parkhurst, S. M. (2009). Wash functions downstream of Rho and links linear and branched actin nucleation factors. Development. https://doi.org/10.1242/dev.035246
- Lock, J. G., & Stow, J. L. (2005). Rab11 in recycling endosomes regulates the sorting and basolateral transport of E-cadherin. Molecular Biology of the Cell, 16(4), 1744–1755. https://doi.org/10.1091/mbc.E04-10-0867
- Lohia, M., Qin, Y., & Macara, I. G. (2012). The Scribble Polarity Protein Stabilizes E-Cadherin/p120-Catenin Binding and Blocks Retrieval of E-Cadherin to the Golgi. PLoS ONE, 7(11). https://doi.org/10.1371/journal.pone.0051130
- Lorenzo, Ó., Urbé, S., & Clague, M. J. (2006). Systematic analysis of myotubularins: Heteromeric interactions, subcellular localisation and endosome-related functions. Journal of Cell Science, 119(14). https://doi.org/10.1242/jcs.03040
- Lou, X. (2018). Sensing exocytosis and triggering endocytosis at synapses: Synaptic vesicle exocytosis–endocytosis coupling. Frontiers in Cellular Neuroscience. https://doi.org/10.3389/fncel.2018.00066
- Lucas, M., Gershlick, D. C., Vidaurrazaga, A., Rojas, A. L., Bonifacino, J. S., & Hierro, A. (2016). Structural Mechanism for Cargo Recognition by the Retromer Complex. Cell, 1–13. https://doi.org/10.1016/j.cell.2016.10.056
- Lucas, M., & Hierro, A. (2017). Retromer. Current Biology, 27(14), R687–R689. https://doi.org/10.1016/j.cub.2017.05.072
- Lupas, A., Van Dyke, M., & Stock, J. (1991). Predicting coiled coils from protein sequences. Science, 252(5009), 1162 LP – 1164. https://doi.org/10.1126/science.252.5009.1162
- Lürick, A., Kümmel, D., & Ungermann, C. (2018). Multisubunit tethers in membrane fusion. Current Biology, 28(8), R417–R420. https://doi.org/10.1016/j.cub.2017.12.012

- Macpherson, I. R., Rainero, E., Mitchell, L. E., van den Berghe, P. V. E., Speirs, C., Dozynkiewicz, M. A., … Norman, J. C. (2014). CLIC3 controls recycling of late endosomal MT1-MMP and dictates invasion and metastasis in breast cancer. Journal of Cell Science. https://doi.org/10.1242/jcs.135947
- Mader, C. C., Oser, M., Magalhaes, M. A. O., Bravo-Cordero, J. J., Condeelis, J., Koleske, A. J., & Gil-Henn, H. (2011). An EGFR-Src-Arg-cortactin pathway mediates functional maturation of invadopodia and breast cancer cell invasion. Cancer Research, 71(5). https://doi.org/10.1158/0008-5472.CAN-10-1432
- Majeed, S. R., Vasudevan, L., Chen, C. Y., Luo, Y., Torres, J. A., Evans, T. M., … Brodsky, F. M. (2014). Clathrin light chains are required for the gyrating-clathrin recycling pathway and thereby promote cell migration. Nature Communications. https://doi.org/10.1038/ncomms4891
- Mallam, A. L., & Marcotte, E. M. (2017). Systems-wide Studies Uncover Commander, a Multiprotein Complex Essential to Human Development. Cell Systems. https://doi.org/10.1016/j.cels.2017.04.006
- Marat, A. L., & Haucke, V. (2016). Phosphatidylinositol 3 -phosphates — at the interface between cell signalling and membrane traffic. The EMBO Journal, 35(Fig 2), 1–19. https://doi.org/10.15252/embj.201593564
- Marchesin, V., Castro-Castro, A., Lodillinsky, C., Castagnino, A., Cyrta, J., Bonsang-Kitzis, H., … Chavrier, P. (2015). ARF6-JIP3/4 regulate endosomal tubules for MT1-MMP exocytosis in cancer invasion. Journal of Cell Biology. https://doi.org/10.1083/jcb.201506002
- Margadant, C., Monsuur, H. N., Norman, J. C., & Sonnenberg, A. (2011). Mechanisms of integrin activation and trafficking. Current Opinion in Cell Biology, 23(5), 607–614. https://doi.org/10.1016/j.ceb.2011.08.005
- Maritzen, T., Zech, T., Schmidt, M. R., Krause, E., Machesky, L. M., & Haucke, V. (2012). Gadkin negatively regulates cell spreading and motility via sequestration of the actin-nucleating ARP2/3 complex. Proceedings of the National Academy of Sciences of the United States of America, 109(26), 10382–10387. https://doi.org/10.1073/pnas.1206468109
- Marx, A., Müller, J., Mandelkow, E. M., Hoenger, A., & Mandelkow, E. (2006). Interaction of kinesin motors, microtubules, and MAPs. Journal of Muscle Research and Cell Motility. https://doi.org/10.1007/s10974-005-9051-4
- Marx, A., Hoenger, A., & Mandelkow, E. (2009). Structures of kinesin motor proteins. In Cell Motility and the Cytoskeleton. https://doi.org/10.1002/cm.20392
- Maxfield, F. R., & McGraw, T. E. (2004). Endocytic recycling. Nature Reviews Molecular Cell Biology, 5(2), 121–132. https://doi.org/10.1038/nrm1315
- McBride, H. M., Rybin, V., Murphy, C., Giner, A., Teasdale, R., & Zerial, M. (1999). Oligomeric complexes link Rab5 effectors with NSF and drive membrane fusion via interactions between EEA1 and syntaxin 13. Cell, 98(3), 377–386. https://doi.org/10.1016/S0092-8674(00)81966-2

- McGough, I. J., & Cullen, P. J. (2013). Clathrin is not required for SNX-BAR-retromermediated carrier formation. Journal of Cell Science, 126(1), 45–52. https://doi.org/10.1242/jcs.112904
- McMillan, K. J., Korswagen, H. C., & Cullen, P. J. (2017). The emerging role of retromer in neuroprotection. Current Opinion in Cell Biology, 47(Figure 1), 72–82. https://doi.org/10.1016/j.ceb.2017.02.004
- McNally, K. E., & Cullen, P. J. (2018). Endosomal Retrieval of Cargo: Retromer Is Not Alone. Trends in Cell Biology, xx, 1–16. https://doi.org/10.1016/j.tcb.2018.06.005
- McNally, K. E., Faulkner, R., Steinberg, F., Gallon, M., Ghai, R., Pim, D., … Cullen, P. J. (2017). Retriever is a multiprotein complex for retromer-independent endosomal cargo recycling. Nature Cell Biology, (January). https://doi.org/10.1038/ncb3610
- Mennella, V., Keszthelyi, B., McDonald, K., Chhun, B., Kan, F., Rogers, G., … Agard, D. (2012). Sub-diffraction-resolution fluorescence microscopy reveals a domain of the centrosome critical for pericentriolar material organization. Nat Cell Biol. https://doi.org/10.1038/jid.2014.371
- Merrifield, C. J., & Kaksonen, M. (2014). Endocytic Accessory Factors and Regulation of Clathrin-Mediated Endocytosis. Cold Spring Harbor Perspectives in Biology, 6(11), 1–16. https://doi.org/10.1101/cshperspect.a016733
- Merrifield, C. J., Moss, S. E., Ballestrem, C., Imhof, B. A., Giese, G., Wunderlich, I., & Almers, W. (1999). Endocytic vesicles move at the tips of actin tails in cultured mast cells. Nature Cell Biology. https://doi.org/10.1038/9048
- Merrifield, C. J., Perrais, D., & Zenisek, D. (2005). Coupling between clathrin-coated-pit invagination, cortactin recruitment, and membrane scission observed in live cells. Cell, 121(4), 593–606. https://doi.org/10.1016/j.cell.2005.03.015
- Messa, M., Fernández-Busnadiego, R., Sun, E. W., Chen, H., Czapla, H., Wrasman, K., … De Camilli, P. (2014). Epsin deficiency impairs endocytosis by stalling the actin-dependent invagination of endocytic clathrin-coated pits. ELife, 3(August2014). https://doi.org/10.7554/eLife.03311
- Mészáros, B., Erdös, G., & Dosztányi, Z. (2018). IUPred2A: Context-dependent prediction of protein disorder as a function of redox state and protein binding. Nucleic Acids Research, 46(W1). https://doi.org/10.1093/nar/gky384
- Miao, Y., Tipakornsaowapak, T., Zheng, L., Mu, Y., & Lewellyn, E. (2018). Phospho-regulation of intrinsically disordered proteins for actin assembly and endocytosis. FEBS Journal, 285(15), 2762–2784. https://doi.org/10.1111/febs.14493
- Mickolajczyk, K. J., & Hancock, W. O. (2017). Kinesin Processivity Is Determined by a Kinetic Race from a Vulnerable One-Head-Bound State. Biophysical Journal. https://doi.org/10.1016/j.bpj.2017.05.007
- Mierzwa, B. E., Chiaruttini, N., Redondo-Morata, L., Moser Von Filseck, J., König, J., Larios, J., … Gerlich, D. W. (2017). Dynamic subunit turnover in ESCRT-III assemblies is regulated by Vps4 to mediate membrane remodelling during cytokinesis. Nature Cell Biology. https://doi.org/10.1038/ncb3559

- Miki, H., Sasaki, T., Takai, Y., & Takenawa, T. (1998). Induction of filopodium formation by a WASP-related actin- depolymerizing protein N-WASP. Nature, 391(6662). https://doi.org/10.1038/34208
- Mills, I. G., Jones, A. T., & Clague, M. J. (1998). Involvement of the endosomal autoantigen EEA1 in homotypic fusion of early endosomes. Current Biology, 8(15). https://doi.org/10.1016/S0960-9822(07)00351-X
- Mindell, J. A. (2012). Lysosomal Acidification Mechanisms. Annual Review of Physiology, 74(1), 69–86. https://doi.org/10.1146/annurev-physiol-012110-142317
- Mirvis, M., Stearns, T., & Nelson, W. J. (2018). Cilium structure, assembly, and disassembly regulated by the cytoskeleton. Biochemical Journal. https://doi.org/10.1042/BCJ20170453
- Miserey-Lenkei, S., Bousquet, H., Pylypenko, O., Bardin, S., Dimitrov, A., Bressanelli, G., … Goud, B. (2017). Coupling fission and exit of RAB6 vesicles at Golgi hotspots through kinesin-myosin interactions. Nature Communications, 8(1). https://doi.org/10.1038/s41467-017-01266-0
- Missirlis, D., Haraszti, T., Kessler, H., & Spatz, J. P. (2017). Fibronectin promotes directional persistence in fibroblast migration through interactions with both its cell-binding and heparin-binding domains. Scientific Reports, 7(1). https://doi.org/10.1038/s41598-017-03701-0
- Mitchison, T., & Kirschner, M. (1984). Dynamic instability of microtubule growth. Nature. https://doi.org/10.1038/312237a0
- Miyashita, Y., & Ozawa, M. (2007). Increased internalization of p120-uncoupled E-cadherin and a requirement for a dileucine motif in the cytoplasmic domain for endocytosis of the protein. Journal of Biological Chemistry, 282(15). https://doi.org/10.1074/jbc.M608351200
- Mojica, F. J., Diez-Villasenor, C., Soria, E. & Juez, G. (2000). Biological significance of a family of regularly spaced repeats in the genomes of Archaea , Bacteria and mitochondria. Mol. Microbiol, 36, 244. https://doi.org/10.1046/j.1365-2958.2000.01838.x
- Montagnac, G., Echard, A., & Chavrier, P. (2008). Endocytic traffic in animal cell cytokinesis. Current Opinion in Cell Biology, 20(4), 454–461. https://doi.org/10.1016/j.ceb.2008.03.011
- Monteiro, P., Rossé, C., Castro-Castro, A., Irondelle, M., Lagoutte, E., Paul-Gilloteaux, P., … Chavrier, P. (2013). Endosomal WASH and exocyst complexes control exocytosis of MT1-MMP at invadopodia. Journal of Cell Biology, 203(6), 1063–1079. https://doi.org/10.1083/jcb.201306162
- Moreno-Layseca, P., Icha, J., Hamidi, H., & Ivaska, J. (2019). Integrin trafficking in cells and tissues. Nature Cell Biology, 21(2), 122–132. https://doi.org/10.1038/s41556-018-0223-z
- Moyer, T. C., & Holland, A. J. (2015). Generation of a conditional analogsensitive kinase in human cells using CRISPR/Cas9-mediated genome engineering. Methods in Cell Biology (Vol. 129). Elsevier. https://doi.org/10.1016/bs.mcb.2015.03.017

- Mullins, R. D., Kelleher, J. F., Xu, J., & Pollard, T. D. (1998). Arp2/3 complex from Acanthamoeba binds profilin and cross-links actin filaments. Molecular Biology of the Cell. https://doi.org/10.1091/mbc.9.4.841
- Murray, D. H., Jahnel, M., Lauer, J., Avellaneda, M. J., Brouilly, N., Cezanne, A., … Zerial, M. (2016). An endosomal tether undergoes an entropic collapse to bring vesicles together. Nature, 537(7618), 107–111. https://doi.org/10.1038/nature19326
- Murray, J. T., Panaretou, C., Stenmark, H., Miaczynska, M., & Backer, J. M. (2002). Role of Rab5 in the recruitment of hVps34/p150 to the early endosome. Traffic, 3(6). https://doi.org/10.1034/j.1600-0854.2002.30605.x
- Muschalik, N., & Munro, S. (2018). Golgins. Current Biology, 28(8), R374–R376. https://doi.org/10.1016/j.cub.2018.01.006
- Nachat, R., Cipolat, S., Sevilla, L. M., Chhatriwala, M., Groot, K. R., & Watt, F. M. (2009). KazrinE is a desmosome-associated liprin that colocalises with acetylated microtubules. Journal of Cell Science, 122(Pt 22), 4035–4041. https://doi.org/10.1242/jcs.047266
- Nader, G. P. F., Ezratty, E. J., & Gundersen, G. G. (2016). FAK, talin and PIPKI 3 regulate endocytosed integrin activation to polarize focal adhesion assembly. Nature Cell Biology, 18(5), 491–503. https://doi.org/10.1038/ncb3333
- Nähse, V., Christ, L., Stenmark, H., & Campsteijn, C. (2017). The Abscission Checkpoint: Making It to the Final Cut. Trends in Cell Biology, 27(1), 1–11. https://doi.org/10.1016/j.tcb.2016.10.001
- Nakai, W., Kondo, Y., Saitoh, A., Naito, T., Nakayama, K., & Shin, H. W. (2013). ARF1 and ARF4 regulate recycling endosomal morphology and retrograde transport from endosomes to the Golgi apparatus. Molecular Biology of the Cell, 24(16). https://doi.org/10.1091/mbc.E13-04-0197
- Naslavsky, N, & Caplan, S. (2011). EHD proteins: Key conductors of endocytic transport. Trends in Cell Biology. https://doi.org/10.1016/j.tcb.2010.10.003.EHD
- Naslavsky, N, Boehm, M., Backlund, P. S., & Caplan, S. (2004). Rabenosyn-5 and EHD1 Interact and Sequentially Regulate Protein Recycling to the Plasma Membrane. Molecular Biology of the Cell, 15(5), 2410–2422. https://doi.org/10.1091/mbc.E03-10-0733
- Naslavsky, N, & Caplan, S. (2018). The enigmatic endosome - Sorting the ins and outs of endocytic trafficking. Journal of Cell Science, 131(13). https://doi.org/10.1242/jcs.216499
- Naslavsky, Naava, Rahajeng, J., Sharma, M., Jović, M., & Caplan, S. (2006). Interactions between EHD proteins and Rab11-FIP2: A role for EHD3 in early endosomal transport. Molecular Biology of the Cell. https://doi.org/10.1091/mbc.E05-05-0466
- Neefjes, J., Jongsma, M. M. L., & Berlin, I. (2017). Stop or Go? Endosome Positioning in the Establishment of Compartment Architecture, Dynamics, and Function Endosomal Compartment Architecture Steers Its Function in Space and Time. Trends in Cell Biology, 1–15. https://doi.org/10.1016/j.tcb.2017.03.002

- Neuhaus, E. M., & Soldati, T. (2000). A myosin I is involved in membrane recycling from early endosomes. Journal of Cell Biology, 150(5). https://doi.org/10.1083/jcb.150.5.1013
- Nieto, M. A., Huang, R. Y.-J., Jackson, R. A., & Thiery, J. P. (2016). Emt: 2016. Cell, 166(1), 21–45. https://doi.org/10.1016/j.cell.2016.06.028
- Nishimura, T., & Kaibuchi, K. (2007). Numb Controls Integrin Endocytosis for Directional Cell Migration with aPKC and PAR-3. Developmental Cell. https://doi.org/10.1016/j.devcel.2007.05.003
- Nordmann, M., Cabrera, M., Perz, A., Bröcker, C., Ostrowicz, C., Engelbrecht-Vandré, S., & Ungermann, C. (2010). The Mon1-Ccz1 complex is the GEF of the late endosomal Rab7 homolog Ypt7. Current Biology. https://doi.org/10.1016/j.cub.2010.08.002
- Nosworthy, N. J., Chhabra, D., Tsubakihara, M., Dedova, I. V, Kekic, M., dos Remedios, C. G., & Berry, D. A. (2003). Actin binding proteins: regulation of cytoskeletal microfilaments. Physiol Rev, 83(2), 433–473.
- Novick, P., Field, C., & Schekman, R. (1980). Identification of 23 complementation groups required for post-translational events in the yeast secretory pathway. Cell, 21(1), 205–215. https://doi.org/10.1016/0092-8674(80)90128-2
- Ohashi, E., Tanabe, K., Henmi, Y., Mesaki, K., Kobayashi, Y., & Takei, K. (2011). Receptor Sorting within Endosomal Trafficking Pathway is Facilitated by Dynamic Actin Filaments. PLoS ONE, 6(5). https://doi.org/10.1371/journal.pone.0019942
- Ohno, H., Stewart, J., Fournier, M. C., Bosshart, H., Rhee, I., Miyatake, S., … Bonifacino, J. S. (1995). Interaction of tyrosine-based sorting signals with clathrin-associated proteins. Science. https://doi.org/10.1126/science.7569928
- Palm, W., & Thompson, C. B. (2017). Nutrient acquisition strategies of mammalian cells. Nature. https://doi.org/10.1038/nature22379
- Parachoniak, C. A., Luo, Y., Abella, J. V., Keen, J. H., & Park, M. (2011). GGA3 functions as a switch to promote met receptor recycling, essential for sustained ERK and cell migration. Developmental Cell, 20(6). https://doi.org/10.1016/j.devcel.2011.05.007
- Pasqualato, S., Senic-Matuglia, F., Renault, L., Goud, B., Salamero, J., & Cherfils, J. (2004). The Structural GDP/GTP Cycle of Rab11 Reveals a Novel Interface Involved in the Dynamics of Recycling Endosomes. Journal of Biological Chemistry, 279(12), 11480–11488. https://doi.org/10.1074/jbc.M310558200
- Pasqualetto, G., Brancale, A., & Young, M. T. (2018). The Molecular Determinants of Small-Molecule Ligand Binding at P2X Receptors . Frontiers in Pharmacology . https://www.frontiersin.org/article/10.3389/fphar.2018.00058
- Paul, N. R., Allen, J. L., Chapman, A., Morlan-Mairal, M., Zindy, E., Jacquemet, G., … Caswell, P. T. (2015). α5β1 integrin recycling promotes Arp2/3-independent cancer cell invasion via the formin FHOD3. Journal of Cell Biology, 210(6), 1013–1031. https://doi.org/10.1083/jcb.201502040

- Paul, N. R., Jacquemet, G., & Caswell, P. T. (2015). Endocytic Trafficking of Integrins in Cell Migration. Current Biology, 25(22), R1092–R1105. https://doi.org/10.1016/j.cub.2015.09.049
- Peglion, F., Llense, F., & Etienne-Manneville, S. (2014). Adherens junction treadmilling during collective migration. Nature Cell Biology, 16(7), 639–651. https://doi.org/10.1038/ncb2985
- Perini, E. D., Schaefer, R., Stöter, M., Kalaidzidis, Y., & Zerial, M. (2014). Mammalian CORVET is required for fusion and conversion of distinct early endosome subpopulations. Traffic, 15(12). https://doi.org/10.1111/tra.12232
- Perrin, L., Lacas-Gervais, S., Gilleron, J., Ceppo, F., Prodon, F., Benmerah, A., … Cormont, M. (2013). Rab4b controls an early endosome sorting event by interacting with the γ-subunit of the clathrin adaptor complex 1. Journal of Cell Science, 126(Pt 21), 4950–4962.
- Peterson, J. R., Bickford, L. C., Morgan, D., Kim, A. S., Ouerfelli, O., Kirschner, M. W., & Rosen, M. K. (2004). Chemical inhibition of N-WASP by stabilization of a native autoinhibited conformation. Nature Structural and Molecular Biology, 11(8), 747–755. https://doi.org/10.1038/nsmb796
- Pfeffer, S. R. (2013). Rab GTPase regulation of membrane identity. Current Opinion in Cell Biology, 25(4), 414–419. https://doi.org/10.1016/j.ceb.2013.04.002
- Picco, A., Irastorza-Azcarate, I., Specht, T., Böke, D., Pazos, I., Rivier-Cordey, A. S., … Gallego, O. (2017). The In Vivo Architecture of the Exocyst Provides Structural Basis for Exocytosis. Cell. https://doi.org/10.1016/j.cell.2017.01.004
- Podinovskaia, M., & Spang, A. (2018). The Endosomal Network: Mediators and Regulators of Endosome Maturation. In C. Lamaze & I. Prior (Eds.), Endocytosis and Signaling (pp. 1–17). Springer.
- Pollard, T. D. (1986). Rate constants for the reactions of ATP- and ADP-actin with the ends of actin filaments. Journal of Cell Biology. https://doi.org/10.1083/jcb.103.6.2747
- Pollard, T. D. (2016). Actin and Actin-Binding Proteins. Cold Spring Harbor Perspect Biol, 1–18.
- Pollard, T. D., & Borisy, G. G. (2003). Cellular motility driven by assembly and disassembly of actin filaments. Cell, 112(4), 453–465. https://doi.org/10.1016/S0092-8674(03)00120-X
- Pollard, T. D., & Cooper, J. A. (2009). Actin, a Central Player in Cell Shape and Movement. Science, 40(6), 1301–1315. https://doi.org/10.1126/science.1175862
- Pollard, T. D., & O'Shaughnessy, B. (2019). Molecular Mechanism of Cytokinesis. Annual Review of Biochemistry, 88(1), 661–689. https://doi.org/10.1146/annurev-biochem-062917-012530
- Popoff, V., Mardones, G. A., Bai, S. K., Chambon, V., Tenza, D., Burgos, P. V., … Johannes, L. (2009). Analysis of articulation between clathrin and retromer in retrograde sorting on early endosomes. Traffic, 10(12), 1868–1880. https://doi.org/10.1111/j.1600-0854.2009.00993.x

- Posor, Y., Eichhorn-Grünig, M., Puchkov, D., Schöneberg, J., Ullrich, A., Lampe, A., … Haucke, V. (2013). Spatiotemporal control of endocytosis by phosphatidylinositol-3,4-bisphosphate. Nature. https://doi.org/10.1038/nature12360
- Posor, Y., Eichhorn-Grünig, M., & Haucke, V. (2015). Phosphoinositides in endocytosis. Biochimica et Biophysica Acta - Molecular and Cell Biology of Lipids, 1851(6), 794–804. https://doi.org/10.1016/j.bbalip.2014.09.014
- Poteryaev, D., Datta, S., Ackema, K., Zerial, M., & Spang, A. (2010). Identification of the switch in early-to-late endosome transition. Cell. https://doi.org/10.1016/j.cell.2010.03.011
- Prekeris, R., Klumperman, J., Chen, Y. A., & Scheller, R. H. (1998). Syntaxin 13 mediates cycling of plasma membrane proteins via tubulovesicular recycling endosomes. Journal of Cell Biology, 143(4), 957–971. https://doi.org/10.1083/jcb.143.4.957
- Prigent, M., Dubois, T., Raposo, G., Derrien, V., Tenza, D., Rossé, C., … Chavrier, P. (2003). ARF6 controls post-endocytic recycling through its downstream exocyst complex effector. Journal of Cell Biology, 163(5). https://doi.org/10.1083/jcb.200305029
- Pu, J., Guardia, C. M., Keren-Kaplan, T., & Bonifacino, J. S. (2016). Mechanisms and functions of lysosome positioning. Journal of Cell Science, 129(23), 4329–4339. https://doi.org/10.1242/jcs.196287
- Puertollano, R., Aguilar, R. C., Gorshkova, I., Crouch, R. J., & Bonifacino, J. S. (2001). Sorting of mannose 6-phosphate receptors mediated by the GGAs. Science, 292(5522). https://doi.org/10.1126/science.1060750
- Puertollano, R., & Bonifacino, J. S. (2004). Interactions of GGA3 with the ubiquitin sorting machinery. Nature Cell Biology, 6(3). https://doi.org/10.1038/ncb1106
- Purushothaman, L. K., & Ungermann, C. (2018). Cargo induces retromer-mediated membrane remodeling on membranes. Molecular Biology of the Cell. https://doi.org/10.1091/mbc.E18-06-0339
- Puthenveedu, M. A., Lauffer, B., Temkin, P., Vistein, R., Carlton, P., Thorn, K., … Mark Von Zastrow. (2010). Sequence-dependent sorting of recycling proteins by actin-stabilized endosomal microdomains. Cell, 143(5), 761–773. https://doi.org/10.1016/j.cell.2010.10.003
- Qualmann, B., Roos, J., DiGregorio, P. J., & Kelly, R. B. (1999). Syndapin I, a synaptic dynamin-binding protein that associates with the neural Wiskott-Aldrich syndrome protein. Molecular Biology of the Cell. https://doi.org/10.1091/mbc.10.2.501
- Rajput, C., Kini, V., Smith, M., Yazbeck, P., Chavez, A., Schmidt, T., … Mehta, D. (2013). Neural Wiskott-Aldrich syndrome protein (N-WASP)-mediated p120-catenin interaction with Arp2-actin complex stabilizes endothelial adherens junctions. Journal of Biological Chemistry, 288(6). https://doi.org/10.1074/jbc.M112.440396
- Ratcliffe, C. D. H., Sahgal, P., Parachoniak, C. A., Ivaska, J., & Park, M. (2016). Regulation of cell migration and β1 integrin trafficking by the endosomal adaptor GGA3. Traffic (Copenhagen, Denmark). https://doi.org/10.1111/tra.12390

- Reck-Peterson, S. L., Redwine, W. B., Vale, R. D., & Carter, A. P. (2018). The cytoplasmic dynein transport machinery and its many cargoes. Nature Reviews Molecular Cell Biology, 19(6), 382–398. https://doi.org/10.1038/s41580-018-0004-3
- Redwine, W. B., DeSantis, M. E., Hollyer, I., Htet, Z. M., Tran, P. T., Swanson, S. K., … Reck-Peterson, S. L. (2017). The human cytoplasmic dynein interactome reveals novel activators of motility. ELife, 6. https://doi.org/10.7554/eLife.28257
- Renard, H. F., Johannes, L., & Morsomme, P. (2018). Increasing Diversity of Biological Membrane Fission Mechanisms. Trends in Cell Biology, 28(4), 274–286. https://doi.org/10.1016/j.tcb.2017.12.001
- Richard Mcintosh, J. (2016). Mitosis. Cold Spring Harbor Perspectives in Biology, 8(9). https://doi.org/10.1101/cshperspect.a023218
- Rivera-Molina, F. E., & Novick, P. J. (2009). A Rab GAP cascade defines the boundary between two Rab GTPases on the secretory pathway. Proceedings of the National Academy of Sciences, 106(34), 14408–14413. https://doi.org/10.1073/PNAS.0906536106
- Rivera, G. M., Briceño, C. A., Takeshima, F., Snapper, S. B., & Mayer, B. J. (2004). Inducible Clustering of Membrane-Targeted SH3 Domains of the Adaptor Protein Nck Triggers Localized Actin Polymerization. Current Biology. https://doi.org/10.1016/j.cub.2003.12.033
- Rizzelli, F., Malabarba, M. G., Sigismund, S., & Mapelli, M. (2020). The crosstalk between microtubules, actin and membranes shapes cell division. Open Biology, 10(3), 190314. https://doi.org/10.1098/rsob.190314
- Robinson, M. S. (2004). Adaptable adaptors for coated vesicles. Trends in Cell Biology. https://doi.org/10.1016/j.tcb.2004.02.002
- Robinson, R. C., Turbedsky, K., Kaiser, D. A., Marchand, J. B., Higgs, H. N., Choe, S., & Pollard, T. D. (2001). Crystal structure of Arp2/3 complex. Science. https://doi.org/10.1126/science.1066333
- Rocca, D. L., Martin, S., Jenkins, E. L., & Hanley, J. G. (2008). Inhibition of Arp2/3-mediated actin polymerization by PICK1 regulates neuronal morphology and AMPA receptor endocytosis. Nature Cell Biology, 10(3), 259–271. https://doi.org/10.1038/ncb1688
- Rohatgi, R., Ho, H. Y. H., & Kirschner, M. W. (2000). Mechanism of N-WASP activation by CDC42 and phosphatidylinositol 4,5-bisphosphate. Journal of Cell Biology, 150(6), 1299–1309. https://doi.org/10.1083/jcb.150.6.1299
- Rosa-Ferreira, C., Christis, C., Torres, I. L., & Munro, S. (2015). The small G protein Arl5 contributes to endosome-to-Golgi traffic by aiding the recruitment of the GARP complex to the Golgi. Biology Open, 4(4), 474–481. https://doi.org/10.1242/bio.201410975
- Rostislavleva, K., Soler, N., Ohashi, Y., Zhang, L., Pardon, E., Burke, J. E., … Williams, R. L. (2015). Structure and flexibility of the endosomal Vps34 complex reveals the basis of its function on membranes. Science, 7365. https://doi.org/10.1126/science.aac7365
- Roth, T. F., & Porter, K. R. (1964). Yolk Protein Uptake in the Oocyte of the Mosquito Aedes Aegypti. L. The Journal of Cell Biology, 20, 313–332. https://doi.org/10.1083/jcb.20.2.313

- Rotty, J. D., Wu, C., & Bear, J. E. (2013). New insights into the regulation and cellular functions of the ARP2/3 complex. Nature Reviews Molecular Cell Biology. https://doi.org/10.1038/nrm3492
- Rouiller, I., Xu, X. P., Amann, K. J., Egile, C., Nickell, S., Nicastro, D., … Hanein, D. (2008). The structural basis of actin filament branching by the Arp2/3 complex. Journal of Cell Biology, 180(5), 887–895. https://doi.org/10.1083/jcb.200709092
- Rubino, M., Miaczynska, M., Lippé, R., & Zerial, M. (2000). Selective membrane recruitment of EEA1 suggests a role in directional transport of clathrin-coated vesicles to early endosomes. Journal of Biological Chemistry, 275(6). https://doi.org/10.1074/jbc.275.6.3745
- Ryder, P. V., Vistein, R., Gokhale, A., Seaman, M. N., Puthenveedu, M. A., & Faundez, V. (2013). The WASH complex, an endosomal Arp2/3 activator, interacts with the Hermansky-Pudlak syndrome complex BLOC-1 and its cargo phosphatidylinositol-4- kinase type IIα. Molecular Biology of the Cell. https://doi.org/10.1091/mbc.E13-02-0088
- Sachse, M., Urbé, S., Oorschot, V., Strous, G. J., & Klumperman, J. (2002). Bilayered clathrin coats on endosomal vacuoles are involved in protein sorting toward lysosomes. Molecular Biology of the Cell. https://doi.org/10.1091/mbc.01-10-0525
- Sadhukhan, S., Sarkar, K., Taylor, M., Candotti, F., & Vyas, Y. M. (2014). Nuclear Role of WASp in Gene Transcription Is Uncoupled from Its ARP2/3-Dependent Cytoplasmic Role in Actin Polymerization. The Journal of Immunology, 193(1). https://doi.org/10.4049/jimmunol.1302923
- Sagona, A. P., Nezis, I. P., Pedersen, N. M., Liestøl, K., Poulton, J., Rusten, T. E., … Stenmark, H. (2010). PtdIns(3)P controls cytokinesis through KIF13A-mediated recruitment of FYVE-CENT to the midbody. Nature Cell Biology, 12(4), 362–371. https://doi.org/10.1038/ncb2036
- Salminen, A., & Novick, P. J. (1987). A ras-like protein is required for a post-Golgi event in yeast secretion. Cell, 49(4), 527–538. https://doi.org/10.1016/0092-8674(87)90455-7
- Sambrook, J., Russell, D.W. (2001). Molecular cloning : a laboratory manual, 3rd ed., Cold Spring Harbor Laboratory Press, Cold Spring Harbor, N.Y. Zool. Res. (Vol. 1). https://doi.org/10.3724/SP.J.1141.2012.01075
- Sanchez, A. D., & Feldman, J. L. (2016). Microtubule-organizing centers: from the centrosome to non-centrosomal sites. Current Opinion in Cell Biology, 1–9. https://doi.org/10.1016/j.ceb.2016.09.003
- Sandri, C., Caccavari, F., Valdembri, D., Camillo, C., Veltel, S., Santambrogio, M., … Serini, G. (2012). The R-Ras/RIN2/Rab5 complex controls endothelial cell adhesion and morphogenesis via active integrin endocytosis and Rac signaling. Cell Research. https://doi.org/10.1038/cr.2012.110
- Sandvig, K., Kavaliauskiene, S., & Skotland, T. (2018). Clathrin-independent endocytosis: an increasing degree of complexity. Histochemistry and Cell Biology, 150(2), 107–118. https://doi.org/10.1007/s00418-018-1678-5

- Sanger, A., Hirst, J., Davies, A. K., & Robinson, M. S. (2019). Adaptor protein complexes and disease at a glance. Journal of Cell Science, 132(20). https://doi.org/10.1242/jcs.222992
- Santos, A. J. M., Raote, I., Scarpa, M., Brouwers, N., & Malhotra, V. (2015). TANGO1 recruits ERGIC membranes to the endoplasmic reticulum for procollagen export. ELife. https://doi.org/10.7554/eLife.10982.001
- Sasaki, T., Hiroki, K., & Yamashita, Y. (2013). The role of epidermal growth factor receptor in cancer metastasis and microenvironment. BioMed Research International. https://doi.org/10.1155/2013/546318
- Sbrissa, D., Ikonomov, O. C., & Shisheva, A. (2002). Phosphatidylinositol 3-phosphate-interacting domains in PIKfyve. Binding specificity and role in PIKfyve endomembrane localization. Journal of Biological Chemistry, 277(8). https://doi.org/10.1074/jbc.M110194200
- Schiel, J. A., Simon, G. C., Zaharris, C., Weisz, J., Castle, D., Wu, C. C., & Prekeris, R. (2012). FIP3-endosome-dependent formation of the secondary ingression mediates ESCRT-III recruitment during cytokinesis. Nature Cell Biology, 14(10), 1068–1078. https://doi.org/10.1038/ncb2577
- Schindler, C., Chen, Y., Pu, J., Guo, X., & Bonifacino, J. S. (2015). EARP is a multisubunit tethering complex involved in endocytic recycling. Nature Cell Biology. https://doi.org/10.1038/ncb3129
- Schlager, M. A., Kapitein, L. C., Grigoriev, I., Burzynski, G. M., Wulf, P. S., Keijzer, N., … Hoogenraad, C. C. (2010). Pericentrosomal targeting of Rab6 secretory vesicles by Bicaudal-D-related protein 1 (BICDR-1) regulates neuritogenesis. EMBO Journal, 29(10), 1637–1651. https://doi.org/10.1038/emboj.2010.51
- Schmelzl, B., & Geli, M. I. (2002). An efficient genetic screen in mammalian cultured cells. EMBO Reports, 3(7), 682–687. https://doi.org/10.1093/embo-reports/kvf131
- Schmid, S. L. (2017). Reciprocal regulation of signaling and endocytosis: Implications for the evolving cancer cell. JCB, 1–10.
- Schmidt, M. R., Maritzen, T., Kukhtina, V., Higman, V. A., Doglio, L., Barak, N. N., … Haucke, V. (2009). Regulation of endosomal membrane traffic by a Gadkin/AP-1/kinesin KIF5 complex. Proceedings of the National Academy of Sciences of the United States of America, 106(36), 15344–15349. https://doi.org/10.1073/pnas.0904268106
- Schnoor, M., Stradal, T. E., & Rottner, K. (2017). Cortactin: Cell Functions of A Multifaceted Actin-Binding Protein. Trends in Cell Biology, 28(2), 79–98. https://doi.org/10.1016/j.tcb.2017.10.009
- Schöneberg, J, Lee, IH. Iwasa, JH., & Hurley, J. H. (2017). Reverse Topology Membrane Scission by the ESCRTs. Nat Rev Mol Cell Biol. https://doi.org/10.1016/j.bpj.2018.11.2488
- Schöneberg, J, Pavlin, M. R., Yan, S., Righini, M., Lee, I. H., Carlson, L. A., … Hurley, J. H. (2018). ATP-dependent force generation and membrane scission by ESCRT-III and Vps4. Science. https://doi.org/10.1126/science.aat1839

- Schu, P. V., Takegawa, K., Fry, M. J., Stack, J. H., Waterfield, M. D., & Emr, S. D. (1993). Phosphatidylinositol 3-kinase encoded by yeast VPS34 gene essential for protein sorting. Science, 260(5104). https://doi.org/10.1126/science.8385367
- Schwob, E., & Martin, R. P. (1992). New yeast actin-like gene required late in the cell cycle. Nature, 355(6356), 179–182. https://doi.org/10.1038/355179a0
- Scita, G., & Di Fiore, P. P. (2010). The endocytic matrix. Nature, 463(7280), 464–473. article. https://doi.org/10.1038/nature08910
- Seaman, M. N. J., McCaffery, J. M., & Emr, S. D. (1998). A membrane coat complex essential for endosome-to-Golgi retrograde transport in yeast. Journal of Cell Biology. https://doi.org/10.1083/jcb.142.3.665
- Semerdjieva, S., Shortt, B., Maxwell, E., Singh, S., Fonarev, P., Hansen, J., … Smythe, E. (2008). Coordinated regulation of AP2 uncoating from clathrin-coated vesicles by rab5 and hRME-6. Journal of Cell Biology, 183(3), 499–511. https://doi.org/10.1083/jcb.200806016
- Sevilla, L. M., Rana, A. A., Watt, F., & Smith, J. C. (2008). KazrinA is required for axial elongation and epidermal integrity in Xenopus tropicalis. Developmental Dynamics, 237(6), 1718–1725. https://doi.org/10.1002/dvdy.21557
- Sevilla, L.M., Nachat, R., Groot, K. R., & Watt, F. M. (2008). Kazrin regulates keratinocyte cytoskeletal networks, intercellular junctions and differentiation. Journal of Cell Science, 121(Pt 21), 3561–3569. https://doi.org/10.1242/jcs.029538
- Sezgin, E., Levental, I., Mayor, S., & Eggeling, C. (2017). The mystery of membrane organization: Composition, regulation and roles of lipid rafts. Nature Reviews Molecular Cell Biology. https://doi.org/10.1038/nrm.2017.16
- Shafaq-Zadah, M., Gomes-Santos, C. S., Bardin, S., Maiuri, P., Maurin, M., Iranzo, J., … Johannes, L. (2016). Persistent cell migration and adhesion rely on retrograde transport of β 1 integrin. Nature Cell Biology. https://doi.org/10.1038/ncb3287
- Shah, C., Hegde, B. G., Morén, B., Behrmann, E., Mielke, T., Moenke, G., … Langen, R. (2014). Structural insights into membrane interaction and caveolar targeting of dynamin-like EHD2. Structure, 22(3). https://doi.org/10.1016/j.str.2013.12.015
- Sharma, M., Giridharan, S. S. P., Rahajeng, J., Naslavsky, N., & Caplan, S. (2009). MICAL-L1 links EHD1 to tubular recycling endosomes and regulates receptor recycling. Molecular Biology of the Cell, 20(24), 5181–5194. https://doi.org/10.1091/mbc.E09-06-0535
- Sharma, M., Naslavsky, N., & Caplan, S. (2008). A role for EHD4 in the regulation of early endosomal transport. Traffic, 9(6), 995–1018. https://doi.org/10.1111/j.1600-0854.2008.00732.x
- Sheff, D. R., Daro, E. A., Hull, M., & Mellman, I. (1999). The receptors recycling pathway contains two distinct populations of early endosomes with different sorting functions. Journal of Cell Biology, 145(1), 123–139. https://doi.org/10.1083/jcb.145.1.123

- Shi, A., Sun, L., Banerjee, R., Tobin, M., Zhang, Y., & Grant, B. D. (2009). Regulation of endosomal clathrin and retromer-mediated endosome to Golgi retrograde transport by the J-domain protein RME-8. EMBO Journal. https://doi.org/10.1038/emboj.2009.272
- Shin, H. W., Hayashi, M., Christoforidis, S., Lacas-Gervais, S., Hoepfner, S., Wenk, M. R., … Zerial, M. (2005). An enzymatic cascade of Rab5 effectors regulates phosphoinositide turnover in the endocytic pathway. Journal of Cell Biology, 170(4). https://doi.org/10.1083/jcb.200505128
- Sicari, Igbaria, & Chevet. (2019). Control of Protein Homeostasis in the Early Secretory Pathway: Current Status and Challenges. Cells, 8(11), 1347. https://doi.org/10.3390/cells8111347
- Sigismund, S., & Scita, G. (2018). The 'endocytic matrix reloaded' and its impact on the plasticity of migratory strategies. Current Opinion in Cell Biology. https://doi.org/10.1016/j.ceb.2018.02.006
- Simonetti, B., Danson, C. M., Heesom, K. J., & Cullen, P. J. (2017). Sequence-dependent cargo recognition by SNX-BARs mediates retromer-independent transport of CI-MPR. Journal of Cell Biology, 216(11), 3695–3712. https://doi.org/10.1083/jcb.201703015
- Simonsen, A., Gaullier, J. M., D'Arrigo, A., & Stenmark, H. (1999). The Rab5 effector EEA1 interacts directly with syntaxin-6. Journal of Biological Chemistry, 274(41), 28857–28860. https://doi.org/10.1074/jbc.274.41.28857
- Simonsen, A., Lippé, R., Christoforidis, S., Gaullier, J. M., Brech, A., Callaghan, J., … Stenmark, H. (1998). EEA1 links PI(3)K function to Rab5 regulation of endosome fusion. Nature, 394(6692), 494–498. https://doi.org/10.1038/28879
- Simunovic, M., Bassereau, P., & Voth, G. A. (2018). Organizing membrane-curving proteins: the emerging dynamical picture. Current Opinion in Structural Biology. https://doi.org/10.1016/j.sbi.2018.03.018
- Simunovic, M., Manneville, J. B., Renard, H. F., Evergren, E., Raghunathan, K., Bhatia, D., … Callan-Jones, A. (2017). Friction Mediates Scission of Tubular Membranes Scaffolded by BAR Proteins. Cell, 170(1), 172-184.e11. https://doi.org/10.1016/j.cell.2017.05.047
- Singla, A., Fedoseienko, A., Giridharan, S. S. P. P., Overlee, B. L., Lopez, A., Jia, D., … Billadeau, D. D. (2019). Endosomal PI(3)P regulation by the COMMD/ CCDC22/CCDC93 (CCC) complex controls membrane protein recycling. Nature Communications, 93(3). https://doi.org/10.1038/s41467-019-12221-6
- Siton, O., Ideses, Y., Albeck, S., Unger, T., Bershadsky, A. D., Gov, N. S., & Bernheim-Groswasser, A. (2011). Cortactin releases the brakes in actin- based motility by enhancing WASP-VCA detachment from Arp2/3 branches. Current Biology. https://doi.org/10.1016/j.cub.2011.11.010
- Skånland, S. S., Wälchli, S., Brech, A., & Sandvig, K. (2009). SNX4 in complex with clathrin and dynein: Implications for endosome movement. PLoS ONE, 4(6), 1–10. https://doi.org/10.1371/journal.pone.0005935

- Skjeldal, F. M., Strunze, S., Bergeland, T., Walseng, E., Gregers, T. F., & Bakke, O. (2012). The fusion of early endosomes induces molecularmotor- driven tubule formation and fission. Journal of Cell Science, 125(8). https://doi.org/10.1242/jcs.092569
- Sochacki, K. A., & Taraska, J. W. (2019). From Flat to Curved Clathrin: Controlling a Plastic Ratchet. Trends in Cell Biology, 29(3), 241–256. https://doi.org/10.1016/j.tcb.2018.12.002
- Solinger, J. A., Rashid, H., Prescianotto-baschong, C., & Spang, A. (2020). FERARI is required for Rab11-dependent endocytic recycling. Nature Cell Biology. https://doi.org/10.1038/s41556-019-0456-5
- Sönnichsen, B., De Renzis, S., Nielsen, E., Rietdorf, J., & Zerial, M. (2000). Distinct membrane domains on endosomes in the recycling pathway visualized by multicolor imaging of Rab4, Rab5, and Rab11. Journal of Cell Biology, 149(4), 901–913. https://doi.org/10.1083/jcb.149.4.901
- Søreng, K., Munson, M. J., Lamb, C. A., Bjørndal, G. T., Pankiv, S., Carlsson, S. R., … Simonsen, A. (2018). SNX 18 regulates ATG 9A trafficking from recycling endosomes by recruiting Dynamin-2 . EMBO Reports. https://doi.org/10.15252/embr.201744837
- Sousa, R., Liao, H. S., Cuéllar, J., Jin, S., Valpuesta, J. M., Jin, A. J., & Lafer, E. M. (2016). Clathrin-coat disassembly illuminates the mechanisms of Hsp70 force generation. Nature Structural and Molecular Biology, 23(9), 821–829. https://doi.org/10.1038/nsmb.3272
- Sousa, S., Cabanes, D., Bougnères, L., Lecuit, M., Sansonetti, P., Tran-van-nhieu, G., & Cossart, P. (2007). Src, cortactin and Arp2/3 complex are required for E-cadherin-mediated internalization of Listeria into cells. Cellular Microbiology, 9(11). https://doi.org/10.1111/j.1462-5822.2007.00984.x
- Spang, A. (2012). The DSL1 Complex: The Smallest but Not the Least CATCHR. Traffic. https://doi.org/10.1111/j.1600-0854.2012.01362.x
- Stamnes, M. A., & Rothman, J. E. (1993). The binding of AP-1 clathrin adaptor particles to Golgi membranes requires ADP-ribosylation factor, a small GTP-binding protein. Cell, 73(5). https://doi.org/10.1016/0092-8674(93)90277-W
- Stein, M. P., Feng, Y., Cooper, K. L., Welford, A. M., & Wandinger-Ness, A. (2003). Human VPS34 and p150 are Rab7 interacting partners. Traffic, 4(11). https://doi.org/10.1034/j.1600-0854.2003.00133.x
- Steinberg, F., Gallon, M., Winfield, M., Thomas, E. C., Bell, A. J., Heesom, K. J., … Cullen, P. J. (2013). A global analysis of SNX27-retromer assembly and cargo specificity reveals a function in glucose and metal ion transport. Nature Cell Biology, 15(5), 461–471. https://doi.org/10.1038/ncb2721
- Stenmark, H. (2009). Rab GTPases as coordinators of vesicle traffic. Nature Reviews Molecular Cell Biology. https://doi.org/10.1038/nrm2728
- Stoorvogel, W., Oorschot, V., & Geuze, H. J. (1996). A novel class of clathrin-coated vesicles budding from endosomes. Journal of Cell Biology, 132(1–2), 21–33. https://doi.org/10.1083/jcb.132.1.21

- Stradal, T. E. B., Rottner, K., Disanza, A., Confalonieri, S., Innocenti, M., & Scita, G. (2004). Regulation of actin dynamics by WASP and WAVE family proteins. Trends in Cell Biology. https://doi.org/10.1016/j.tcb.2004.04.007
- Sugino, H., & Hatano, S. (1982). Effect of fragmin on actin polymerization: Evidence for enhancement of nucleation and capping of the barbed end. Cell Motility. https://doi.org/10.1002/cm.970020505
- Sun, Q., Westphal, W., Wong, K. N., Tan, I., & Zhong, Q. (2010). Rubicon controls endosome maturation as a Rab7 effector. Proceedings of the National Academy of Sciences of the United States of America. https://doi.org/10.1073/pnas.1010554107
- Sun, Z., & Brodsky, J. L. (2019). Protein quality control in the secretory pathway. Journal of Cell Biology. https://doi.org/10.1083/jcb.201906047
- Suyama, K., Shapiro, I., Guttman, M., & Hazan, R. B. (2002). A signaling pathway leading to metastasis is controlled by N-cadherin and the FGF receptor. Cancer Cell. https://doi.org/10.1016/S1535-6108(02)00150-2
- Svitkina, T. (2018). The actin cytoskeleton and actin-based motility. Cold Spring Harbor Perspectives in Biology, 10(1), 1–22. https://doi.org/10.1101/cshperspect.a018267
- Svitkina, T., & Borisy, G. G. (1999). Arp2/3 complex and actin depolymerizing factor/cofilin in dendritic organization and treadmilling of actin filament array in lamellipodia. Journal of Cell Biology. https://doi.org/10.1083/jcb.145.5.1009
- Szebenyi, G., Hall, B., Yu, R., Hashim, A. I., & Krämer, H. (2007). Hook2 localizes to the centrosome, binds directly to centriolin/CEP110 and contributes to centrosomal function. Traffic, 8(1). https://doi.org/10.1111/j.1600-0854.2006.00511.x
- Tanabe, K., Ohashi, E., Henmi, Y., & Takei, K. (2011). Receptor sorting and actin dynamics at early endosomes. Communicative & Integrative Biology, 4(6), 742–744. https://doi.org/10.4161/cib.17628
- Tanaka, N., Kyuuma, M., & Sugamura, K. (2008). Endosomal sorting complex required for transport proteins in cancer pathogenesis, vesicular transport, and non-endosomal functions. Cancer Science. https://doi.org/10.1111/j.1349-7006.2008.00825.x
- Taunton, J., Rowning, B. A., Coughlin, M. L., Wu, M., Moon, R. T., Mitchison, T. J., & Larabell, C. A. (2000). Actin-dependent propulsion of endosomes and lysosomes by recruitment of N-WASP. The Journal of Cell Biology, 148(3), 519–530. http://www.pubmedcentral.nih.gov/articlerender.fcgi?artid=2174808&tool=pmcentrez&rendertype=abstract
- Taylor, M. J., Perrais, D., & Merrifield, C. J. (2011). A high precision survey of the molecular dynamics of mammalian clathrin-mediated endocytosis. PLoS Biology, 9(3). https://doi.org/10.1371/journal.pbio.1000604
- Tisdale, E. J., Bourne, J. R., Khosravi-Far, R., Der, C. J., & Balch, W. E. (1992). GTP-binding mutants of Rab1 and Rab2 are potent inhibitors of vesicular transport from the endoplasmic reticulum to the golgi complex. Journal of Cell Biology, 119(4). https://doi.org/10.1083/jcb.119.4.749

- Titus, M. A. (2018). Myosin-Driven Intracellular Transport. Cold Spring Harbor Perspectives in Biology, 1–16.
- Tovey, C. A., & Conduit, P. T. (2018). Microtubule nucleation by γ-tubulin complexes and beyond. Essays in Biochemistry, 62(6), 765–780. https://doi.org/10.1042/EBC20180028
- Traer, C. J., Rutherford, A. C., Palmer, K. J., Wassmer, T., Oakley, J., Attar, N., … Cullen, P. J. (2007). SNX4 coordinates endosomal sorting of TfnR with dynein-mediated transport into the endocytic recycling compartment. Nature Cell Biology, 9(12), 1370–1380. https://doi.org/10.1038/ncb1656
- Tran, D. T., Masedunskas, A., Weigert, R., & Ten Hagen, K. G. (2015). Arp2/3-mediated F-actin formation controls regulated exocytosis in vivo. Nature Communications, 6. https://doi.org/10.1038/ncomms10098
- Traub, L. M. (2003). Sorting it out: AP-2 and alternate clathrin adaptors in endocytic cargo selection. Journal of Cell Biology. https://doi.org/10.1083/jcb.200309175
- Tsarouhas, V., Liu, D., Tsikala, G., Fedoseienko, A., Zinn, K., Matsuda, R., … Samakovlis, C. (2019). WASH phosphorylation balances endosomal versus cortical actin network integrities during epithelial morphogenesis. Nature Communications, 10(1), 2193. https://doi.org/10.1038/s41467-019-10229-6
- Uemura, T., & Waguri, S. (2020). Emerging roles of Golgi/endosome-localizing monomeric clathrin adaptors GGAs. Anatomical Science International, 95(1), 12–21. https://doi.org/10.1007/s12565-019-00505-2
- Ullrich, O., Reinsch, S., Urbé, S., Zerial, M., & Parton, R. G. (1996). Rab11 regulates recycling through the pericentriolar recycling endosome. Journal of Cell Biology, 135(4). https://doi.org/10.1083/jcb.135.4.913
- Ungermann, C., & Kümmel, D. (2019). Structure of membrane tethers and their role in fusion. Traffic, 20(7), 479–490. https://doi.org/10.1111/tra.12655
- Urbé, S., Huber, L. A., Zerial, M., Tooze, S. A., & Parton, R. G. (1993). Rab11, a small GTPase associated with both constitutive and regulated secretory pathways in PC12 cells. FEBS Letters, 334(2). https://doi.org/10.1016/0014-5793(93)81707-7
- Urnavicius, L., Lau, C. K., Elshenawy, M. M., Morales-Rios, E., Motz, C., Yildiz, A., & Carter, A. P. (2018). Cryo-EM shows how dynactin recruits two dyneins for faster movement. Nature, 554(7691), 202–206. https://doi.org/10.1038/nature25462
- Uruno, T., Liu, J., Zhang, P., Fan, Y. X., Egile, C., Li, R., … Zhan, X. (2001). Activation of Arp2/3 complex-mediated actin polymerization by cortactin. Nature Cell Biology. https://doi.org/10.1038/35060051
- van Dam, E. M., & Stoorvogel, W. (2002). Dynamin-dependent transferrin receptor recycling by endosome-derived clathrin-coated vesicles. Molecular Biology of the Cell. https://doi.org/10.1091/mbc.01-07-0380

- van der Beek, J., Jonker, C., van der Welle, R., Liv, N., & Klumperman, J. (2019). CORVET, CHEVI and HOPS – Multisubunit tethers of the endo-lysosomal system in health and disease. Journal of Cell Science, 132(10). https://doi.org/10.1242/jcs.189134
- van der Sluijs, P., Hull, M., Webster, P., Mâle, P., Goud, B., & Mellman, I. (1992). The small GTP-binding protein rab4 controls an early sorting event on the endocytic pathway. Cell, 70(5), 729–740. https://doi.org/10.1016/0092-8674(92)90307-X
- van Weering, J. R. T., Verkade, P., & Cullen, P. J. (2012). SNX-BAR-mediated endosome tubulation is co-ordinated with endosome maturation. Traffic, 13(1), 94–107. https://doi.org/10.1111/j.1600-0854.2011.01297.x
- Völlner, F., Ali, J., Kurrle, N., Exner, Y., Eming, R., Hertl, M., … Tikkanen, R. (2016). Loss of flotillin expression results in weakened desmosomal adhesion and Pemphigus vulgaris-like localisation of desmoglein-3 in human keratinocytes. Scientific Reports, 6. https://doi.org/10.1038/srep28820
- Vyas, J. M., Kim, Y.-M., Artavanis-Tsakonas, K., Love, J. C., Van der Veen, A. G., & Ploegh, H. L. (2007). Tubulation of Class II MHC Compartments Is Microtubule Dependent and Involves Multiple Endolysosomal Membrane Proteins in Primary Dendritic Cells. The Journal of Immunology, 178(11). https://doi.org/10.4049/jimmunol.178.11.7199
- Wandinger-Ness, A., & Zerial, M. (2014). Rab Proteins and the Compatmentalization of the Endosomal System. Cold Spring Harbor Perspectives in Biology, 6(11), a022616. https://doi.org/10.1101/cshperspect.a022616
- Wang, H., Lo, W. T., & Haucke, V. (2019). Phosphoinositide switches in endocytosis and in the endolysosomal system. Current Opinion in Cell Biology. https://doi.org/10.1016/j.ceb.2019.03.011
- Wang, J., Fedoseienko, A., Chen, B., Burstein, E., Jia, D., & Billadeau, D. D. (2018). Endosomal receptor trafficking: Retromer and beyond. Traffic, (May), 578–590. https://doi.org/10.1111/tra.12574
- Wang, Qian, Chen, X. W., & Margolis, B. (2007). PALS1 regulates E-cadherin trafficking in mammalian epithelial cells. Molecular Biology of the Cell. https://doi.org/10.1091/mbc.E06-07-0651
- Wang, Qiong, Liu, M., Li, X., Chen, L., & Tang, H. (2009). Kazrin F is involved in apoptosis and interacts with BAX and ARC. Acta Biochimica et Biophysica Sinica, 41(9), 763–772. http://www.ncbi.nlm.nih.gov/pubmed/19727525
- Wang, Y. J., Wang, J., Sun, H. Q., Martinez, M., Sun, Y. X., Macia, E., … Yin, H. L. (2003). Phosphatidylinositol 4 phosphate regulates targeting of clathrin adaptor AP-1 complexes to the Golgi. Cell, 114(3), 299–310. https://doi.org/10.1016/S0092-8674(03)00603-2
- Wang, Z., Zhang, F., He, J., Wu, P., Tay, L. W. R., Cai, M., … Du, G. (2017). Binding of PLD2-Generated Phosphatidic Acid to KIF5B Promotes MT1-MMP Surface Trafficking and Lung Metastasis of Mouse Breast Cancer Cells. Developmental Cell, 43(2), 186-197.e7. https://doi.org/10.1016/j.devcel.2017.09.012

– Warner, C. L., Stewart, A., Luzio, J. P., Steel, K. P., Libby, R. T., Kendrick-Jones, J., & Buss, F. (2003). Loss of myosin VI reduces secretion and the size of the Golgi in fibroblasts from Snell's waltzer mice. EMBO Journal, 22(3), 569–579. https://doi.org/10.1093/emboj/cdg055

– Warner, S. J., & Longmore, G. D. (2009). Cdc42 antagonizes Rho1 activity at adherens junctions to limit epithelial cell apical tension. Journal of Cell Biology, 187(1), 119–133. https://doi.org/10.1083/jcb.200906047

– Wassmer, T., Attar, N., Harterink, M., van Weering, J. R. T., Traer, C. J., Oakley, J., … Cullen, P. J. (2009). The Retromer Coat Complex Coordinates Endosomal Sorting and Dynein-Mediated Transport, with Carrier Recognition by the trans-Golgi Network. Developmental Cell, 17(1), 110–122. https://doi.org/10.1016/j.devcel.2009.04.016

– Watanabe, S., & Boucrot, E. (2017). Fast and ultrafast endocytosis. Current Opinion in Cell Biology. https://doi.org/10.1016/j.ceb.2017.02.013

– Weaver, A. M., Hussaini, I. M., Mazar, A., Henkin, J., & Gonias, S. L. (1997). Embryonic fibroblasts that are genetically deficient in low density lipoprotein receptor-related protein demonstrate increased activity of the urokinase receptor system and accelerated migration on vitronectin. Journal of Biological Chemistry, 272(22). https://doi.org/10.1074/jbc.272.22.14372

– Weaver, A. M., Karginov, A. V., Kinley, A. W., Weed, S. A., Li, Y., Parsons, J. T., & Cooper, J. A. (2001). Cortactin promotes and stabilizes Arp2/3-induced actin filament network formation. Current Biology. https://doi.org/10.1016/S0960-9822(01)00098-7

– Wegner, A. (1976). Head to tail polymerization of actin. Journal of Molecular Biology. https://doi.org/10.1016/S0022-2836(76)80100-3

– Wei, J., Fu, Z. Y., Li, P. S., Miao, H. H., Li, B. L., Ma, Y. T., & Song, B. L. (2014). The clathrin adaptor proteins ARH, Dab2, and numb play distinct roles in Niemann-Pick C1-Like 1 versus low density lipoprotein receptor-mediated cholesterol uptake. Journal of Biological Chemistry. https://doi.org/10.1074/jbc.M114.593764

– Welz, T., Wellbourne-Wood, J., & Kerkhoff, E. (2014). Orchestration of cell surface proteins by Rab11. Trends in Cell Biology, 24(7), 407–414. https://doi.org/10.1016/j.tcb.2014.02.004

– Wenzel, E. M., Schultz, S. W., Schink, K. O., Pedersen, N. M., Nähse, V., Carlson, A., … Raiborg, C. (2018). Concerted ESCRT and clathrin recruitment waves define the timing and morphology of intraluminal vesicle formation. Nature Communications, 9(1). https://doi.org/10.1038/s41467-018-05345-8

– White, D. P., Caswell, P. T., & Norman, J. C. (2007). alphavbeta3 and alpha5beta1 integrin recycling pathways dictate downstream Rho kinase signaling to regulate persistent cell migration. The Journal of Cell Biology, 177(3), 515–525. https://doi.org/10.1083/jcb.200609004

- Wickner, W., & Rizo, J. (2017). A cascade of multiple proteins and lipids catalyzes membrane fusion. Molecular Biology of the Cell, 28(6), 707–711. https://doi.org/10.1091/mbc.E16-07-0517
- Wilson, B. J., Allen, J. L., & Caswell, P. T. (2018). Vesicle trafficking pathways that direct cell migration in 3D matrices and in vivo. Traffic, 19(12), 899–909. https://doi.org/10.1111/tra.12605
- Wilson, G. M., Fielding, A. B., Simon, G. C., Yu, X., Andrews, P. D., Haines, R. S., … Prekeris, R. (2005). The FIP3-Rab11 protein complex regulates recycling endosome targeting to the cleavage furrow during late cytokinesis. Molecular Biology of the Cell, 16(2), 849–860. https://doi.org/10.1091/mbc.E04-10-0927
- Winckler, B., & Choo Yap, C. (2011). Endocytosis and Endosomes at the Crossroads of Regulating Trafficking of Axon Outgrowth-Modifying Receptors. Traffic. https://doi.org/10.1111/j.1600-0854.2011.01213.x
- Witkos, T. M., & Lowe, M. (2017). Recognition and tethering of transport vesicles at the Golgi apparatus. Current Opinion in Cell Biology. https://doi.org/10.1016/j.ceb.2017.02.003
- Wittinghofer, A., Franken, S. M., Scheidig, A. J., Rensland, H., Lautwein, A., Pai, E. F., & Goody, R. S. (1993). Three-dimensional structure and properties of wild-type and mutant H-ras-encoded p21. Ciba Foundation Symposium. https://doi.org/10.1002/9780470514450.ch2
- Xiao, K., Garner, J., Buckley, K. M., Vincent, P. A., Chiasson, C. M., Dejana, E., … Kowalczyk, A. P. (2005). p120-catenin regulates clathrin-dependent endocytosis of VE-cadherin. Molecular Biology of the Cell, 16(11). https://doi.org/10.1091/mbc.E05-05-0440
- Xing, M., Peterman, M. C., Davis, R. L., Oegema, K., Shiau, A. K., & Field, S. J. (2016). GOLPH3 drives cell migration by promoting Golgi reorientation and directional trafficking to the leading edge. Molecular Biology of the Cell. https://doi.org/10.1091/mbc.E16-01-0005
- Yamada, A., Mamane, A., Lee-Tin-Wah, J., Di Cicco, A., Prévost, C., Lévy, D., … Bassereau, P. (2014). Catch-bond behaviour facilitates membrane tubulation by non-processive myosin 1b. Nature Communications, 5. https://doi.org/10.1038/ncomms4624
- Yang, T. T., Chong, W. M., Wang, W. J., Mazo, G., Tanos, B., Chen, Z., … Liao, J. C. (2018). Super-resolution architecture of mammalian centriole distal appendages reveals distinct blade and matrix functional components. Nature Communications. https://doi.org/10.1038/s41467-018-04469-1
- Yorimitsu, T., Sato, K., & Takeuchi, M. (2014). Molecular mechanisms of Sar/Arf GTPases in vesicular trafficking in yeast and plants. Frontiers in Plant Science. https://doi.org/10.3389/fpls.2014.00411
- Yudowski, G. A., Puthenveedu, M. A., Henry, A. G., & Von Zastrow, M. (2009). Cargo-mediated regulation of a rapid Rab4-dependent recycling pathway. Molecular Biology of the Cell, 20(11), 2774–2784. https://doi.org/10.1091/mbc.E08-08-0892

- Zahoor, M., & Farhan, H. (2018). Crosstalk of Autophagy and the Secretory Pathway and Its Role in Diseases. In International Review of Cell and Molecular Biology (Vol. 337). https://doi.org/10.1016/bs.ircmb.2017.12.004
- Zeng, Q., Tran, T. T. H., Tan, H. X., & Hong, W. (2003). The cytoplasmic domain of Vamp4 and Vamp5 is responsible for their correct subcellular targeting: The N-terminal extension of Vamp4 contains a dominant autonomous targeting signal for the trans-Golgi network. Journal of Biological Chemistry, 278(25), 23046–23054. https://doi.org/10.1074/jbc.M303214200
- Zhang, G., Kashimshetty, R., Ng, K. E., Tan, H. B., & Yeong, F. M. (2006). Exit from mitosis triggers Chs2p transport from the endoplasmic reticulum to mother-daughter neck via the secretory pathway in budding yeast. The Journal of Cell Biology, 174(2), 207–220. https://doi.org/10.1083/jcb.200604094
- Zhang, X. M., Ellis, S., Sriratana, A., Mitchell, C. A., & Rowe, T. (2004). Sec15 is an effector for the Rab11 GTPase in mammalian cells. Journal of Biological Chemistry, 279(41), 43027–43034. https://doi.org/10.1074/jbc.M402264200
- Zhao, Y., & Keen, J. H. (2008). Gyrating clathrin: Highly dynamic clathrin structures involved in rapid receptor recycling. Traffic. https://doi.org/10.1111/j.1600-0854.2008.00819.x
- Zhen, Y., & Stenmark, H. (2015). Cellular functions of Rab GTPases at a glance. Journal of Cell Science, 128(17), 3171–3176. https://doi.org/10.1242/jcs.166074
- Zhukovsky, M. A., Filograna, A., Luini, A., Corda, D., & Valente, C. (2019). Protein Amphipathic Helix Insertion: A Mechanism to Induce Membrane Fission. Frontiers in Cell and Developmental Biology, 7(December), 1–29. https://doi.org/10.3389/fcell.2019.00291
- Zimmet, A., Van Eeuwen, T., Boczkowska, M., Rebowski, G., Murakami, K., & Dominguez, R. (2020). Cryo-EM structure of NPF-bound human Arp2/3 complex and activation mechanism. Science Advances, 6(23), eaaz7651. https://doi.org/10.1126/sciadv.aaz7651